AGE-RELATED CHANGES IN SYNAPTIC, CALCIUM AND COGNITIVE MECHANISMS IN THE BASAL FOREBRAIN USING AN OPTOGENETIC MOUSE MODEL

A Dissertation

by

EUNYOUNG BANG

Submitted to the Office of Graduate and Professional Studies of
Texas A&M University
in partial fulfillment of the requirements for the degree of

DOCTOR OF PHILOSOPHY

Chair of Committee,	William H. Griffith
Committee Members,	Jun Wang
	Rahul Srinivasan
	James Grau
Head of Department,	Farida Sohrabji

August 2021

Major Subject: Neuroscience

ABSTRACT

Age-relate cognitive decline is a devastating disorder often associated with serious neurological disease and neurodegeneration. The increased prevalence of neurological diseases, as a result of the aging population, only reinforces the importance of understanding the neurobiological basis of aging and the need for better therapeutics to treat age-related dysfunction. In the current work, studies were designed to utilize our new optogenetic aging mouse model of the basal forebrain (BF) to test the efficacy of a pharmacological treatment across aging and to test the effects of late-onset, short-term intermittent fasting (IF) on well-characterized age-related changes in synaptic and Ca^{2+} signaling. Finally, we tested whether both synaptic excitation (E) and inhibition (I) changed during aging. Our model utilized a bacterial artificial chromosome (BAC) transgenic mouse line with stable expression of the channelrhodopsin-2 (ChR2) variant H134R [VGAT-ChR2(H134R)-EYFP] in a reduced synaptic preparation that allows for specific optogenetic light stimulation on GABAergic synaptic terminals across aging. Our first study showed that clinically relevant concentrations of amitriptyline (AMI) reduced the frequency of spontaneous inhibitory postsynaptic currents (sIPSCs) and reduced quantal content in both young and aged mice. These results suggest a presynaptic mechanism of action of the drug that does not diminish with age. Our second study showed the late-onset, short-term IF reversed age-related changes in Ca^{2+} buffering and GABAergic synaptic transmission in BF neurons of aged mice. We performed quantal analysis using the method of failures and showed that IF reverses the

age-related decrease in quantal content of GABAergic synapses. Our results suggest that late-onset, short-term IF, may show comparable beneficial effects as those of life-long caloric restriction (CR) to improve brain health. Few therapeutics are currently available to treat age-related neurological dysfunction and IF may provide a healthy therapeutic alternative. Finally, we demonstrated that the E/I balance increased with age due to no change in synaptic excitation coupled with decrease in synaptic inhibition in the BF brain slices. E/I imbalance within neural circuits has been implicated in age-related brain dysfunction. Our studies will help advance our knowledge of the neurobiology of the aging and suggest possible new avenues for drug research mechanisms and/or lifestyle changes.

ACKNOWLEDGEMENTS

I would like to thank my committee chair, Dr. William H. Griffith, and my committee members, Dr. Jun Wang, Dr. Rahul Srinivasan, and Dr. James Grau for their guidance, and support throughout the entire Ph.D. program.

Thanks also go to my friends and colleagues and the department faculty, Dr. David A. Murchison and Dr. Karienn S. Montgomery and staff, Ms. Annette S. Fincher for making my time at Texas A&M University a great experience.

Finally, thanks to my parents, Jumsook Lee and Kichul Bang and brother, Jaehyun Bang for their encouragement and to my husband, Eui Seop Kim and my daughter, Lina Kim for her/his patience and love.

CONTRIBUTORS AND FUNDING SOURCES

Contributors

This work was supervised by a dissertation committee consisting of Regents Professor William H. Griffith [advisor], Associate Professor Jun Wang, and Assistant Professor Rahul Srinivasan of the Department of Neuroscience and Experimental Therapeutics and Mary Tucker Currie Professor James Grau of the Department of Psychology.

For Chapter II, Ms. Annette S. Fincher, Dr. Karienn S. Montgomery, and Professor David J. Earnest helped contribute to the circadian study, while Dr. Angelika Tobery contributed measurements of calcium currents in rat basal forebrain neurons. Some of the fura-2 calcium imaging experiments for Chapter II was conducted by Dr. David A. Murchison. The behavior experiments for Chapter III were assisted by Ms. Sophie Nader. All graphic illustrations were drawn by Ms. Annette S. Fincher. The mouse breeding colony was maintained by Ms. Annette S. Fincher.

All other work conducted for the dissertation was independently completed by the graduate student, Eunyoung Bang.

Funding Sources

This work was also made possible in part by grants from the National Institute of Aging AG047652, Department of Neuroscience and Experimental Therapeutics, College of Medicine, Janell and Jo Marek ’57 Alzheimer’s disease research fund. Its contents

are solely the responsibility of the authors and do not necessarily represent the official views of the granting agencies mentioned above.

NOMENCLATURE

Aβ	Amyloid beta
ACh	Acetylcholine
AChE	Cholinesterases
AD	Alzheimer disease
AL	Ad libitum
ALS	Amyotrophic lateral sclerosis
AMI	Amitriptyline
AMPA	α-amino-3-hydroxy-5-methyl-4-isoxazolepropionic acid
APP	Amyloid precursor protein
APV	2-amino-5-phosphonopentanoic acid
ATM	Ataxia telangiectasia
ATP	Adenosine triphosphate
BAC	Bacterial artificial chromosome
BDNF	Brain derived neurotrophic factor
BF	Basal forebrain
BLA	Basolateral amygdala
BMI	Body mass index
CBP	Calcium binding proteins
CAT	Catalase
ChAT	Choline acetyltransferase

ChR	Channelrhodopsin
CR	Caloric restriction
CS	Cockayne syndrome
CSB	Cockayne syndrome complementation group B
DNA	Deoxyribonucleic acid
DNQX	6,7-dinitroquinoxaline-2,3-dione
E	Excitation
EEG	Electroencephalogram
ER	Endoplasmic reticulum
EYFP	Enhanced yellow fluorescent protein
fMRI	Functional magnetic resonance imaging
FDA	Food and drug administration
FTO	Fat mass and obesity-associated
GABA	γ-aminobutyric acid
GAD	Glutamic acid decarboxylase
GAL	Galanin
GAT	GABA transporter
GFAP	Glial fibrillary acidic protein
GRP	Glucose-regulated proteins
GSH	Glutathione
HD	Huntington’s disease
HNE	4-hydroxynonenal, lipid peroxidation product

HSP	Heat shock proteins
HVA	High-voltage-activated
I	Inhibition
Idh	Isocitrate dehydrogenase
IF	Intermittent fasting
IGF	Insulin-like growth factor
IL	Interleukins
IPSC	Inhibitory postsynaptic current
LD 12:12	A standard 12h light/12h dark cycle
LTP	Long-term potentiation
LVA	Low-voltage activated
mAChR	Muscarinic acetylcholine receptor
MAOI	Monoamine oxidase inhibitor
MCI	Mild cognitive impairment
mEPSCs	Miniature excitatory postsynaptic currents
mIPSCs	Miniature inhibitory postsynaptic currents
mPFC	Medial prefrontal cortex
mPTP	Mitochondrial permeability transition pore
MS/DB	Medial septum/diagonal band nucleus
MS/VDB	Medial septum/vertical diagonal band nucleus
mtDNA	Mitochondrial DNA
nAChR	Nicotinic acetylcholine receptors

NAD	Nicotinamide adenine dinucleotide
NADH	Nicotinamide adenine dinucleotide + Hydrogen
NADPH	Nicotinamide adenine dinucleotide phosphate
NCAM	Neural cell adhesion molecule
NFκB	Nuclear factor kappa-light-chain enhancer of activated B cells
NGF	Nerve growth factor
NMDA	N-methyl-D-aspartate
NPY	Neuropeptide Y
NSF	N-Ethylmaleimide sensitive factor
oIPSCs	Optically-evoked inhibitory postsynaptic currents
OXPHOS	Oxidative phosphorylation
PD	Parkinson’s disease
PFA	Paraformaldehyde
PFC	Prefrontal cortex
PSA-NCAM	Polysialylated form of neural cell adhesion molecule
REM	Rapid eye movement
ROS	Reactive oxygen species
RRP	Readily releasable pool
sAHP	Slow after-hyperpolarization
sEPSCs	Spontaneous excitatory postsynaptic currents
sER	Smooth endoplasmic reticulum
sIPSCs	Spontaneous inhibitory postsynaptic currents

SIRT	Sirtuin
SI/EA	Substantia innominate/extended amygdala
SK	Small conductance calcium-activated potassium
SNRI	Selective norepinephrine reuptake inhibitor
SOD	Superoxide dismutase
SSRI	Selective serotonin reuptake inhibitor
SVC	Synaptic vesicle cycle
SWS	Slow-wave sleep
TLR	Toll-like receptor
TNF	Tumor necrosis factor
VAChT	Vesicular acetylcholine transporter
VEGF	Vascular endothelial cell growth factor
VGAT	Vesicular GABA transporter
Vgluts	Vesicular glutamate transporters
v-SNARE	Vesicular soluble NSF attachment protein receptor
WRN	Werner protein
WS	Werner syndrome
WT	Wildtype

TABLE OF CONTENTS

Page

LIST OF FIGURES

Page

SPECIFIC AIMS

Aim 1: To determine the actions of the antidepressant drug amitriptyline on GABAergic synaptic transmission across aging.

Hypothesis: Amitriptyline will act presynaptically to block GABAergic synaptic neurotransmitter and this inhibition will increase during aging.

Aim 2: To determine if late-onset, short-term intermittent fasting (4-6 weeks) alleviates age-related changes in intracellular calcium buffering, inhibitory synaptic transmission and cognitive impairment.

Hypothesis: Late-onset, short-term intermittent fasting will reverse age-related changes in intracellular calcium buffering, inhibitory synaptic transmission and cognitive impairment.

Aim 3: To examine glutamatergic synaptic excitation in the basal forebrain and determine the excitatory/inhibitory (E/I) synaptic ratio during aging.

Hypothesis: The excitatory/inhibitory (E/I) synaptic ratio will increase in the mouse BF neurons during aging due to a decrease in synaptic inhibition with no change in synaptic excitation.

CHAPTER I

GENERAL INTRODUCTION

1.1 Significance of studying brain aging

Experiments were conducted to study a number of parameters of the aging brain with the hopes of achieving a better understanding of factors contributing to age-related physiological and cognitive dysfunction. The importance of understanding and maintaining healthy aging cannot be overemphasized. The number of individuals over the age of 65 is projected to rise to 88.5 million in 2050, which will more than double the number of 40.2 million in 2010 (Vicent & Velkoff, 2010). There were approximately 4.2 million adults suffering from dementia in the United States in 2010 and more than 135 million worldwide (Hurd et al., 2013; Prince et al., 2013). Associated with this increasing population is the growing number of cases of age-related cognitive impairment and devastating neurological disease resulting in an explosion of health care costs and the need for new and effective therapies (Hurd et al., 2013; Wimo et al., 2013). Importantly, lifestyle changes such as exercise and caloric restriction have proven to be beneficial to facilitate healthy aging. Caloric restriction has proven very effective in facilitating benefits in human aging (Sohal and Weindruch, 1996; Redman and Ravussin, 2011; Most et al., 2016), however, the mechanisms are unknown. This dissertation focuses on two main aspects of age-related brain function including synaptic transmission by asking how does a commonly used antidepressant drug, amitriptyline (AMI) acts on synaptic transmission across aging. AMI will be used as a prototype drug to test whether therapeutic concentrations of this antidepressant prove efficacious during

aging and whether presynaptic actions to regulate neurotransmitter release are important mechanisms. Secondly, does an increasingly popular type of caloric restriction (referred to as late-onset intermittent fasting) act to reverse of prevent previously described cellular changes in the basal forebrain during aging.

1.2 Overview of the neurobiology of aging

The aging process is accompanied by structural and physiological changes in the brain. In the human brain, both gray and white matter are reduced during normal aging along with enlargement of the cerebral ventricles, resulting in brain shrinkage (Drayer, 1988). Functional magnetic resonance imaging (fMRI) studies found that the functional integration between brain areas is disrupted during normal aging which is associated with white matter degradation and poor cognitive performance (Andrews-Hanna et al., 2007). In addition to a global loss of integrative function in the brain networks, reduced metabolic activity in the brain is observed in normal aging as well as Alzheimer's disease (AD) (Small et al., 2002). Histological analyses have revealed that a combination of dendritic regression and the loss of neuronal cells leads to brain atrophy during aging (West et al., 1994; Dumitriu et al., 2010). Recent studies in cellular and molecular biology have enhanced our knowledge of the basic mechanisms of brain aging including, neuronal/synaptic dysfunction, dysregulation of neuronal calcium homeostasis, mitochondrial dysfunction by accumulation of oxidatively damaged molecules, impaired lysosome and proteasome function, compromised DNA repair and inflammation. All of these processes may contribute to age-related cognitive decline and disrupt health aging. An overview of these mechanisms associated with brain aging are discussed below.

1.2.1 Neuronal/synaptic dysfunction

The structural integrity and well-balanced synaptic activities of different neurotransmitter systems are essential for normal brain function. More specifically, synaptic contacts on the dendrites of neurons are structurally well organized. On excitatory neurons, GABAergic inputs make their synapses on or adjacent to the cell body while glutamatergic inputs often make synapses on distal dendrites, and various modulatory synapses from basal forebrain cholinergic neurons, midbrain dopaminergic neurons, and brainstem serotonergic and noradrenergic neurons are located proximal to the distal glutamatergic inputs (Mattson and Arumugam, 2018). However, numerous physiological and structural changes in neurons have been observed during aging, such as decreased size of soma (de Brabander et al., 1998; Wong et al., 2000), loss/regression of dendrites and dendritic spines (Jacobs et al., 1997; Peters et al., 1998; Page et al., 2002; Duan et al., 2003), synapse loss (Chen et al., 1995; Wong et al., 1998), neurotransmitter receptors changes (Post-Munson et al., 1994; Rosene and Nicholson, 1999) and/or decreased response to neurotransmitters (Fieber et al., 2010; Akhmedov et al., 2013; Kempsell and Fieber, 2014). These age-related alterations in physiology and structure of neuronal cells may induce age-related impairments in neuronal networks and synaptic activities.

Synaptic dysfunction has been considered as one of hall marks of brain aging thought to contribute to cognitive decline (Lehmann et al., 2012; McQuail et al., 2015; Rozycka et al., 2017; Kwakowsky et al., 2018a,b; Ren et al., 2018). During aging, disruption of excitation/inhibition (E/I) synaptic balances occur as a result of impaired

GABAergic signaling (Heise et al., 2013; Richardson et al., 2013; McQuail et al., 2015; Porges et al., 2017). In the hippocampus, reduced GABAergic signaling and aberrant excitability are observed during aging. For example, electrophysiological studies demonstrate a reduced frequency of spontaneous inhibitory postsynaptic potentials (IPSPs) in granule cells of the aged dentate gyrus (Patrylo et al., 2007). Furthermore, both the amplitude and frequency of $GABA_AR$-mediated currents, as well as the amplitude and duration of the slow $GABA_BR$-mediated IPSP, are attenuated in aged CA1 pyramidal neurons (Potier et al., 1992, 2006). Likewise, age-related alterations in GABAergic signaling occur in aged prefrontal cortex (PFC) (Bañuelos et al., 2014; Bories et al., 2013; Luebke et al., 2004). Medial prefrontal cortex (mPFC) in aged rat showed an increased expression of GAD, the enzyme for GABA synthesis, and decreased expression of GAT-1, the GABA transporter, indicating an increase in GABA production and a decrease in clearance of extracellular GABA in the aged PFC (Bañuelos et al., 2014). In addition, inhibitory postsynaptic currents (IPSCs) increase in mPFC of both rats and primates with age, suggesting an increase in inhibitory transmission in aged PFC (Bories et al., 2013; Luebke et al., 2004). Therefore, different brain areas demonstrate different functional changes in associated with aging.

One mechanism that has not been studied in detail in central synapses during aging is the quantal analysis of neurotransmitter release. Studies may be lacking due to difficulty in recording postsynaptic currents from aged neurons and the ability to stimulate minimal synaptic events. Chapters II and III will utilize quantal analysis across aging in a reduced synaptic preparation. Finally, overall synaptic change during aging could be due to an

imbalance of excitation/inhibition balance as mentioned above. The final chapter in this dissertation will study both excitatory and inhibitory synaptic transmission in the basal forebrain across aging using brain slices to determine directly the relationship between excitation and inhibition across basal forebrain aging.

1.2.2 Dysregulation of neuronal calcium homeostasis during aging

The contribution of calcium has been well appreciated in the neuronal functions. Calcium is a major trigger of neurotransmitter release and a conventional diffusible second messenger. Moreover, it is importantly involved in synaptic plasticity as well as neuronal cell death. Given its critical role in the neuronal functions, there is no doubt that calcium concentration is tightly regulated in the neuronal cells, which is called "calcium homeostasis". Ca^{2+} has a very large concentration difference between inside and outside of neurons, from ~1-2 mM Ca^{2+} outside, to ~100 nM Ca^{2+} inside the cell. Therefore, it is important to maintain the low concentration of Ca^{2+} inside the cell for proper cell signaling. Intracellular calcium concentration ($[Ca^{2+}]_i$) can be increased by extracellular calcium influx via channels on the plasma membrane and the calcium release from the intracellular organelles such as endoplasmic reticulum (ER) and mitochondria. Once $[Ca^{2+}]_i$ rises by Ca^{2+} influx, a number of mechanisms including calcium binding proteins (CBP) act immediately to bind Ca^{2+} and regulate the peak of free Ca^{2+} concentration, which is called "rapid buffering". On the other hand, various pumps and exchangers on the plasma membrane and organelles contribute to slower buffering by exporting Ca^{2+} outside of the neuron or store Ca^{2+} ions within the organelles.

Studies have accumulated substantial evidence for alterations in neuronal calcium homeostasis during aging. In hippocampal CA1 pyramidal neurons of aged animals, age-related enhancement of Ca^{2+} influx through voltage-gated Ca^{2+} channels was reported in many studies (Landfield, 1987; Pitler and Landfield, 1990; Thibault et al., 2001; Power et al., 2002), and L-type Ca^{2+} channels are thought to be the major component causing the enhancement (Landfield, 1994; Moyer and Disterhoft, 1994; Thibault et al., 1995; Campbell et al., 1996). Enhancement of Ca^{2+} influx during aging results in spike-mediated Ca^{2+} accumulation, which leads to activation of slow, Ca^{2+}-activated K^+ current-mediated by small conductance calcium-activated potassium (SK) channels. As a result, a slow afterhyperpolarization (sAHP) is increased in neurons from aged animals, leading to less ability for neurons to fire. On the other hand, the expression of NMDA receptors that are the most permeable to Ca^{2+} ions (Garaschuk et al., 1996) is declined with age, specifically in the hippocampus (Kumar and Foster, 2019; Barnes et al., 1997; Eckles-Smith et al., 2000; Zhao et al., 2009), suggesting a possible compensatory mechanism to limit intracellular Ca^{2+} concentrations. However, such a mechanism can exacerbate synaptic dysfunction during aging (Barnes et al., 1996). Moreover, compromised Ca^{2+} buffering is also observed with reduced levels of Ca^{2+}-binding proteins such as calbindin (Iacopino and Christakos, 1990; Mattson et al., 1991; de Jong et al., 1996) and impaired mitochondrial and endoplasmic reticulum Ca^{2+} handling (Mattson et al., 2008; Stutzmann and Mattson, 2011). Alterations in Ca^{2+} regulation and Ca^{2+} dependent physiology during aging contributes to altered synaptic function and neural degeneration and has been thought to account for the age-related

cognitive impairment (Disterhoft et al., 1996; Thibault and Landfield, 1996; Foster and Norris, 1997; Foster, 1999, 2007, 2012; Tombaugh et al., 2005; Murphy et al., 2006; Gant et al., 2015, 2018; Kumar and Foster, 2019; Abu-Omar et al., 2018).

1.2.3 Mitochondrial dysfunction and accumulation of oxidatively damaged molecules during aging

The brain is a high energy-consuming organ which consumes 20% of energy produced by body. Mitochondria are located throughout the cytoplasm of neuronal dendrites and axons, are the main energy source for neurons. Neurons generate ATP which is required for most of neuronal activity including cell survival and death, the regulation of intracellular calcium homeostasis, synaptic plasticity, and neurotransmitter synthesis (Mattson et al., 2008). Although mitochondria provide cellular energy necessary for neuronal survival, it also produces reactive oxygen species (ROS) such as hydrogen peroxide (H_2O_2), superoxide anion (O^{2-}), and hydroxyl radicals (OH^-) which can provoke damage to neurons when exceeds the cellular antioxidant defense system. However, the mitochondrial ROS generated in the normal conditions have critical roles in cell homeostasis and the regulation of cell survival, thus maintaining reduction-oxidation (redox) homeostasis is another critical role of mitochondria (Harman, 1956; Jezek and Hlavata, 2005; Goldstein and Merenyi, 2008; Brown and Borutaite, 2002).

A growing body of evidence has shown how aging impacts mitochondrial functions in neuronal cells in the brain. Mitochondria in axons of aged mice shows an increase in size and these structural alterations correlate with lower ATP levels and increased generation of nitric oxide, protein nitration, and lipid peroxidation. Moreover,

in the same animals, mitochondria-smooth endoplasmic reticulum(sER) interactions are compromised, indicating a dysregulation of Ca^{2+} homeostasis during aging (Stahon et al., 2016). On the other hand, Morozov et al. found mitochondrial fragmentation in prefrontal cortex neurons from aged rhesus macaques (Morozov et al., 2017). More importantly, the aging process is associated with an increase in brain oxidative stress, and it has been observed that the mitochondrial regulation of redox homeostasis in the brain is impaired during aging. For example, in senescence-accelerated mice, the activities of antioxidants molecules such as superoxide dismutase (SOD) and the glutathione (GSH) were reduced, indicating deficits in the brain antioxidant system. In line with these findings, an increased oxidative damage to mitochondrial DNA (mtDNA) was observed (Kim and Chan, 2001; Santos et al., 2013). The opening of the mitochondrial permeability transition pore (mPTP) which can lead to apoptosis via membrane depolarization and uncoupling of the oxidative phosphorylation (OXPHOS), is also involved in the aging process (Toman and Fiskum, 2011). Mitochondrial Ca^{2+} accumulation or increased oxidative stress can stimulate mPTP to open, and during aging, a reduced threshold Ca^{2+} concentration to induce mPTP opening is observed in rat mitochondria (Krestinina et al., 2015).

Excessive production of ROS with age-related mitochondrial dysfunction disrupts the redox homeostasis, resulting in oxidative stress and ROS-mediated damage to important molecules such as DNA and proteins. In the human brain, oxidative damage to specific gene promoters which plays central roles in synaptic plasticity results in gene silencing (Lu et al., 2004). In addition to damaged gene expression, increased levels of

irreversible protein modification such as protein carbonylation and nitration are observed in the olfactory bulb of aged mice in which loss of olfaction is a common feature of aging (Vaishnav et al., 2007). In line, accumulation of the lipid peroxidation product 4-hydroxynonenal (HNE) is associated with amyloid deposits in the brains of old dogs (Papaioannou et al., 2001).

As mentioned above, neurons are equipped with antioxidants system which neutralize or remove ROS, including SOD, GSH, and catalase (CAT) (Sena and Chandel, 2012; Circu and Aw, 2010). Oxidatively modified molecules can also be removed by proteasomal degradation or by the process of autophagy (Nixon, 2013). However, in the aged brain, antioxidant defense machineries as well as the function of proteasomes and lysosomes are diminished, which can accelerate aging (Melov et al., 1998; Paul et al., 2007; Keller et al., 2002; Butler and Bahr, 2006; Zhang et al., 2017).

1.2.4 Impaired ubiquitin-proteasome and autophagy-lysosome system during aging

Neurons are fully differentiated non-dividing cells which need to preserve their structural and functional stability during the entire lifetime, and hence the function of proteasomes and lysosomes are particularly important for neurons. The ubiquitin-proteasome system is a major proteolytic system in neuronal cells. It regulates concentration of many regulatory proteins in various biological processes as well as terminates damaged proteins. Once a protein is tagged with ubiquitins, it is degraded by the proteasome (Finely, 2009). Similarly, autophagy is an intracellular catabolic process which degrades cytoplasmic materials and organelles. It is activated under metabolic stress, including nutrient deprivation, DNA damage, hypoxia or oxidative and

endoplasmic reticulum (ER) stress, to support energy balance by degrading many cellular components (Egan et al., 2011; Rubinsztein et al., 2011). In addition to stress response, autophagy contributes to housekeeping function and quality-control by preventing or removing aggregated proteins (Nixon, 2013). Lysosomes are single-membrane vesicles that contains acid hydrolases, such as proteases, glycosidases, and lipases, for autophagic degradation system.

The ability to maintain a functional ubiquitin-proteasome or autophagy-lysosome system, declines during aging. The reduced autophagy function shortens lifespan and induces neurodegeneration (Simonsen et al., 2008; Juhász et al., 2007; Hara et al., 2006; Komatsu et al., 2006). In Huntington's disease (HD), the age-related decrease in the expression of beclin 1, a gene essential for autophagy leads to a reduction of autophagic activity during aging, which results in the intracellular accumulation of mutant huntingtin protein (Shibata et al., 2006). In addition, aging reduces the function of proton pump, vacuolar ATPase on the membrane of lysosomes, resulting in the pH dysregulation of lysosomes in which hydrolases is most active at the acidic pH of the lysosomal lumen (Colacurcio and Nixon, 2016). Similar to autophagy-lysosome system, ubiquitin-proteasome dysfunction also occurs during aging (Graham and Liu, 2017). In neurodegenerative disorders such as AD, HD, and Parkinson's disease (PD), abnormal amounts of ubiquitin and the accumulation of ubiquitylated protein aggregates are observed, suggesting an impairment of ubiquitin-proteasome activity (Tanaka and Matsuda, 2014; Nixon, 2013; Matsuda and Tanaka, 2010). Furthermore, decreased

proteasomal activity enhances the neurodegenerative phenotype (Nixon, 2013; Saez and Vilchez, 2014).

1.2.5 Impaired DNA repair during aging

DNA damages continue to happen by both exogenous (radiation, chemicals, and diet) and endogenous (depurination, spontaneous DNA replication errors, and ROS) sources. In healthy young cells, damaged DNA is rapidly repaired in DNA repair pathways that include base excision repair, nucleotide excision repair, mismatch repair, and double-strand break repair. Base excision repair excises mostly oxidative and alkylation DNA damage, nucleotide excision repair removes bulky, helix-distorting lesions from DNA, mismatch repair reverses replication errors, and double-strand break repair is specific for repairing double strand breaks, mainly by homologous recombination, single-strand annealing, and non-homologous end-joining.

Unrepaired DNA damage can cause genomic instability and accelerate aging mechanisms. In many studies of genetically modified mice with defects in DNA repair, normal aging phenotypes are observed, indicating impaired DNA repair can lead to aging process and premature aging (de Boer et al., 2002; Andressoo et al., 2006; Garinis et al., 2008; Gredilla et al., 2012). The human diseases showing premature aging such as Werner syndrome (WS), Cockayne syndrome (CS), and ataxia telangiectasia are caused by mutations in proteins involved in DNA repair and patients with those syndromes shows accelerated brain aging. For example, Werner syndrome patients whose *WRN* (Werner protein) is mutated, exhibit AD-like neuropathology and cognitive deficits (Leverenz et al., 1998; Rekik et al., 2017). The *CSB* (Cockayne syndrome

complementation group B) mutation in Cockayne patients is characterized with degeneration of cerebellar Purkinje cells and cochlear and retinal neurons (Weidenheim et al., 2009). In mice with mutation of *CSB* gene, hearing loss and mitochondrial dysfunction in hippocampal and cortical neurons are observed at an early age (Nagtegaal et al., 2015; Thomsen et al., 2018). In ataxia telangiectasia patients who have *ATM* (Ataxia Telangiectasia) gene deficiency, neuropathological abnormalities in the cerebrum, brain stem and spinal cord have been observed with diffuse degeneration of cerebellar Purkinje cells and granule neurons, which results in impaired control of body movements (Rothblum-Oviatt et al., 2016). Consistently, normal aging also exhibits impaired DNA repair system in the brain. In neuronal cells which are post-mitotic, base excision repair is particularly important, but during aging, the activities of mitochondrial glycosylase which recognize the damaged base are reduced in hippocampus, frontal cortex, brainstem, and cerebellum of old mice compared to young mice (Imam et al., 2006). In addition, the expression of Polβ that integrates a new undamaged base into the DNA strand is decreased in the aging brain (Cabelof et al., 2013).

1.2.6 Inflammation during neurodegenerative disease

The inflammation response is an essential immunological defense system in living organisms, subsequent to trauma or infection, and it is also a common feature of brain aging. Microarray analysis have demonstrated that a gene expression profile suggestive of a marked inflammatory response is upregulated in the aged brain (Prolla, 2002; Godbout et al., 2005). Additionally, the major immune cells for the brain such as microglia are activated with an ameboid morphology and release proinflammatory

cytokines like tumor necrosis factor-α (TNF- α) and interleukins (IL-1β, IL-6) (Sparkman and Johnson, 2008; Campuzano et al., 2009; Cribbs et al., 2012; Norden and Godbout, 2013). The activated microglia in the aged brain exhibit an exaggerated response to infection and stress (Dilger and Johnson, 2008; Henry et al. 2008; Rosczyk et al. 2008; Godbout et al. 2005). In addition to activated microglia and the production of proinflammatory cytokines, the complement system may also be activated during aging (Arumugam et al., 2007; Shi et al., 2015; Hong et al., 2016). The complement system is a major part of the immune system that promotes both innate and acquired immune system. However, it has been known that complement system can be recruited and activated by antibodies generated by the adaptive immune system. Activation of the complement system involves the sequential cleavage of proteins and results in stimulation of phagocytes to clear foreign and damaged material. Although liver is the primary source of complement synthesis, brain is also capable of synthesizing complement proteins in microglia, astrocytes, and neurons. In AD brain, complement components which is highly colocalized with amyloid plaques and neurofibrillary tangles are observed (Shen et al., 2001). In line, biochemical assays have revealed that Aβ and aggregated tau can activate the complement pathways in an antibody-independent fashion (Shen et al., 2001; Salminen et al., 2009; Bradt et al., 1998; Jiang et al., 1994). Furthermore, the activation of Toll-like receptors (TLRs) which plays a critical role in innate immune response by recognizing pathogen-derived molecules can be the one of causal effects of neuroinflammation during aging (Okun et al., 2011). It has been shown that TLRs are upregulated in brains of neurodegenerative diseases such

as AD (Liu et al., 2005), PD and amyotrophic lateral sclerosis (ALS) (van Noort and Bsibsi, 2009; De Paola et al., 2012; Lee et al., 2015). Likely TLR4-dependent activation of microglia which can induce neuroinflammatory process is observed in neurodegenerative diseases such as AD and PD (Heneka et al., 2005; Song et al., 2011).

1.3 Caloric restriction during aging

Caloric restriction (CR) is the most potent intervention to slow the rate of aging and to prevent or ameliorate the age-related diseases such as cardiovascular disease, hypertension, cancer, and cognitive impairment (Sohal and Weindruch, 1996; Redman and Ravussin, 2011; Most et al., 2016). The therapeutic potentials of CR have been substantially demonstrated in human as well as animal model of aging and neurological diseases (Mattson, 2012). Although the mechanisms of beneficial CR effect are complex and not fully understood, it has been extensively studied in attempts to explain its mechanisms underlying neuroprotective properties. Recent studies suggested that caloric restriction activates numerous adaptive cellular stress response pathways that mediate hormesis. CR attenuates oxidative stress by upregulating the plasma membrane redox system which contributes to the regulation of the cellular redox homeostasis through the maintenance of $NAD(P)^+$/NAD(P)H ratios (Hyun et al., 2006; Merker et al., 2002) as well as increasing antioxidant enzymes such as SOD, GSH and glutathione peroxidase activity (Gong et al., 1997; Sreekumar et al., 2002; Agarwal et al., 2005; Rankin et al., 2006). Likewise, the production of ROS in the mitochondria is decreased in response to CR (Merry, 2002; Gredilla and Barja, 2005). Moreover, CR delays age-related oxidative damage to DNA, proteins, and lipids (Merry, 2004; Hunt et al., 2006).

Sirtuins are a large and diverse family of enzymes that regulate gene expression and are necessary to reduce oxidative stress. It has been demonstrated that downregulation of SIRT3, a mitochondria deacetylase causes the mitochondria dysfunction, resulting in senescence (Wiley et al., 2016). During CR, SIRT3 expression is upregulated, which, in turn, deacetylates and activates mitochondrial isocitrate dehydrogenase 2 (Idh2), resulting in increased NADPH levels and an increased ratio of reduced to oxidized glutathione in mitochondria, indicating that CR may protect mitochondria by the action of SIRT3 (Someya et al., 2010). However, in mice lacking SIRT3, the preventative effect of CR on age-related hearing loss which is a common age-related disorder associated with oxidative stress is diminished. Similarly, CR increases the expression of SIRT2, a class III histone deacetylase of which increased activity extends lifespan, but it cannot extend lifespans in SIR2 knockouts (Kaeberlein et al., 1999; Lin et al., 2000, 2004).

The abnormal accumulation of misfolded self-aggregating proteins is a feature of aging and neurodegenerative disorders such as AD and PD as mentioned above in section 1.2.4. Chaperones are highly conserved and ubiquitous proteins that prevent misfolding and aggregation of polypeptides. They include several families of heat shock proteins (HSP) and glucose-regulated proteins (GRP). A study demonstrated that intermittent fasting, a type of CR, increases the cytosolic protein chaperone HSP-70 and the endoplasmic reticulum chaperone GRP-78 in the cerebral cortex and striatum of rats and mice when compared to ad libitum control animals (Arumugam et al., 2010). CR can

also upregulate the function of autophagy, which can remove damaged proteins, membranes, and organelles (Alirezaei et al., 2010).

Inflammation has been demonstrated to be linked with aging and various neurological disorders (Chung et al., 2002; Sarkar and Fisher, 2006). The nuclear factor NFkB pathway has long been believed to be a proinflammatory signaling pathway since NFkB is activated by reactive oxygen species or amyloid Aβ, which in turn induces increased transcription of various cytokines such as interleukins (IL1β, IL2, IL4, IL6) and tumor necrosis factors (TNFα and TNFβ) in various tissues, including the brain (Gloire et al., 2006; Valerio et al., 2006). However, it is demonstrated that CR reduces NFkB levels and blocks the synthesis of interleukins and TNFα (Spaulding et al., 1997; Bhattacharya et al., 2006; Ugochukwu and Figgers, 2007).

Lastly, it is suggested that neurogenesis is also enhanced with CR by upregulating the expression of neurotrophic factors such as brain derived neurotrophic factor (BDNF), insulin-like growth factor 1 (IGF-1), and vascular endothelial cell growth factor (VEGF) (Lee et al., 2002; Cheng et al., 2003; Joseph D'Ercole and Ye, 2008).

1.3.1 Caloric restriction and cognitive function

Caloric dietary intake is a key factor for successful cognitive aging. Overeating and obesity are related to increased risks for the development of late-life cognitive impairment and Alzheimer's disease (Willeumier et al., 2011; Gunstad et al., 2010; Luchsinger et al., 2007; Toro et al., 2009). In the study in which a total of 36 healthy adults (16 men and 20 women) were recruited, an elevated body mass index (BMI) is

related to decreased cerebral blood flow in the prefrontal cortex, indicating that elevated BMI may be a risk factor for decreased prefrontal cortex function and potentially impaired executive function (Willeumier et al., 2011). It is also demonstrated that multiple obesity indices (i.e., BMI, waist circumferences, and waist to hip ratio) were associated with poorer performance in a variety of cognitive domains, including global screening measures, memory, and verbal fluency tasks (Gunstad et al., 2010). Individuals who are overweight in midlife are at increased risk for AD (Fitzpatrick et al., 2009; Hassing et al., 2009; Dahl et al., 2013). Excess body fat has been associated with impaired glucose metabolism and insulin resistance, and in the population with a high prevalence of diabetes, there are significant higher risk of amnestic mild cognitive impairment (MCI) (Luchsinger et al., 2007). The vulnerability to AD is also more increased particularly with insulin resistance (de la Monte, 2009) and diabetes (Profenno et al., 2010). Individuals carrying the rs9939609 A allele of the fat mass and obesity-associated (FTO) gene are genetically susceptible to developing obesity (Dina et al., 2007), and elderly FTO A allele carriers showed a reduced volume in the frontal lobe (Ho et al., 2010) as well as increased risk for incident Alzheimer disease (Keller et al., 2011). Moreover, obese but not normal weight FTO rs9939609 A allele carriers at the age of 82 years showed poor performance on verbal fluency even without the clinically apparent cognitive impairment, suggesting that the FTO gene primarily affects frontal lobe-dependent cognitive process (retrieval of verbal memory) in elderly men (Benedict et al., 2011).

On the other hand, dietary caloric restriction can alleviate age-related cognitive decline (Witte et al., 2009; Mattson, 2012, Mattson and Arumugam, 2018). Considerable evidence from animal models supports the beneficial effects of calorie restriction (CR). Rats maintained for several months on intermittent fasting (IF) exhibited increased resistance to excitotoxin-induced memory impairment and this was correlated with reduced vulnerability of hippocampal CA3 neurons to degeneration (Bruce-Keller et al., 1999). CR also prevented age-related deficits in LTP and NMDA and AMPA glutamate receptor levels in the rat hippocampus (Eckles-Smith et al., 2000; Shi et al., 2007). Moreover, CR can reduce the accumulation of Aβ in the brains of amyloid precursor protein (APP) mutant transgenic mice and old monkeys (Patel et al., 2005; Wang et al., 2005). In the study which compared the effect of CR and IF, both CR and IF diets ameliorated the cognitive deficit in the 3 X TgAD mice. Interestingly, however, the IF diet did not decrease the amyloid or tau pathologies although CR diet reduced the levels of amyloid β-peptide and hyperphosphorylated tau in their hippocampus compared to 3 X TgAD mice on the *ad libitum* diet. It is speculated that IF diet preserves synaptic function by activating adaptive cellular stress response pathway even in the presence of considerable amyloid and tau pathology (Halagappa et al., 2007). In rat basal forebrain (BF), life-long CR prevented age-related increase of rapid calcium buffering which is associated with altered spontaneous synaptic transmission and cognitive impairment (Murchison and Griffith, 2007; Murchison et al., 2009; Griffith et al., 2014). Furthermore, studies have shown that even late onset, short-term regimens produce changes seen in long-term CR animals. For example, Cao and colleagues (2001)

reported that 4-week short-term CR reproduced 64% and 77% of the effects of long-term CR on the expression of genes that were increased during aging and on the gene expression that were downregulated during aging of control mice, respectively. In addition, late onset, short-term (3 months) IF can reverse changes in expression of neuronal plasticity markers, the neural cell adhesion molecule (NCAM) and polysialylated form of neural cell adhesion molecule (PSA-NCAM) which are gradually downregulated with age. The expression of astrocytic marker glial fibrillary acidic protein (GFAP) which is progressively increased during aging can also be reversed. NCAM and PSA-NCAM expression are known to mediate cell interactions to enhance synaptic plasticity, learning and memory functions and neuro-regeneration (Kaur et al., 2008).

1.4 Amitriptyline

Amitriptyline is a traditional tricyclic antidepressant which is named after its chemical structure of three rings of atoms. It was discovered in 1960 and approved by the US Food and Drug Administration (FDA) in 1961. Although it has been increasingly replaced by other antidepressants with less side effect and better safety profile, including selective serotonin reuptake inhibitor (SSRI), selective norepinephrine reuptake inhibitor (SNRI), and monoamine oxidase inhibitor (MAOI) due to its toxicity in overdose, it is still considered to be highly effective and used as a second-line treatment for depressive disorders as well as other neurological disorders such as anxiety, neuropathic pain disorders and migraine (Baldessarini, 2006; Couch et al., 2011; Moore et al., 2015). Because of its diverse therapeutic applications, AMI continues to be used throughout life

span, and overall antidepressant use among patients over 65 years of age has more than tripled from 1995 to 2005 (National Center for Health Statistics, 2007).

1.5 Basal forebrain

The basal forebrain (BF) was chosen for this dissertation because of the importance of this brain are in age-related diseases and neurodegeneration. The BF which is located close to the medial and ventral surfaces of the cerebral hemispheres develops from the subpallium, and consists of the medial septum, vertical and horizontal limbs of the diagonal band, pallidal regions (ventral pallidum and globus pallidus) and the substantia innominate/extended amygdala (Zaborszky et al., 2012, 2015). This brain regions plays an important role in attention, sleep-wake control, memory, and neuropsychiatric disorders such as Alzheimer's disease, Parkinson's disease, schizophrenia, and drug abuse. However, because the BF contains a heterogenous and complex set of cell types based upon transmitter content, morphology, and projection pattern, such as cholinergic, GABAergic, glutamatergic, various calcium binding protein (CBP, calbindin, calretinin, and parvalbumin) containing neurons and peptidergic (neuropeptide Y (NPY), somatostatin, and galanin) projection and interneurons, understanding the BF functional role is difficult (Zaborszky et al., 2012, 2015).

1.5.1 The various cell types in the basal forebrain

1.5.1.1 Cholinergic neurons

The major cell type in the BF is cholinergic neurons located in the medial septum, the vertical and horizontal limbs of the diagonal band and in the substantia innominata/nucleus basalis (Mesulam et al., 1983b; Zaborszky et al., 2012, 2015). The

estimated number of cholinergic neurons in the nucleus basalis is approximately 6,632 ± 1,105 in C57BL/6J non-transgenic mice (Perez et al., 2007). In rats, the number of cholinergic neurons in the medial septum/vertical diagonal band nucleus (MS/VDB) was reported to be 9,647 ± 504, with 26,390 ± 1097 cholinergic neurons found in the entire basal forebrain (Miettinen et al., 2002). Most cholinergic cells are large and multipolar with extensive dendritic fields (Záborszky et al., 1986; Walker et al., 1989). Cholinergic neurons in the BF provide the major source of acetylcholine (ACh) to various brain areas throughout the brain. The synthesis and release of ACh requires the expression of three genes: choline acetyltransferase (ChAT), the vesicular acetylcholine transporter (VAChT) and the choline transport 1, while cholinesterases (AChE) degrades ACh. Among seven different forms of ChAT mRNAs, basal forebrain cholinergic neurons mostly express the R1 and R2 types. The differentiation of cholinergic neurons is regulated by the neurotrophin nerve growth factor (NGF) via TrkA and $p75^{NTR}$ which are high and low affinity receptors, respectively (Fagan et al., 1997; Yuen et al., 1996). BF cholinergic neurons express various types of receptors such as adrenergic, glutamatergic, GABAergic (De Souza Silva et al., 2006; Kiss et al., 1993; Zaborszky et al., 2004), receptors for estrogen (Miettinen et al., 2002) and endocannabinoids (Harkany et al., 2003). When it comes to the electrophysiological properties, cholinergic neurons in BF have low threshold calcium spikes, generating a rhythmic firing pattern. Moreover, cholinergic neurons in the medial septum/diagonal band of Broca neurons (MS/DB) are slow-firing neurons (Duque et al., 2000; Simon et al., 2006). Slow firing neurons are characterized by slow firing rates and pronounced slow afterhyperpolarization (sAHP) produced by a

calcium-activated potassium current (Griffith, 1988; Griffith et al., 2000). In addition, these neurons display fast inward rectification at hyperpolarized membrane potentials. In head-fixed rats, cholinergic neurons of the basal forebrain show the highest firing rate during the wake state as compared to slow-wave sleep or rapid eye movement (REM) sleep (Hassani et al., 2009). Furthermore, a recent study demonstrated that basal forebrain cholinergic neurons can be differentiated into two electrophysiologically different subtypes: early and late firing neurons. Early firing neurons, which comprise 70% of basal forebrain cholinergic neurons, are more excitable when compared to the late firing neurons, and they are completely silenced after initial action potentials. Also, they have a higher density of low voltage activated (LVA) calcium currents. Late firing neurons, which are 30% of basal forebrain cholinergic neurons, are less excitable, but they maintain a tonic discharge at low frequencies (Unal, 2015).

1.5.1.2 GABAergic neurons

GABAergic neurons are also identified in the rat BF, and they outnumber cholinergic neurons: approximately 39,000 – 119,000 GAD^+ cells (Gritti et al., 1993, 2006). Most GABAergic neurons are smaller than cholinergic neurons even though some of them are large and medium-sized cells, suggesting that many GABAergic neurons may play a role as interneurons and send inhibitory signals locally to cholinergic, GABAergic or glutamatergic neurons in the BF. Medium- to large GABAergic neurons, which resemble cholinergic neurons, may also represent inhibitory signal but outside of the BF (i.e., cortex, hippocampus, or hypothalamus) as projecting neurons (Gritti et al.,1994, 1997, 2003; Henderson et al., 2010). GABAergic neurons are divided into subgroups

based on the co-expression of CBPs. From dual immunostaining for the CBPs and glutamic acid decarboxylase (GAD) in the rat BF, it turns out that most of the parvalbumin group (~90%) is colocalized with GAD, and many of septohippocampal GABAergic neurons express parvalbumin. Only a small portion (10%) of the calbindin or calretinin is GAD (Gritti et al., 2003). Furthermore, it has been reported that a small percentage of cholinergic neurons coexpress GAD (Brashear et al., 1986; Sotty et al., 2003).

1.5.1.3 CBPs-containing neurons

CBPs such as parvalbumin, calretinin, calbindin and secretagogin are valuable markers for classifying the neuronal cell types in the brain, and they can act as Ca^{2+} sensors or buffers, modulating neurotransmitter release and intracellular signaling pathways. As mentioned above, in the rat BF, abundant parvalbumin neurons are coexpressed with GAD and project to the cerebral cortex and hippocampus (Celio et al., 1990; Gritti et al., 1993, 2003; Zaborszky et al., 1999; Henderson et al., 2010). Most of cholinergic neurons in the primate BF express calbindin-D-28, a vitamin D-dependent calbindin. In aged individuals or Alzheimer's disease patients, there are not only substantial loss of cholinergic neurons but also a dramatic loss of calbindin in the remaining cholinergic neurons (Geula et al., 2003). On the other hand, it is reported that the rat BF cholinergic neurons have no calbindin immunoreactivity (Celio and Norman, 1985; Chang and Kuo, 1991; Smith et al., 1994). The rat BF calbindin and calretinin cells which are non-cholinergic neurons but need to be determined for the type of neurotransmitters project to the cortex (Zaborszky et al., 1999). Lastly, secretagogin+ cells were found in the interstitial nucleus of the posterior limb of the anterior commissure, in the ventral pallidum, horizontal limb of the

diagonal band nucleus and the dorsal part of the substantia innominate/extended amygdala (SI/EA), and they are colocalized with ChAT+ neurons both in the primate (Mulder et al., 2009) and the mouse basal forebrain (Gyengesi et al., 2013).

1.5.1.4 Glutamatergic neurons

In the rat BF, approximately 5-30% of neurons are believed to be glutamatergic excitatory neurons which contain, one of vesicular glutamate transporters (Vgluts 1-3) (Gritti et al., 2003; Hur and Zaborszky, 2005). In the rat BF, a small percentage of these Vglut2-containing glutamatergic neurons project to the prefrontal and somatosensory cortices (Hur and Zaborszky, 2005). In the medial septum diagonal band complex (MS/DB) of mouse BF, Vglut2-positive neurons project to the hippocampus (Henderson et al., 2010). Some of Vglut2-positive neurons exert local excitatory influence in the MS/DB of rat BF (Hajszan et al., 2004). For example, the presence of glutamate receptors such metabotropic, AMPA, and NMDA receptors in the BF indicates that BF neurons receive inputs directly from glutamate neurons (Petralia and Wenthold, 1992; Kiss et al., 1993; Martin et al., 1993; Page and Everitt, 1995; Standaert et al., 1996; De Souza Silva et al., 2006). In accordance, the ACh release in the cortex is significantly increased with the administration of glutamate agonists kainic acid and NMDA into the BF (Fadel et al., 2001; Fournier et al., 2004). However, the specific glutamate receptor subtypes expressed by cholinergic and non-cholinergic neurons have yet to be fully characterized.

1.5.1.5 Neuropeptide-containing neurons

1.5.1.5.1 Neuropeptide-Y

Neuropeptide-Y (NPY)-immunoreactivity is identified in the BF. NPY is colocalized with GABA (Aoki and Pickel, 1989) and/or somatostatin (Köhler et al. 1987) in many forebrain neurons. NPY axons have been shown to synapse with cholinergic neurons in the BF (Zaborszky and Duque, 2000) even though the origin of NPY synapses on cholinergic neurons is hard to be determined due to lots of NPY expression in the brainstem ascending projection neurons to BF cholinergic neurons (Zaborszky and Cullinan, 1996; Hajszán and Zaborszky, 2002). NPY neurons has the opposite patterns of cell firing of cholinergic neurons when studied with cortical electroencephalogram (EEG) (Duque et al., 2000). In addition, NPY injection into the BF induces changes in cortical EEG in both anesthetized and freely moving rats (Tóth et al., 2005; 2007). Given that NPY neurons are colocalized with GABA in the forebrain, NPY neurons may affect cortical EEG by inhibiting the cholinergic corticopetal neurons as interneurons in the BF. On the other hands, there are specific receptors that NPY binds to, including Y1, Y2, Y4 and Y5, and in the mouse BF, Y2 receptor-positive neurons were found (Stanić et al., 2006). Moreover, Y1 receptor-mediated inhibition of NPY on cholinergic neurons was demonstrated by in vitro electrophysiological study (Záborszky et al., 2009).

1.5.1.5.2 Somatostatin

Somatostatin, a 14- or 28-amino acid-containing neuropeptide, has been identified in synapses on cholinergic projection neurons (Zaborszky, 1989), and some portion of somatostatin-positive neurons may be originated locally from the ventral pallidum,

substantia innominate, and around horizontal diagonal band (Zarborszky and Duque, 2000). Somatostatin has been known to inhibit both GABA and glutamate release presynaptically on BF cholinergic neurons (Momiyama and Zaborszky, 2006).

1.5.1.5.3 Galanin

The neuropeptide galanin (GAL)-immunoreactivity which innervates cholinergic neurons in the BF also has been identified (Henderson and Morris, 1997; Mufson et al., 2003). It is demonstrated that GAL inhibits cholinergic signals in the hippocampus and induces cognitive impairment in rodent models (Elvander et al., 2004). In Alzheimer's disease (AD), increased galanin-containing fibers show hyperinnervation of cholinergic neurons in the BF. Similarly, in the transgenic mice with overexpression of GAL, a reduced number of cholinergic neurons in the horizontal limb of the diagonal band and spatial memory impairments were observed, which is similar characteristics to AD. However, the role of GAL in BF cholinergic neurons is still controversial. A study suggested a neuroprotective effect of GAL on BF cholinergic neurons (Counts et al., 2009). In line, it is demonstrated that GAL blocks the cholinergic-induced increase in GABA release and reduces inhibitory input onto cholinergic neurons. This study suggests that the disinhibition of cholinergic neurons by GAL could serve as a compensatory mechanism for the degeneration of BF cholinergic neurons during the progression of AD (Damborsky et al., 2017).

1.5.2 Basal forebrain cholinergic functions in behavior

Basal forebrain cholinergic neurons play a critical role in attention, sleep, wakefulness, and cognitive function. Recent studies demonstrated the role of basal

forebrain cholinergic neurons in the attentional processing. It has been observed that acetylcholine transients are increased in PFC in response to attention task-related cues (Sarter et al., 2016). In addition, optogenetic study has shown that stimulation of cholinergic signals enhances the cue-associated cholinergic transient and improves cue detection, while blocking the ACh transients with optogenetic inhibition of basal forebrain cholinergic neurons results in many failures for the animals to detect cue (Gritton et al., 2016). Furthermore, it is suggested that basal forebrain cholinergic neurons contribute to a decorrelation in sensory cortex. In sensory cortex, a behaviorally relevant cue is detected by increasing signal-to-noise ratio. In other words, the firing rate of task-relevant sensory cortical neurons increases, and the intra-cortical noise decreases, which is called decorrelation and measured as "desynchronization" (Cohen and Maunsell, 2009; Mitchell et al., 2009). Optogenetic stimulation of basal forebrain cholinergic inputs in the primary visual cortex (V1) mediates desynchronization whereas optogenetic inhibition of cholinergic neurons in the basal forebrain causes increased synchronization of cortical neurons. These studies suggest that basal forebrain cholinergic signaling is important in attentional processing in PFC and sensory cortex (Chen et al., 2015; Pinto et al., 2013).

Basal forebrain cholinergic signaling is known to play an important role in the waking state as well as REM sleep by promoting cortical activation. Cholinergic activity and acetylcholine release increase to the highest levels during REM sleep and wakefulness (Vazquez and Baghdoyan, 2001; Lee et al., 2005; Marrosu et al., 1995). In addition, the selectively stimulated cholinergic neurons in the basal forebrain by neurotensin-induced cortical activation decreased slow-wave sleep (SWS), enhanced REM sleep, and increased

quiet waking state (Cape et al., 2000). In contrast, it is demonstrated that the ablation of cholinergic basal forebrain neurons in rats significantly inhibits cortical activation, but it has no effect on sleep and wake (Berntson et al., 2002). In recent studies, optogenetic stimulation of basal forebrain cholinergic neurons has shown to suppress SWS and enhance wakefulness and REM sleep (Han et al., 2014) whereas optogenetic inhibition prolonged SWS but had no effect on the duration of wakefulness or REM sleep (Shi et al., 2015). To summarize, basal forebrain cholinergic neurons may play a major role for controlling SWS, but they jointly modulate wakefulness and REM sleep with other regions or other types of neurons in the brain.

Lastly, cholinergic neurons in the basal forebrain contribute to memory and cognitive functions. It has been known that ACh release in the hippocampus is increased during the various memory tasks and blocking muscarinic acetylcholine receptor (mAChR) signaling in the hippocampus impairs memory (Mitsushima et al., 2013; Roland et al., 2014; Wallenstein and Vago, 2001). In addition, it has been demonstrated that cholinergic signaling through α7 nicotinic acetylcholine receptors (nAChRs) and M1 mAChRs is important for long-term potentiation (LTP) and plasticity in hippocampus (Cheng and Yakel, 2015; Gu et al., 2012; Gu and Yakel, 2011). Moreover, basal forebrain cholinergic signaling is involved in the formation of fear memories and anxiety-like behaviors with the amygdala. Recent work demonstrated that stimulation of cholinergic terminal fields in the amygdala in awake-behaving mice during training in a cued fear-conditioning delayed the extinction of fear memory. In contrast, inhibition of cholinergic signaling during training reduced the acquisition of learned fear behaviors. The underlying

mechanisms shown in their work is that the activation of cholinergic activity increased firing of basolateral amygdala (BLA) principal neurons and glutamatergic synaptic transmission in the BLA as well as induced LTP of cortical-amygdala circuits (Jiang, 2016). Interestingly however, activation of cholinergic signaling in the amygdala displayed a state-dependent inhibitory effect on the principal BLA neurons. When the principal BLA neurons were quiescent, cholinergic neurons projected from basal forebrain induced muscarinic (M1) IPSPs (Unal et al., 2015). In contrast, substantial cholinergic deficits are demonstrated in neurodegenerative disorders such Alzheimer's disease (AD) and Parkinson's disease (PD) (Cantero et al., 2009; Bohnen and Albin, 2011; Mesulam, 2013; Zeighami et al., 2015; Schmitz and Nathan Spreng, 2016). The reduction in basal forebrain volume and degeneration of basal forebrain cholinergic neurons is a reliable marker for AD (Fernández-Cabello et al., 2020), and mild cognitive decline (MCI) shows basal forebrain atrophy (Zhang et al., 2011b; Grothe et al., 2016). Griffith and his colleagues (2014) have demonstrated that the frequency of spontaneous inhibitory postsynaptic currents (sIPSCs) in the rat BF was reduced during aging, and this was seen in cognitively impaired aged animals.

1.6 Optogenetic mouse model of aging and basal forebrain preparation

Optogenetics is the neuromodulation method in which genetic and optic are combined to control individual neuronal activities in living tissue and behaving animals (Deisseroth, 2011). It employs bacterial opsins most of which are fast light-activated channels, pumps, and enzymes like channelrhodopsin (ChRs), halorhodopsin, and archaerhodopsin (Zhang et al., 2011a). The ChRs are retinylidene proteins which are

seven-transmembrane proteins and contain the light-isomerizable chromophore all-*trans*-retinal. The ChR1 and ChR2 are the first identified as a light-gated ion channel in *Chlamydomonas reinhardtii*, a green unicellular alga from temperate freshwater environments (Nagel et al., 2002). The natural ChR2 absorbs blue light with an absorption maximum at 480 nm. When the all-*trans*-retinal complex absorbs a photon, it opens the pore and conduct H^+, Na^+, K^+ and Ca^{2+} by inducing a conformational change from all-*trans* to 13-*cis*-retinal. The light-gated ion pumps have been also found in archaea, which is called halorhodopsin. Similar to ChRs, halorhodopsin contains the essential light-isomerizable vitamin A derivative all-*trans*-retinal. It opens up the ability to silence excitable cells with brief pulses of yellow light by transferring Cl^- ions into the cell. The peak absorbance of the halorhodopsin retinal complex is about 570 nm (Han and Boyden, 2007; Zhang et al., 2007, 2011a). Archaerhodopsins are light-driven H^+ ion transporters which pumps one H^+ ions from the cytosol to the extracellular medium in presence of green-yellow light (peak response spectra at 566 nm), thus driving the hyperpolarization of the cell membrane and inhibiting action potential firing of neurons (Chow et al., 2010).

The optogenetic methods that allows precise temporal manipulation with a great specificity in intact system have emerged as powerful tools for studying neuronal networks and functions, providing a comprehensive understanding of various neurological disorders that were poorly understood before due to the complexity of the neural systems. However, these methods have not been widely used in aging studies and little is known about the functional expression of optogenetic actuators like ChRs,

halorhodopsin, and archaerhodopsin in neurons across aging. In the recent study of our laboratory, it has been demonstrated that expression of the ChR2 in the VGAT-ChR2(H134R)-EYFP transgenic mice is functionally maintained throughout the entire lifespan of the mice (Montgomery et al., resubmission). VGAT is vesicular γ-aminobutyric acid (GABA) transporter which is specifically expressed in GABAergic neurons and glycinergic neurons (Sagné et al., 1997; Gasnier, 2000). In this mouse line, a Bacterial Artificial Chromosome (BAC) transgenic strategy is employed to express ChR2(H134R)-EYFP under the control of VGAT promoter to enable specific functional activation of GABAergic neuronal population (Zhao et al., 2011). Therefore, in this dissertation study, we extend the use of this optogenetic mouse line to study age-related physiological changes in the BF.

The preparations of BF that will be used in this dissertation involve three different types depending on the different experimental preference (Figure 1.1). Once the whole brain is sliced three different sections are produced. The blue area within the slices highlights the BF region. For electrophysiological measurements, BF are prepared either in brain slice or enzyme-free, acutely dissociated neurons. For calcium imaging with standard fura-2 ratiometric microfluorimetry, enzyme-treated, acutely dissociated neurons are prepared. Figure 1.1 illustrates each experimental preparation. More detailed information is in the materials and methods sections for each research chapter.

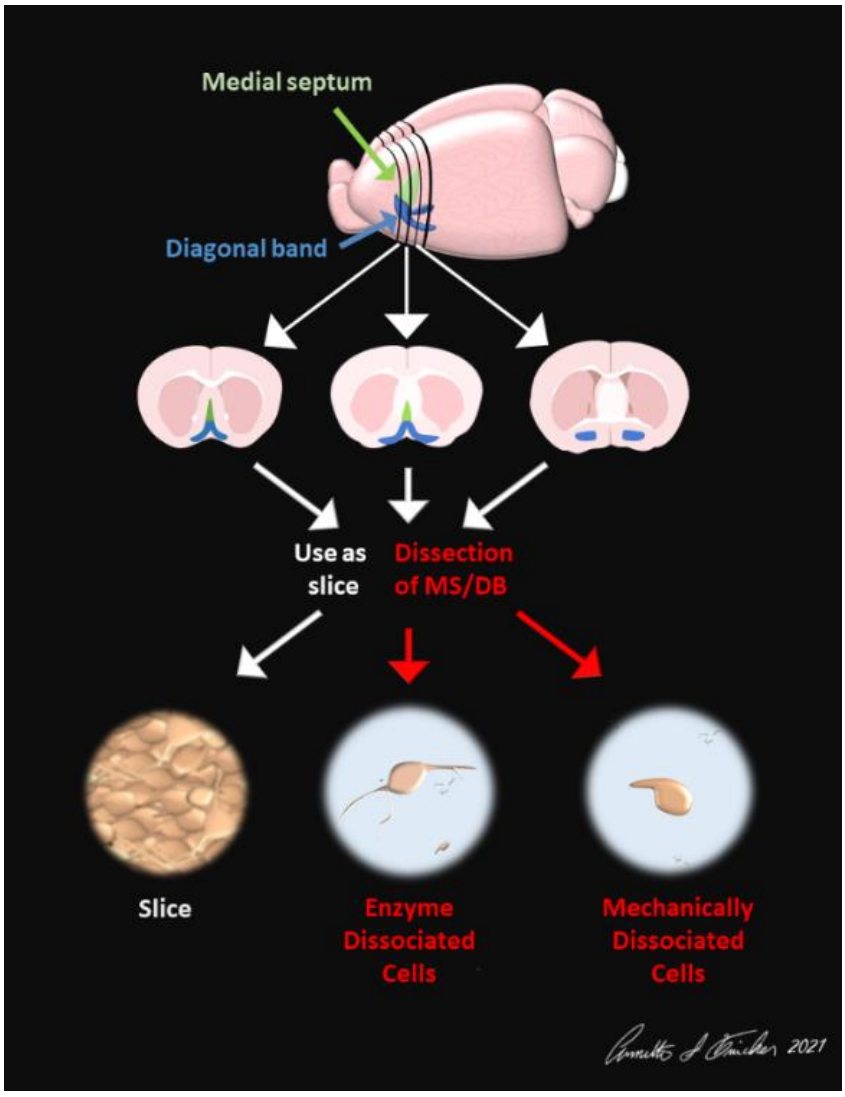

Figure 1.1. Diagram of the mouse basal forebrain preparation.
The brain is quickly removed and placed in a chilled cutting solution (top). After blocking of the brain by trimming the cerebellum and olfactory bulb with a razor blade, the brain is immediately glued on a cutting stage of a tissue slicer and immersed in carbogen-equilibrated (95% O_2/5%CO_2) cutting solution at < 4°C. From rostral to caudal, brain slices containing the BF medial septum and nucleus of the diagonal band (MS/nDB) region are cut using a vibrating tissue slicer. For electrophysiology experiment, either brain slice (left) or enzyme-free, mechanically dissociated neurons (right) were prepared. For calcium imaging, enzyme-treated, acutely dissociated neurons were used (middle).

1.7 References

Abu-Omar, N., Das, J., Szeto, V., Feng, Z.P. (2018). Neuronal ryanodine receptors in development and aging. *Mol. Neurobiol.* 55, 1183-1192. doi: 10.1007/s12035-016-0375-4.

Agarwal, S., Sharma, S., Agrawal, V., Roy, N. (2005). Caloric restriction augments ROS defense in S. cerevisiae, by a Sir2p independent mechanism. *Free Radic. Res.* 39, 55-62. doi: 10.1080/10715760400022343.

Akhmedov, K., Rizzo, V., Kadakkuzha, B.M., Carter, C.J., Magoski, N.S., Capo, T.R., Puthanveettil, S.V. (2013). Decreased response to acetylcholine during aging of aplysia neuron R15. *PLoS One* 8, e84793. doi: 10.1371/journal.pone.0084793.

Alirezaei, M., Kemball, C.C., Flynn, C.T., Wood, M.R., Whitton, J.L., Kiosses, W.B. (2010). Short-term fasting induces profound neuronal autophagy. *Autophagy* 6, 702-10. doi: 10.4161/auto.6.6.12376.

Andressoo, J.O., Hoeijmakers, J.H., Mitchell, J.R. (2006). Nucleotide excision repair disorders and the balance between cancer and aging. *Cell Cycle* 5, 2886-8. doi: 10.4161/cc.5.24.3565.

Andrews-Hanna, J.R., Snyder, A.Z., Vincent, J.L., Lustig, C., Head, D., Raichle, M.E., Buckner, R.L. (2007). Disruption of large-scale brain systems in advanced aging. *Neuron* 56, 924-35. doi: 10.1016/j.neuron.2007.10.038.

Aoki, C., Pickel, V.M. (1989). Neuropeptide Y in the cerebral cortex and the caudate-

putamen nuclei: ultrastructural basis for interactions with GABAergic and non-GABAergic neurons. *J. Neurosci.* 9, 4333-54. doi: 10.1523/JNEUROSCI.09-12-04333.1989.

Arumugam, T.V., Phillips, T.M., Cheng, A., Morrell, C.M., Mattson, M.P., Wan, R. (2010). Age and energy intake interact to modify cell stress pathways and stroke outcome. *Ann. Neurol.* 67, 41-52. doi: 10.1002/ana.21798.

Arumugam, T.V., Tang, S.C., Lathia, J.D., Cheng, A., Mughal, M.R., Chigurupati, S., Magnus, T., Chan, S.L., Jo, D.G., Ouyang, X., Fairlie, D.P., Granger, D.N., Vortmeyer, A., Basta, M., Mattson, M.P. (2007). Intravenous immunoglobulin (IVIG) protects the brain against experimental stroke by preventing complement-mediated neuronal cell death. *Proc. Natl. Acad. Sci. U S A.* 104, 14104-9. doi: 10.1073/pnas.0700506104.

Baldessarini, R. J. (2006). "Drug therapy of depression and anxiety disorders" in *Goodman & Gilman's. The pharmacological basis of therapeutics, 11th edition (New York, NY: McGraw Hill)*, 429-459.

Bañuelos, C., Beas, B.S., McQuail, J.A., Gilbert, R.J., Frazier, C.J., Setlow, B., Bizon, J.L. (2014). Prefrontal cortical GABAergic dysfunction contributes to age-related working memory impairment. *J. Neurosci.* 34, 3457-66. doi: 10.1523/JNEUROSCI.5192-13.2014.

Barnes, C.A., Rao, G., Shen, J. (1997). Age-related decrease in the N-Methyl-d-AspartateR-mediated excitatory postsynaptic potential in hippocampal region CA1. *Neurobiol. Aging.* 18, 445-52. doi: 10.1016/s0197-4580(97)00044-4.

Barnes, C.A., Rao, G., McNaughton, B.L. (1996). Functional integrity of NMDA-dependent LTP induction mechanisms across the lifespan of F-344 rats. Learn. Mem. 3, 124-37. doi: 10.1101/lm.3.2-3.124.

Benedict, C., Jacobsson, J.A., Rönnemaa, E., Sällman-Almén, M., Brooks, S., Schultes, B., Fredriksson, R., Lannfelt, L., Kilander, L., Schiöth, H.B. (2011). The fat mass and obesity gene is linked to reduced verbal fluency in overweight and obese elderly men. *Neurobiol. Aging.* 32, 1159.e1-5. doi: 10.1016/j.neurobiolaging.2011.02.006.

Berntson, G.G., Shafi, R., Sarter, M. (2002). Specific contributions of the basal forebrain corticopetal cholinergic system to electroencephalographic activity and sleep/waking behaviour. *Eur. J. Neurosci.* 16, 2453-61. doi: 10.1046/j.1460-9568.2002.02310.x.

Bhattacharya, A., Chandrasekar, B., Rahman, M.M., Banu, J., Kang, J.X., Fernandes, G. (2006). Inhibition of inflammatory response in transgenic fat-1 mice on a calorie-restricted diet. *Biochem. Biophys. Res. Commun.* 349, 925-30. doi: 10.1016/j.bbrc.2006.08.093.

Bohnen, N.I., Albin, R.L. (2011). The cholinergic system and Parkinson disease. *Behav. Brain Res.* 221, 564-73. doi: 10.1016/j.bbr.2009.12.048.

Bories, C., Husson, Z., Guitton, M.J., De Koninck, Y. (2013). Differential balance of prefrontal synaptic activity in successful versus unsuccessful cognitive aging. *J. Neurosci.* 33, 1344-56. doi: 10.1523/JNEUROSCI.3258-12.2013.

Bradt, B.M., Kolb, W.P., Cooper, N.R. (1998). Complement-dependent proinflammatory

properties of the Alzheimer's disease beta-peptide. *J. Exp. Med.* 188, 431-438. doi: 10.1084/jem.188.3.431.

Brashear, H.R., Zaborszky, L., Heimer, L. (1986). Distribution of GABAergic and cholinergic neurons in the rat diagonal band. *Neuroscience* 17, 439-51. doi: 10.1016/0306-4522(86)90258-7.

Brown, G.C., Borutaite, V. (2002). Nitric oxide inhibition of mitochondrial respiration and its role in cell death. *Free Radic. Biol. Med.* 33, 1440-50. doi: 10.1016/s0891-5849(02)01112-7.

Bruce-Keller, A.J., Umberger, G., McFall, R., Mattson, M.P. (1999). Food restriction reduces brain damage and improves behavioral outcome following excitotoxic and metabolic insults. *Ann. Neurol.* 45, 8-15.

Butler, D., Bahr, B.A. (2006). Oxidative stress and lysosomes: CNS-related consequences and implications for lysosomal enhancement strategies and induction of autophagy. *Antioxid. Redox. Signal.* 8, 185-96. doi: 10.1089/ars.2006.8.185.

Cabelof, D.C., Yanamadala, S., Raffoul, J.J., Guo, Z., Soofi, A., Heydari, A.R. (2003). Caloric restriction promotes genomic stability by induction of base excision repair and reversal of its age-related decline. *DNA Repair (Amst).* 2, 295-307. doi: 10.1016/s1568-7864(02)00219-7.

Campbell, L.W., Hao, S.Y., Thibault, O., Blalock, E.M., Landfield, P.W. (1996). Aging changes in voltage-gated calcium currents in hippocampal CA1 neurons. *J. Neurosci.* 16, 6286-95. doi: 10.1523/JNEUROSCI.16-19-06286.1996.

Campuzano, O., Castillo-Ruiz, M.M., Acarin, L., Castellano, B., Gonzalez, B. (2009). Increased levels of proinflammatory cytokines in the aged rat brain attenuate injury-induced cytokine response after excitotoxic damage. *J. Neurosci. Res.* 87, 2484–2497

Cantero, J.L., Atienza, M., Lage, C., Zaborszky, L., Vilaplana, E., Lopez-Garcia, S., Pozueta, A., Rodriguez-Rodriguez, E., Blesa, R., Alcolea, D., Lleo, A., Sanchez-Juan, P., Fortea, J; Alzheimer's disease neuroimaging initiative. (2020). Atrophy of basal rorebrain initiates with tau pathology in individuals at risk for Alzheimer's disease. *Cereb. Cortex.* 30, 2083-2098. doi: 10.1093/cercor/bhz224.

Cao, S.X., Dhahbi, J.M., Mote, P.L., Spindler, S.R. (2001). Genomic profiling of short- and long-term caloric restriction effects in the liver of aging mice. *Proc. Natl. Acad. Sci. U S A.* 98, 10630-5. doi: 10.1073/pnas.191313598.

Cape, E.G., Manns, I.D., Alonso, A., Beaudet, A., Jones, B.E. (2000). Neurotensin-induced bursting of cholinergic basal forebrain neurons promotes gamma and theta cortical activity together with waking and paradoxical sleep. *J. Neurosci.* 20, 8452-61. doi: 10.1523/JNEUROSCI.20-22-08452.2000.

Celio, M.R. (1990). Calbindin D-28k and parvalbumin in the rat nervous system. *Neuroscience* 35, 375-475. doi: 10.1016/0306-4522(90)90091-h.

Celio, M.R., Norman, A.W. (1985). Nucleus basalis Meynert neurons contain the vitamin D-induced calcium-binding protein (Calbindin-D 28k). *Anat. Embryol (Berl).* 173, 143-8. doi: 10.1007/BF00316296.

Chang, H.T., Kuo, H. (1991). Calcium-binding protein (calbindin D-28k)

immunoreactive neurons in the basal forebrain of the monkey and the rat: relationship with the cholinergic neurons. *Adv. Exp. Med. Biol.* 295, 119-26. doi: 10.1007/978-1-4757-0145-6_4.

Chen, K.S., Masliah, E., Mallory, M., Gage, F.H. (1995). Synaptic loss in cognitively impaired aged rats is ameliorated by chronic human nerve growth factor infusion. *Neuroscience* 68, 19-27. doi: 10.1016/0306-4522(95)00099-5.

Chen, N., Sugihara, H., Sur, M. (2015). An acetylcholine-activated microcircuit drives temporal dynamics of cortical activity. *Nat. Neurosci.* 18, 892–902. doi: 10.1038/nn.4002.

Cheng, A., Wang, S., Cai, J., Rao, M.S., Mattson, M.P. (2003). Nitric oxide acts in a positive feedback loop with BDNF to regulate neural progenitor cell proliferation and differentiation in the mammalian brain. *Dev. Biol.* 258, 319-333. doi: 10.1016/s0012-1606(03)00120-9.

Cheng, Q., Yakel, J.L. (2015). The effect of α7 nicotinic receptor activation on glutamatergic transmission in the hippocampus. *Biochem. Pharmacol.* 97, 439-444. doi: 10.1016/j.bcp.2015.07.015.

Chow, B.Y., Han, X., Dobry, A.S., Qian, X., Chuong, A.S., Li, M., Henninger, M.A., Belfort, G.M., Lin, Y., Monahan, P.E., Boyden, E.S. (2010). High-performance genetically targetable optical neural silencing by light-driven proton pumps. *Nature* 463, 98-102. doi: 10.1038/nature08652.

Chung, H.Y., Kim, H.J., Kim, K.W., Choi, J.S., Yu, B.P. (2002). Molecular

inflammation hypothesis of aging based on the anti-aging mechanism of calorie restriction. *Microsc. Res. Tech.* 59, 264-272. doi: 10.1002/jemt.10203.

Circu, M.L., Aw, T.Y. (2010). Reactive oxygen species, cellular redox systems, and apoptosis. *Free Radic. Biol. Med.* 48, 749-62. doi: 10.1016/j.freeradbiomed.2009.12.022.

Cohen, M.R., and Maunsell, J.H. (2009). Attention improves performance primarily by reducing interneuronal correlations. *Nat. Neurosci.* 12, 1594-600. doi: 10.1038/nn.2439.

Colacurcio, D.J., Nixon, R.A. (2016). Disorders of lysosomal acidification-The emerging role of v-ATPase in aging and neurodegenerative disease. *Ageing Res. Rev.* 32, 75-88. doi: 10.1016/j.arr.2016.05.004.

Couch, J.R.; Amitriptyline Versus Placebo Study Group. (2011). Amitriptyline in the prophylactic treatment of migraine and chronic daily headache. *Headache* 51, 33-51. doi: 10.1111/j.1526-4610.2010.01800.x.

Counts, S.E., He, B., Che, S., Ginsberg, S.D., Mufson, E.J. (2009). Galanin fiber hyperinnervation preserves neuroprotective gene expression in cholinergic basal forebrain neurons in Alzheimer's disease. *J. Alzheimers Dis.*18, 885-96. doi: 10.3233/JAD-2009-1196.

Cribbs, D.H., Berchtold, N.C., Perreau, V., Coleman, P.D., Rogers, J., Tenner, A.J., Cotman, C.W. (2012). Extensive innate immune gene activation accompanies brain aging, increasing vulnerability to cognitive decline and neurodegeneration: a microarray study. *J. Neuroinflammation* 9, 179. doi: 10.1186/1742-2094-9-179.

Dahl, A.K., Hassing, L.B. (2013). Obesity and cognitive aging. *Epidemiol. Rev.* 35, 22-32. doi: 10.1093/epirev/mxs002.

Damborsky, J.C., Smith, K.G., Jensen, P., Yakel, J.L. (2017). Local cholinergic-GABAergic circuitry within the basal forebrain is modulated by galanin. *Brain Struct. Funct.* 222, 1385-1400. doi: 10.1007/s00429-016-1283-0.

de Boer, J., Andressoo, J.O., de Wit, J., Huijmans, J., Beems, R.B., van Steeg, H., Weeda, G., van der Horst, G.T., van Leeuwen, W., Themmen, A.P., Meradji, M., Hoeijmakers, J.H. (2002). Premature aging in mice deficient in DNA repair and transcription. *Science* 296, 1276-9. doi: 10.1126/science.1070174.

de Brabander, J.M., Kramers, R.J., Uylings, H.B. (1998). Layer-specific dendritic regression of pyramidal cells with ageing in the human prefrontal cortex. *Eur. J. Neurosci.* 10, 1261-9. doi: 10.1046/j.1460-9568.1998.00137.x.

de Jong, G.I., Naber, P.A., Van der Zee, E.A., Thompson, L.T., Disterhoft, J.F., Luiten, P.G. (1996). Age-related loss of calcium binding proteins in rabbit hippocampus. *Neurobiol. Aging* 17, 459-65. doi: 10.1016/0197-4580(96)00030-9.

de la Monte, S.M., Longato, L., Tong, M., Wands, J.R. (2009). Insulin resistance and neurodegeneration: roles of obesity, type 2 diabetes mellitus and non-alcoholic steatohepatitis. *Curr. Opin. Investig. Drugs.* 10, 1049-60.

De Paola, M., Mariani, A., Bigini, P., Peviani, M., Ferrara, G., Molteni, M., et al. (2012). Neuroprotective effects of toll-like receptor 4 antagonism in spinal cord cultures and in a mouse model of motor neuron degeneration. *Mol. Med.* 18, 971–981. doi: 10.2119/molmed.2012.00020

Deisseroth, K. (2011). Optogenetics. *Nat. Methods.* 8, 26-9. doi: 10.1038/nmeth.f.324.

De Souza Silva, M.A., Dolga, A., Pieri, I., Marchetti, L., Eisel, U.L., Huston, J.P., Dere, E. (2006). Cholinergic cells in the nucleus basalis of mice express the N-methyl-D-aspartate-receptor subunit NR2C and its replacement by the NR2B subunit enhances frontal and amygdaloid acetylcholine levels. *Genes Brain Behav.* 5, 552-60. doi: 10.1111/j.1601-183X.2006.00206.x.

Dilger, R.N., Johnson, R.W. (2008). Aging, microglial cell priming, and the discordant central inflammatory response to signals from the peripheral immune system. *J. Leukoc. Biol.* 84, 932-9. doi: 10.1189/jlb.0208108.

Dina, C., Meyre, D., Gallina, S., Durand, E., Körner, A., Jacobson, P., Carlsson, L.M., Kiess, W., Vatin, V., Lecoeur, C., Delplanque, J., Vaillant, E., Pattou, F., Ruiz, J., Weill, J., Levy-Marchal, C., Horber, F., Potoczna, N., Hercberg, S., Le Stunff, C., Bougnères, P., Kovacs, P., Marre, M., Balkau, B., Cauchi, S., Chèvre, J.C., Froguel, P. (2007). Variation in FTO contributes to childhood obesity and severe adult obesity. *Nat. Genet.* 39, 724-6. doi: 10.1038/ng2048.

Disterhoft, J.F., Thompson, L.T., Moyer, J.R. Jr., Mogul, D.J. (1996). Calcium-dependent afterhyperpolarization and learning in young and aging hippocampus. *Life Sci.* 59, 413-20. doi: 10.1016/0024-3205(96)00320-7.

Drayer, B.P. (1988). Imaging of the aging brain. Part I. Normal findings. *Radiology* 166, 785-96. doi: 10.1148/radiology.166.3.3277247.

Duan, H., Wearne, S.L., Rocher, A.B., Macedo, A., Morrison, J.H., Hof, P.R. (2003).

Age-related dendritic and spine changes in corticocortically projecting neurons in macaque monkeys. *Cereb. Cortex.* 13, 950-61. doi: 10.1093/cercor/13.9.950.

Dumitriu, D., Hao, J., Hara, Y., Kaufmann, J., Janssen, W.G., Lou, W., Rapp, P.R., Morrison, J.H. (2010). Selective changes in thin spine density and morphology in monkey prefrontal cortex correlate with aging-related cognitive impairment. *J. Neurosci.* 30, 7507-15. doi: 10.1523/JNEUROSCI.6410-09.2010.

Duque, A., Balatoni, B., Detari, L., Zaborszky, L. (2000). EEG correlation of the discharge properties of identified neurons in the basal forebrain. *J. Neurophysiol.* 84, 1627–35. doi: 10.1152/jn.2000.84.3.1627.

Eckles-Smith, K., Clayton, D., Bickford, P., Browning, M.D. (2000). Caloric restriction prevents age-related deficits in LTP and in NMDA receptor expression. *Brain Res. Mol. Brain Res.* 78, 154-62. doi: 10.1016/s0169-328x(00)00088-7.

Egan, D., Kim, J., Shaw, R.J., Guan, K.L. (2011). The autophagy initiating kinase ULK1 is regulated via opposing phosphorylation by AMPK and mTOR. *Autophagy* 7, 643-4. doi: 10.4161/auto.7.6.15123.

Elvander, E., Schött, P.A., Sandin, J., Bjelke, B., Kehr, J., Yoshitake, T., Ogren, S.O. (2004). Intraseptal muscarinic ligands and galanin: influence on hippocampal acetylcholine and cognition. *Neuroscience* 126, 541-57. doi: 10.1016/j.neuroscience.2004.03.058.

Fadel, J., Sarter, M., Bruno, J.P. (2001). Basal forebrain glutamatergic modulation of cortical acetylcholine release. *Synapse* 39, 201-12. doi: 10.1002/1098-2396(20010301)39:3<201::AID-SYN1001>3.0.CO;2-3.

Fagan, A.M., Garber, M., Barbacid, M., Silos-Santiago, I., Holtzman, D.M. (1997). A role for TrkA during maturation of striatal and basal forebrain cholinergic neurons in vivo. *J. Neurosci.* 17, 7644-54. doi: 10.1523/JNEUROSCI.17-20-07644.1997.

Fernández-Cabello, S., Kronbichler, M., Van Dijk, K.R.A., Goodman, J.A., Spreng, R.N., Schmitz, T.W.; Alzheimer's Disease Neuroimaging Initiative. (2020). Basal forebrain volume reliably predicts the cortical spread of Alzheimer's degeneration. *Brain* 143, 993-1009. doi: 10.1093/brain/awaa012.

Fieber, L.A., Carlson, S.L., Capo, T.R., Schmale, M.C. (2010). Changes in D-aspartate ion currents in the Aplysia nervous system with aging. *Brain Res.* 1343, 28-36. doi: 10.1016/j.brainres.2010.05.001.

Finley, D. (2009). Recognition and processing of ubiquitin-protein conjugates by the proteasome. *Annu. Rev. Biochem.* 78, 477-513. doi: 10.1146/annurev.biochem.78.081507.101607.

Fitzpatrick, A.L., Kuller, L.H., Lopez, O.L., Diehr, P., O'Meara, E.S., Longstreth, W.T. Jr., Luchsinger, J.A. (2009). Midlife and late-life obesity and the risk of dementia: cardiovascular health study. *Arch. Neurol.* 66, 336-42. doi: 10.1001/archneurol.2008.582.

Foster, T.C. (1999). Involvement of hippocampal synaptic plasticity in age-related memory decline. *Brain Res. Brain Res. Rev.* 30, 236-49. doi: 10.1016/s0165-0173(99)00017-x.

Foster, T.C. (2007). Calcium homeostasis and modulation of synaptic plasticity in the

aged brain. *Aging Cell* 6, 319-25. doi: 10.1111/j.1474-9726.2007.00283.x.

Foster, T.C. (2012). Dissecting the age-related decline on spatial learning and memory tasks in rodent models: N-methyl-D-aspartate receptors and voltage-dependent Ca2+ channels in senescent synaptic plasticity. *Prog. Neurobiol.* 96, 283-303. doi: 10.1016/j.pneurobio.2012.01.007.

Foster, T.C., Norris, C.M. (1997). Age-associated changes in Ca(2+)-dependent processes: relation to hippocampal synaptic plasticity. *Hippocampus* 7, 602-12. doi: 10.1002/(SICI)1098-1063(1997)7:6<602::AID-HIPO3>3.0.CO;2-G.

Fournier, G.N., Materi, L.M., Semba, K., Rasmusson, D.D. (2004). Cortical acetylcholine release and electroencephalogram activation evoked by ionotropic glutamate receptor agonists in the rat basal forebrain. *Neuroscience* 123, 785-92. doi: 10.1016/j.neuroscience.2003.10.021.

Gant, J.C., Blalock, E.M., Chen, K.C., Kadish, I., Thibault, O., Porter, N.M., Landfield, P.W. (2018). FK506-binding protein 12.6/1b, a negative regulator of [Ca^{2+}], rescues memory and restores genomic regulation in the hippocampus of aging rats. *J. Neurosci.* 38, 1030-1041. doi: 10.1523/JNEUROSCI.2234-17.2017.

Gant, J.C., Chen, K.C., Kadish, I., Blalock, E.M., Thibault, O., Porter, N.M., Landfield, P.W. (2015). Reversal of aging-related neuronal Ca2+ dysregulation and cognitive impairment by delivery of a transgene encoding FK506-binding protein 12.6/1b to the hippocampus. *J. Neurosci.* 35, 10878-87. doi: 10.1523/JNEUROSCI.1248-15.2015.

Garaschuk, O., Schneggenburger, R., Schirra, C., Tempia, F., Konnerth, A. (1996).

Fractional Ca2+ currents through somatic and dendritic glutamate receptor channels of rat hippocampal CA1 pyramidal neurones. *J. Physiol.* 491, 757-72. doi: 10.1113/jphysiol.1996.sp021255.

Garinis, G.A., van der Horst, G.T., Vijg, J., Hoeijmakers, J.H. (2008). DNA damage and ageing: new-age ideas for an age-old problem. *Nat. Cell Biol.* 10, 1241-7. doi: 10.1038/ncb1108-1241.

Gasnier, B. (2000). The loading of neurotransmitters into synaptic vesicles. *Biochimie.* 82, 327–337.

Geula, C., Bu, J., Nagykery, N., Scinto, L.F., Chan, J., Joseph, J., Parker, R., Wu, C.K. (2003). Loss of calbindin-D28k from aging human cholinergic basal forebrain: relation to neuronal loss. *J. Comp. Neurol.* 455, 249-59. doi: 10.1002/cne.10475.

Gloire, G., Legrand-Poels, S., Piette, J. (2006). NF-kappaB activation by reactive oxygen species: fifteen years later. *Biochem Pharmacol.* 72, 1493-505. doi: 10.1016/j.bcp.2006.04.011.

Godbout, J.P., Chen, J., Abraham, J., Richwine, A.F., Berg, B.M., Kelley, K.W., Johnson, R.W. (2005). Exaggerated neuroinflammation and sickness behavior in aged mice following activation of the peripheral innate immune system. *FASEB J.* 19, 1329-31. doi: 10.1096/fj.05-3776fje.

Goldstein, S., Merényi, G. (2008). The chemistry of peroxynitrite: implications for biological activity. *Methods Enzymol.* 436, 49-61. doi: 10.1016/S0076-6879(08)36004-2.

Gong, X., Shang, F., Obin, M., Palmer, H., Scrofano, M.M., Jahngen-Hodge, J., Smith,

D.E., Taylor, A. (1997). Antioxidant enzyme activities in lens, liver and kidney of calorie restricted Emory mice. *Mech. Ageing Dev.* 99, 181-92. doi: 10.1016/s0047-6374(97)00102-4.

Graham, S.H., Liu, H. (2017). Life and death in the trash heap: The ubiquitin proteasome pathway and UCHL1 in brain aging, neurodegenerative disease and cerebral ischemia. *Ageing Res. Rev.* 34, 30-38. doi: 10.1016/j.arr.2016.09.011.

Gredilla, R., Barja, G. (2005). Minireview: the role of oxidative stress in relation to caloric restriction and longevity. *Endocrinology* 146, 3713-3717. doi: 10.1210/en.2005-0378.

Gredilla, R., Garm, C., Stevnsner, T. (2012). Nuclear and mitochondrial DNA repair in selected eukaryotic aging model systems. *Oxid. Med. Cell Longev.* 2012, 282438. doi: 10.1155/2012/282438.

Griffith, W.H. (1988). Membrane properties of cell types within guinea pig basal forebrain nuclei *in vitro*. *J. Neurophysiol.* 59, 1590-612. doi: 10.1152/jn.1988.59.5.1590.

Griffith, W.H., Dubois, D.W., Fincher, A., Peebles, K.A., Bizon, J.L., Murchison, D. (2014). Characterization of age-related changes in synaptic transmission onto F344 rat basal forebrain cholinergic neurons using a reduced synaptic preparation. *J. Neurophysiol.* 111, 273-86. doi: 10.1152/jn.00129.2013.

Griffith, W.H., Jasek, M.C., Bain, S.H., Murchison, D. (2000). Modification of ion channels and calcium homeostasis of basal forebrain neurons during aging. *Behv. Brain Res.* 115, 219-33. doi: 10.1016/s0166-4328(00)00260-6.

Gritti, I., Henny, P., Galloni, F., Mainville, L., Mariotti, M., Jones, B.E. (2006). Stereological estimates of the basal forebrain cell population in the rat, including neurons containing choline acetyltransferase, glutamic acid decarboxylase or phosphate-activated glutaminase and colocalizing vesicular glutamate transporters. *Neuroscience* 143, 1051-64. doi: 10.1016/j.neuroscience.2006.09.024.

Gritti, I., Mainville, L., Jones, B.E. (1993). Codistribution of GABA- with acetylcholine-synthesizing neurons in the basal forebrain of the rat. *J. Comp. Neurol.* 329, 438-57. doi: 10.1002/cne.903290403. PMID: 8454735.

Gritti, I., Mainville, L., Jones, B.E. (1994). Projections of GABAergic and cholinergic basal forebrain and GABAergic preoptic-anterior hypothalamic neurons to the posterior lateral hypothalamus of the rat. *J. Comp. Neurol.* 339, 251-68. doi: 10.1002/cne.903390206.

Gritti, I., Mainville, L., Mancia, M., Jones, B.E. (1997). GABAergic and other noncholinergic basal forebrain neurons, together with cholinergic neurons, project to the mesocortex and isocortex in the rat. *J. Comp. Neurol.* 383, 163-77.

Gritti, I., Manns, I.D., Mainville, L., Jones, B.E. (2003). Parvalbumin, calbindin, or calretinin in cortically projecting and GABAergic, cholinergic, or glutamatergic basal forebrain neurons of the rat. *J. Comp. Neurol.* 458, 11-31. doi: 10.1002/cne.10505.

Gritton, H.J., Howe, W.M., Mallory, C.S., Hetrick, V.L., Berke, J.D., Sarter, M. (2016).

Cortical cholinergic signaling controls the detection of cues. *Proc. Natl. Acad. Sci. U S A.* 113, E1089-97. doi: 10.1073/pnas.1516134113.

Grothe, M.J., Heinsen, H., Amaro, E. Jr., Grinberg, L.T., Teipel, S.J. (2016). Cognitive correlates of basal forebrain atrophy and associated cortical hypometabolism in mild cognitive impairment. *Cereb. Cortex.* 26, 2411-2426. doi: 10.1093/cercor/bhv062.

Gu, Z., Lamb, P.W., Yakel, J.L. (2012). Cholinergic coordination of presynaptic and postsynaptic activity induces timing-dependent hippocampal synaptic plasticity. *J. Neurosci.* 32, 12337-48. doi: 10.1523/JNEUROSCI.2129-12.2012.

Gu, Z., Yakel, J.L. (2011). Timing-dependent septal cholinergic induction of dynamic hippocampal synaptic plasticity. *Neuron* 71, 155-65. doi: 10.1016/j.neuron.2011.04.026.

Gunstad, J., Lhotsky, A., Wendell, C.R., Ferrucci, L., Zonderman, A.B. (2010). Longitudinal examination of obesity and cognitive function: results from the baltimore longitudinal study of aging. *Neuroepidemiology* 34, 222-9. doi: 10.1159/000297742.

Gyengesi, E., Andrews, Z.B., Paxinos, G., Zaborszky, L. (2013). Distribution of secretagogin-containing neurons in the basal forebrain of mice, with special reference to the cholinergic corticopetal system. *Brain Res. Bull.* 94, 1-8. doi: 10.1016/j.brainresbull.2013.01.009.

Hajszan, T., Alreja, M., Leranth, C. (2004). Intrinsic vesicular glutamate transporter 2-

immunoreactive input to septohippocampal parvalbumin-containing neurons: novel glutamatergic local circuit cells. *Hippocampus* 14, 499-509. doi: 10.1002/hipo.10195.

Hajszán, T., Zaborszky, L. (2002). Direct catecholaminergic-cholinergic interactions in the basal forebrain. III. Adrenergic innervation of choline acetyltransferase-containing neurons in the rat. *J. Comp. Neurol.* 449, 141-57. doi: 10.1002/cne.10279.

Halagappa, V.K., Guo, Z., Pearson, M., Matsuoka, Y., Cutler, R.G., Laferla, F.M., Mattson, M.P. (2007). Intermittent fasting and caloric restriction ameliorate age-related behavioral deficits in the triple-transgenic mouse model of Alzheimer's disease. *Neurobiol. Dis.* 26, 212-20. doi: 10.1016/j.nbd.2006.12.019.

Han, X., Boyden, E.S. (2007). Multiple-color optical activation, silencing, and desynchronization of neural activity, with single-spike temporal resolution. *PLoS One* 2, e299. doi: 10.1371/journal.pone.0000299.

Han, Y., Shi, Y.F., Xi, W., Zhou, R., Tan, Z.B., Wang, H., Li, X.M., Chen, Z., Feng, G., Luo, M., Huang, Z.L., Duan, S., Yu, Y.Q. (2014). Selective activation of cholinergic basal forebrain neurons induces immediate sleep-wake transitions. *Curr. Biol.* 24, 693-8. doi: 10.1016/j.cub.2014.02.011.

Hara, T., Nakamura, K., Matsui, M., Yamamoto, A., Nakahara, Y., Suzuki-Migishima, R., Yokoyama, M., Mishima, K., Saito, I., Okano, H., Mizushima, N. (2006). Suppression of basal autophagy in neural cells causes neurodegenerative disease in mice. *Nature* 441, 885-9. doi: 10.1038/nature04724.

Harkany, T., Härtig, W., Berghuis, P., Dobszay, M.B., et al. (2003). Complementary distribution of type 1 cannabinoid receptors and vesicular glutamate transporter 3 in basal forebrain suggests input-specific retrograde signaling by cholinergic neurons. *Eur. J. Neurosci.* 18, 1979–1992. doi: 10.1046/j.1460-9568.2003.02898.x.

Harman, D. (1965). The free radical theory of aging: effect of age on serum copper levels. *J. Gerontol.* 20, 151-3. doi: 10.1093/geronj/20.2.151.

Hassani, O.K., Lee, M.G., Henny, P., Jones, B.E. (2009). Discharge profiles of identified GABAergic in comparision to cholinergic and putative glutamatergic basal forebrain neurons across the sleep-wwake cycle. *J. Neurosci.* 29, 11828–40. doi: 10.1523/JNEUROSCI.1259-09.2009.

Hassing, L.B., Dahl, A.K., Thorvaldsson, V., Berg, S., Gatz, M., Pedersen, N.L., Johansson, B. (2009). Overweight in midlife and risk of dementia: a 40-year follow-up study. *Int. J. Obes. (Lond).* 33, 893-8. doi: 10.1038/ijo.2009.104.

Heise, K.F., Zimerman, M., Hoppe, J., Gerloff, C., Wegscheider, K., Hummel, F.C. (2013). The aging motor system as a model for plastic changes of GABA-mediated intracortical inhibition and their behavioral relevance. *J. Neurosci.* 33, 9039-49. doi: 10.1523/JNEUROSCI.4094-12.2013.

Henderson, Z., Lu, C.B., Janzsó, G., Matto, N., McKinley, C.E., Yanagawa, Y., Halasy, K. (2010). Distribution and role of Kv3.1b in neurons in the medial septum diagonal band complex. *Neuroscience* 166, 952-69. doi: 10.1016/j.neuroscience.2010.01.020.

Henderson, Z., Morris, N. (1997). Galanin-immunoreactive synaptic terminals on basal forebrain cholinergic neurons in the rat. *J. Comp. Neurol.* 383, 82-93. doi: 10.1002/(sici)1096-9861(19970623)383:1<82::aid-cne7>3.0.co;2-h.

Heneka, M.T., Sastre, M., Dumitrescu-Ozimek, L., Dewachter, I., Walter, J., Klockgether, T., Van Leuven, F. (2005). Focal glial activation coincides with increased BACE1 activation and precedes amyloid plaque deposition in APP[V717I] transgenic mice. *J. Neuroinflammation* 2, 22. doi: 10.1186/1742-2094-2-22.

Henry, C.J., Huang, Y., Wynne, A., Hanke, M., Himler, J., Bailey, M.T., Sheridan, J.F., Godbout, J.P. (2008). Minocycline attenuates lipopolysaccharide (LPS)-induced neuroinflammation, sickness behavior, and anhedonia. *J. Neuroinflammation* 5, 15. doi: 10.1186/1742-2094-5-15.

Ho, A.J., Stein, J.L., Hua, X., Lee, S., Hibar, D.P., Leow, A.D., Dinov, I.D., Toga, A.W., Saykin, A.J., Shen, L., Foroud, T., Pankratz, N., Huentelman, M.J., Craig, D.W., Gerber, J.D., Allen, A.N., Corneveaux, J.J., Stephan, D.A., DeCarli, C.S., DeChairo, B.M., Potkin, S.G., Jack, C.R. Jr., Weiner, M.W., Raji, C.A., Lopez, O.L., Becker, J.T., Carmichael, O.T., Thompson, P.M.; Alzheimer's Disease Neuroimaging Initiative. (2010). A commonly carried allele of the obesity-related FTO gene is associated with reduced brain volume in the healthy elderly. *Proc. Natl. Acad. Sci. U S A.* 107, 8404-9. doi: 10.1073/pnas.0910878107.

Hong, S., Beja-Glasser, V.F., Nfonoyim, B.M., Frouin, A., Li, S., Ramakrishnan, S.,

Merry, K.M., Shi, Q., Rosenthal, A., Barres, B.A., Lemere, C.A., Selkoe, D.J., Stevens, B. (2016). Complement and microglia mediate early synapse loss in Alzheimer mouse models. *Science* 352, 712-716. doi: 10.1126/science.aad8373.

Hur, E.E., Zaborszky, L. (2005). Vglut2 afferents to the medial prefrontal and primary somatosensory cortices: a combined retrograde tracing in situ hybridization study [corrected]. *J. Comp. Neurol.* 483, 351-73. doi: 10.1002/cne.20444.

Hurd, M.D., Martorell, P., Langa, K.M. (2013). Monetary costs of dementia in the United States. *N. Engl. J. Med.* 369, 489-90. doi: 10.1056/NEJMc1305541.

Hyun, D.H., Emerson, S.S., Jo, D.G., Mattson, M.P., de Cabo, R. (2006). Calorie restriction up-regulates the plasma membrane redox system in brain cells and suppresses oxidative stress during aging. *Proc. Natl. Acad. Sci. U S A* 103, 19908-12. doi: 10.1073/pnas.0608008103.

Iacopino, A.M., Christakos, S. (1990). Specific reduction of calcium-binding protein (28-kilodalton calbindin-D) gene expression in aging and neurodegenerative diseases. *Proc. Natl. Acad. Sci. U S A* 87, 4078-82. doi: 10.1073/pnas.87.11.4078.

Imam, S.Z., Karahalil, B., Hogue, B.A., Souza-Pinto, N.C., Bohr, V.A. (2006). Mitochondrial and nuclear DNA-repair capacity of various brain regions in mouse is altered in an age-dependent manner. *Neurobiol. Aging.* 27, 1129-36. doi: 10.1016/j.neurobiolaging.2005.06.002.

Jacobs, B., Driscoll, L., Schall, M. (1997). Life-span dendritic and spine changes in

areas 10 and 18 of human cortex: a quantitative Golgi study. *J. Comp. Neurol.* 386, 661-80.

Jezek, P., Hlavatá, L. (2005). Mitochondria in homeostasis of reactive oxygen species in cell, tissues, and organism. *Int. J. Biochem. Cell Biol.* 37, 2478-503. doi: 10.1016/j.biocel.2005.05.013.

Jiang, H., Burdick, D., Glabe, C.G., Cotman, C.W., Tenner, A.J. (1994). beta-Amyloid activates complement by binding to a specific region of the collagen-like domain of the C1q A chain. *J. Immunol.* 152, 5050-9.

Jiang, L., Kundu, S., Lederman, J.D., López-Hernández, G.Y., Ballinger, E.C., Wang, S., Talmage, D.A., Role, L.W. (2016). Cholinergic signaling controls conditioned fear behaviors and enhances plasticity of cortical-amygdala circuits. *Neuron* 90, 1057-70. doi: 10.1016/j.neuron.2016.04.028.

Joseph D'Ercole, A., Ye, P. (2008). Expanding the mind: insulin-like growth factor I and brain development. *Endocrinology* 149, 5958-62. doi: 10.1210/en.2008-0920.

Juhász, G., Erdi, B., Sass, M., Neufeld, T.P. (2007). Atg7-dependent autophagy promotes neuronal health, stress tolerance, and longevity but is dispensable for metamorphosis in Drosophila. *Genes Dev.* 21, 3061-6. doi: 10.1101/gad.1600707.

Kaeberlein, M., McVey, M., Guarente, L. (1999). The SIR2/3/4 complex and SIR2 alone promote longevity in Saccharomyces cerevisiae by two different mechanisms. *Genes Dev.* 13, 2570-80. doi: 10.1101/gad.13.19.2570.

Kaur, M., Sharma, S., Kaur, G. (2008). Age-related impairments in neuronal plasticity

markers and astrocytic GFAP and their reversal by late-onset short term dietary restriction. *Biogerontology* 9, 441-54. doi: 10.1007/s10522-008-9168-0.

Kempsell, A.T., Fieber, L.A. (2014). Behavioral aging is associated with reduced sensory neuron excitability in Aplysia californica. *Front. Aging Neurosci.* 6, 84. doi: 10.3389/fnagi.2014.00084.

Köhler, C., Eriksson, L.G., Davies, S., Chan-Palay, V. (1987). Co-localization of neuropeptide tyrosine and somatostatin immunoreactivity in neurons of individual subfields of the rat hippocampal region. *Neurosci. Lett.* 78, 1-6. doi: 10.1016/0304-3940(87)90551-9.

Kwakowsky, A., Calvo-Flores Guzmán, B., Govindpani, K., Waldvogel, H.J., Faull, R.L. (2018a). Gamma-aminobutyric acid A receptors in Alzheimer's disease: highly localized remodeling of a complex and diverse signaling pathway. *Neural. Regen. Res.* 13, 1362-1363. doi: 10.4103/1673-5374.235240.

Kwakowsky, A., Calvo-Flores Guzmán, B., Pandya, M., Turner, C., Waldvogel, H.J., Faull, R.L. (2018b). $GABA_A$ receptor subunit expression changes in the human Alzheimer's disease hippocampus, subiculum, entorhinal cortex and superior temporal gyrus. *J. Neurochem.* 145, 374-392. doi: 10.1111/jnc.14325.

Keller, J.N., Gee, J., Ding, Q. (2002). The proteasome in brain aging. *Ageing Res. Rev.* 1, 279-93. doi: 10.1016/s1568-1637(01)00006-x.

Keller, L., Xu, W., Wang, H.X., Winblad, B., Fratiglioni, L., Graff, C. (2011). The

obesity related gene, FTO, interacts with APOE, and is associated with Alzheimer's disease risk: a prospective cohort study. *J. Alzheimers. Dis.* 23, 461-9. doi: 10.3233/JAD-2010-101068.

Kim, G.W., Chan, P.H. (2001). Oxidative stress and neuronal DNA fragmentation mediate age-dependent vulnerability to the mitochondrial toxin, 3-nitropropionic acid, in the mouse striatum. *Neurobiol. Dis.* 8, 114-26. doi: 10.1006/nbdi.2000.0327.

Kiss, J., Jane, J.A., Zaborszky, L. (1993). Distribution of neurons containing immunoreactivity for metabotropic-1α glutamate receptors (MGluR-1α) in the rat basal forebrain complex. *Soc. Neurosci. Abstr.*19, 287.

Komatsu, M., Waguri, S., Chiba, T., Murata, S., Iwata, J., Tanida, I., Ueno, T., Koike, M., Uchiyama, Y., Kominami, E., Tanaka, K. (2006). Loss of autophagy in the central nervous system causes neurodegeneration in mice. *Nature* 441, 880-4. doi: 10.1038/nature04723.

Krestinina, O., Azarashvili, T., Baburina, Y., Galvita, A., Grachev, D., Stricker, R., Reiser, G. (2015). In aging, the vulnerability of rat brain mitochondria is enhanced due to reduced level of 2',3'-cyclic nucleotide-3'-phosphodiesterase (CNP) and subsequently increased permeability transition in brain mitochondria in old animals. *Neurochem. Int.* 80, 41-50. doi: 10.1016/j.neuint.2014.09.008.

Kumar, A., and Foster, T.C. (2019). Alteration in NMDA receptor mediated glutama tergic neurotransmission in the hippocampus during senescence. *Neurochem. Res.* 44, 38-48. doi: 10.1007/s11064-018-2634-4.

Landfield, P.W. (1987). 'Increased calcium-current' hypothesis of brain aging. *Neurobiol. Aging* 8, 346-7. doi: 10.1016/0197-4580(87)90074-1.

Landfield, P.W. (1994). Increased hippocampal Ca2+ channel activity in brain aging and dementia. Hormonal and pharmacologic modulation. *Ann. N. Y. Acad. Sci.* 747, 351-64. doi: 10.1111/j.1749-6632.1994.tb44422.x.

Lee, J., Duan, W., Mattson, M.P. (2002). Evidence that brain-derived neurotrophic factor is required for basal neurogenesis and mediates, in part, the enhancement of neurogenesis by dietary restriction in the hippocampus of adult mice. *J. Neurochem.* 82, 1367-75. doi: 10.1046/j.1471-4159.2002.01085.x.

Lee, M.G., Hassani, O.K., Alonso, A., Jones, B.E. (2005). Cholinergic basal forebrain neurons burst with theta during waking and paradoxical sleep. *J. Neurosci.* 25, 4365-9. doi: 10.1523/JNEUROSCI.0178-05.2005.

Lee, J. Y., Lee, J. D., Phipps, S., Noakes, P. G., Woodruff, T. M. (2015). Absence of toll-like receptor 4 (TLR4) extends survival in the hSOD1G93A mouse model of amyotrophic lateral sclerosis. *J. Neuroinflammation* 12, 90. doi: 10.1186/s12974-015-0310-z

Lehmann, K., Steinecke, A., Bolz, J. (2012). GABA through the ages: regulation of cortical function and plasticity by inhibitory interneurons. *Neural. Plast.* 2012, 892784. doi: 10.1155/2012/892784.

Leverenz, J.B., Yu, C.E., Schellenberg, G.D. (1998). Aging-associated neuropathology in Werner syndrome. *Acta. Neuropathol.* 96, 421-4. doi: 10.1007/s004010050914.

Lin, S.J., Defossez, P.A., Guarente, L. (2000). Requirement of NAD and SIR2 for life-span extension by calorie restriction in Saccharomyces cerevisiae. *Science* 289, 2126-2128. doi: 10.1126/science.289.5487.2126.

Lin, S.J., Ford, E., Haigis, M., Liszt, G., Guarente, L. (2004). Calorie restriction extends yeast life span by lowering the level of NADH. *Genes Dev.* 18, 12-6. doi: 10.1101/gad.1164804.

Liu, Y., Walter, S., Stagi, M., Cherny, D., Letiembre, M., Schulz-Schaeffer, W., Heine, H., Penke, B., Neumann, H., Fassbender, K. (2005). LPS receptor (CD14): a receptor for phagocytosis of Alzheimer's amyloid peptide. *Brain* 128, 1778–1789. doi: 10.1093/brain/awh531.

Lu, T., Pan, Y., Kao, S.Y., Li, C., Kohane, I., Chan, J., Yankner, B.A. (2004). Gene regulation and DNA damage in the ageing human brain. *Nature* 429, 883-91. doi: 10.1038/nature02661.

Luchsinger, J.A., Reitz, C., Patel, B., Tang, M.X., Manly, J.J., Mayeux, R. (2007). Relation of diabetes to mild cognitive impairment. *Arch. Neurol.* 64, 570-5. doi: 10.1001/archneur.64.4.570.

Luebke, J.I., Chang, Y.M., Moore, T.L., Rosene, D.L. (2004). Normal aging results in decreased synaptic excitation and increased synaptic inhibition of layer 2/3 pyramidal cells in the monkey prefrontal cortex. *Neuroscience* 125, 277-88. doi: 10.1016/j.neuroscience.2004.01.035.

Marrosu, F., Portas, C., Mascia, M.S., Casu, M.A., Fà, M., Giagheddu, M., Imperato, A.,

Gessa, G.L. (1995). Microdialysis measurement of cortical and hippocampal acetylcholine release during sleep-wake cycle in freely moving cats. *Brain Res.* 671, 329-32. doi: 10.1016/0006-8993(94)01399-3.

Martin, L.J., Blackstone, C.D., Levey, A.I., Huganir, R.L., Price, D.L. (1993). Cellular localizations of AMPA glutamate receptors within the basal forebrain magnocellular complex of rat and monkey. *J. Neurosci.* 13, 2249-63. doi: 10.1523/JNEUROSCI.13-05-02249.1993.

Matsuda, N., and Tanaka, K. (2010). Does impairment of the ubiquitin-proteasome system or the autophagy-lysosome pathway predispose individuals to neurodegenerative disorders such as Parkinson's disease? *J. Alzheimers Dis.* 19, 1–9. doi: 10.3233/JAD-2010-1231.

Mattson, M.P. (2012). Energy intake and exercise as determinants of brain health and vulnerability to injury and disease. *Cell Metab.* 16, 706-22. doi: 10.1016/j.cmet.2012.08.012.

Mattson, M.P., Arumugam, T.V. (2018). Hallmarks of brain aging: adaptive and pathological modification by metabolic states. *Cell Metab.* 27, 1176-1199. doi: 10.1016/j.cmet.2018.05.011.

Mattson, M.P., Gleichmann, M., Cheng, A. (2008). Mitochondria in neuroplasticity and neurological disorders. *Neuron* 60, 748-66. doi: 10.1016/j.neuron.2008.10.010.

Mattson, M.P., Rychlik, B., Chu, C., Christakos, S. (1991). Evidence for calcium-

reducing and excito-protective roles for the calcium-binding protein calbindin-D28k in cultured hippocampal neurons. *Neuron* 6, 41-51. doi: 10.1016/0896-6273(91)90120-o.

McQuail, J.A., Frazier, C.J., Bizon, J.L. (2015). Molecular aspects of age-related cognitive decline: the role of GABA signaling. *Trends. Mol. Med.* 21, 450-60. doi: 10.1016/j.molmed.2015.05.002.

Melov, S., Schneider, J.A., Day, B.J., Hinerfeld, D., Coskun, P., Mirra, S.S., Crapo, J.D., Wallace, D.C. (1998). A novel neurological phenotype in mice lacking mitochondrial manganese superoxide dismutase. *Nat. Genet.* 18, 159-63. doi: 10.1038/ng0298-159.

Merker, M.P., Bongard, R.D., Kettenhofen, N.J., Okamoto, Y., Dawson, C.A. (2002). Intracellular redox status affects transplasma membrane electron transport in pulmonary arterial endothelial cells. *Am. J. Physiol. Lung Cell. Mol. Physiol.* 282, L36–L43. doi: 10.1152/ajplung.00283.2001.

Merry, B.J. (2002). Molecular mechanisms linking calorie restriction and longevity. *Int. J. Biochem. Cell Biol.* 34, 1340-1354. doi: 10.1016/s1357-2725(02)00038-9.

Merry, B.J. (2004). Oxidative stress and mitochondrial function with aging—the effects of calorie restriction. *Aging Cell* 3, 7-12. doi: 10.1046/j.1474-9728.2003.00074.x.

Mesulam, M.M. (2013). Cholinergic circuitry of the human nucleus basalis and its fate in Alzheimer's disease. *J. Comp. Neurol.* 521, 4124-44. doi: 10.1002/cne.23415.

Mesulam, M.M., Mufson, E.J., Wainer, B.H., Levey, A.I. (1983b). Central cholinergic

pathways in the rat: an overview based on an alternative nomenclature (Ch1-Ch6). *Neuroscience* 10, 1185–201. doi: 10.1016/0306-4522(83)90108-2.

Miettinen, R.A., Kalesnykas, G., Koivisto, E.H. (2002). Estimation of the total number of cholinergic neurons containing estrogen receptor-alpha in the rat basal forebrain. *J. Histochem. Cytochem.* 50, 891-902. doi: 10.1177/002215540205000703.

Mitchell, J.F., Sundberg, K.A., Reynolds, J.H. (2009). Spatial attention decorrelates intrinsic activity fluctuations in macaque area V4. *Neuron* 63, 879-88. doi: 10.1016/j.neuron.2009.09.013.

Mitsushima, D., Sano, A., Takahashi, T. (2013). A cholinergic trigger drives learning-induced plasticity at hippocampal synapses. *Nat. Commun.* 4, 2760. doi: 10.1038/ncomms3760.

Momiyama, T., Zaborszky, L. (2006). Somatostatin presynaptically inhibits both GABA and glutamate release onto rat basal forebrain cholinergic neurons. *J. Neurophysiol.* 96, 686-94. doi: 10.1152/jn.00507.2005.

Moore, R. A., Derry, S., Aldington, D., Cole, P., and Wiffen, P. J. (2015). Amitriptyline for neuropathic pain in adults. Cochrane. *Database. Sys. Rev.* 7, CD008242. doi: 10.1002/14651858.CD008242.pub3

Morozov, Y.M., Datta, D., Paspalas, C.D., Arnsten, A.F.T. (2017). Ultrastructural evidence for impaired mitochondrial fission in the aged rhesus monkey dorsolateral prefrontal cortex. *Neurobiol. Aging* 51, 9-18. doi: 10.1016/j.neurobiolaging.2016.12.001.

Most, J., Tosti, V., Redman, L.M., Fontana, L. (2016). Calorie restriction in humans: An update. *Ageing Res. Rev.* 39, 36-45. doi: 10.1016/j.arr.2016.08.005.

Moyer, J.R. Jr., Disterhoft, J.F. (1994). Nimodipine decreases calcium action potentials in rabbit hippocampal CA1 neurons in an age-dependent and concentration-dependent manner. *Hippocampus* 4, 11-7. doi: 10.1002/hipo.450040104.

Murchison, D., Griffith, W.H. (2007). Calcium buffering systems and calcium signaling in aged rat basal forebrain neurons. *Aging Cell.* 6, 297-305. doi: 10.1111/j.1474-9726.2007.00293.x.

Murchison, D., McDermott, A.N., Lasarge, C.L., Peebles, K.A., Bizon, J.L., Griffith, W.H. (2009). Enhanced calcium buffering in F344 rat cholinergic basal forebrain neurons is associated with age-related cognitive impairment. *J. Neurophysiol.* 102, 2194-207. doi: 10.1152/jn.00301.2009.

Mufson, E.J., Ginsberg, S.D., Ikonomovic, M.D., DeKosky, S.T. (2003). Human cholinergic basal forebrain: chemoanatomy and neurologic dysfunction. *J. Chem. Neuroanat.* 26, 233-42. doi: 10.1016/s0891-0618(03)00068-1.

Mulder, J., Zilberter, M., Spence, L., Tortoriello, G., Uhlén, M., Yanagawa, Y., Aujard, F., Hökfelt, T., Harkany, T. (2009). Secretagogin is a Ca2+-binding protein specifying subpopulations of telencephalic neurons. *Proc. Natl. Acad. Sci. U S A* 106, 22492-7. doi: 10.1073/pnas.0912484106.

Murphy, G.G., Rahnama, N.P., Silva, A.J. (2006). Investigation of age-related cognitive decline using mice as a model system: behavioral correlates. *Am. J. Geriatr. Psychiatry.* 14, 1004-11. doi: 10.1097/01.JGP.0000209405.27548.7b.

Nagel, G., Ollig, D., Fuhrmann, M., Kateriya, S., Musti, A.M., Bamberg, E., Hegemann, P. (2002). Channelrhodopsin-1: a light-gated proton channel in green algae. *Science* 296, 2395-8. doi: 10.1126/science.1072068.

Nagtegaal, A.P., Rainey, R.N., van der Pluijm, I., Brandt, R.M., van der Horst, G.T., Borst, J.G., Segil, N. (2015). Cockayne syndrome group B (Csb) and group a (Csa) deficiencies predispose to hearing loss and cochlear hair cell degeneration in mice. *J. Neurosci.* 35, 4280-6. doi: 10.1523/JNEUROSCI.5063-14.2015.

National Center for Health Statistics. (2007). Health, United States, 2007 with chartbook on trends in the health of Americans. https://www.cdc.gov/nchs/data/hus/hus07.pdf [Accessed January 5, 2021]

Nixon, R.A. (2013). The role of autophagy in neurodegenerative disease. *Nat. Med.* 19, 983-97. doi: 10.1038/nm.3232.

Norden, D.M., Godbout, J.P. (2013). Review: microglia of the aged brain: primed to be activated and resistant to regulation. *Neuropathol. Appl. Neurobiol.* 39, 19-34. doi: 10.1111/j.1365-2990.2012.01306.x.

Okun, E., Griffioen, K.J., Mattson, M.P. (2011). Toll-like receptor signaling in neural plasticity and disease. *Trends. Neurosci.* 34, 269-81. doi: 10.1016/j.tins.2011.02.005.

Page, T.L., Einstein, M., Duan, H., He, Y., Flores, T., Rolshud, D., Erwin, J.M., Wearne, S.L., Morrison, J.H., Hof, P.R. (2002). Morphological alterations in neurons forming corticocortical projections in the neocortex of aged Patas monkeys. *Neurosci. Lett.* 317, 37-41. doi: 10.1016/s0304-3940(01)02428-4.

Page, K.J., Everitt, B.J. (1995). The distribution of neurons coexpressing immunoreactivity to AMPA-sensitive glutamate receptor subtypes (GluR1-4) and nerve growth factor receptor in the rat basal forebrain. *Eur. J. Neurosci.* 7, 1022-33. doi: 10.1111/j.1460-9568.1995.tb01090.x.

Papaioannou, N., Tooten, P.C., van Ederen, A.M., Bohl, J.R., Rofina, J., Tsangaris, T., Gruys, E. (2001). Immunohistochemical investigation of the brain of aged dogs. I. Detection of neurofibrillary tangles and of 4-hydroxynonenal protein, an oxidative damage product, in senile plaques. *Amyloid* 8, 11-21. doi: 10.3109/13506120108993810.

Patel, N.V., Gordon, M.N., Connor, K.E., Good, R.A., Engelman, R.W., Mason, J., Morgan, D.G., Morgan, T.E., Finch, C.E. (2005). Caloric restriction attenuates Abeta-deposition in Alzheimer transgenic models. *Neurobiol. Aging.* 26, 995-1000. doi: 10.1016/j.neurobiolaging.2004.09.014.

Patrylo, P.R., Tyagi, I., Willingham, A.L., Lee, S., Williamson, A. (2007). Dentate filter function is altered in a proepileptic fashion during aging. *Epilepsia* 48, 1964-78. doi: 10.1111/j.1528-1167.2007.01139.x.

Paul, A., Belton, A., Nag, S., Martin, I., Grotewiel, M.S., Duttaroy, A. (2007). Reduced mitochondrial SOD displays mortality characteristics reminiscent of natural aging. *Mech. Ageing Dev.* 128, 706-16. doi: 10.1016/j.mad.2007.10.013.

Perez, S.E., Dar. S., Ikonomovic, M.D., DeKosky, S.T., Mufson, E.J. (2007). Cholinergic forebrain degeneration in the APPswe/PS1DeltaE9 transgenic mouse. *Neurobiol. Dis.* 28, 3-15. doi: 10.1016/j.nbd.2007.06.015.

Peters, A., Sethares, C., Moss, M.B. (1998). The effects of aging on layer 1 in area 46 of prefrontal cortex in the rhesus monkey. *Cereb. Cortex.* 8, 671-84. doi: 10.1093/cercor/8.8.671.

Petralia, R.S., Wenthold, R.J. (1992). Light and electron immunocytochemical localization of AMPA-selective glutamate receptors in the rat brain. *J. Comp. Neurol.* 318, 329-54. doi: 10.1002/cne.903180309.

Pinto, L., Goard, M.J., Estandian, D., Xu, M., Kwan, A.C., Lee, S.H., Harrison, T.C., Feng, G., Dan, Y. (2013). Fast modulation of visual perception by basal forebrain cholinergic neurons. *Nat. Neurosci.* 16, 1857-1863. doi: 10.1038/nn.3552.

Pitler, T.A., Landfield, P.W. (1990). Aging-related prolongation of calcium spike duration in rat hippocampal slice neurons. *Brain Res.* 508, 1-6. doi: 10.1016/0006-8993(90)91109-t.

Porges, E.C., Woods, A.J., Edden, R.A., Puts, N.A., Harris, A.D., Chen, H., Garcia, A.M., Seider, T.R., Lamb, D.G., Williamson, J.B., Cohen, R.A. (2017). Frontal gamma-aminobutyric acid concentrations are associated with cognitive performance in older adults. *Biol. Psychiatry. Cogn. Neurosci. Neuroimaging.* 2, 38-44. doi: 10.1016/j.bpsc.2016.06.004.

Post-Munson, D.J., Lum-Ragan, J.T., Mahle, C.D., Gribkoff, V.K. (1994). Reduced bicuculline response and GABAA agonist binding in aged rat hippocampus. *Neurobiol. Aging* 15, 629-33. doi: 10.1016/0197-4580(94)00057-3.

Potier, B., Jouvenceau, A., Epelbaum, J., Dutar, P. (2006). Age-related alterations of

GABAergic input to CA1 pyramidal neurons and its control by nicotinic acetylcholine receptors in rat hippocampus. *Neuroscience* 142, 187-201. doi: 10.1016/j.neuroscience.2006.06.040.

Potier, B., Rascol, O., Jazat, F., Lamour, Y., Dutar, P. (1992). Alterations in the properties of hippocampal pyramidal neurons in the aged rat. *Neuroscience* 48, 793-806. doi: 10.1016/0306-4522(92)90267-6.

Power, J.M., Wu, W.W., Sametsky, E., Oh, M.M., Disterhoft, J.F. (2002). Age-related enhancement of the slow outward calcium-activated potassium current in hippocampal CA1 pyramidal neurons in vitro. *J. Neurosci.* 22, 7234-43. doi: 10.1523/JNEUROSCI.22-16-07234.2002.

Profenno, L.A., Porsteinsson, A.P., Faraone, S.V. (2010). Meta-analysis of Alzheimer's disease risk with obesity, diabetes, and related disorders. *Biol. Psychiatry* 67, 505-12. doi: 10.1016/j.biopsych.2009.02.013.

Prolla, T.A. (2002). DNA microarray analysis of the aging brain. *Chem. Senses.* 27, 299-306. doi: 10.1093/chemse/27.3.299.

Prince, M., Bryce, R., Albanese, E., Wimo, A., Ribeiro, W., Ferri, C.P. (2013). The global prevalence of dementia: a systematic review and metaanalysis. *Alzheimers Dement.* 9, 63-75.e2. doi: 10.1016/j.jalz.2012.11.007.

Rankin, J.W., Shute, M., Heffron, S.P., Saker, K.E. (2006). Energy restriction but not protein source affects antioxidant capacity in athletes. *Free Radic. Biol. Med.* 41, 1001-9. doi: 10.1016/j.freeradbiomed.2006.06.019.

Redman, L.M., Ravussin, E. (2011). Caloric restriction in humans: impact on

physiological, psychological, and behavioral outcomes. *Antioxid. Redox Signal.* 14, 275-87. doi: 10.1089/ars.2010.3253.

Rekik, K., Francés, B., Valet, P., Dray, C., Florian, C. (2017). Cognitive deficit in hippocampal-dependent tasks in Werner syndrome mouse model. *Behav. Brain. Res.* 323, 68-77. doi: 10.1016/j.bbr.2017.01.034.

Ren, S.Q., Yao, W., Yan, J.Z., Jin, C., Yin, J.J., Yuan, J., Yu, S., Cheng, Z. (2018). Amyloid β causes excitation/inhibition imbalance through dopamine receptor 1-dependent disruption of fast-spiking GABAergic input in anterior cingulate cortex. *Sci. Rep.* 8, 302. doi: 10.1038/s41598-017-18729-5.

Richardson, B.D., Ling, L.L., Uteshev, V.V., Caspary, D.M. (2013). Reduced GABA(A) receptor-mediated tonic inhibition in aged rat auditory thalamus. *J. Neurosci.* 33, 1218-27a. doi: 10.1523/JNEUROSCI.3277-12.2013.

Roland, J.J., Stewart, A.L., Janke, K.L., Gielow, M.R., Kostek, J.A., Savage, L.M., Servatius, R.J., Pang, K.C. (2014). Medial septum-diagonal band of Broca (MSDB) GABAergic regulation of hippocampal acetylcholine efflux is dependent on cognitive demands. *J. Neurosci.* 34, 506-14. doi: 10.1523/JNEUROSCI.2352-13.2014.

Rosczyk, H.A., Sparkman, N.L., Johnson, R.W. (2008). Neuroinflammation and cognitive function in aged mice following minor surgery. *Exp. Gerontol.* 43, 840-6. doi: 10.1016/j.exger.2008.06.004.

Rosene, D., and Nicholson, T. (1999). “Neurotransmitter receptor changes in the

hippocampus and cerebral cortex in normal aging," in *Cerebral Cortex*, eds A. Peters and J. Morrison (New York, Philadelphia: Springer), 111-128.

Rothblum-Oviatt C, Wright J, Lefton-Greif MA, McGrath-Morrow SA, Crawford TO, Lederman HM. Ataxia telangiectasia: a review. *Orphanet. J. Rare. Dis.* 11, 159. doi: 10.1186/s13023-016-0543-7.

Rozycka, A., Liguz-Lecznar, M. (2017). The space where aging acts: focus on the GABAergic synapse. *Aging Cell* 16, 634-643. doi: 10.1111/acel.12605.

Rubinsztein, D.C., Mariño, G., Kroemer, G. (2011). Autophagy and aging. *Cell* 146, 682-95. doi: 10.1016/j.cell.2011.07.030.

Saez, I., Vilchez, D. (2014). The mechanistic links between proteasome activity, aging and age-related diseases. *Curr. Genomics* 15, 38-51. doi: 10.2174/138920291501140306113344.

Sagné, C., El Mestikawy, S., Isambert, M.F., Hamon, M., Henry, J.P., Giros, B., Gasnier, B. (1997). Cloning of a functional vesicular GABA and glycine transporter by screening of genome databases. *FEBS Lett.* 417, 177-83. doi: 10.1016/s0014-5793(97)01279-9.

Salminen, A., Ojala, J., Kauppinen, A., Kaarniranta, K., Suuronen, T. (2009). Inflammation in Alzheimer's disease: amyloid-beta oligomers trigger innate immunity defence via pattern recognition receptors. *Prog. Neurobiol.* 87, 181-94. doi: 10.1016/j.pneurobio.2009.01.001.

Santos, R.X., Correia, S.C., Zhu, X., Smith, M.A., Moreira, P.I., Castellani, R.J.,

Nunomura, A., Perry, G. (2013). Mitochondrial DNA oxidative damage and repair in aging and Alzheimer's disease. *Antioxid. Redox. Signal.* 18, 2444-57. doi: 10.1089/ars.2012.5039.

Sarkar, D., Fisher, P.B. (2006). Human polynucleotide phosphorylase (hPNPase old-35): an RNA degradation enzyme with pleiotrophic biological effects. *Cell Cycle* 5, 1080-4. doi: 10.4161/cc.5.10.2741.

Sarter, M., Lustig, C., Berry, A.S., Grittone, H., Howe, W.M., Parikh, V. (2016). What do phasic cholinergic signals do? *Neurobiol. Learn. Mem.* 130, 135-41. doi: 10.1016/j.nlm.2016.02.008.

Schmitz, T.W., Nathan, Spreng. R; Alzheimer's Disease Neuroimaging Initiative. (2016). Basal forebrain degeneration precedes and predicts the cortical spread of Alzheimer's pathology. *Nat. Commun.* 7, 13249. doi: 10.1038/ncomms13249.

Sena, L.A., Chandel, N.S. (2012). Physiological roles of mitochondrial reactive oxygen species. *Molecular Cell* 48, 158-67 doi: 10.1016/j.molcel.2012.09.025.

Shen, Y., Lue, L., Yang, L., Roher, A., Kuo, Y., Strohmeyer, R., Goux, W.J., Lee, V., Johnson, G.V., Webster, S.D., Cooper, N.R., Bradt, B., Rogers, J. (2001). Complement activation by neurofibrillary tangles in Alzheimer's disease. *Neurosci. Lett.* 305, 165-168. doi: 10.1016/s0304-3940(01)01842-0.

Shi, L., Adams, M.M., Linville, M.C., Newton, I.G., Forbes, M.E., Long, A.B., Riddle, D.R., Brunso-Bechtold, J.K. (2007). Caloric restriction eliminates the aging-related decline in NMDA and AMPA receptor subunits in the rat hippocampus

and induces homeostasis. *Exp. Neurol.* 206, 70-9. doi: 10.1016/j.expneurol.2007.03.026.

Shi, Q., Colodner, K.J., Matousek, S.B., Merry, K., Hong, S., Kenison, J.E., Frost, J.L., Le, K.X., Li, S., Dodart, J.C., Caldarone, B.J., Stevens, B., Lemere, C.A. (2015). Complement C3-deficient mice fail to display age-related hippocampal decline. *J. Neurosci.* 35, 13029-42. doi: 10.1523/JNEUROSCI.1698-15.2015.

Shi, Y.F., Han, Y., Su, Y.T., Yang, J.H., Yu, Y.Q. (2015). Silencing of cholinergic basal forebrain neurons using archaerhodopsin prolongs slow-wave sleep in mice. *PLoS One* 10, e0130130. doi: 10.1371/journal.pone.0130130.

Shibata, M., Lu, T., Furuya, T., Degterev, A., Mizushima, N., Yoshimori, T., MacDonald, M., Yankner, B., Yuan, J. (2006). Regulation of intracellular accumulation of mutant Huntingtin by Beclin 1. *J. Biol. Chem.* 281, 14474-85. doi: 10.1074/jbc.M600364200.

Simon, A.P., Poindessous-Jazat, F., Dutar, P., Epelbaum, J., Bassant, M-H. (2006). Firing properties of anatomically identified neurons in the medial septum of anesthetized and unanesthetized restrained rats. *J. Neurosci.* 26, 9038–46. doi: 10.1523/JNEUROSCI.1401-06.2006.

Simonsen, A., Cumming, R.C., Brech, A., Isakson, P., Schubert, D.R., Finley, K.D. (2008). Promoting basal levels of autophagy in the nervous system enhances longevity and oxidant resistance in adult Drosophila. *Autophagy* 4, 176-84. doi: 10.4161/auto.5269.

Small, S.A., Tsai, W.Y., DeLaPaz, R., Mayeux, R., Stern, Y. (2002). Imaging

hippocampal function across the human life span: is memory decline normal or not? *Ann. Neurol.* 51, 290-5. doi: 10.1002/ana.10105.

Smith, M.L., Hale, B.D., Booze, R.M. (1994). Calbindin-D28k immunoreactivity within the cholinergic and GABAergic projection neurons of the basal forebrain. *Exp. Neurol.* 130, 230-6. doi: 10.1006/exnr.1994.1201.

Sohal, R.S., Weindruch, R., 1996. Oxidative stress, caloric restriction, and aging. Science 273, 59-67. doi: 10.1126/science.273.5271.59.

Someya, S., Yu, W., Hallows, W.C., Xu, J., Vann, J.M., Leeuwenburgh, C., Tanokura, M., Denu, J.M., Prolla, T.A. (2010). Sirt3 mediates reduction of oxidative damage and prevention of age-related hearing loss under caloric restriction. Cell 143, 802-12. doi: 10.1016/j.cell.2010.10.002.

Song, M., Jin, J., Lim, J.E., Kou, J., Pattanayak, A., Rehman, J.A., Kim, H.D., Tahara, K., Lalonde, R., Fukuchi, K. (2011). TLR4 mutation reduces microglial activation, increases Abeta deposits and exacerbates cognitive deficits in a mouse model of Alzheimer's disease. *J. Neuroinflammation* 8, 92. doi: 10.1186/1742-2094-8-92.

Sotty, F., Danik, M., Manseau, F., Laplante, F., Quirion, R., Williams, S. (2003). Distinct electrophysiological properties of glutamatergic, cholinergic and GABAergic rat septohippocampal neurons: novel implications for hippocampal rhythmicity. *J. Physiol.* 551, 927-43. doi: 10.1113/jphysiol.2003.046847.

Sparkman, N.L., Johnson, R.W. (2008). Neuroinflammation associated with aging

sensitizes the brain to the effects of infection or stress. *Neuroimmunomodulation* 15, 323–30 doi: 10.1159/000156474.

Spaulding, C.C., Walford, R.L., Effros, R.B. (1997). Calorie restriction inhibits the age-related dysregulation of the cytokines TNF-alpha and IL-6 in C3B10RF1 mice. *Mech. Ageing Dev.* 93, 87-94. doi: 10.1016/s0047-6374(96)01824-6.

Sreekumar, R., Unnikrishnan, J., Fu, A., Nygren, J., Short, K.R., Schimke, J., Barazzoni, R., Nair, K.S. (2002). Effects of caloric restriction on mitochondrial function and gene transcripts in rat muscle. *Am. J. Physiol. Endocrinol. Metab.* 283, E38-43. doi: 10.1152/ajpendo.00387.2001.

Stahon, K.E., Bastian, C., Griffith, S., Kidd, G.J., Brunet, S., Baltan, S. (2016). Age-related changes in axonal and mitochondrial ultrastructure and function in white matter. *J. Neurosci.* 36, 9990-10001. doi: 10.1523/JNEUROSCI.1316-16.2016.

Standaert, D.G., Landwehrmeyer, G.B., Kerner, J.A., Penney, J.B. Jr., Young, A.B. (1996). Expression of NMDAR2D glutamate receptor subunit mRNA in neurochemically identified interneurons in the rat neostriatum, neocortex and hippocampus. *Brain Res. Mol. Brain Res.* 42, 89-102. doi: 10.1016/s0169-328x(96)00117-9.

Stanić, D., Brumovsky, P., Fetissov, S., Shuster, S., Herzog, H., Hökfelt, T. (2006). Characterization of neuropeptide Y2 receptor protein expression in the mouse brain. I. Distribution in cell bodies and nerve terminals. *J. Comp. Neurol.* 499, 357-90. doi: 10.1002/cne.21046.

Stutzmann, G.E., Mattson, M.P. (2011). Endoplasmic reticulum Ca(2+) handling in

excitable cells in health and disease. *Pharmacol. Rev.* 63, 700-27. doi: 10.1124/pr.110.003814.

Tanaka, K., Matsuda, N. (2014). Proteostasis and neurodegeneration: the roles of proteasomal degradation and autophagy. *Biochim. Biophys. Acta.* 1843, 197-204. doi: 10.1016/j.bbamcr.2013.03.012.

Thibault, O., Hadley, R., Landfield, P.W. (2001). Elevated postsynaptic [Ca2+]i and L-type calcium channel activity in aged hippocampal neurons: relationship to impaired synaptic plasticity. *J. Neurosci.* 21, 9744-56. doi: 10.1523/JNEUROSCI.21-24-09744.2001.

Thibault, O., and Landfield, P.W. (1996). Increase in single L-type calcium channels in hippocampal neurons during aging. *Science* 272, 1017-20. doi: 10.1126/science.272.5264.1017.

Thibault, O., Mazzanti, M.L., Blalock, E.M., Porter, N.M., Landfield, P.W. (1995). Single-channel and whole-cell studies of calcium currents in young and aged rat hippocampal slice neurons. *J. Neurosci. Methods.* 59, 77-83. doi: 10.1016/0165-0270(94)00196-n.

Thomsen, K., Yokota, T., Hasan-Olive, M.M., Sherazi, N., Fakouri, N.B., Desler, C., Regnell, C.E., Larsen, S., Rasmussen, L.J., Dela, F., Bergersen, L.H., Lauritzen, M. (2018). Initial brain aging: heterogeneity of mitochondrial size is associated with decline in complex I-linked respiration in cortex and hippocampus. *Neurobiol. Aging* 61, 215-224. doi: 10.1016/j.neurobiolaging.2017.08.004.

Toman, J., Fiskum, G. (2011). Influence of aging on membrane permeability transition

in brain mitochondria. *J. Bioenerg. Biomembr.* 43, 3-10. doi: 10.1007/s10863-011-9337-8.

Tombaugh, G.C., Rowe, W.B., Rose, G.M. (2005). The slow afterhyperpolarization in hippocampal CA1 neurons covaries with spatial learning ability in aged Fisher 344 rats. *J. Neurosci.* 25, 2609-16. doi: 10.1523/JNEUROSCI.5023-04.2005.

Toro, P., Schonknecht, P., Schroder, J. (2009). Type II diabetes in mild cognitive impairment and Alzheimer's disease: results from a prospective population-based study in Germany. *J. Alzheimers. Dis.* 16, 687-91. doi: 10.3233/JAD-2009-0981.

Tóth, A., Hajnik, T., Záborszky, L., Détári, L. (2007). Effect of basal forebrain neuropeptide Y administration on sleep and spontaneous behavior in freely moving rats. *Brain Res. Bull.* 72, 293-301. doi: 10.1016/j.brainresbull.2007.01.006.

Tóth, A., Záborszky, L., Détári, L. (2005). EEG effect of basal forebrain neuropeptide Y administration in urethane anaesthetized rats. *Brain Res. Bull.* 66, 37-42. doi: 10.1016/j.brainresbull.2005.03.008.

Ugochukwu, N.H., Figgers, C.L. (2007). Caloric restriction inhibits up-regulation of inflammatory cytokines and TNF-alpha, and activates IL-10 and haptoglobin in the plasma of streptozotocin-induced diabetic rats. *J. Nutr. Biochem.* 18, 120-6. doi: 10.1016/j.jnutbio.2006.03.008.

Unal, C.T., Pare, D., Zaborszky, L. (2015). Impact of basal forebrain cholinergic inputs on basolateral amygdala neurons. *J. Neurosci.* 35, 853-63. doi: 10.1523/JNEUROSCI.2706-14.2015.

Valerio, A., Boroni, F., Benares, M., Sarnico, I., Ghisi, V., Bresciani, L.G., Ferrario, M., Borsani, G., Spano, P., Pizzi, M. (2006). NF-kappaB pathway: a target for preventing beta-amyloid (Abeta)-induced neuronal damage and Abeta42 production. *Eur. J. Neurosci.* 23, 1711-20. doi: 10.1111/j.1460-9568.2006.04722.x.

van Noort, J. M., and Bsibsi, M. (2009). Toll-like receptors in the CNS: implications for neurodegeneration and repair. *Prog. Brain Res.* 175, 139–148. doi: 10.1016/S0079-6123(09)17509-X.

Vaishnav, R.A., Getchell, M.L., Poon, H.F., Barnett, K.R., Hunter, S.A., Pierce, W.M., Klein, J.B., Butterfield, D.A., Getchell, T.V. (2007). Oxidative stress in the aging murine olfactory bulb: redox proteomics and cellular localization. *J. Neurosci. Res.* 85, 373-85. doi: 10.1002/jnr.21130.

Vazquez, J., Baghdoyan, H.A. (2001). Basal forebrain acetylcholine release during REM sleep is significantly greater than during waking. *Am. J. Physiol. Regul. Integr. Comp. Physiol.* 280, R598-601. doi: 10.1152/ajpregu.2001.280.2.R598.

Vincent, G. K., Velkoff, V. A. (2010). The next four decades: The older population in the United States: 2010 to 2050. *Current Population Reports* 25-1138. U.S. Census Bureau; Washington, DC.

Walker, L.C., Price, D.L., Young, W.S. 3rd. (1989). GABAergic neurons in the primate basal forebrain magnocellular complex. *Brain Res.* 499, 188-92. doi: 10.1016/0006-8993(89)91152-9.

Wallenstein, G.V., Vago, D.R. (2001). Intrahippocampal scopolamine impairs both

acquisition and consolidation of contextual fear conditioning. *Neurobiol. Learn. Mem.* 75, 245-52. doi: 10.1006/nlme.2001.4005.

Wang, J., Ho, L., Qin, W., Rocher, A.B., Seror, I., Humala, N., Maniar, K., Dolios, G., Wang, R., Hof, P.R., Pasinetti, G.M. (2005). Caloric restriction attenuates beta-amyloid neuropathology in a mouse model of Alzheimer's disease. *FASEB J.* 19, 659-61. doi: 10.1096/fj.04-3182fje.

Weidenheim, K.M., Dickson, D.W., Rapin, I. (2009). Neuropathology of Cockayne syndrome: Evidence for impaired development, premature aging, and neurodegeneration. *Mech. Ageing Dev.* 130, 619-36. doi: 10.1016/j.mad.2009.07.006.

West, M.J., Coleman, P.D., Flood, D.G., Troncoso, J.C. (1994). Differences in the pattern of hippocampal neuronal loss in normal ageing and Alzheimer's disease. *Lancet* 344, 769-72. doi: 10.1016/s0140-6736(94)92338-8.

Wiley, C.D., Velarde, M.C., Lecot, P., Liu, S., Sarnoski, E.A., Freund, A., Shirakawa, K., Lim, H.W., Davis, S.S., Ramanathan, A., Gerencser, A.A., Verdin, E., Campisi, J. (2016). Mitochondrial dysfunction induces senescence with a distinct secretory phenotype. *Cell Metab.* 23, 303-14. doi: 10.1016/j.cmet.2015.11.011.

Willeumier, K.C., Taylor, D.V., Amen, D.G. (2011). Elevated BMI is associated with decreased blood flow in the prefrontal cortex using SPECT imaging in healthy adults. *Obesity (Silver Spring)* 19, 1095-7. doi: 10.1038/oby.2011.16.

Wimo, A., Jönsson, L., Bond, J., Prince, M., Winblad, B. (2013). Alzheimer Disease

International. The worldwide economic impact of dementia 2010. *Alzheimers Dement.* 9, 1-11.e3. doi: 10.1016/j.jalz.2012.11.006.

Witte, A.V., Fobker, M., Gellner, R., Knecht, S., Flöel, A. (2009). Caloric restriction improves memory in elderly humans. *Proc. Natl. Acad. Sci. U S A* 106, 1255-60. doi: 10.1073/pnas.0808587106.

Wong, T.P., Campbell, P.M., Ribeiro-da-Silva, A., Cuello, A.C. (1998). Synaptic numbers across cortical laminae and cognitive performance of the rat during ageing. *Neuroscience* 84, 403-12. doi: 10.1016/s0306-4522(97)00485-5.

Wong, T.P., Marchese, G., Casu, M.A., Ribeiro-da-Silva, A., Cuello, A.C., De Koninck, Y. (2000). Loss of presynaptic and postsynaptic structures is accompanied by compensatory increase in action potential-dependent synaptic input to layer V neocortical pyramidal neurons in aged rats. *J. Neurosci.* 20, 8596-606. doi: 10.1523/JNEUROSCI.20-22-08596.2000.

Yuen, E.C., Howe, C.L., Li, Y., Holtzman, D.M., Mobley, W.C. (1996). Nerve growth factor and the neurotrophic factor hypothesis. *Brain Dev.* 18, 362-8. doi: 10.1016/0387-7604(96)00051-4.

Zaborszky, L. (1989). Afferent connections of the forebrain cholinergic projection neurons, with special reference to monoaminergic and peptidergic fibers. *EXS.* 57, 12-32. doi: 10.1007/978-3-0348-9138-7_2.

Zaborszky, L., Cullinan, W.E. (1996). Direct catecholaminergic-cholinergic interactions

in the basal forebrain. I. Dopamine-beta-hydroxylase- and tyrosine hydroxylase input to cholinergic neurons. *J. Comp. Neurol.* 374, 535-54. doi: 10.1002/(SICI)1096-9861(19961028)374:4<535::AID-CNE5>3.0.CO;2-2.

Zaborszky, L., Duque, A. (2000). Local synaptic connections of basal forebrain neurons. *Behav. Brain Res.* 115, 143-58. doi: 10.1016/s0166-4328(00)00255-2.

Záborszky, L., Duque, A., Alreja, M., Saak, S.V. (2009). Effect of NPY in the cholinergic basal forebrain in rat: a double-immunolabeling electron microscopy and in vitro electrophysiological studies. *Soc. Neurosci. Abstr.* 35, P2.1.04.

Zaborszky, L., Duque, A., Gielow, M., Gombkoto, P., Nadasdy, Z., Somogyi, J. (2015). Chapter 19 - Organization of the basal forebrain cholinergic projection system: specific or diffuse? *The rat nervous system (fourth edition)* 491–507. doi: 10.1016/B978-0-12-374245-2.00019-X.

Záborszky, L., Heimer, L., Eckenstein, F., Leranth, C. (1986). GABAergic input to cholinergic forebrain neurons: an ultrastructural study using retrograde tracing of HRP and double immunolabeling. *J. Comp. Neurol.* 250, 282-95. doi: 10.1002/cne.902500303.

Zaborszky, L., Pang, K., Somogyi, J., Nadasdy, Z., Kallo, I. (1999). The basal forebrain corticopetal system revisited. *Ann. N. Y. Acad. Sci.* 877, 339-67. doi: 10.1111/j.1749-6632.1999.tb09276.x.

Zaborszky, L., Pol, A. van den, Gyengesi, E. (2012). Chapter 28 - The basal forebrain cholinergic projection system in mice. *The mouse nervous system* 684–718. doi: 10.1016/B978-0-12-369497-3.10028-7.

Zaborszky, L., Rosin, D.L., Kiss, J. (2004). Alpha-adrenergic receptor (alpha(2A)) is colocalized in basal forebrain cholinergic neurons: a light and electron microscopic double immunolabeling study. *J. Neurocytol.* 33, 265-76. doi: 10.1023/B:NEUR.0000044188.67442.9d.

Zeighami, Y., Ulla, M., Iturria-Medina, Y., Dadar, M., Zhang, Y., Larcher, K.M., Fonov, V., Evans, A.C., Collins, D.L., Dagher, A. (2015). Network structure of brain atrophy in de novo Parkinson's disease. *Elife* 4, e08440. doi: 10.7554/eLife.08440.

Zhang, S., Eitan, E., Mattson, M.P. (2017). Early involvement of lysosome dysfunction in the degeneration of cerebral cortical neurons caused by the lipid peroxidation product 4-hydroxynonenal. *J. Neurochem.* 140, 941-954. doi: 10.1111/jnc.13957.

Zhang, F., Vierock, J., Yizhar, O., Fenno, L.E., Tsunoda, S., Kianianmomeni, A., Prigge, M., Berndt, A., Cushman, J., Polle, J., Magnuson, J., Hegemann, P., Deisseroth, K. (2011a). The microbial opsin family of optogenetic tools. *Cell* 147, 1446-57. doi: 10.1016/j.cell.2011.12.004.

Zhang, F., Wang, L.P., Brauner, M., Liewald, J.F., Kay, K., Watzke, N., Wood, P.G., Bamberg, E., Nagel, G., Gottschalk, A., Deisseroth, K. (2007). Multimodal fast optical interrogation of neural circuitry. *Nature* 446, 633-9. doi: 10.1038/nature05744.

Zhang, H., Trollor, J.N., Wen, W., Zhu, W., Crawford, J.D., Kochan, N.A., Slavin, M.J., Brodaty, H., Reppermund, S., Kang, K., Mather, K.A., Sachdev, P.S. (2011b). Grey matter atrophy of basal forebrain and hippocampus in mild cognitive

impairment. *J. Neurol. Neurosurg. Psychiatry* 82, 487-93. doi: 10.1136/jnnp.2010.217133.

Zhao, X., Rosenke, R., Kronemann, D., Brim, B., Das, S.R., Dunah, A.W., Magnusson, K.R. (2009). The effects of aging on N-methyl-D-aspartate receptor subunits in the synaptic membrane and relationships to long-term spatial memory. *Neuroscience* 162, 933-45. doi: 10.1016/j.neuroscience.2009.05.018.

Zhao, S., Ting, J.T., Atallah, H.E., Qiu, L., Tan, J., Gloss, B., Augustine, G.J., Deisseroth, K., Luo, M., Graybiel, A.M., Feng, G. (2011). Cell type–specific channelrhodopsin-2 transgenic mice for optogenetic dissection of neural circuitry function. *Nat. Methods.* 8, 745-52. doi: 10.1038/nmeth.1668.

CHAPTER II

AMITRIPTYLINE DECREASES GABAERGIC TRANSMISSION IN BASAL FOREBRAIN NEURONS USING AN OPTOGENETIC MODEL OF AGING[*]

2.1 Abstract

The antidepressant drug amitriptyline is used in the treatment of clinical depression and a variety of neurological conditions such as anxiety, neuropathic pain disorders and migraine. Antidepressants are associated with both therapeutic and untoward effects, and their use in the elderly has tripled since the mid-1990s. Because of this widespread use, we are interested in testing the acute effects of amitriptyline on synaptic transmission at therapeutic concentrations well below those that block voltage-gated calcium channels. We found that 3 μM amitriptyline reduced the frequency of spontaneous GABAergic inhibitory postsynaptic currents (IPSCs) and reduced quantal content in mice at ages of 7-10 mo. and 23-25 mo., suggesting a presynaptic mechanism of action that does not diminish with age. We employed a reduced synaptic preparation of the basal forebrain (BF) and a new optogenetic aging model utilizing a bacterial artificial chromosome (BAC) transgenic mouse line with stable expression of the channelrhodopsin-2 (ChR2) variant H134R specific for GABAergic neurons [VGAT-ChR2(H134R)-EYFP]. This model enables optogenetic light stimulation of specific

---

[*] This chapter is re-printed with permission from "Amitriptyline decreases GABAergic transmission in basal forebrain neurons using an optogenetic model of aging" by Bang E, Tobery A, Montgomery KS, Fincher AS, Earnest DJ, Murchison DA, Griffith WH, 2021. *Frontiers in Aging Neuroscience*, 13, 673155, Copyright [2021] by Creative Commons license ("CC BY").

GABAergic synaptic terminals across aging. Age-related impairment of circadian behavior was used to confirm predictable age-related changes associated with this model. Our results suggest that low concentrations of amitriptyline act presynaptically to reduce neurotransmitter release and that this action is maintained during aging.

2.2 Introduction

Amitriptyline (AMI) is a tricyclic antidepressant used for various neurological disorders such as anxiety, depression, neuropathic pain disorders and migraine (Baldessarini, 2006; Couch et al., 2011; Moore et al., 2015; Urquhart et al., 2018). Because of its diverse therapeutic applications, AMI continues to be used throughout life span, and overall antidepressant use among patients over 65 years of age has more than tripled from 1995 to 2005 (National Center for Health Statistics, 2007). Although the actions of AMI to block reuptake of norepinephrine and serotonin have been studied for many years, much less is known about the additional cellular mechanisms of AMI that may contribute to its therapeutic efficacy. For example, AMI acts to inhibit ion channels such as the voltage-gated sodium, calcium and potassium channels (Nicholson et al., 2002; Yan et al., 2010; Wu et al., 2012). AMI also acts as an antagonist of the serotonin, the α1-adrenergic, the histamine, and the muscarinic acetylcholine receptors (Richelson, 1979; Kachur et al., 1988; Pandey et al., 2010; Nojimoto et al., 2010; Liu et al., 2012). Moreover, it possesses neurotrophic activity by acting as an agonist of TrkA and TrkB receptor which BDNF activates (Jang et al., 2009). Many, but not all, of these actions to block ion channels occur at higher than therapeutic concentrations of approximately 3-6 μM (Glotzbach and Preskorn, 1982; Lavoie et al., 1990; Baldessarini, 2006). Importantly

chronic low dose AMI, within the therapeutic range, is an effective therapy for lower back pain (Urquhart et al, 2018), reducing nicotine-induced increase in C-fiber excitability in humans (Freysoldt et al., 2009), and prevention of age-related impairment in the water maze task in rats (Yau et al., 2002). However, some human studies demonstrate the negative effects of AMI on cognitive function within the therapeutic ranges of depression treatment (Peck et al., 1979; Branconnier et al., 1982; Linnoila et al., 1983; Curran et al., 1988). Therefore, the purpose of the present study is to investigate whether therapeutic concentrations of AMI interfere with synaptic transmission in the basal forebrain (BF) using a new synaptic optogenetic model and whether these actions are maintained during aging.

The BF contains a heterogeneous population of cholinergic and noncholinergic neurons located in the medial septum, diagonal band, nucleus basalis, ventral pallidum, substantia innominata, globus pallidus and the internal capsule (Wainer et al., 1985; Zaborszky et al., 1999; Hajszan et al., 2004; Manseau et al., 2005). These neurons play an important role in cognitive functions such as attention, arousal, and memory (see review, Zaborszky et al., 2018) and our laboratory has been studying calcium homeostasis, voltage-gated calcium currents and synaptic transmission in these neurons across aging for many years (Griffith and Murchison, 1995; Murchison and Griffith, 1996, 1998, 2007; Murchison et al., 2009). Using a reduced synaptic preparation, we have shown that decreased GABAergic inhibitory synaptic transmission in BF is associated with age-related cognitive impairment in rats (Griffith et al. 2014). We have recently reproduced many of these earlier results in a new optogenetic aging model

utilizing a bacterial artificial chromosome (BAC) transgenic mouse line with stable expression of the channelrhodopsin-2 (ChR2) variant H134R specific for GABAergic neurons [VGAT-ChR2(H134R)-EYFP] (Montgomery et al., resubmission). In the present study, we have used this optogenetic aging model with whole-cell voltage-clamp, Ca^{2+}-sensitive fluorescent imaging and the reduced synaptic preparation to examine the effect of AMI on inhibitory synaptic transmission in the BF. The great advantage of the reduced synaptic preparation is that it is possible to selectively stimulate GABAergic nerve terminals on well-clamped isolated BF neurons. This model allows us to calculate relative changes in quantal content (m) of transmitter release and identify presumed presynaptic functions. Finally, age-related changes in circadian wheel-running activity were used to further characterize the VGAT optogenetic mouse as a viable aging model.

2.3 Results

2.3.1 Optogenetic aging model and reduced synaptic preparation

We recently demonstrated that the expression of ChR2 in mice carrying the VGAT-ChR2-EYFP transgene is functionally maintained across aging, thus this mouse line is useful for aging neuroscience (Montgomery et al., resubmission). In mice hemizygous for VGAT-ChR2-EYFP BAC transgene, the ChR2-EYFP fusion protein is expressed in GABAergic neuronal populations by the mouse vesicular GABA transporter (VGAT) promoter on the BAC transgene (Figure 2.1A), which enables specific optical stimulation of GABAergic neurons. Whole brain coronal images showed strong ChR2-EYFP expression in a section of the BF (Figure 2.1C).

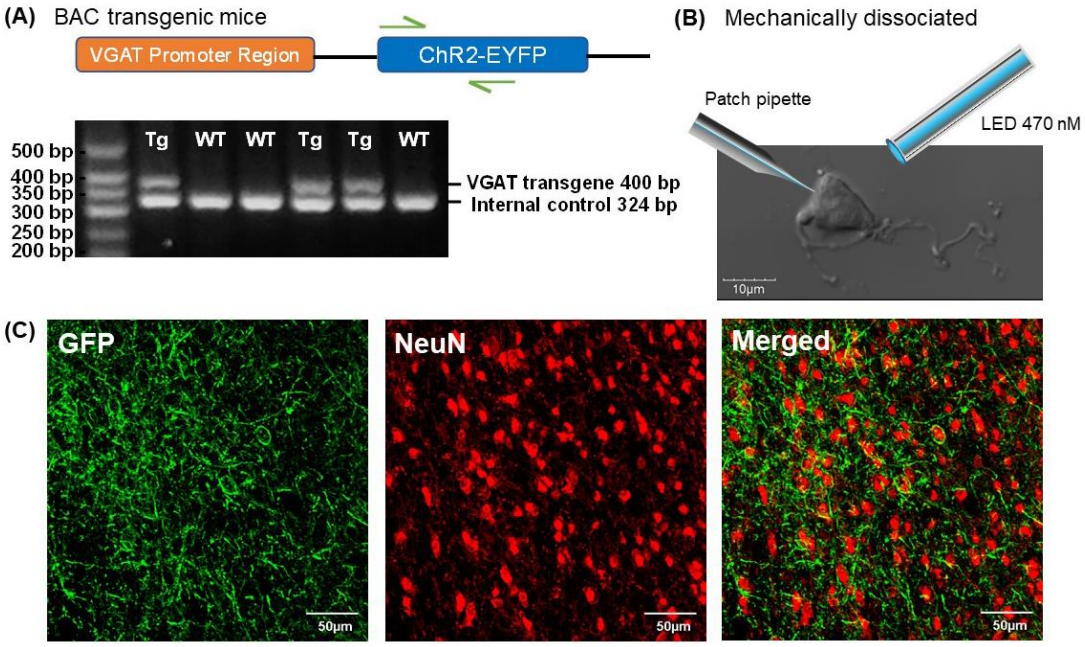

Figure 2.1. Characterization of ChR2-EYFP expression in VGAT-ChR2(H134R)-EYFP transgenic mice. (A) Schematic representation of VGAT-ChR2-EYFP transgene (top) and an example of PCR gel electrophoresis (bottom). The first lane is the DNA size standard and the fragment size is given in base pairs on the left. The genotypes are described at the top of each lane. (B) The representative mechanically dissociated BF neuron with the illustrations of patch pipette and 470-nm LED light stimulation. (C) Confocal images of mouse BF slice show strong ChR2-EYFP expression in GABAergic neurons of VGAT-ChR2(H134R)-EYFP transgenic mice.

Our ‘reduced synaptic preparation’ was designed to investigate synaptic physiology during aging with greater efficiency than in an aged slice preparation. This reduced preparation consists of acutely dissociated neurons that are not exposed to the usual proteolytic enzyme treatment and therefore retain functional presynaptic inputs on somas and proximal dendrites (Akaike and Moorhouse, 2003). Figure 2.1B shows an enzyme-free, acutely dissociated BF neuron and an illustration of the patch pipette and optogenetic light-stimulation.

2.3.2 Effects of AMI on calcium

The effect of AMI on whole-cell high-voltage-activated (HVA) calcium currents was investigated by applying a series of concentrations to acutely dissociated BF neurons from juvenile rats. The effect of AMI on calcium current inhibition was tested at the following five concentrations: 3 μM (n=5), 10 μM (n=8), 30 μM (n=7), 100 μM (n=6) and 300 μM (n=3) with AMI inhibiting calcium currents by 1.87 ± 0.65%, 16.02 ± 6.37%, 30.25 ± 3.42%, 46.29 ± 6.31% and 99.26 ± 0.74%, respectively (Figure 2.2A). Increasing concentrations were applied on the same neuron and the concentration-response curve for AMI is shown in Figure 2.2B. It is well known that high concentrations of AMI block voltage-gated Ca^{2+} channels (see Introduction), so the purpose of this experiment was to identify those concentrations of AMI below significant Ca^{2+} inhibition. The curve has a Hill coefficient of 1.2 and an EC_{50} (effective concentration for 50% inhibition) of approximately 100 μM.

To confirm that AMI acts in a similar manner on calcium signalling in the mouse, we used the ratiometric calcium-sensitive fluorescent probe fura-2 and induced

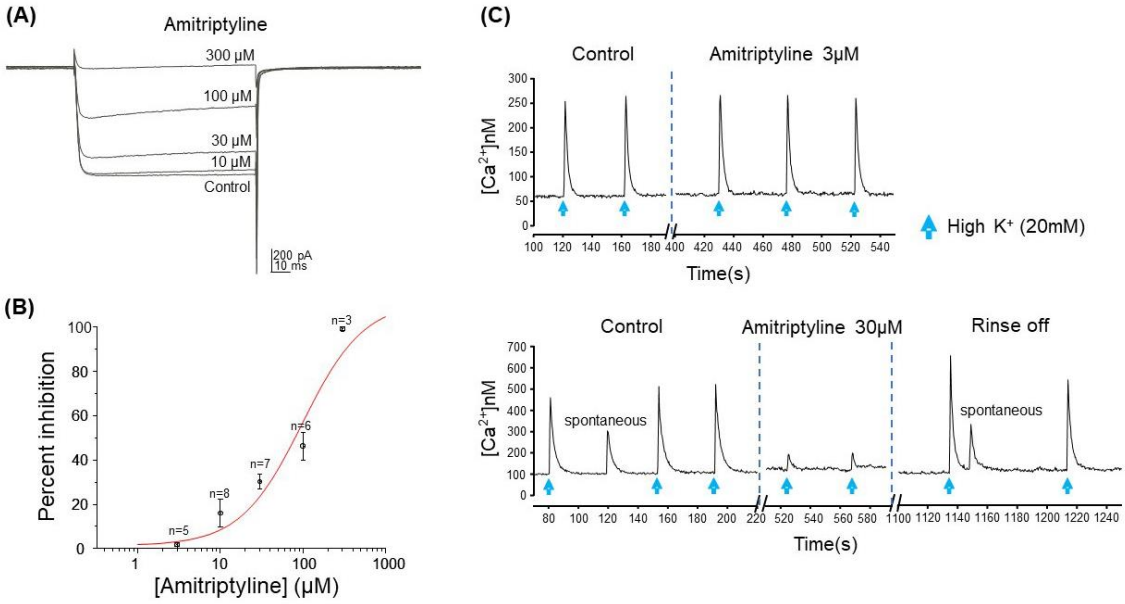

Figure 2.2. AMI effect on calcium current and intracellular calcium transients. (A) Whole-cell perforated-patch voltage-clamp recordings of calcium currents from a rat BF neuron show reduced current amplitude in the presence of increasing concentrations of AMI. Currents were elicited by a depolarizing test pulse to -15 mV (V_h = -70mV, 20 s between traces). (B) Cumulative concentration-response curve for AMI inhibition of calcium current in rat BF neurons. Percent inhibition of calcium current observed at five different concentrations (3, 10, 30, 100 and 300 µM) was plotted (± S.E.M.), yielding an EC_{50} of 98.02 µM. (C) Fura-2 microfluorimetric recordings of intracellular calcium transients evoked by picospritzer application of 20 mM K^+ (blue arrows, top panel: 600 ms, lower panel: 400 ms duration) show the effects of AMI on mouse BF neurons. The upper figure shows no effect of 3 µM AMI on the amplitude of calcium transients. In a different cell, the lower figure shows reversible inhibition of calcium transient amplitude by 30 µM AMI (n=4). Spontaneous Ca^{2+} events are seen in the lower panel, as well.

robust intracellular calcium transients in acutely dissociated BF neurons by applying 20 mM KCl (High $[K^+]$) by focal picospritzer. High $[K^+]$ depolarizes the membrane and activates voltage-gated Ca^{2+} channels. We then tested the ability of AMI to inhibit these transients (Figure 2.2C). AMI (30 μM) significantly inhibited high $[K^+]$-induced calcium transients by approximately 72% (Figure 2.2C, bottom panel, control: 238 ± 58.67 nM, and 30 μM AMI: 65.5 ± 19.85 nM, n=4, *$p<0.05$). On the other hand, 3 μM AMI had no effect on transient amplitude which is consistent with the previous rat BF data showing very little inhibition of Ca^{2+} currents at that concentration. We next determined the concentration-response relationship for AMI inhibition of synaptic transmission.

2.3.3 AMI decreases inhibitory synaptic transmission in mouse BF neurons

To study synaptic transmission in mouse BF neurons, we used whole-cell voltage-clamp and the reduced synaptic preparation previously described in rats (Griffith et al., 2014). Briefly, this preparation utilizes acutely dissociated neurons, without enzyme treatment, resulting in isolated cells with functional synapses. The predominant spontaneous synaptic events in this preparation are GABAergic IPSCs. These currents are easily identified, from the very infrequent spontaneous EPSCs, by their larger amplitude (using Cl^-filled electrodes, V_h = -60 mV) and long-time course compared to the smaller and very fast spontaneous EPSCs (Griffith et al., 2014). We visually identified and measured spontaneous IPSCs in both WT and VGAT mice.

Six different concentrations of AMI were tested in young mouse BF neurons: 300 pM (n=6), 1 nM (n=5), 3 nM (n=10), 3 μM (n=10), 10 μM (n=8), and 30 μM (n=11). Figure 2.3A shows whole-cell voltage-clamp recordings of sIPSCs from the BF

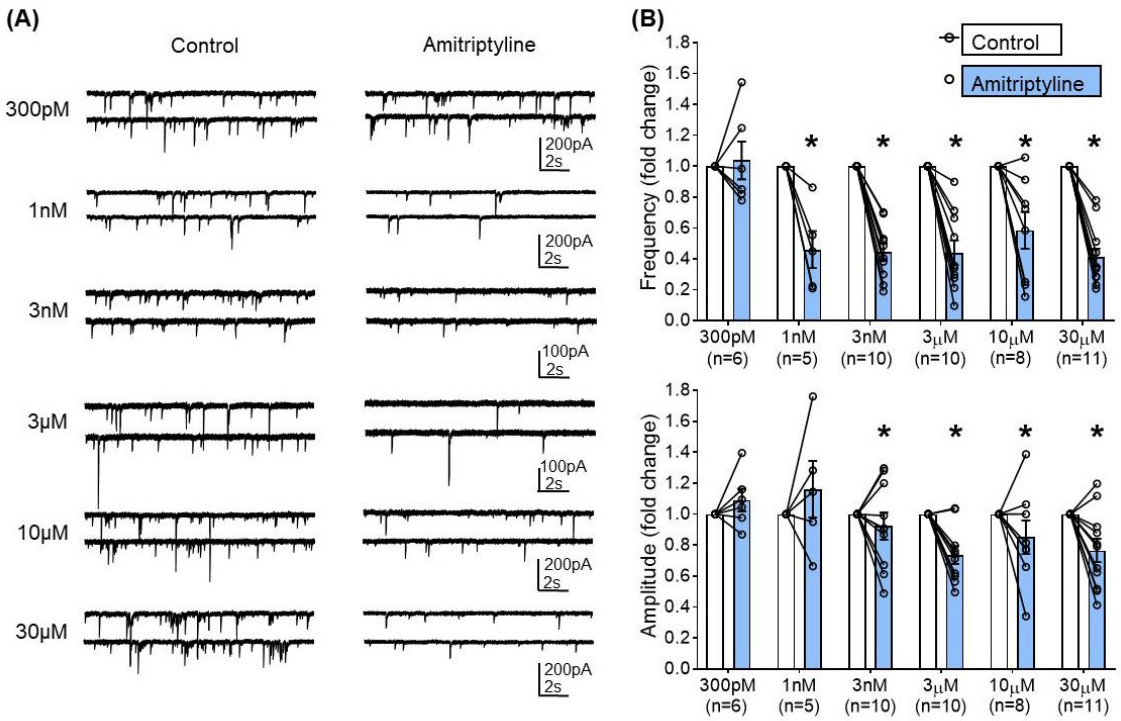

Figure 2.3. Concentration-dependent changes in the frequency and amplitude of spontaneous IPSCs using a reduced synaptic preparation of BF neurons. (A) Representative whole-cell voltage-clamp recordings (Vh = -60 mV) from young BF neurons in control (left) and AMI (right). Concentrations are shown to the left and each neuron only received one concentration of AMI. Frequency and amplitude of sIPSCs were decreased in a concentration-dependent manner by application of AMI. (B) Summary data showing the normalized frequency change in AMI (top, 300pM: 1.038 ± 0.123, 1nM: 0.460 ± 0.120, 3nM: 0.44 ± 0.06, 3μM: 0.44 ± 0.08, 10μM: 0.58 ± 0.12, 30μM: 0.41 ± 0.06) and normalized amplitude change in AMI (bottom, 300pM: 1.09 ± 0.07, 1nM: 1.11 ± 0.16, 3nM: 0.92 ± 0.09, 3μM: 0.74 ± 0.06, 10μM: 0.85 ± 0.11, 30μM: 0.77 ± 0.07). Results are presented as mean ± SEM. Individual cells (n) were paired for control and AMI (paired t-test, *$p<0.05$). N = 23 mice.

neurons in paired control and AMI for each concentration (V_h = -60 mV). The frequency of sIPSCs was significantly reduced in the presence of AMI at almost all concentrations tested (Figure 2.3B, top). The amplitude of sIPSCs was also significantly reduced by most concentrations of AMI (Figure 2.3B, bottom, paired t-test, *p<0.05). We performed the remainder of the experiments using 3 μM AMI because this concentration had minimal effect on calcium currents and transients but significantly reduced the frequency of sIPSCs. Furthermore, 3-6 μM AMI is considered a clinically relevant concentration for depression treatment (Glotzbach and Preskorn, 1982; Lavoie et al., 1990; Baldessarini, 2006).

2.3.4 AMI decreases spontaneous IPSCs in both young and aged BF neurons

The remaining experiments used both young (7-10 mo.) and aged (23-25 mo.) VGAT-ChR2-EYFP mice. In addition, these cohorts were monitored for wheel-running behavior in order to confirm the well-known age-related changes in patterns of circadian entrainment (Figure 2.7).

In young neurons, both mean frequency and mean amplitude of sIPSCs were significantly reduced by 3 μM AMI. Figure 2.4A shows whole-cell voltage-clamp recordings of sIPSCs from young BF neurons in control and AMI (V_h = -60 mV). The mean sIPSC frequencies were 1.05 ± 0.13 Hz for control and 0.24 ± 0.07 Hz in AMI (left in Figure 2.4C, paired t-test, *p<0.05), and the inhibition normalized to control frequency is shown on the right (paired t-test, *p<0.05). For sIPSC amplitude, the means were 50.06 ± 6.62 pA in control and 31.37 ± 4.44 pA in AMI (left in Figure 2.4E, paired

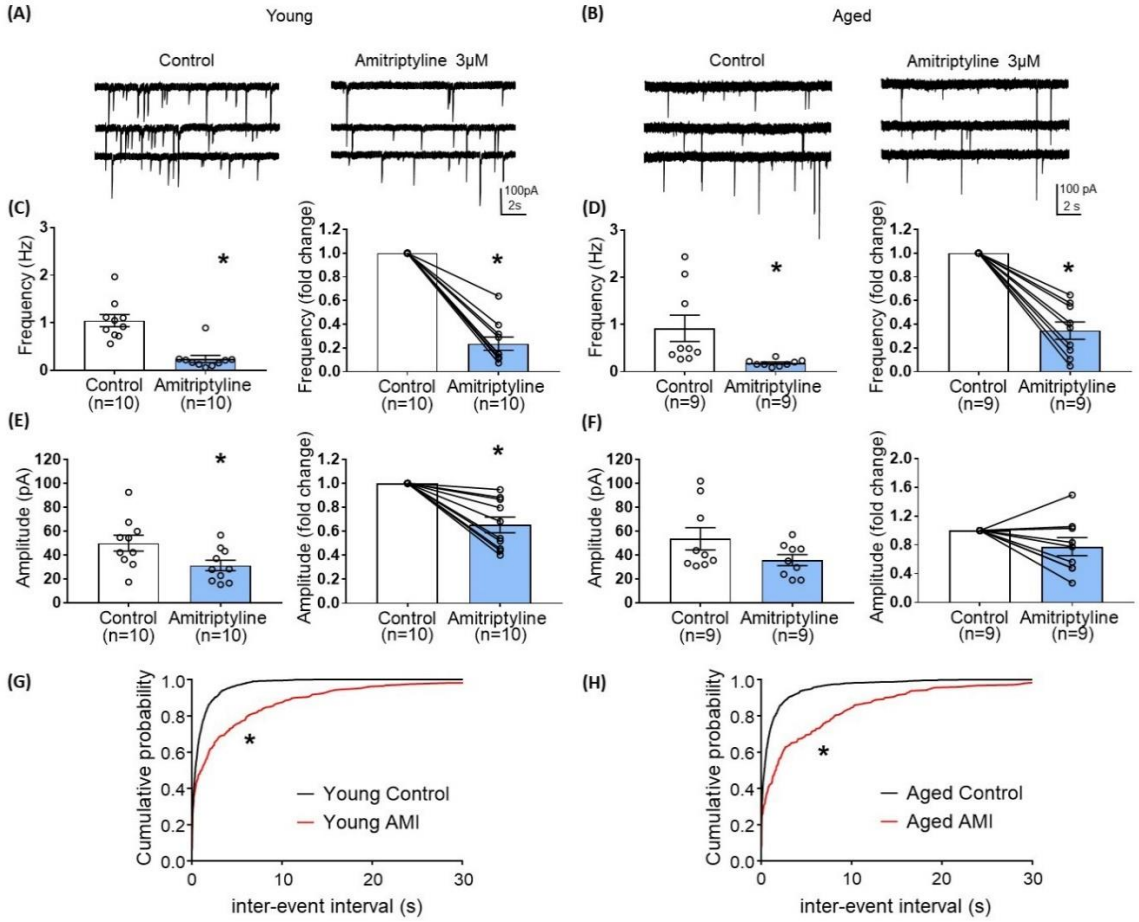

Figure 2.4. The effect of AMI (3 μM) on spontaneous IPSC frequency and amplitude in BF neurons from young and aged VGAT mice using the reduced synaptic preparation. Representative whole-cell voltage-clamp recordings (V_h = -60 mV) from a young (A) and aged (B) BF neuron in control (left) and 3 μM AMI (right). (C) Scatter plots with mean ± SEM of frequency (left panel, 1.05 ± 0.13 Hz for control, 0.24 ± 0.07 Hz in 3 μM AMI, paired t-test, *p<0.05) and graph of normalized fold change in frequency (right panel, 0.24 ± 0.06 for 3 μM AMI, paired t-test, *p<0.05) show that AMI decreases the frequency of sIPSCs in young BF neurons. (D) Scatter plots with mean ± SEM of frequency (left, control: 0.92 ± 0.28 Hz, 3 μM AMI: 0.18 ± 0.02 Hz, paired t-test, *p<0.05) and graph of normalized fold change in frequency (right, 3 μM AMI: 0.35 ± 0.07, paired t-test, *p<0.05) show that AMI decreases the frequency of sIPSCs in aged BF neurons. (E) Scatter plots with mean ± SEM of amplitude (left panel, 50.06 ± 6.62 pA in control, 31.37 ± 4.44 pA in 3 μM AMI, paired t-test, *p<0.05) and graph of normalized fold change in amplitude (right panel, 0.65 ± 0.07 in 3 μM AMI, paired t-test, *p<0.05) show that AMI decreases the amplitude of sIPSCs in young BF neurons. (F) Scatter plots with mean ± SEM of amplitude (left, control: 53.75 ± 9.32 pA, 3 μM AMI: 35.9 ± 4.58 pA, paired t-test, p=0.07) and graph of normalized fold change in amplitude (right, 3 μM AMI: 0.78 ± 0.13, paired t-test, p=0.11) show that

AMI did not significantly alter the amplitude of sIPSCs in aged BF neurons. (G) Cumulative probability plots of sIPSC inter-event intervals in young mouse BF neurons (n=10). (H) Cumulative probability plots of sIPSC inter-event intervals in aged mouse BF neurons (n=9). In AMI, the cumulative probability curves were significantly different from control (*$p<0.01$, K-S test). N = 5 young and N = 5 aged mice.

t-test, *p<0.05), and the normalized change is shown on the right (paired t-test, *p<0.05). Figures 2.4G and 2.4H show the cumulative probability curves of young and aged sIPSC frequencies in control (black) and in 3 μM AMI (red). These curves are significantly different by the Kolmogorov-Smirnov test (*p<0.01).

The same experiments were repeated in aged BF neurons (Figure 2.4B, D, F, H). Whole-cell voltage-clamp recordings (V_h = -60 mV) from the same neuron are shown in Figure 2.4B. Similar to young mice, the mean frequency of sIPSCs in aged BF neurons was significantly reduced by AMI (Figure 2.4D left, control: 0.92 ± 0.28 Hz, 3 μM AMI: 0.18 ± 0.02 Hz, paired t-test, *p<0.05). At the right on Figure 2.4D, the normalized difference between control and AMI also was significant (paired t-test, *p<0.05). Although the mean amplitude of sIPSCs in the aged group was reduced in the presence of 3 μM AMI, the change was not significant (left in Figure 2.4F, control: 53.75 ± 9.32 pA, AMI: 35.9 ± 4.58 pA, paired t-test, p=0.07). The normalized change in the sIPSC amplitude between control and AMI in aged BF neurons also was not significant (Figure 2.4F right, paired t-test, p=0.11). Despite the lack of significant effect of 3 μM AMI on aged sIPSC amplitude, the reduction of both young and aged sIPSC frequency suggests that AMI remains efficacious during aging.

2.3.5 AMI decreases light-induced oIPSCs in both young and aged BF neurons

To examine further synaptic mechanisms of AMI on inhibitory synaptic transmission, light-induced oIPSCs were measured before and after treatment with 3 μM AMI in BF neurons from young and aged VGAT mice. As seen in superimposed voltage-clamp (Vh = -60 mV) recordings in Figure 2.5A, AMI significantly decreased

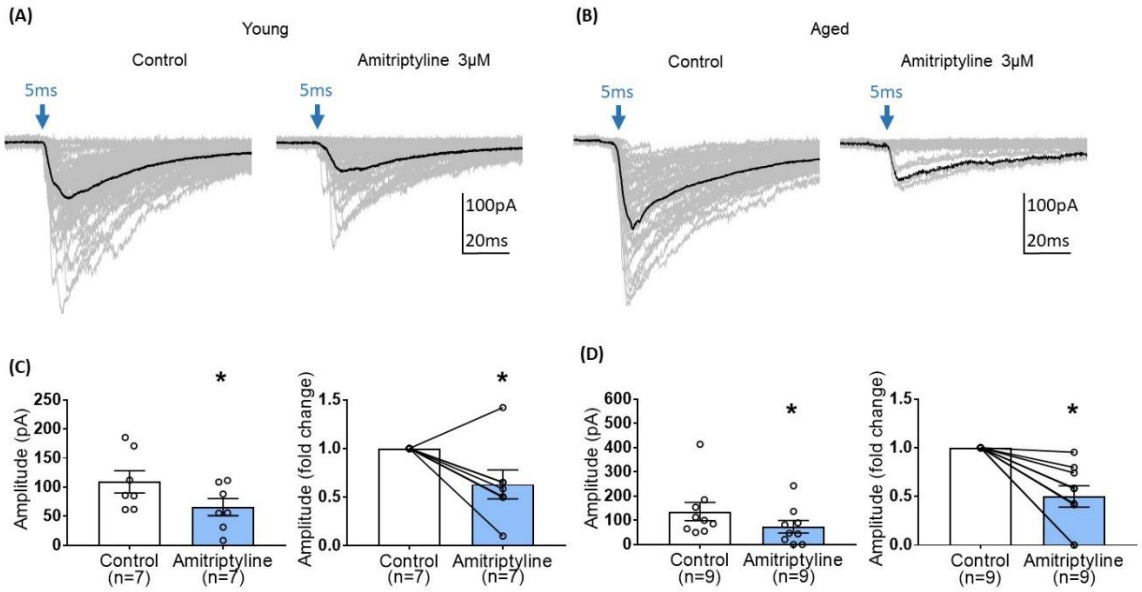

Figure 2.5. The effect of AMI (3 μM) on light-induced optical IPSC (oIPSC) amplitude in BF neurons of young and aged VGAT mice in the reduced synaptic preparation. (A and B) Superimposed (50 traces) whole-cell voltage-clamp recordings (V_h = -60 mV) of evoked oIPSCs from a young (A) and an aged (B) BF neuron in control (left) and 3 μM AMI (right). The evoking stimulus was a 5 ms pulse of 470 nm light at constant intensity (blue arrow). The black trace represents the mean oIPSC and failures were not included in the calculation. (C) Scatter plots with mean data ± SEM of oIPSC amplitude (left panel, control: 109.3 ± 19.05 pA, 3 μM AMI: 65.85 ± 14.75 pA, paired t-test, *p<0.05) and normalized fold change of oIPSC amplitude (3 μM AMI: 0.63 ± 0.15, paired t-test, *p<0.05) show that AMI significantly decreases the amplitude of light-induced oIPSCs in young BF neurons compared to control. (D) Scatter plots with mean ± SEM of oIPSC amplitude (left panel, control: 136 ± 37.88 pA, 3 μM AMI: 73.8 ± 25.83 pA, paired t-test, *p<0.05) and normalized fold change of oIPSC amplitude (3 μM AMI: 0.50 ± 0.11, paired t-test, *p<0.05) show that AMI significantly decreases the amplitude of light-induced oIPSCs in aged BF neurons. N = 5 young and N = 4 aged mice.

the amplitude of light-induced (470 nm, 5 ms, constant intensity at blue arrow) oIPSCs in young BF neurons (left in Figure 2.5C, control: 109.3 ± 19.05 pA, AMI: 65.85 ± 14.75 pA, paired t-test, *p<0.05) and the normalized amplitude (Figure 2.5C right, paired t-test, *p<0.05). Parallel experiments on oIPSCs using BF neurons from aged VGAT mice are seen in Figure 2.5B and D. Similarly, the amplitude of light-induced oIPSC (Figure 2.5B) was significantly decreased by 3 μM AMI (left in Figure 2.5D, control: 136 ± 37.88 pA, 3 μM AMI: 73.8 ± 25.83 pA, paired t-test, *p<0.05). The normalized amplitude change is shown on the right of Figure 2.5D (paired t-test, *p<0.05). In Figure 2.5A,B, the superimposed gray traces represent 50 repetitions of the stimulus and the black trace is the average. Failures were not included in the measurement of the mean amplitudes.

To investigate further a possible presynaptic contribution of AMI to reduced oIPSCs, we performed quantal analysis using the method of failures. Quantal content (m) was determined by m=ln(N/N0) as described in the methods. The power of this analysis is that no assumptions concerning synaptic number are necessary. Figures 2.6A and 6B show that minimal light stimulation (5 ms, blue arrow) generates both light-evoked currents and failures in both young and aged neurons. In the presence of AMI (3 μM), the number of failures increased in both age groups. Analysis revealed that quantal content was significantly decreased by 3 μM AMI in both young (left in Figure 2.6C, m = 2.46 ± 0.32 for control and 0.54 ± 0.11 for AMI) and aged (left in Figure 2.6D, m = 1.61 ± 0.47 for control and 0.26 ± 0.10 for AMI; paired t-test, *p<0.05). The normalized

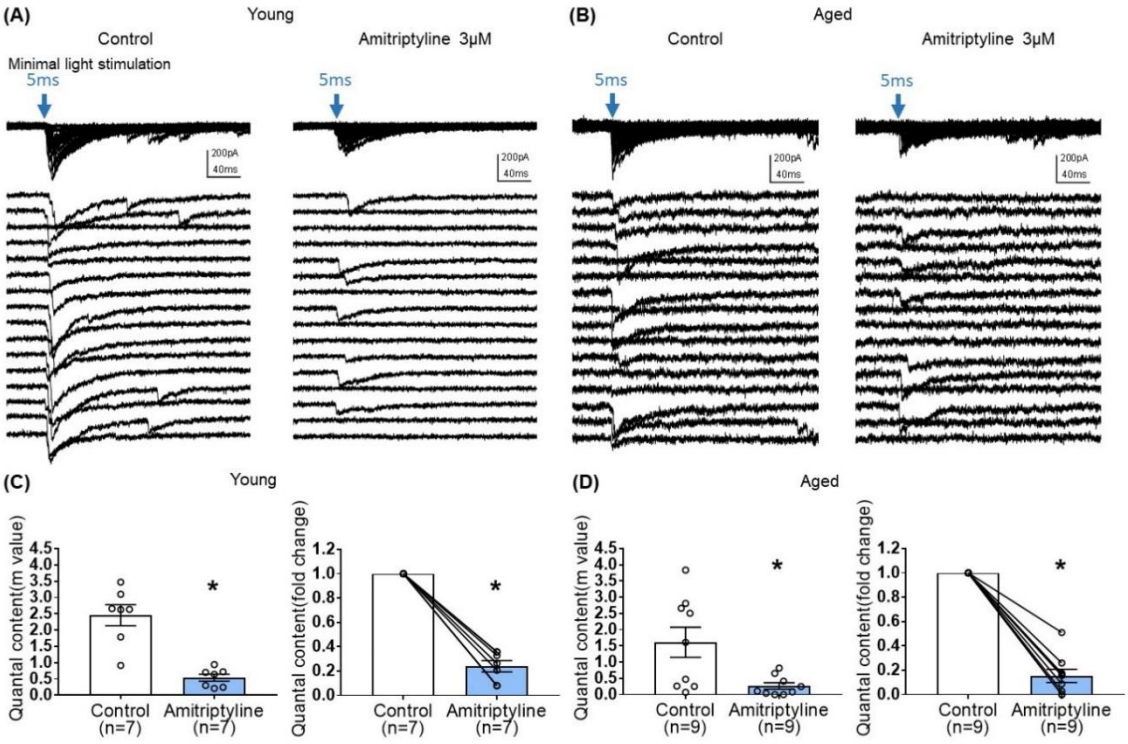

Figure 2.6. AMI (3 μM) decreases quantal content of inhibitory synaptic transmission in both young and aged BF neurons in the reduced synaptic preparation of VGAT mice. (A and B) Representative whole-cell voltage-clamp recordings (V_h = -60 mV) of oIPSCs superimposed (top) and expanded (below) in young and aged mice (left: control, right: 3 μM AMI). Blue arrow indicates 470nm light stimulation with 5-ms duration and constant minimal intensity. The expanded traces show 16 representative sweeps of the 50-100 stimulus repetitions recorded for each cell. (C) Scatter plots showing mean quantal content (m) in control and 3 μM AMI at left (m = 2.46 ± 0.32 for control, 0.54 ± 0.11 for 3 μM AMI, paired t-test, *p<0.05) and on the right panel showing normalized fold change of quantal content by AMI in young BF neurons (3 μM AMI: 0.24 ± 0.05, paired t-test, *p<0.05). (D) Graphs showing quantal content (m) in control and 3 μM AMI in aged BF neurons (left, m = 1.61 ± 0.47 for control, 0.26 ± 0.10 for 3 μM AMI, paired t-test, *p<0.05) and normalized fold change of quantal content by 3 μM AMI in aged BF neurons (right, 3 μM AMI: 0.15 ± 0.05, paired t-test, *p<0.05). Quantal content (m) of inhibitory synaptic transmission was significantly decreased by application of AMI both in young and aged BF neurons. Bars represent mean ± SEM. N = 5 young and N = 4 aged mice.

fold change in quantal content between control and AMI is shown to the right in Figure 2.6C,D (paired t-test, *p<0.05).

2.3.6 Effect of age on daily circadian wheel-running entrainment

For our electrophysiology experiments described above using VGAT mice (Figures 2.4-2.6), we utilized the well characterized circadian wheel-running entrainment model to validate our optogenetic aging model. During exposure to LD 12:12, entrainment of the activity rhythm was observed in all WT and VGAT mice. Representative actograms of young and aged animals from both WT (Figure 2.7A) and VGAT (Figure 2.7B) mice are shown and constitute the raw data from which the analysis (Figure 2.7C-E) was conducted. During entrainment to LD 12:12, young and aged mice of both genotypes were distinguished by robust differences in the total amount of daily wheel-running activity. Daily activity levels (wheel revolutions/24hr) were significantly and up to 8-fold greater in young WT and VGAT mice compared to aged subjects (Figure 2.7C, two-way ANOVA, age effect; $F(1,28) = 51.02$, *$p<0.0001$). No effect of genotype was observed in daily wheel-running activity (two-way ANOVA, genotype effect; $F(1,28) = 0.85$, $p = 0.36$). In both WT and VGAT mice, the young and aged cohorts were characterized by clear differences in their patterns of circadian entrainment. In the young mice, daily onsets of activity occurred near or shortly after lights-off such that the average phase angle (Ψ) between the activity onsets and the offset of the photoperiod was -7.70 ± 2.63 for WT and -4.97 ± 0.97 min for VGAT (Figure 2.7D). In contrast, the activity rhythms of aged mice were distinguished by an altered phase angle of entrainment to LD 12:12 such that their daily onsets of activity were delayed and

occurred at later times relative to young animals, commencing more than 20 minutes after lights-off for most animals (Figures 2.7A, B and D). In the aged WT and VGAT groups, the average phase angles were –28.76 ± 3.94 and –30.93 ± 3.57 min, respectively. These values were significantly greater than those observed in young animals for each genotype (Figure 2.7D, two-way ANOVA, age effect; $F(1,28) = 41.74$, $^*p<0.0001$). There was no effect of genotype on phase angle of activity (two-way ANOVA, effect of genotype; $F(1,28) = 0.01$, $p = 0.95$). In addition to the delayed onsets of daily activity, aged WT and VGAT animals showed unstable patterns of entrainment to LD 12:12 as indicated by high variability in the timing of their activity onsets between successive days (Figures 2.7A, B and E). During exposure to LD 12:12, the activity onsets in individual aged WT and VGAT mice occurred at (earlier or later) times that differed on average respectively by 54.88 ± 5.70 and 61.21 ± 6.49 minutes from the preceding day. Whereas the average day-to-day variability in activity onset times of young animals was only 18.38 ± 5.03 (WT) and 24.33 ± 5.84 (VGAT) minutes (Figure 2.7E). The values for day-to-day variation in the onsets of activity in the aged WT and VGAT groups were significantly greater (two-way ANOVA, age effect; $F(1,28) = 33.29$, $^*p<0.0001$) than those observed in their young counterparts. No significant difference in day-to-day variability in activity onset times was observed between age-matched WT and VGAT mice (two-way ANOVA, effect of genotype; $F(1,28) = 0.93$, $p = 0.34$).

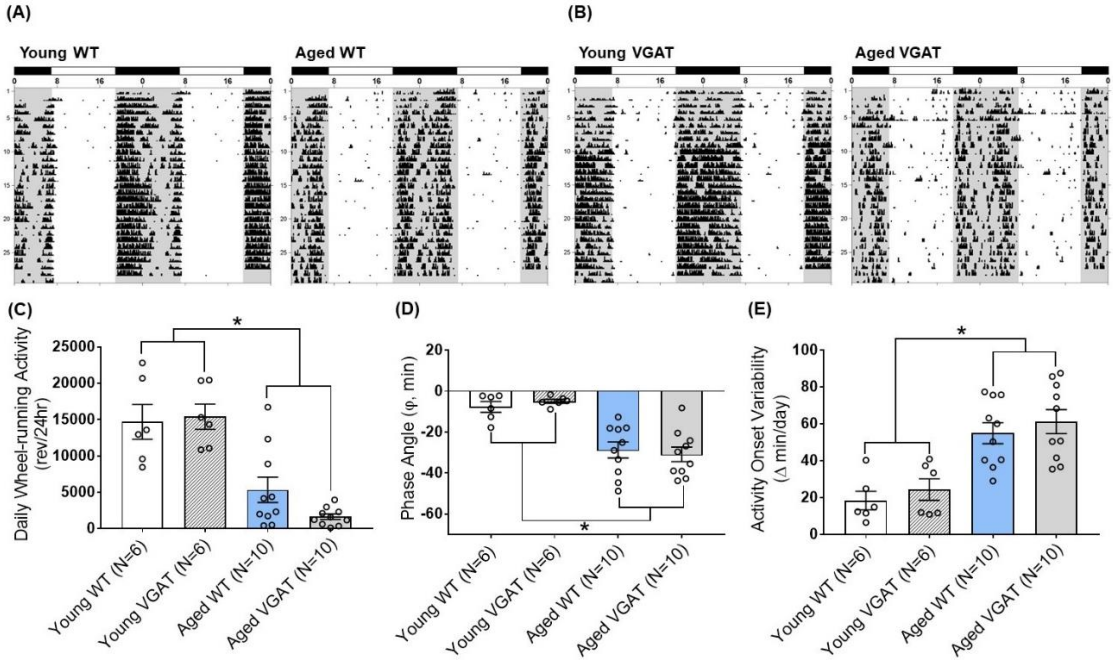

Figure 2.7. **Effects of aging on light-dark entrainment and other properties of the circadian rhythm of wheel-running activity in WT and VGAT mice.** Representative records of circadian wheel-running behavior in WT (A) and VGAT (B) mice comparing the activity rhythms of young (left) and aged (right) animals during entrainment to LD 12:12. Actograms are double-plotted over a 48-hour period. Each dot on the actogram represents 50-wheel rotations per 10-minute window. The closed bars at the top and shading on the records signify the timing of the dark phase in the LD 12:12 cycle. (C) Total daily wheel-running activity of young and aged mice for each genotype (WT, VGAT). Bars depict average wheel revolutions per 24hr (±SEM) (Young WT: 14695 ± 2387, Young VGAT: 15410 ± 1740, Aged WT: 5358 ± 1744, Aged VGAT: 1655 ± 382.7, two-way ANOVA, age effect; $F(1,28) = 51.02$, *$p<0.0001$, genotype effect; $F(1,28) = 0.85$, $p = 0.36$). (D) Phase angle between daily activity onsets and lights-off during LD 12:12 entrainment in young and aged WT and VGAT mice. Bars represent the mean (± SEM) phase angle of entrainment (Ψ) to LD 12:12 in minutes. Negative values indicate that daily onsets of activity occur after lights-off whereas positive values denote that activity onsets precede the end of the light phase (Young WT: -7.70 ± 2.63 min, Young VGAT: -4.97 ± 0.97 min, Aged WT: -28.76 ± 3.94 min, Aged VGAT: -30.93 ± 3.57 min, two-way ANOVA, age effect; $F(1,28) = 41.74$, *$p<0.0002$, effect of genotype; $F(1,28) = 0.01$, $p = 0.95$). (E) Absolute day-to-day variability in daily onsets of activity. Absolute differences in the timing of activity onsets on successive days were analyzed in individual animals and bars represent mean (± SEM) determinations in minutes (Young WT: 18.38 ± 5.03 min, Young VGAT: 24.33 ± 5.84 min, Aged WT: 54.88 ± 5.70 min, Aged VGAT: 61.21 ± 6.49 min, two-way ANOVA, age effect; $F(1,28) = 33.29$, *$p<0.0001$, effect of genotype; $F(1,28) = 0.93$, $p = 0.34$). There were no significant differences between genotypes. N = 6 young and N = 10 aged mice for each genotype.

2.4 Discussion

In the present study, we show that therapeutic concentrations of AMI decrease spontaneous and light-evoked IPSCs in BF neurons at concentrations below those that block HVA Ca^{2+} currents. Importantly, this synaptic inhibition is preserved during aging. The therapeutic concentrations of AMI for the treatment of depression are 3-6 μM (Lavoie et al., 1990; Glotzbach and Preskorn, 1982), while lower concentrations are also effective for chronic pain and migraine (Suga et al., 2019; Riediger et al., 2017; Urquhart et al., 2018). These therapeutic actions of AMI are maintained in the elderly (Barber and Gibson, 2009). Our data suggest that inhibition of GABAergic synaptic transmission may be one of the mechanisms by which AMI acts therapeutically across aging. In our model, a low concentration of AMI, in the therapeutic range, reduced inhibitory synaptic transmission, whereas higher concentrations were required to block HVA Ca^{2+} currents and high K^+ induced intracellular Ca^{2+} transients.

AMI has a broad profile of pharmacological actions, including inhibition of biogenic amine reuptake, antagonism of serotonin, muscarinic, α1-adrenergic, and histamine receptors (Pandey et al., 2010; Nojimoto et al., 2010; Liu et al., 2012; Richelson, 1979; Kachur et al., 1988). It also acts to block Ca^{2+} and Na^+ channels (Brau et al., 2001; Nicholson et al., 2002; Yan et al., 2010; Wu et al., 2012). Additional actions of AMI are described for the NMDA receptor ion channel complex that may contribute to efficacy against neuropathic pain, including the enhancement of Ca^{2+}-dependent receptor desensitization and acting as an open channel blocker of NMDARs (Stepanenko et al., 2019). The enhancement of NMDA receptor desensitization shows a strong

dependence on extracellular [Ca^{2+}] concentrations with an e-fold shift in IC_{50} achieved by a [Ca^{2+}] change of 0.63 mM (Stepanenko et al., 2019). These actions on the NMDA receptor provide a likely mechanism for results showing that AMI inhibited the NMDA-dependent LTP in the hippocampus (Watanabe et al., 1993). Also, the Stepanenko study reported an IC_{50} value of 4.9 μM in [2mM] Ca^{2+} that is very similar to the concentration used in our experiments (Figures 2.4-2.6) and suggests that AMI may mediate important actions to regulate neurotransmitters by a mechanism that does not involve voltage-gated channels. However, a slight inhibition of presynaptic I_{Ca} cannot be ruled out, as concentrations of AMI as low as 1 μM have been shown to modestly inhibit I_{Ca} in trigeminal ganglion neurons (Wu et al., 2012).

The probability of neurotransmitter release is directly proportional to the Ca^{2+} change within the synaptic terminal (Zucker, 1993; Wu and Saggau, 1997) and AMI regulation of synaptic transmission by this mechanism has been shown using mechanically isolated medullary dorsal horn neurons (Cho et al., 2012). Here, glycinergic neurotransmission is enhanced by higher concentrations of AMI (30 μM) through a suggested presynaptic mechanism to increase neurotransmitter release. These authors provide evidence that AMI increases spontaneous miniature glycinergic IPSCs onto acutely isolated neurons by increasing the interterminal Ca^{2+} concentration, which might be mediated by the Ca^{2+} release from the Ca^{2+} stores rather than the Ca^{2+} influx from the extracellular space. (Cho et al., 2012). Chronic AMI (and other antidepressant) treatments have been shown to affect synaptic plasticity in the hippocampus (Zarei et al., 2014; Zhang et al., 2020) with fewer studies focusing on the acute actions of AMI to

regulate synaptic transmission (Watanabe et al., 1993). It is interesting to speculate that, in our study, AMI may decrease the frequency of sIPSCs by a mechanism that regulates intraterminal Ca^{2+} stores. We did not measure directly the change in intraterminal Ca^{2+} concentrations induced by AMI but did not observe a change in somatic baseline [Ca^{2+}] on exposure to either 3 or 30 μM AMI (Figure 2.2). Whereas, presynaptic modulation of neurotransmitter release has been long tied to modulating terminal Ca^{2+} channels, other mechanisms may also come into play to modulate synaptic transmission including fast acting neurotropic factors (Berninger and Poo, 1996; Kovalchuk et al., 2004) and transmembrane regulation of synapses (Tang et al., 2016; Biederer et al., 2017; Han et al., 2021).

Neurotrophins have been implicated in the therapeutic effects of antidepressants with brain derived neurotrophic factor (BDNF) acting as one of the most popular candidates (reviewed Dwivedi 2009; Colucci-D'Amato et al., 2020). Interestingly, AMI possesses neurotrophic effects by acting directly as an agonist of TrkA and TrkB receptors which BDNF triggers (Jang et al., 2009). AMI may exert neurotrophic effects in primary cortical neurons by activation of a Trk/MAPK signaling pathway and possibly alleviating the loss of synaptic connections under conditions where atrophy and loss of synaptic connections may contribute to progression of neurological diseases (O'Neill et al., 2016). Because BDNF has been proposed as a key transducer of the effects of antidepressants (Björkholm et al., 2016), it is no surprise that the ability of BDNF to rapidly modulate synaptic transmission has been studied extensively (Kim et al., 1994; Berninger and Poo, 1996; Kovalchuk et al., 2004; Poo, 2001). In the

hippocampus, BDNF decreases inhibitory GABAergic transmission (Tanaka et al., 1997; Frerking et al., 1998) whereas BDNF increases excitatory transmission (Tyler et al., 2006). This bidirectional control of synaptic transmission by BDNF would be consistent with the observed effects of AMI if it was acting on synaptic transmission through Trk receptors. While our results showed that acute AMI can decrease synaptic transmission by a presynaptic mechanism to decrease quantal release, in cultured organotypic slices of brainstem noradrenergic neurons in the A1 and A2 area, one-week treatment of 10 μM AMI increased quantal size and shifted the distribution of events (Chiti and Teschemacher, 2007). It is possible that AMI either acts directly or indirectly through neurotrophins to regulate synaptic transmission depending upon the specific synapses and releasable pools of transmitter (Tyler et al., 2006).

Previously, we found that sIPSC frequency in cholinergic BF neurons is reduced during aging and is associated with cognitive impairment in rats (Griffith et al., 2014). In the present study, AMI decreased the frequency of sIPSCs in young and aged BF neurons of mice. This suggests that AMI could have a negative influence on cognitive function, particularly in the aged. There are numerous studies reporting the effects of AMI on memory and cognitive functions both in humans and in rodent models, however, conclusions differ depending on the experimental conditions. For studies reporting cognitive impairment following AMI treatment, in most cases, a single dose of AMI was administered (Branconnier et al., 1982; Curran et al., 1988; Parra et al., 2002). On the other hand, chronic treatment with AMI demonstrated beneficial effects on cognitive function in clinical and in animal studies (Sternberg and Jarvik, 1976; Staton et al., 1981;

Yau et al., 2002; Chadwick et al., 2011). Chronic AMI has been shown to prevent age-related decline and impairment in the water maze task in rats when treatment was initiated at 16 months of age and then tested at 24 months (Yau et al., 2002). These authors suggest that the use of antidepressants may serve as a useful therapeutic approach possibly to ameliorate cognitive impairments in aged individuals.

In our study, we demonstrated that the actions of AMI to reduce synaptic transmission continued during aging in our optogenetic model. We utilized circadian behavioral activity to establish that a parameter of normal aging occurred in this model. Circadian rhythm alterations and disturbances are part of the normal aging process in humans, and these changes in circadian function are further amplified in patients with symptomatic Alzheimer disease (AD) (Witting et al., 1990; Harper et al., 2005). Age- and AD-related changes in circadian rhythms are most pronounced in the sleep-wake cycle (Olivier-Martin et al., 1975; Peter-Derex et al., 2015). Circadian disturbances of sleep-wake rhythms in aging and AD include rhythm fragmentation over the entire cycle with increased nighttime and decreased daytime bouts of activity in conjunction with a decrease in rhythm amplitude (Weitzman et al., 1982; Satlin et al., 1995; Harper et al., 2005; Peter-Derex et al.,2015, Musiek et al., 2018). In AD, these changes in the sleep-wake cycle are often accompanied by a phase delay in peak daily activity that is associated with an increased risk of moderate to severe dementia (Tranah et al., 2011). The effects of aging on rodent circadian rhythms are comparable to those observed in human aging and AD. Common alterations in the circadian activity of aged rodents include alterations in the amplitude and day-to-day accuracy of the activity rhythm and

in its entrainment to light-dark cycles (Rusak and Zucker, 1979; Ingram et al., 1982). Consistent with the age-related changes in sleep-wake rhythms reported in humans and rodents, aged WT and VGAT mice in the present study were distinguished by phase delays and increased day-to-day variability in the activity onsets during entrainment to the daily light-dark cycle. Consequently, these findings establish the utility of the VGAT-ChR2 optogenetic mouse as a model to study the relationship between aging and circadian rhythm disturbances. As such, future studies will determine whether this circadian dysfunction precedes cognitive impairment during aging and thus provide a biomarker of preclinical dementia.

Our laboratory recently developed a new optogenetic aging model which demonstrated that expression of the channelrhodopsin in the VGAT mouse line remained functional throughout the lifespan of the mice and there is no effect of genotype (wild type versus VGAT-ChR2-EYFP) on aging-related physiological and behavioral properties (Montgomery et al., resubmission). Here we present data showing that therapeutically relevant concentrations of AMI inhibited sIPSC frequency in the mouse BF neurons regardless of animal age. Given that changes in the frequency reflect changes in probability of neurotransmitter release from presynaptic sites, reduction in sIPSC frequency by AMI suggests that AMI is likely to act presynaptically to decrease the probability of spontaneous GABA release on BF neurons. AMI also significantly decreased the amplitude of sIPSCs in young BF neurons but not quite significantly in aged BF neurons. This indicates that AMI may work on both pre- and post-synaptic sites, perhaps with a greater impact at pre-synaptic sites. This conclusion was supported

by the findings that AMI significantly decreased the amplitude of light-induced oIPSCs as well as the quantal content in both young and aged BF neurons without age-related differences. Future studies will be needed to investigate further possible pre-and postsynaptic mechanisms of AMI.

2.5 Materials and Methods

2.5.1 Animals and Treatments

Preliminary experiments to construct a concentration response curve for AMI inhibition of high voltage-activated (HVA) calcium currents utilized juvenile Fischer 344 rats. We have experience studying the physiology and pharmacology of Ca^{2+} currents in basal forebrain neurons of Fischer 344 rats (Murchison and Griffith, 1996, 1998), and therefore, used juvenile rats to confirm the concentration range for Ca^{2+} current inhibition by AMI. Pregnant F344 dams were obtained (Harlan, Indianapolis, IN) and allowed to give birth. Juveniles of both sexes were used between 10 and 30 days of age. For all other experiments we used VGAT-ChR2(H134R)-EYFP and wildtype (WT) C57 Bl/6 mice. Breeding pairs were purchased from Jackson Labs (Stock 014548; Zhao et al., 2011) and we established an aging colony where mice of all ages and both genotypes could be obtained. Mice were identified as WT or VGAT by standard tail-clip genotyping methods after weaning. Genotyping was done on a MJ PTC-100 Thermocycler (Bio-Rad Laboratories, Hercules, CA) using the EZ BioResearch Fast Tissue/Tail PCR Genotyping Kit (EZ BioResearch, St. Louis, MO) with value oligo primers from ThermoFisher (Waltham, MA) and sequence from Jackson Lab (Bar Harbor, ME): transgene (~400 bp): forward primer 11678: 5′-ACC CTT CTG TCC TTT

TCT CC-3′, reverse primer 10493: 5′-GCA AGG TAG AGC ATA GAG GG-3′ and internal control (324 bp): forward primer oIMR7338: 5′-CTA GGC CAC AGA ATT GAA AGA TCT-3′, reverse primer oIMR7339: 5′-GTA GGT GGA AAT TCT AGC ATC C-3′. Samples were run with Bulldog Bioflex S50 DNA ladder (Portsmouth, NH) on 2% Agarose gel using 1 X TBE buffer with SYBR Safe DNA gel stain for 1.5hr and imaged either on a Flourchem Q or an Accuris Smartdoc.

For the data in Figure 2.3, to determine the concentration response relationship for AMI inhibition of spontaneous synaptic transmission, young mice were between 2 and 7 months of age (N=23). For all other studies for age and AMI comparisons (Figures 2.4-2.6) all mice underwent circadian wheel-running prior to drug testing. For wheel-running behavior, young wildtype (WT, N=6) and VGAT (N=6) mice were 7-10 months while aged WT (N=10) and VGAT (N=10) mice were 23-25 months. ‘N’ refers to the number of mice, while ’n’ is the number of neurons. All rodents were maintained in the AAALAC-accredited vivarium at the Texas A&M University Health Science Center under controlled conditions (22 – 25°C; lights 0700-1900 h; mouse chow and water ad lib) in accordance with policies of the Texas A&M University Laboratory Animal Care Committee and NIH guidelines. TAMU animal protocol number 2019-0362.

2.5.2 Immunohistochemistry

Mice were deeply anesthetized with isoflurane and transcardially perfused with ice-cold phosphate-buffered saline (PBS, 0.01 M, pH 7.4) followed by a fixative, 4% paraformaldehyde (PFA) in PBS. Brains were quickly removed from the skull and post-fixed overnight in the same solution at 4 °C followed by dehydration in 30% sucrose

solution overnight at 4 °C. The brain was cut into 40-μm coronal sections using a freezing microtome. Sections were washed 3 times in Tris-buffered saline (TBS, 100 mM Tris-HCl, 150 mM NaCl, pH 7.5) and then permeabilized with TBST (0.1% Triton X-100 in TBS) for 30 minutes at room temperature (RT). After permeabilization, sections were blocked (1.5 hr at RT) with 5% normal donkey serum in TBST and were incubated in primary antibody with blocking solution overnight at 4 °C. After incubation with primary antibody, sections were washed in TBS three times and incubated in secondary antibody with blocking solution for 2 hr at RT followed by three-time wash in TBS. Lastly, they were mounted in Vectashield (Vector Laboratories, Burlingame, CA) and examined under a confocal laser-scanning microscope (FV1200, Olympus, Shinjuku City, Tokyo). Antibodies targeting the following proteins were used: GFP (1:5000; Abcam, Cambridge, MA) and NeuN (1:1000; Millipore, Burlington, MA). The Alexa Fluor 488-conjugated goat anti-chicken IgY (H+L) antibody (1:300; Invitrogen, Carlsbad, CA) and Alexa Fluor 647-conjugated donkey anti-mouse IgG (H+L) antibody (1:300; Invitrogen, Carlsbad, CA) were used for secondary antibodies.

2.5.3 Circadian wheel running measurements

For circadian measurements of wheel- running activity, mice were housed individually in cages equipped with running wheels. Animals were maintained on a standard 12h light/12h dark cycle (LD 12:12; lights-on at 0600 h) and their circadian rhythms of wheel-running were continuously recorded for 30 days. Revolutions were summed and stored in 10-min bins, graphically depicted in actograms and analyzed using a computer running ClockLab data collection and analysis software (ActiMetrics,

Evanston, IL). Entrainment and qualitative parameters of the activity rhythm were measured over the same interval for all animals. During entrainment to LD 12:12, the onset of activity for a given cycle was identified as the first bin during which an animal attained 10% of peak running-wheel revolutions (i.e. intensity). To measure angle of entrainment, least squares analyses was used to establish a regression line through the daily onsets of activity during the period of entrainment (30 days), and then the number of minutes before (positive) or after (negative) the time of lights-off in the LD cycle (1800 h) was determined for each animal. Total daily activity was calculated by averaging the number of wheel revolutions per 24 h over the 30-day interval of analysis.

2.5.4 Acutely dissociated neurons and reduced synaptic preparation

Rats and mice, were decapitated after isoflurane anesthetization and brain slices (400 μm for rats, 320 μm for mice) were micro dissected to isolate the medial septum and nucleus of the diagonal band (MS/nDB), as described previously (Murchison and Griffith, 1996; Griffith et al., 2014). This tissue was kept suspended in a holding solution (mM): 140 NaCl, 2.7 KCl, 0.5 $CaCl_2$, 1.2 $MgCl_2$, 10 HEPES, and 33 D-glucose (pH 7.4 with NaOH, 310-330 mOsm) by a small magnetic stir bar and was continuously oxygenated with 100% O_2 in a holding chamber. Individual tissue pieces were triturated in a pair of fire-polished glass pipettes, and the dissociated cells were dispersed and allowed to settle onto the glass floor of a recording chamber containing bath solution (mM): 140 NaCl, 2.7 KCl, 2 $CaCl_2$, 1.2 $MgCl_2$, 10 HEPES, and 33 D-glucose, then perfused at a rate of about 2ml/min. Experiments were performed at room temperature within 5 h of dispersal. For the rat whole-cell Ca^{2+}-current experiments and mouse fura-2

experiments depicted in Figure 2.2, the pieces of BF slices were treated with trypsin (Sigma, type XI or type I, St. Louis, MO) as described previously (Murchison and Griffith 1996, 1998). Importantly, for the synaptic studies in mice, no enzyme was used prior to dissociation in order to preserve presynaptic terminals on the reduced synaptic preparation (Griffith et al., 2014). This method is similar to that described by Akaike and Moorhouse (2003) to obtain a nerve-bouton preparation, however we have refined this technique to include aging neurons.

2.5.5 Electrophysiology

Whole-cell and perforated-patch voltage-clamp recordings were used. Whole-cell recording techniques were used for measuring spontaneous inhibitory postsynaptic currents (sIPSCs) and optically-evoked IPSCs (oIPSCs) while perforated-patch recordings were used for the calcium current experiment. Voltage-clamp recordings were performed using a Multiclamp 700B amplifier or Axopatch 200A (Molecular Devices, San Jose, CA), Digidata 1440A interface and pClamp 10 software (Molecular Devices, San Jose, CA). Membrane capacitance (pF) was obtained by digital cancellation of whole-cell capacitance transients. Recordings for sIPSCs and oIPSCs were made from a holding potential of -60mV, low-pass filtered at 2 kHz and digitized at 10 kHz. Patch pipettes were pulled from glass capillary tubing (KG-33, 1.5mm OD, King Precision Glass, Claremont, CA) on a Flaming/Brown P-87 pipette puller (Sutter Instrument ®, Novato, CA) with resistance 4-8 MΩ when filled with a pipette solution. The internal pipette solution for whole-cell recordings contained (mM): CsCl, 130; ethylene glycol-bis (β-aminoethyl ether) N,N,N',N'-tetraacetic acid (EGTA), 10; $MgCl_2$,

2; HEPES, 10; Mg-ATP, 4; GTP, 0.1; pH 7.2 with CsOH; 295-300 mOsm, as described previously (Murchison and Griffith, 1996). For perforated-patch recordings, the internal solution contained (mM): CsAc, 120; CsCl, 15; HEPES, 20; EGTA, 0.4; and amphotericin B (240 mg/ml), pH 7.2, 290-300 mOsm. AMI (Sigma, St. Louis, MO) was prepared as a 10mM stock solution in distilled water and diluted in external bath solution for each experiment just before use.

2.5.5.1 Measuring Calcium currents from rat BF neurons

Acutely dissociated neurons from juvenile rats were used for these studies, as describe above in section 2.5.4. For experiments studying calcium currents, barium (2 mM) was used as the charge carrier and voltage-clamp was obtained by the perforated-patch method using amphotericin B (240 mg/ml) (Murchison et al., 2009). Amphotericin B was included in the patch pipette and neurons were allowed to dialyze (~4 minutes after maximum perforation) prior to recording. Cells were held at -70 mV and a test pulse (to -15 mV, 90 ms duration) was applied every 20 s. Barium replaces calcium as the charge carrier in the bath recording solution to prevent calcium-dependent processes and was used throughout the experiment as described in our previous studies (Murchison et al., 2009). Increasing concentrations of AMI were applied by focal drug barrel until a stable current was obtained. Currents were measured from 0 mV to peak, and the percent inhibition of HVA calcium current by AMI was plotted.

2.5.5.2 Optically-induced current recordings and quantal content analysis

Neurons in the reduced synaptic preparation were mechanically dissociated from small sections of basal forebrain as describe above and dispersed onto a recording

chamber. Optical stimulation was applied using 5-ms duration of 470 nm light at 15 s intervals using an optogenetic illumination system (DC2100, Thor Labs, Ann Arbor, MI) and 50-100 traces of optically-induced inhibitory postsynaptic currents (oIPSCs) were recorded. For the quantal content analysis, minimal stimulation was used in order to ensure a sufficient number of failures. LED intensity was controlled by adjusting the drive current (1mA-1A). Power density was calculated by dividing the measured power by the measured illuminated area using a PM200 optical power and energy meter (ThorLabs, Ann Arbor, MI) connected to an S120C photodiode sensor (ThorLabs, Ann Arbor, MI). Initial measurements using a 400 μm cannula revealed a maximum power density of approximately 10 mW/mm^2, and a power density of 1.76 mW/mm^2 corresponding to 100mA drive current. For the quantal content analysis, using the method of failures ($m = \ln(N/N_0)$) in the Poisson model, quantal content (m) was calculated where N is total number of stimuli, and N_0 is the number of failures where stimulation failed to evoke a synaptic response.

2.5.5.3 Electrophysiological analysis

Mini Analysis (6.0.7; Synaptosoft, Decatur, GA) and Clampfit 10 (Molecular Devices, San Jose, CA) software were employed for the analysis. The evoked response was calculated as the peak current over 20 ms from the time when response begins. Mean data were compared using a paired t-test with significance determined by $p< 0.05$ (GraphPad, San Diego, CA). Values were expressed as mean ± S.E.M.

2.5.6 Calcium imaging

Standard fura-2 ratiometric microfluorimetry (Murchison and Griffith, 1998, 2007; Murchison et al., 2009) was used to measure intracellular calcium changes in enzyme-treated mouse BF neurons. Neurons were acutely dissociated and dispersed onto a cover slip and were loaded with ratiometric fluorescent Ca^{2+}-indicator fura-2AM (1 μM, Molecular Probes, Eugene, OR) from the bath for 12 min in the presence of 10 μM pluronic acid (Invitrogen, Carlsbad CA) followed by 40-45 min washout to allow for fura de-esterification. The resulting fluorescence is equivalent to ~100 μM impermeable salt of fura-2 (pentapotassium salt, fura-2 K^{+}_{5}). Fluorescence was recorded with 340 nm and 380 nm excitation and the 340/380 ratio, which increases with increasing $[Ca^{2+}]$ was calculated. In order to achieve an adequate sampling rate for the fura-2 data shown in Figure 2.2, the pixels were binned and the fluorescent intensities were measured from a region of interest, centered on and smaller than the cell soma. Intracellular calcium concentrations ($[Ca^{2+}]_i$) were estimated as described previously (Murchison and Griffith, 1998). Ca^{2+}-transients ($\Delta[Ca^{2+}]_i$) were triggered by focal picospritzer (Picospritzer II, General Valve, Fairfield NJ) application of recording solution with elevated $[K^{+}]$ (20mM) solution (High $[K^{+}]$). Fluorescent signals were recorded using a Sutter lambda DG-4 excitation switcher (Sutter Instrument ®, Novato, CA), a Hamamatsu ORCA flash2.8 CCD camera (Hamamatsu Photonics, Bridgewater Township, NJ), an Olympus IX70 fluorescent scope and Metafluor imaging software (Molecular Devices, San Jose, CA).

2.5.7 Statistical analysis

Comparisons were performed using a paired t-test with significance determined by $p<0.05$ (GraphPad, San Diego, CA). Values are expressed as means ± S.E.M. For wheel-running statistical analyses, raw data were analyzed using a two-way ANOVA to determine the significance of age and genotype effects on circadian properties and quantitative parameters of the activity rhythm. In each case, differences in circadian behavior were considered significant at $p<0.05$.

2.6 References

Akaike, N., and Moorhouse, A. J. (2003). Techniques: applications of the nerve-bouton preparation in neuropharmacology. Trends. Pharmacol. Sci. 24, 44-47. doi: 10.1016/s0165-6147(02)00010-x

Baldessarini, R. J. (2006). "Drug therapy of depression and anxiety disorders" in Goodman & Gilman's. The pharmacological basis of therapeutics, 11th edition (New York, NY: McGraw Hill), 429-459.

Barber, J. B., and Gibson, S. J. (2009). Treatment of chronic non-malignant pain in the elderly. *Drug-Safety* 32, 457-474. doi: 10.2165/00002018-200932060-00003

Biederer, T., Kaeser, P. S., and Blanpied, T. A. (2017). Transcellular nanoalignment of synaptic function. *Neuron.* 96, 680-696. doi: 10.1016/j.neuron.2017.10.006

Björkholm, C., and Monteggia, L. M. (2016). BDNF - a key transducer of antidepressant effects. *Neuropharmacology.* 102, 72-79. doi: 10.1016/j.neuropharm.2015.10.034

Branconnier, R. J., Devitt, D. R., Cole, J. O. and Spera, K. F. (1982). Amitriptyline

selectively disrupts verbal recall from secondary memory of the normal aged. *Neurobiol. Aging* 3, 55-59. doi: 10.1016/0197-4580(82)90061-6

Brau, M. E., Dreimann, M., Olschewski, A., Vogel, W., and Hempelmann, G. (2001). Effect of drugs used for neuropathic pain management on tetrodotoxin-resistant Na(+) currents in rat sensory neurons. *Anesthesiology* 94, 137-144. doi: 10.1097/00000542-200101000-00024

Berninger, B., and Poo, M. M. (1996). Fast actions of neurotrophic factors. *Curr. Opin. Neurobiol.* 6, 324-330. doi: 10.1016/s0959-4388(96)80115-2

Chadwick, W., Mitchell, N., Caroll, J., Zhou, Y., Park, S-S., Wang, L., Becker, K. G., Zhang, Y., Lehrmann, E., Ill, W. H. W., Martin, B., and Maudsley, S. (2011). Amitriptyline-mediated cognitive enhancement in aged 3XTg Alzheimer's disease mice is associated with neurogenesis and neurotrophic activity. *PLoS One* 6, e21660. doi: 10.1371/journal.pone.0021660

Chiti, Z., and Teschemacher, A. G. (2007). Exocytosis of norepinephrine at axon varicosities and neuronal cell bodies in the rat brain. *FASEB J.* 21, 2540-2550. doi: 10.1096/fj.06-7342com

Cho, J. H., Choi, I. S., Lee, M. G., and Jang, I. S. (2012). Effect of amitriptyline on glycinergic transmission in rat medullary dorsal horn neurons. *Brain Res.* 1455, 10-18. doi: 10.1016/j.brainres.2012.03.030

Colucci-D'Amato, L., Speranza, L., and Volpicelli, F. (2020). Neurotrophic factor

BDNF, physiological functions and therapeutic potential in depression, neurodegeneration and brain cancer. *Int. J. Mol. Sci.* 21, 7777. doi: 10.3390/ijms21207777

Couch, J. R., Amitriptyline Versus Placebo Study Group (2011). Amitriptyline in the prophylactic treatment of migraine and chronic daily headache. *Headache* 51, 33-51. doi: 10.1111/j.1526-4610.2010.01800.x

Curran, H. V., Sakulsripron, M., and Lader, M. (1988). Antidepressants and human memory: An investigation of four drugs with different sedative and anticholinergic profiles. *Psychopharmacology* 95, 520-527. doi: 10.1007/BF00172967

Dwivedi, Y. (2009). Brain-derived neurotrophic factor: role in depression and suicide. *Neuropsychiatr. Dis. Treat.* 5, 433-449. doi: 10.2147/ndt.s5700

Frerking, M., Malenka, R. C., and Nicoll, R. A. (1998). Brain-derived neurotrophic factor (BDNF) modulates inhibitory, but not excitatory, transmission in the CA1 region of the hippocampus. *J. Neurophysiol.* 80, 3383-3386. doi: 10.1152/jn.1998.80.6.3383

Freysoldt, A., Fleckenstein, J., Lang, P. M., Irnich, D., Grafe, P., and Carr, R. W. (2009). Low concentrations of amitriptyline inhibit nicotinic receptors in unmyelinated axons of human peripheral nerve. *Br. J. Pharmacol.* 158, 797-805. doi: 10.1111/j.1476-5381.2009.00347.x

Glotzbach, R. K., and Preskorn, S. H. (1982). Brain concentrations of tricyclic

antidepressants: single-dose kinetics and relationship to plasma concentrations in chronically dosed rats. *Psychopharmacology (Berl).* 78, 25-27. doi: 10.1007/BF00470582

Griffith, W. H., Dubois, D. W., Fincher, A., Peebles, K. A., Bizon, J. L., and Murchison, D. (2014). Characterization of age-related changes in synaptic transmission onto F344 rat basal forebrain cholinergic neurons using a reduced synaptic preparation. *J. Neurophysiol.* 111, 273-286. doi: 10.1152/jn.00129.2013

Griffith, W. H. and Murchison, D. A. (1995). Enhancement of GABA-activated membrane currents in aged Fischer 344 rat basal forebrain neurons. *J. Neurosci.* 15, 2407-2416. doi: 10.1523/JNEUROSCI.15-03-02407.1995

Hajszan, T., Alreja, M., and Leranth, C. (2004). Intrinsic vesicular glutamate transporter 2-immunoreactive input to septohippocampal parvalbumin-containing neurons: novel glutamatergic local circuit cells. *Hippocampus* 14, 499-509. doi: 10.1002/hipo.10195

Han, W., Shepard, R. D., and Lu, W. (2021). Regulation of $GABA_A$Rs by transmembrane accessory proteins. *Trends Neurosci.* 44, 152-165. doi: 10.1016/j.tins.2020.10.011

Harper, D. G., Volicer, L., Stopa, E. G., McKee, A. C., Nitta, M., and Satlin, A. (2005). Disturbance of endogenous circadian rhythm in aging and Alzheimer disease. *Am. J. Geriatr. Psychiatry* 13, 359-368. doi: 10.1176/appi.ajgp.13.5.359

Ingram, D. K., London, E. D., and Reynolds, M. A. (1982). Circadian rhythmicity and

sleep: effects of aging in laboratory animals. *Neurobiol. Aging* 3, 287-297. doi: 10.1016/0197-4580(82)90017-3

Jang, S. W., Liu, X., Chan, C. B., Weinshenker, D., Hall, R. A., Xiao, G., and Ye, K. (2009). Amitriptyline is a TrkA and TrkB receptor agonist that promotes TrkA/TrkB heterodimerization and has potent neurotrophic activity. *Chemistry & Biology* 16, 644-656. doi: 10.1016/j.chembiol.2009.05.010

Kachur, J. F., Allbee, W. E., and Gaginella, T. S. (1988). Antihistaminic and antimuscarinic effects of amitriptyline on guinea pig ileal electrolyte transport and muscle contractility in vitro. *J. Pharmacol. Exp. Ther.* 245, 455-459.

Kim, H. G., Wang, T., Olafsson, P., and Lu, B. (1994). Neurotrophin 3 potentiates neuronal activity and inhibits gamma-aminobutyratergic synaptic transmission in cortical neurons. *Proc. Natl. Acad. Sci. U.S.A.* 91, 12341-12345. doi: 10.1073/pnas.91.25.12341

Kovalchuk, Y., Holthoff, K., and Konnerth, A. (2004). Neurotrophin action on a rapid timescale. *Curr. Opin. Neurobiol.* 14, 558-563. doi: 10.1016/j.conb.2004.08.014

Lavoie, P. A., Beauchamp, G., and Elie, R. (1990). Tricyclic antidepressants inhibit voltage-dependent calcium channels and Na(+)-Ca2+ exchange in rat brain cortex synaptosomes. *Can. J. Physiol. Pharmacol.* 68, 1414-1418, doi: 10.1139/y90-215

Linnoila, M., Johnson, J., Dubyoski, T., Ross, R., Buchsbaum, M., Potter, W. Z., and Weingartner, H. (1983). Effects of amitriptyline, desipramine and zimeldine, alone and in combination with ethanol, on information processing and memory in

healthy volunteers. Acta. Psychiatr. Scand. Suppl. 308,175-181. doi: 10.1111/j.1600-0447.1983.tb11121.x

Liu, J., Reid, A. R., and Sawynok, J. (2012). Spinal serotonin 5-HT7 and adenosine A1 receptors, as well as peripheral adenosine A1 receptors, are involved in antinociception by systemically administered amitriptyline. *Eur. J. Pharmacol.* 698, 213-219. doi: 10.1016/j.ejphar.2012.10.042

Manseau, F., Danik, M., and Williams, S. (2005). A functional glutamatergic neurone network in the medial septum and diagonal band area. *J. Physiol.* 566, 865-884. doi: 10.1113/jphysiol.2005.089664

Moore, R. A., Derry, S., Aldington, D., Cole, P., and Wiffen, P. J. (2015). Amitriptyline for neuropathic pain in adults. Cochrane. *Database. Sys. Rev.* 7, CD008242. doi: 10.1002/14651858.CD008242.pub3

Murchison, D., and Griffith, W. H. (1996). High-voltage-activated calcium currents in basal forebrain neurons during aging. *J. Neurophysiol.* 76, 158-174. doi: 10.1152/jn.1996.76.1.158

Murchison, D., and Griffith, W. H. (1998). Increased calcium buffering in basal forebrain neurons during aging. *J. Neurophysiol.* 80, 350-364. doi: 10.1152/jn.1998.80.1.350

Murchison, D. and Griffith, W. H. (2007). Calcium buffering systems and calcium signaling in aged rat basal forebrain neurons. *Aging Cell* 6, 297–305. doi: 10.1111/j.1474-9726.2007.00293.x

Murchison, D., McDermott, A. N., LaSarge, C. L., Peeble, K. A., Bizon, J. L., and

Griffith, W. H. (2009). Enhanced calcium buffering in F344 rat cholinergic basal forebrain neurons is associated with age-related cognitive impairment. *J. Neurophysiol.* 102, 2194-2207. doi: 10.1152/jn.00301.2009

Musiek, E. S., Bhimasani, M., Zangrilli, M. A., Morris, J. C., Holtzman, D. M., and Ju, Y. S. (2018). Circadian rest-activity pattern changes in aging and preclinical Alzheimer Disease. *JAMA Neurol.* 75, 582–590. doi: 10.1001/jamaneurol.2017.4719

National Center for Health Statistics. (2007). Health, United States, 2007 with chartbook on trends in the health of Americans. https://www.cdc.gov/nchs/data/hus/hus07.pdf [Accessed January 5, 2021]

Nicholson, G. M., Blanche, T., Mansfield, K., and Tran, Y. (2002). Differential blockade of neuronal voltage-gated Na(+) and K(+) channels by antidepressant drugs. Eur. *J. Pharmacol.* 452, 35-48. doi: 10.1016/s0014-2999(02)02239-2

Nojimoto, F. D., Mueller, A., Hebeler-Barbosa, F., Akinaga, J., Lima, V., Kiguti, L. R., and Pupo, A. S. (2010). The tricyclic antidepressants amitriptyline, nortriptyline and imipramine are weak antagonists of human and rat alpha1B-adrenoceptors. *Neuropharmacology* 59(1-2), 49-57. doi: 10.1016/j.neuropharm.2010.03.015

Olivier-Martin, R., Cendron, H. and Vallery-Masson, J. (1975). Sleep in the aged subject. *Am. Med. Psychol.* 1, 77-90.

O'Neill, E., Kwok, B., Day, J. S., Connor, T. J., and Harkin, A. (2016). Amitriptyline

protects against TNF-α-induced atrophy and reduction in synaptic markers via a Trk-dependent mechanism. *Pharmacol. Res. Perspect.* 4, e00195. doi: 10.1002/prp2.195

Pandey, D. K., Mahesh, R., Kumar, A. A., Rao, V. S., Arjun, M., and Rajkumar, R. (2010). A novel 5-HT(2A) receptor antagonist exhibits antidepressant-like effects in a battery of rodent behavioural assays: approaching early-onset antidepressants. *Pharmacol. Biochem. Behav.* 94, 363-373. doi: 10.1016/j.pbb.2009.09.018

Parra, A., Everss, E., Monleón, S., Vinader-Caerols, C., and Arenas, M. C. (2002). Effects of acute amitriptyline administration on memory, anxiety and activity in male and female mice. *Neurosci. Res. Comm.* 31, 135-144. doi: 10.1002/nrc.10046

Peck, A. W., Bye, C. E., Clubley, M., Henson, T., and Riddington, C. (1979). A comparison of bupropion hydrochloride with dexamphetamine and amitriptyline in healthy subjects. *Br. J. Clin. Pharmacol.* 7, 469-78. doi: 10.1111/j.1365-2125.1979.tb00988.x.

Peter-Derex, L., Yammine, P., Bastuji, H., and Croisile, B. (2015). Sleep and Alzheimer's disease. *Sleep Med. Rev.* 19, 29-38. doi: 10.1016/j.smrv.2014.03.007

Poo, M. M. (2001). Neurotrophins as synaptic modulators. *Nat. Rev. Neurosci.* 2, 24-32. doi: 10.1038/35049004

Richelson, E. (1979). Tricyclic antidepressants and histamine H1 receptors. *Mayo. Clin.*

Proc. 54, 669-674.

Riediger, C., Schuster, T., Barlinn, K., Maier, S., Weitz, J., and Siepmann, T. (2017). Adverse effects of antidepressants for chronic pain: A systematic review and meta-analysis. *Front. Neurol.* 8, 307. doi: 10.3389/fneur.2017.00307

Rusak, B. and Zucker, I. (1979). Neural regulation of circadian rhythms. *Physiol. Rev.* 59, 449-526. doi: 10.1152/physrev.1979.59.3.449

Satlin, A., Volicer, L., Stopa, E. G., and Harper, D. (1995). Circadian locomotor activity and core-body temperature rhythms in Alzheimer's disease. *Neurobiol. Aging* 16, 765-771. doi: 10.1016/0197-4580(95)00059-n.

Staton, R. D., Wilson, H., and Brumback, R. A. (1981). Cognitive improvement associated with tricyclic antidepressant treatment of childhood major depressive illness. *Percept. Mot. Skills* 53, 219-234. doi: 10.2466/pms.1981.53.1.219

Stepanenko, Y. D., Boikov, S. I., Sibarov, D. A., Abushik, P. A., Vanchakova, N. P., Belinskaia, D., Shestakova, N. N., and Antonov, S. M. (2019). Dual action of amitriptyline on NMDA receptors: enhancement of Ca-dependent desensitization and trapping channel block. *Sci. Rep.* 9, 19454. doi: 10.1038/s41598-019-56072-z.

Sternberg, D. E., and Jarvik, M. E. (1976). Memory functions in depression. *Arch. Gen. Psychiatry* 33, 219-224. doi: 10.1001/archpsyc.1976.01770020055009

Suga, T., Takenoshita, M., Watanabe, T., Tu, T. T., Mikuzuki, L., Hong, C., Miura, K.,

Yoshikawa, T., Nagamine, T., and Toyofuku, A. (2019). Therapeutic dose of amitriptyline for older patients with burning mouth syndrome. *Neuropsychiatr. Dis. Treat.* 15, 3599-3607. doi: 10.2147/NDT.S235669

Tanaka, T., Saito, H., and Matsuki, N. (1997). Inhibition of GABAA synaptic responses by brain-derived neurotrophic factor BDNF in rat hippocampus. *J. Neurosci.* 17, 2959–2966. doi: 10.1523/JNEUROSCI.17-09-02959.1997

Tang, A. H., Chen, H., Li, T. P., Metzbower, S. R., MacGillavry, H. D., and Blanpied, T. A. (2016). A trans-synaptic nanocolumn aligns neurotransmitter release to receptors. *Nature* 536, 210-214. doi: 10.1038/nature19058

Tranah, G. J., Blackwell, T., Stone, K. L., Ancoli-Israel, S., Paudel, M. L., Ensrud, K. E., Cauley, J. A., Redline, S., Hillier, T. A., Cummings, S. R., and Yaffe, K. (2011). Circadian activity rhythms and risk of incident dementia and mild cognitive impairment in older women. *Ann. Neurol.* 70, 722-732. doi: 10.1002/ana.22468

Tyler, W. J., Zhang, X. L., Hartman, K., Winterer, J., Muller, W., Stanton, P. K., and Pozzo-Miller, L. (2006). BDNF increases release probability and the size of a rapidly recycling vesicle pool within rat hippocampal excitatory synapses. *J. Physiol.* 574, 787-803. doi: 10.1113/jphysiol.2006.111310

Urquhart, D. M., Wluka, A. E., van Tulder, M., Heritier, S., Forbes, A., Fong, C., Wang, Y., Sim, M. R., Gibson, S. J., Arnold, C., and Cicuttini, F. M. (2018). Efficacy of low-dose amitriptyline for chronic low back pain: a randomized clinical trial. *JAMA Intern. Med.* 178, 1474-1481. doi: 10.1001/jamainternmed.2018.4222

Wainer, B. H., Levey, A. I., Rye, D. B., Mesulam, M. M., and Mufson, E. J. (1985).

Cholinergic and non-cholinergic septohippocampal pathways. *Neurosci. Lett.* 54, 45-52. doi: 10.1016/s0304-3940(85)80116-6

Watanabe, Y., Saito, H., and Abe, K. (1993). Tricyclic antidepressants block NMDA receptor-mediated synaptic responses and induction of long-term potentiation in rat hippocampal slices. *Neuropharmacology.* 32, 479-486. doi: 10.1016/0028-3908(93)90173-z

Weitzman, E. D., Moline, M. L., Czeisler, C. A. and Zimmerman, J. C. (1982). Chronobiology of Aging: temperature, sleep-wake rhythms and entrainment. *Neurobiol. Aging* 3, 299-309. doi: 10.1016/0197-4580(82)90018-5

Witting, W., Kwa I. H., Eikelenboom, P., Mirmiran, M., and Swaab, D. F. (1990). Alterations in the circadian rest-activity rhythm in aging and Alzheimer's disease. *Biol. Psychiatry* 27, 563-572. doi: 10.1016/0006-3223(90)90523-5

Wu, L. G., and Saggau, P. (1997). Presynaptic inhibition of elicited neurotransmitter release. *Trends Neurosci.* 20, 204-212. doi: 10.1016/s0166-2236(96)01015-6

Wu, W., Ye, Q., Wang, W., Yan, L., Wang, Q., Xiao, H., and Wan, Q. (2012). Amitriptyline modulates calcium currents and intracellular calcium concentration in mouse trigeminal ganglion neurons. *Neurosci. Lett.* 506, 307-311. doi: 10.1016/j.neulet.2011.11.031

Yan, L., Wang, Q., Fu, Q., Ye, Q., Xiao, H., and Wan, Q. (2010). Amitriptyline inhibits currents and decreases the mRNA expression of voltage-gated sodium channels in cultured rat cortical neurons, *Brain Res.* 1336, 1-9. doi: 10.1016/j.brainres.2010.04.016

Yau, J. L. W., Noble, J., Hibberd, C., Rowe, W. B., Meaney, M. J., Morris, R. G. M., and Seckl, J. R. (2002). Chronic treatment with the antidepressant amitriptyline prevents impairments in water maze learning in aging rats. *J. Neurosci.* 22, 1436-1442. doi: 10.1523/JNEUROSCI.22-04-01436.2002

Záborszky, L., Gombkoto, P., Varsanyi, P., Gielow, M. R., Poe, G., Role, L. W., Ananth, M., Rajebhosale, P., Talmage, D. A., Hasselmo, M. E., Dannenberg, H., Minces, V. H., and Chiba, A. A. (2018). Specific basal forebrain-cortical cholinergic circuits coordinate cognitive operations. *J. Neurosci.* 38, 9446-9458. doi: 10.1523/JNEUROSCI.1676-18.2018

Zaborszky, L., Pang, K., Somogyi, J., Nadasdy, Z., and Kallo, I. (1999). The basal forebrain corticopetal system revisited. *Ann. N. Y. Acad. Sci.* 877, 339-367. doi: 10.1111/j.1749-6632.1999.tb09276.x

Zarei, G., Reisi, P., Alaei, H., and Javanmard, S. H. (2014). Effects of amitriptyline and fluoxetine on synaptic plasticity in the dentate gyrus of hippocampal formation in rats. *Adv. Biomed. Res.* 3, 199. doi: 10.4103/2277-9175.142044.

Zhang, M., Liu, Y., Hu, G., Kang, L., Ran, Y., Su, M., and Yu, S. (2020). Cognitive impairment in a classical rat model of chronic migraine may be due to alterations in hippocampal synaptic plasticity and N-methyl-D-aspartate receptor subunits. *Mol. Pain.* 16, 1744806920959582. doi: 10.1177/1744806920959582

Zhao, S., Ting, J. T., Atallah, H. E., Qiu, L., Tan, J., Gloss, B., Augustine, G. J.,

Deisseroth, K., Luo, M., Graybiel, A. M., and Feng, G. (2011). Cell type–specific channelrhodopsin-2 transgenic mice for optogenetic dissection of neural circuitry function. *Nat. Methods.* 8, 745-752. doi: 10.1038/nmeth.1668.

Zucker, R. S. (1993). Calcium and transmitter release. *J. Physiol. Paris.* 87, 25-36. doi: 10.1016/0928-4257(93)90021-k.

CHAPTER III

LATE-ONSET SHORT-TERM INTERMITTENT FASTING REVERSES AGE-RELATED CHANGES IN CALCIUM BUFFERING AND INHIBITORY SYNAPTIC TRANSMISSION BUT NOT COGNITIVE FUNCTION IN MOUSE BASAL FOREBRAIN NEURONS

3.1 Abstract

Aging is often associated with cognitive decline and recurrent cellular and molecular impairments. While life-long caloric restriction (CR) has been shown to delay age-related cognitive deterioration as well as the onset of neurological disease, recent studies suggest that late-onset, short-term intermittent fasting (IF), may show comparable beneficial effects as those of life-long CR to improve brain health. We used a new optogenetic aging model to study the effects of late-onset (>18 months), short-term (4-6 weeks) IF on age-related changes in GABAergic synaptic transmission, intracellular calcium (Ca^{2+}) buffering and cognitive status. We utilized a bacterial artificial chromosome (BAC) transgenic mouse line with stable expression of the channelrhodopsin-2 (ChR2) variant H134R [VGAT-ChR2(H134R)-EYFP] in a reduced synaptic preparation that allows for specific optogenetic light stimulation on GABAergic synaptic terminals across aging. We performed quantal analysis using the method of failures in this model and show that short-term IF reverses the age-related decrease in quantal content of GABAergic synapses. Likewise, short-term IF also reversed age-related changes in Ca^{2+} buffering and spontaneous GABAergic synaptic transmission in basal

forebrain (BF) neurons of aged mice. Although age-related cognitive impairment was reduced following short-term IF, it was not prevented. Our findings suggest that late-onset short-term IF can reverse age-related physiological impairments in mouse BF neurons but that 4 weeks IF is not sufficient to reverse age-related cognitive decline.

3.2 Significance statement

Here we demonstrate plasticity of the aging brain and reversal of well-defined hallmarks of brain aging using short-term intermittent fasting initiated later in life. Few therapeutics are currently available to treat age-related neurological dysfunction while synaptic dysfunction during aging and neurological disease is a topic of intense research. Using a new reduced synaptic preparation and optogenetic stimulation we are able to study age-related synaptic mechanisms in greater detail. Several neurophysiological parameters including quantal content were altered during aging and were reversed with short-term intermittent fasting. These methods can be used to identify potential therapies to reverse physiological dysfunction during aging.

3.3 Introduction

Age-related cognitive impairment is a substantial burden on society today. The number of individuals over the age of 65 is projected to rise to 88.5 million in 2050, which is more than double that from 2010 (Vicent & Velkoff, 2010). Approximately 4.2 million adults were suffering from dementia in the United States in 2010 and more than 135 million worldwide (Hurd et al., 2013; Prince et al., 2013). The estimated cost attributable to cognitive decline was $200 billion per year in the United States (Hurd et

al., 2013) and $600 billion worldwide (Wimo et al., 2013). It is critical to understand the mechanisms of brain aging and to identify potential therapeutics.

Calorie restriction (CR), whether resulting from reduced calorie intake or intermittent fasting (IF), is a well-established paradigm to promote healthy brain aging and possibly, delay or prevent age-related cognitive dysfunction (Cauwenberghe et al., 2016)). CR may induce beneficial effects by various cellular/molecular mechanisms such as delayed oxidative damage (Merry, 2004; Hunt et al., 2006), increased protein chaperone activity (Arumugam et al., 2010), reduced inflammation (Spaulding et al., 1997; Bhattacharya et al., 2006; Ugochukwu and Figgers, 2007), or by increased neurogenesis and upregulation of neurotrophic factors (BDNF, IGF-1, VEGF; Lee et al., 2002; Cheng et al., 2003; Joseph D'Ercole and Ye, 2008; Mattson, 2010). Interestingly, synaptic function was shown to improve following only days (Campanelli et al., 2021) or months (Dasgupta et al., 2018) of diet restriction or IF. In the hippocampus, short-term dietary restriction increased the number of glutamate receptors at synapses responsible for an enhanced long-term potentiation (Babits et al.,2016) and increased AMPA receptor membrane incorporation (Ribeiro et al., 2014). The beneficial effects of CR on cognition also have been reported in human subjects after only 3 to 24 months (Witte et al., 2008; Horie et al., 2016; Leclerc et al., 2019). Healthy elderly individuals on CR (30% reduction) for three months showed a significant increase in their verbal memory performance (Witte et al., 2008). Other studies have shown that late-onset short-term dietary regimens may produce comparable benefits to life-long CR (Goto 2006, 2007; Kaur et al., 2008; Witte et al., 2009; Sharma et al., 2010; Singh et al., 2012).

Although it is known that CR can reduce age-associated cognitive decline in animals and humans, the cellular/molecular mechanisms underlying these effects remain unclear. We have been studying calcium (Ca^{2+}) homeostasis, synaptic physiology and cognitive status during aging of rat basal forebrain (BF) neurons for many years (Griffith and Murchison, 1995; Murchison and Griffith, 1996, 1998, 2007; Murchison et al., 2009, 2014). The BF plays an important role in cognitive functions such as attention, arousal, and learning and memory and projects to widespread brain areas such as neocortex and hippocampus where it modulates cortical and hippocampal neurons (Zaborszky et al., 2018). We have previously reported that enhanced Ca^{2+} buffering during aging is associated with age-related deficits in the frequency of spontaneous inhibitory postsynaptic currents (sIPSCs) in rat BF neurons, and that these changes were most prominent in cognitively impaired subjects (Murchison et al., 2009; Griffith et al., 2014). An increase in Ca^{2+} buffering was prevented in aged rats by life-long 40% reduced calorie intake (Murchison and Griffith, 2007).

We have extended these studies to mice using a bacterial artificial chromosome (BAC) transgenic line with stable expression of the channelrhodopsin-2 (ChR2) variant H134R (VGAT-ChR2(H134R)-EYFP) specific for GABAergic neurons (Zhao et al., 2011; Bang et al., 2021). We used acutely dissociated BF neurons and a reduced synaptic preparation (Griffith et al., 2014; Bang et al., 2021), to examine the effect of late-onset short-term IF diet (24hr-alternate day fasting for 4-6 weeks) on age-related changes in inhibitory synaptic transmission and Ca^{2+} buffering in behaviorally characterized mice. This optogenetic aging model enabled us to selectively stimulate

GABAergic nerve terminals on voltage-clamped BF neurons, and calculate quantal content (m) of inhibitory neurotransmitter release. We report that age-related changes in Ca^{2+} homeostasis and inhibitory synaptic transmission are correlated with cognitive status. We show that this IF protocol can reverse age-related neurophysiological changes, but it is not efficacious on cognitive function.

3.4 Result

3.4.1 Optogenetic mouse model and reduced synaptic preparation

Experiments were conducted using WT C57/Bl6 mice and VGAT-ChR2(H134R)-EYFP optogenetic mice on a C57/Bl6 background. The expression of the channelrhodopsin-EYFP construct is under control of the vesicular GABA transporter (VGAT) promotor and is only expressed in GABAergic neurons (Figure 3.1A). This permits specific excitation of GABAergic neurons by 470 nm light stimulation and light-evoked optogenetic IPSCs (oIPSCs) can be recorded in post-synaptic targets, as shown in Figure 3.1B. For our experiments we employed a reduced synaptic preparation that consists of acutely dissociated BF neurons that receive no enzyme treatment and presynaptic terminals remain attached. In this preparation, GABAergic neurons can be identified by their bright EYFP fluorescence, while non-GABAergic neurons (presumably cholinergic) feature fluorescent puncta that are putatively GABAergic terminals (Figure 3.1C).

3.4.2 Changes in body weight and food consumption by intermittent fasting (IF) diet

Young and aged mice were maintained on ad libitum (AL) diets prior to the start of the experimental protocols. Control subjects continued on the AL diet for the duration

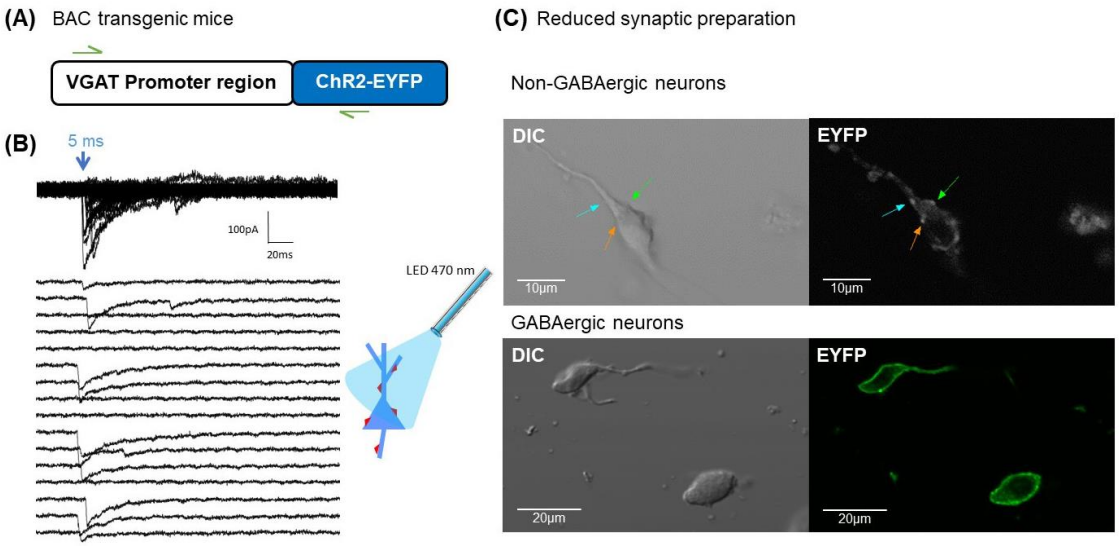

Figure 3.1. Reduced synaptic preparation in VGAT-ChR2-EYFP BAC optogenetic mice allows stimulation of light-evoked inhibitory postsynaptic currents (oIPSCs). (A) Schematic diagram of the transgenic construct present in the GABAergic neurons of these mice. (B) Examples of light-induced oIPSCs (Vh = -60mV). Top records show superimposed traces with individual responses and failures below. Minimal intensity light stimulation of 5 ms duration (470 nm) is indicated at blue arrow. A stylized diagram of a dissociated neuron with blue light excitation is shown also. Presynaptic GABAergic terminals are depicted in red to illustrate how they can be activated with light. (C) Confocal DIC and fluorescent images of GABAergic and non-GABAergic acutely dissociated neurons in the reduced synaptic preparation. Top panels show a DIC image of a live (non-GABAergic) neuron and colored arrows point out the position of presumed presynaptic terminals. The EYFP fluorescence image to the right shows more clearly the location of the fluorescent puncta that are thought to be GABAergic synaptic terminals (arrows). In this preparation non-GABAergic neurons are likely cholinergic and display only very dim autofluorescence. In contrast below, live GABAergic neurons are seen as DIC images (left) and displaying bright EYFP fluorescence (right). Note that in this single confocal plane scan, ChR2-EYFP fluorescence is predominately located around the cell surface where functioning ChR2 channels are located.

of the protocols, while mice on IF diets commenced 4 weeks prior to Barnes maze training and continued during the remaining protocol (6 weeks total), as shown in Figure 3.2A. Therefore, aged cohorts received late-onset IF that was started six weeks before they were utilized for experimental studies. Body weight and food consumption were monitored throughout the experiment. Aged mice on IF diet gradually decreased their body weight during the 6-week IF and showed 7% reduction in body weight after the 6-week IF period compared to their initial body weight, while aged control maintained their body weight throughout the 6-week diet period. Young control mice showed a gradual increase of their body weight during the 6-week period, resulting in a 3% increase of body weight. The young IF group also increased body weight during the first 2-weeks of the IF diets, however, their body weights eventually began to decrease and were reduced by 1.4% at the end of 6 weeks. This change in body weight was significantly different for the aged IF diet group (Figure 3.2B). Both young and aged mice placed on IF diet were observed to binge on feeding day, and their daily food intake on feeding day was 67% and 63% higher than young and aged control, respectively (Figure 3.2C, left). Despite binge eating behavior, total food consumption during the 6-week diet period was reduced by 14% and 17% in young and aged IF mice compared to respective controls (Figure 3.2C, right).

3.4.3 IF reverses age-related alterations in calcium buffering in WT mouse BF neurons

In order to determine the functional consequences of a 6 week IF diet, we started by testing the previously described age-related enhancement of rapid intracellular Ca^{2+}

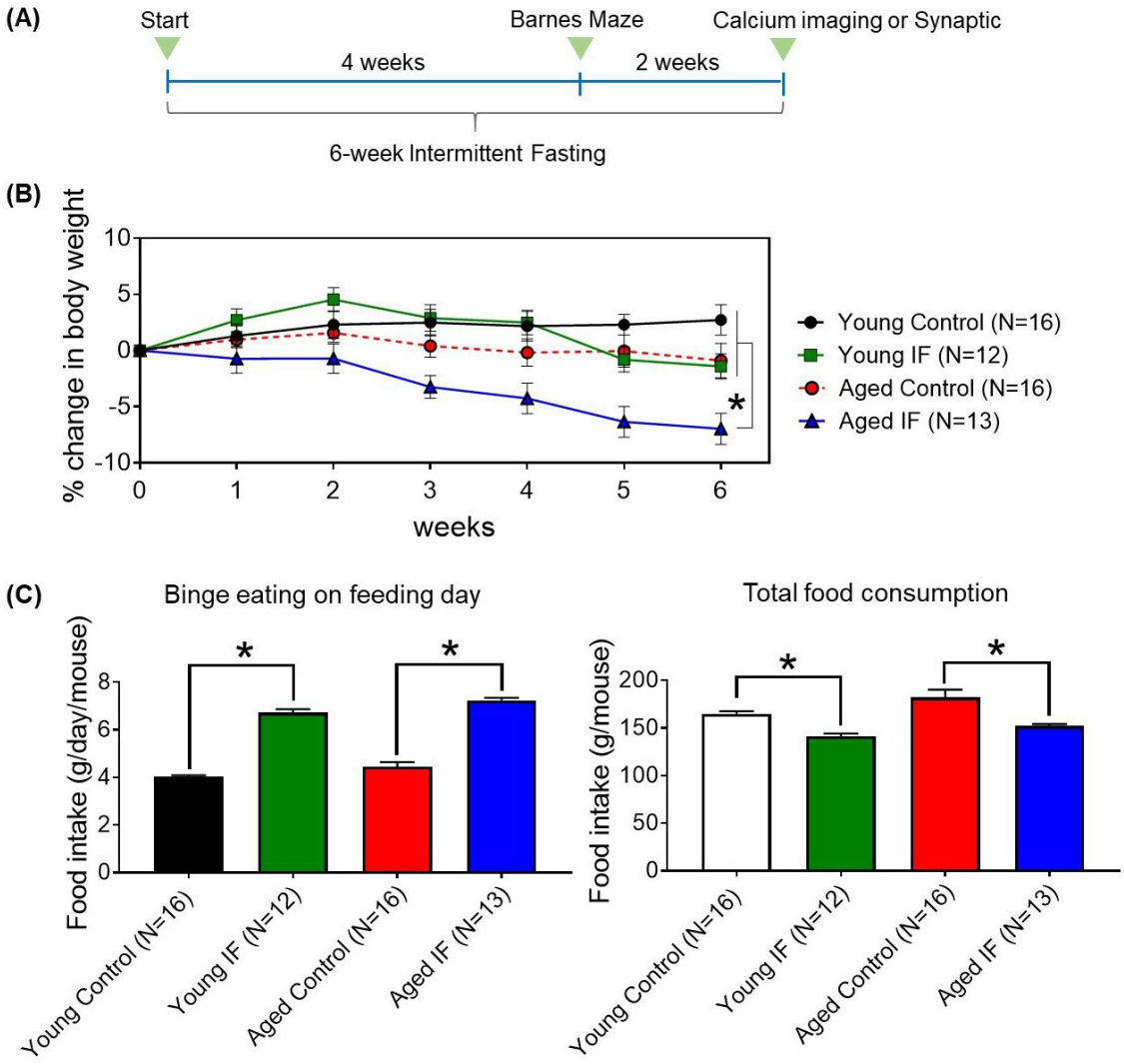

Figure 3.2. The effect of intermittent fasting (IF) on body weight and food consumption. (A) Overview of the timeline and experimental design of the IF experiments. All mice were initially fed ad libitum (AL) then maintained for 6 weeks on either an IF diet or continued on the AL (control) diet. To assess cognitive function, all mouse groups (young control and IF, aged control and IF) were trained in the Barnes maze task starting 4 weeks after the implementation of the IF diets. Barnes maze training continued for 2 weeks before mice were utilized to measure either calcium buffering or synaptic transmission. Diets were maintained until sacrifice. (B) Plot of percent (%) change in body weights of control and IF mice in both young and aged during the 6-week diet period (weeks: $F_{3.084,\ 163.4} = 10.29$, $p < 0.0001$, age: $F_{1,\ 53} = 13.53$, $p < 0.001$, diet: $F_{1,\ 53} = 5.070$, $p < 0.05$, interaction (weeks x age): $F_{6,\ 318} = 4.701$, $p < 0.001$, interaction (weeks x diet): $F_{6,\ 318} = 7.810$, $p < 0.0001$, interaction (age x diet): $F_{1,\ 53} = 3.109$, $p = 0.083$, interaction (weeks x age x diet): $F_{6,\ 318} = 1.070$, $p = 0.3806$, N = 12-16 per group). For IF mice, the body weights were measured after feeding days. (C) Graphs

of average of daily food intake per mouse (left, interaction: $F_{1,53} = 0.09763$, $p = 0.7559$; age: $F_{1,53} = 11.47$, $p < 0.01$; diet: $F_{1,53} = 395.4$, $p < 0.0001$, N = 12-16 per group) and average of total food consumption per mouse during the 6-week diet period (right, interaction: $F_{1,53} = 0.45$, $p = 0.5052$; age: $F_{1,53} = 7.986$, $p < 0.01$; diet: $F_{1,53} = 29.72$, $p < 0.0001$, N = 12-16 per group). All data are expressed as mean ± SEM and are pooled from the WT and VGAT cohorts. The data in panel B were analyzed by a repeated-measures three-way ANOVA with Fisher's LSD post hoc test. The data included in panel C were analyzed by a two-way ANOVA with Fisher's LSD post hoc test. *$p < 0.05$. Values of 'N' indicate number of mice.

buffering that occurs in rat BF neurons and is associated with age-related cognitive impairment (Murchison et al., 2009) and reversed by life-long caloric restriction (Murchison and Griffith, 2007). We first replicated the reversal of the age-related increase in Ca^{2+} buffering in life-long CR mice (Supplementary Figure 3.1). These mice were obtained from the NIA aging colony and were maintained on a 60% of control diet starting in adolescence. We then hypothesized that age-related increases in rapid Ca^{2+} buffering can be reversed by late-onset short-term IF diet. We used a simplified method (Bang et al., 2021) to assess the relative Ca^{2+} buffering of the young and aged mice in each diet group. Acutely dissociated BF neurons from behaviorally characterized (Barnes maze) WT mice were loaded with the ratiometric calcium-sensitive fluorescent probe fura-2 AM and Ca^{2+} transients were evoked by focal picospritzer application of elevated $[K^+]$ (20mM) solution (High $[K^+]$), as shown in Figure 3.3A. Representative Ca^{2+} transients from visually identified neurons of each diet group are shown in Figure 3.3B. Transients of increasing amplitude were generated by stimuli of increasing duration. The amplitude of the transients (peak $\Delta[Ca^{2+}]_i$ - baseline $[Ca^{2+}]_i$) was plotted against the stimulus intensity (stimulus duration X 10) to calculate buffering slopes (Figure 3.3C). The stimulus intensities in these plots are in arbitrary units and a greater slope value is indicative of lower rapid Ca^{2+} buffering. The calculated slopes for all neurons from each group were plotted in Figure 3.3D (left) and the slope values averaged from individual animals is shown at right. Consistent with our earlier findings, Ca^{2+} buffering in aged control is significantly greater (lower slope) compared to young

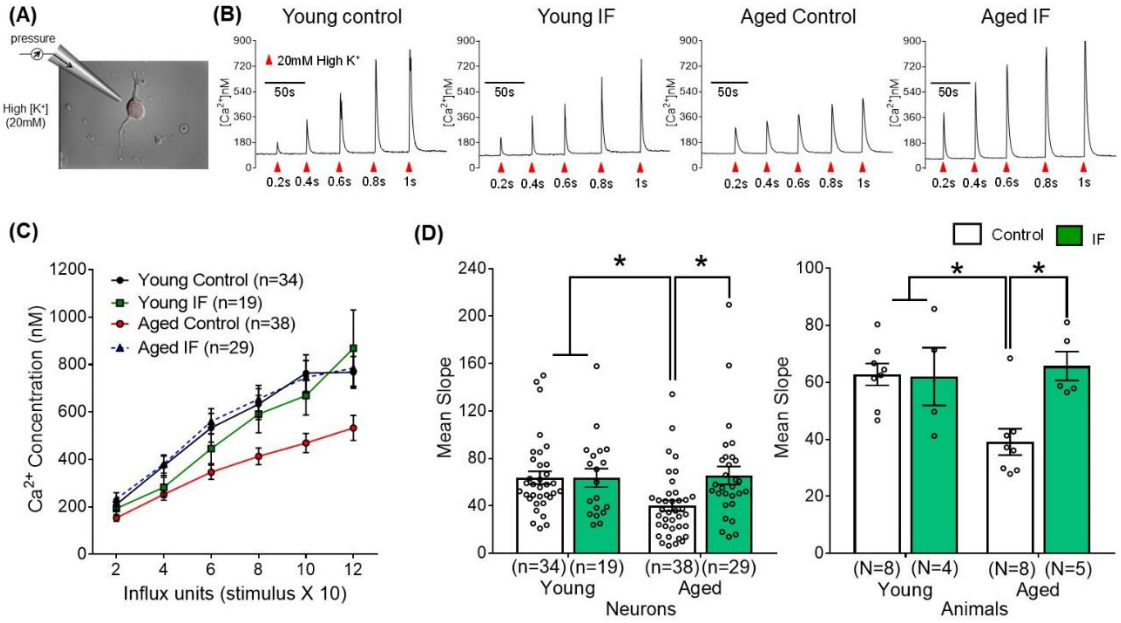

Figure 3.3. Increased Ca^{2+} buffering in WT mouse basal forebrain neurons during aging is reversed by late-onset short-term intermittent fasting. (A) DIC image of an acutely dissociated mouse BF neuron with an illustration of the focal picospritzer method for application of elevated $[K^+]$ (20 mM) solution (High $[K^+]$). The red circle depicts the region of interest from which the fura-2 fluorescent intensity data is collected. (B) Representative traces of ratiometric fura-2 Ca^{2+}-sensitive fluorescence in BF neurons from young and aged control and IF mice. Ca^{2+}-transients were generated by depolarizing the neurons with picospritzer applications of high $[K^+]$ with increasing durations (red arrows). Note that smaller transients in aged neurons indicate increased $[Ca^{2+}]_i$ buffering. Estimated $[Ca^{2+}]_i$ was determined using standard *in vitro* calibration (see methods) (C) Summary data of buffering slope plots for BF neurons from each mouse group (n = 19-38 per group). The stimulus duration was multiplied by 10 in order to avoid fractional slopes. Greater slopes indicate lower calcium buffering. The dashed line depicts the aged IF data. (D) Bar graphs and scatter plots show the mean buffering slopes in both young and aged control and IF diet groups (left panel from individual neurons, interaction, $F_{1,116} = 4.216$, $p < 0.05$, n = 19-38 per group; right panel by animals, interaction, $F_{1,21} = 6$, $p < 0.05$, N = 4-8 per group). All data are mean ± SEM. The data in panel D were analyzed by a two-way ANOVA with Fisher's LSD post hoc test. *$p < 0.05$. Values of 'n' indicate number of neurons and values of 'N' indicate number of mice.

control. However, Ca^{2+} buffering plots in aged late onset IF showed significantly higher slope when compared to aged control but was not different from young control and IF. This demonstrates that increased calcium buffering during aging was reversed by late-onset short-term IF diet. There was no significant difference in calcium buffering values between young control and young IF. In addition, we did not observe any differences in somatic baseline $[Ca^{2+}]_i$ between groups both in neurons and animals: Young control: 88.18 ± 3.85 nM, Young IF: 83.74 ± 5.15 nM, Aged control: 89.84 ± 3.95 nM, Aged IF: 84.83 ± 4.83 nM, interaction, $F_{1, 116} = 0.004037$, $p = 0.9494$, age, $F_{1, 116} = 0.0928$, $p = 0.7612$, diet, $F_{1, 116} = 1.092$, $p = 0.2983$, n = 19-38 per group.

3.4.4 Age-related decrease in frequency of spontaneous inhibitory postsynaptic currents (sIPSCs) is reversed by late-onset IF in VGAT optogenetic mice

Our laboratory has reported that the frequency of sIPSCs in BF neurons is reduced with age both in rats (Griffith et al., 2014) and mice (Bang, et al., 2021) and that this reduction in sIPSC frequency is associated with cognitive impairment in rats (Griffith et al., 2014). We further proposed that increased intracellular calcium buffering contributes to cognitive impairment by affecting synaptic function during aging (Murchison et al., 2009; Griffith et al., 2014). In order to examine whether late-onset short-term IF can reverse the age-related decrease in sIPSC frequency, we utilized standard whole-cell voltage-clamp (V_h = -60 mV) in the reduced synaptic preparation and measured sIPSCs in BF neurons from VGAT mice that had been behaviorally characterized by Barnes maze training. Figure 3.4 shows that late-onset IF reverses the decline in frequency of

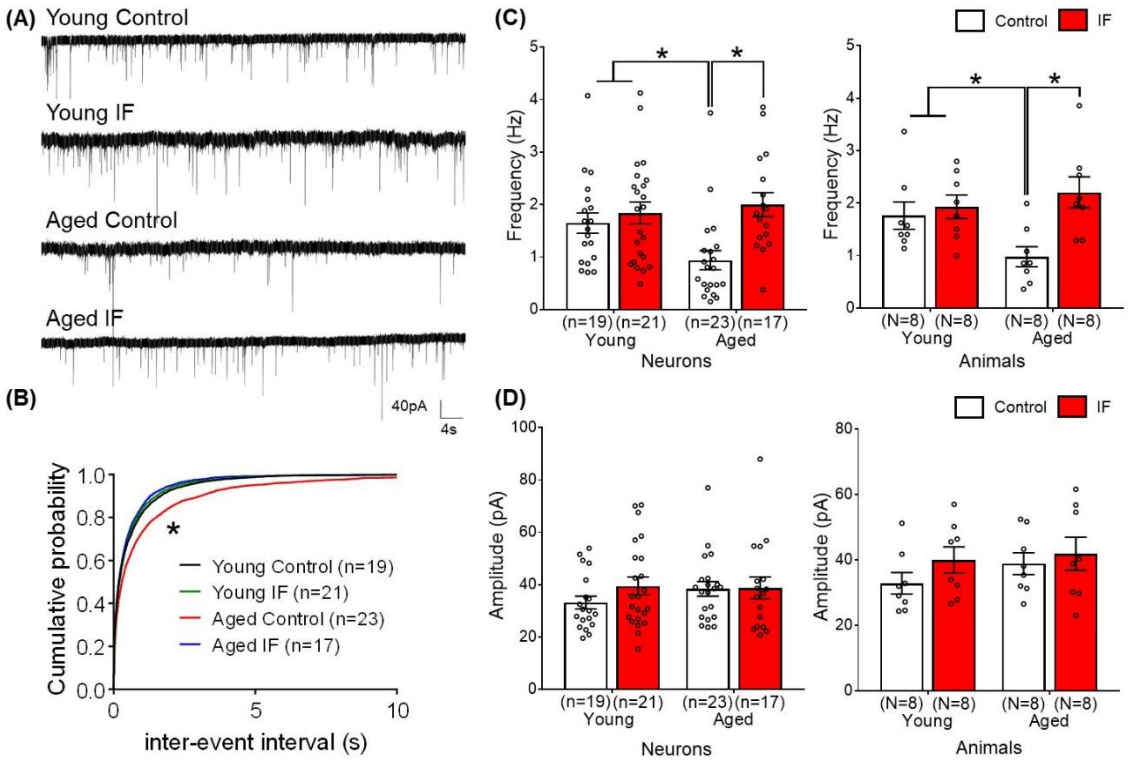

Figure 3.4. The effect of late-onset short-term intermittent fasting on frequency and amplitude of spontaneous inhibitory postsynaptic currents (sIPSCs) in basal forebrain neurons of VGAT optogenetic mice in the reduced synaptic preparation. (A) Representative whole-cell voltage-clamp recordings (V_h = -60mV) from an acutely dissociated basal forebrain neuron in each group of mice. (B) Cumulative probability plots of sIPSC inter-event intervals (n = 17-23 neurons per group * $p < 0.01$, K-S test). (C) Bar graphs and scatter plots show mean ± SEM of sIPSC frequency (left panel from individual neurons, interaction, $F_{1,76} = 4.484$, $p < 0.05$, n = 17-23 per group; right panel by animals, interaction, $F_{1,28} = 4.645$, $p < 0.05$, N = 8 per group). (D) Bar graphs and scatter plots with mean ± SEM of sIPSC amplitude (left panel from individual neurons, n = 17-23 per group; right panel by animals, N = 8 per group). There were no significant differences in sIPSC amplitudes in either neurons (left) or animals (right) regardless of age and diet. The data included in panels C and D are expressed as mean ± SEM and were analyzed by a two-way ANOVA with Fisher's LSD post hoc test. *$p < 0.05$. Values of 'n' indicate number of neurons and values of 'N' indicate number of mice.

sIPSCs observed during aging with no significant effect on amplitude. Example currents from each test group are shown in Figure 3.4A, while Figure 3.4B shows cumulative probability plots of sIPSC inter-event intervals (n = 17-23 neurons per group * $p<0.01$, K-S test) along with reversal of the age-related increases in inter-event duration by late-onset IF. Figure 3.4C shows scatter plots and mean ± SEM of sIPSC frequency (left panel from individual neurons, interaction, $F_{1,76} = 4.484$, $p < 0.05$, n = 17-23 per group; right panel by animals, interaction, $F_{1,28} = 4.645$, $p < 0.05$, N = 8 per group). The sIPSC frequencies of aged late-onset IF diet mice were not significantly different from that of young mice of either diet regimen, while showing a significantly higher sIPSC frequency than aged controls. Figure 3.4D shows scatter plots with mean ± SEM of sIPSC amplitude (left panel from individual neurons, n = 17-23 per group; right panel by animals, N = 8 per group). There were no significant differences in sIPSC amplitudes in either neurons or animals regardless of age and diet. The data included in Figure 3.4C and D were analyzed by a two-way ANOVA with Fisher's LSD post hoc test. Our results demonstrate that late-onset short-term IF can reverse age-related reductions in sIPSC frequency in the mouse BF.

3.4.5 Late-onset short-term IF restores age-related changes in quantal content of VGAT optogenetic mice BF neurons

Changes in the frequency of synaptic transmission are often mediated by changes in the probability of neurotransmitter release at the presynaptic sites. Therefore, we next examined whether there are observable presynaptic changes in inhibitory synaptic mechanisms during aging and if these alterations can be restored by late-onset short-term

IF diet. We used whole-cell voltage-clamp (V_h = -60 mV) to record light-evoked oIPSCs in the reduced synaptic preparation of BF neurons from behaviorally characterized VGAT mice. By applying 5 ms minimal intensity light stimulation, quantal content (m) was calculated using the method of failures (see Methods) Figure 3.5A shows representative traces of oIPSCs from each test group with traces superimposed (top) and distributed (below). Note the failures (lack of response) visible in the individual traces. Figure 3.5B shows scatter plots and mean quantal content (m) data calculated by the method of failures for both young and aged diet groups. The data on the left is from individual neurons (interaction, $F_{1, 51} = 4.085$, $p < 0.05$, n = 9-19 per group) and data on the right is averaged by individual animals (interaction, $F_{1, 24} = 1.947$, $p = 0.1757$, age, $F_{1,24} = 2.42$, $p = 0.1329$, diet, $F_{1, 24} = 2.871$, $p = 0.1031$, N = 6-8 per group). The m-values are significantly reduced in the BF neurons of aged control as compared to young control and late-onset IF, suggesting that there is an age-related decrease in quantal content at GABAergic synapses in mouse BF neurons and that this decrease is reversed by late-onset IF. The data averaged by animals (Figure 3.5B, right) did not show statistical significance of either interaction between aging and diet or main effects for aging and diet on quantal content, possibly due to the small number of animals and the large scatter. None-the-less, the animal data very much resembles the individual neuron data. Overall, these results suggest that late-onset short-term IF diet can reverse the age-related reduction in presynaptic quantal content (m) of BF neurons. We observed no significant changes in the amplitude of light-induced oIPSCs (Figure 3.5C). The data in

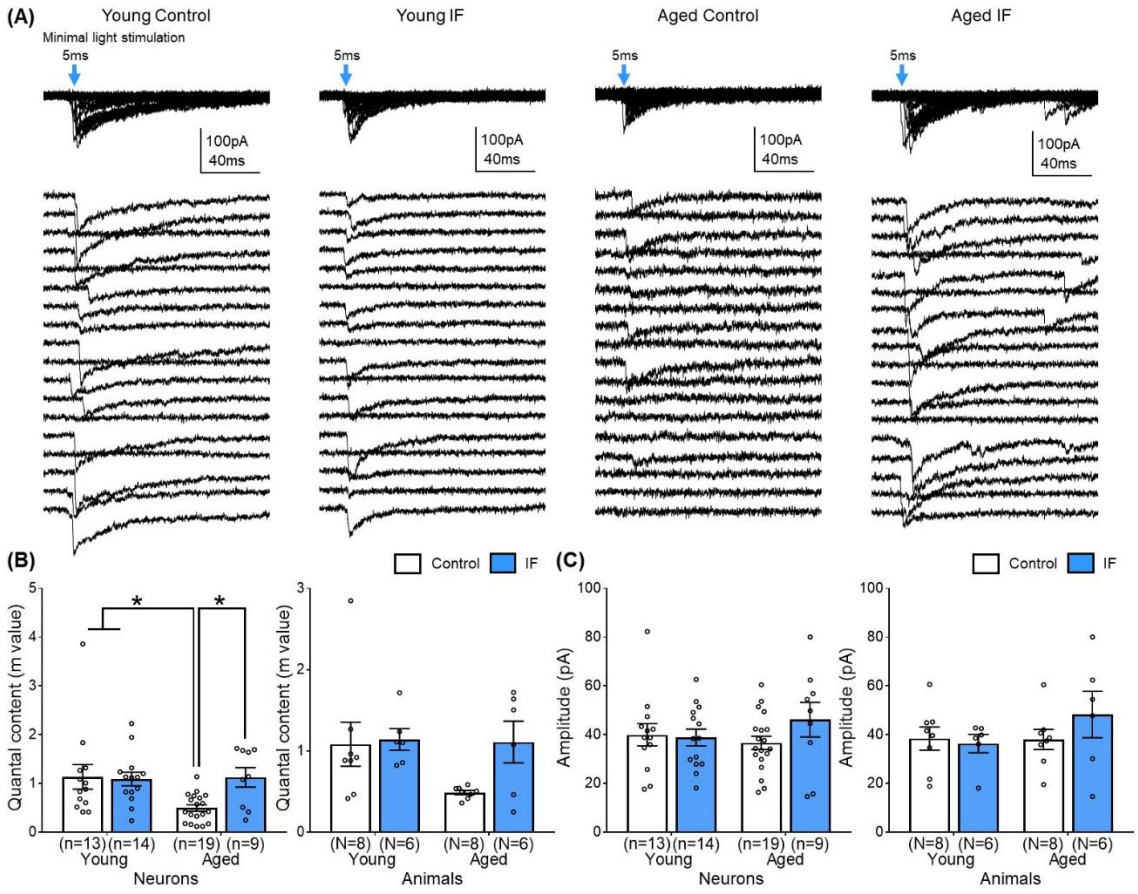

Figure 3.5. Late-onset short-term intermittent fasting reverses an age-related reduction in quantal content of inhibitory synaptic transmission in basal forebrain neurons of VGAT optogenetic mice in the reduced synaptic preparation. (A) Representative whole-cell voltage-clamp recordings (V_h = -60 mV) of oIPSCs superimposed (top) and distributed (below). Blue arrow indicates minimal intensity light stimulation (470 nm, 5 ms). (B) Graphs showing mean quantal content (m) calculated by the method of failures for both young and aged diet groups. The data on the left is from individual neurons (interaction, $F_{1, 51} = 4.085$, $p < 0.05$, n = 9-19 per group) and data on the right is averaged by individual animals (interaction, $F_{1, 24} = 1.947$, $p = 0.1757$, age, $F_{1,24} = 2.42$, $p = 0.1329$, diet, $F_{1, 24} = 2.871$, $p = 0.1031$, N = 6-8 per group). (C) Amplitude data of similar bar graphs for oIPSCs show no significant differences for age or diet. All data are mean ± SEM. The data in B and C were analyzed by a two-way ANOVA with Fisher's LSD post hoc test. *$p < 0.05$. Values of 'n' indicate number of neurons and values of 'N' indicate number of mice.

Figure 3.5B and C were analyzed by a two-way ANOVA with Fisher's LSD post hoc test. *$p < 0.05$.

3.4.6 Late-onset short-term IF did not reverse age-associated decline in cognitive function

After 4 weeks on the IF diets, Barnes maze training was performed to assess cognitive function in all mice (young and aged, VGAT and WT). In order to familiarize mice with the room and maze table, as well as to decrease their anxiety which may affect their behavior, all the mouse subjects went through habituation and pre-training prior to the acquisition and reversal training sessions (Figure 3.6A). The Barnes maze diagrams for acquisition and reversal training are shown in Figure 3.6B. Note that the location of the escape hole in reversal training is 180° opposite of the acquisition location. During the acquisition and reversal training days, distance traveled (cm) was measured and analyzed with repeated measurements ANOVA. In the acquisition training (Figure 3.6C, left), all four tested groups showed a decrease in the distance traveled to reach the escape hole from the start position (maze center) between days 1 and 4. However, the aged controls took significantly longer path-lengths than young controls. Although both IF groups displayed path-lengths generally intermediate between the young and aged controls, the aged IF was not different from aged control. Both aged control and aged IF showed delayed learning but eventually acquired the task such that there were no significant differences in distance travelled between the groups by day 4. Interestingly, young IF showed significantly longer distance on day 1 and day 2. when compared to young control, suggesting that the IF regimen in this study may be stressful and have

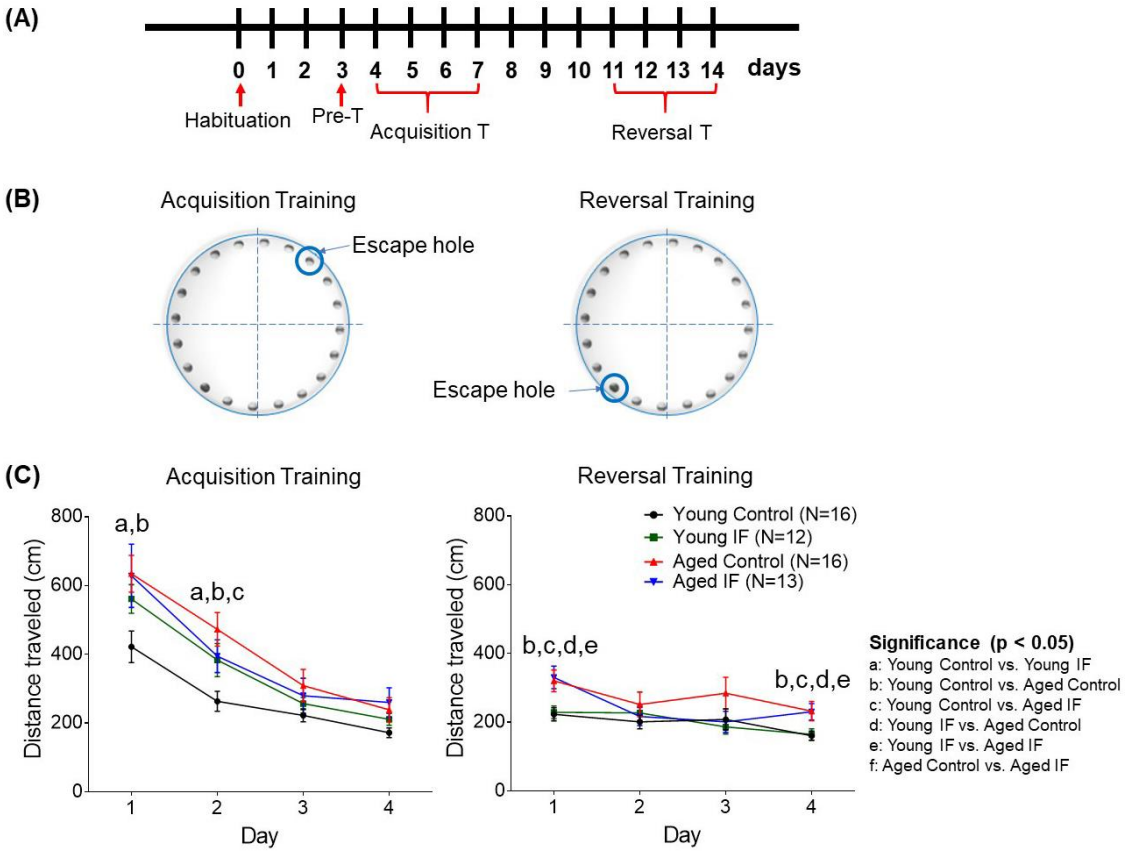

Figure 3.6. Age-related learning delay is not reversed by late-onset short-term intermittent fasting. (A) Diagram of the experimental timeline for Barnes maze training is shown. Numerals represent days of training. (B) Schematic representation of Barnes maze is depicted. Acquisition training (T) is shown on the left and reversal training is shown on the right. Note that escape hole position in the reversal training is changed 180˚ from its previous location in the acquisition training. The non-escape holes lack the escape compartment. (C) Graphs are shown of distance traveled per day to the escape hole in acquisition training (left, day, $F_{2.211, 117.2} = 69.14$, $p < 0.0001$; age, $F_{1, 53} = 8.281$, $p < 0.01$; diet, $F_{1, 53} = 0.9082$, $p = 0.3449$; no interaction between day and age, day and diet, age and diet, or day, age and diet) and reversal training (right, day, $F_{2.376, 125.9} = 7.445$, $p < 0.001$; age, $F_{1, 53} = 9.125$, $p < 0.01$; diet, $F_{1, 53} = 0.3886$, $p = 0.5357$; no interaction between day and age, day and diet, age and diet, or day, age and diet). All data are mean ± SEM and are pooled from WT and VGAT cohorts. The data included in panel C were analyzed by a repeated measure three-way ANOVA with Fisher's LSD post hoc test. Significance ($p < 0.05$) is shown in the figure with multiple comparisons indicated by letters a-f. Values of 'N' indicate number of mice.

some detrimental effect on the cognitive function in young animals. On the other hand, in the reversal training where animals are required to learn the new location of the escape box (Figure 3.6C, right), there was no difference in the performance of young control and young IF. Aged controls took longer paths than young controls or young IF during reversal training, and this deficit was only marginally improved by IF diet. These data suggest that aged mice showed delayed learning and less cognitive flexibility as compared to young mice and that the IF regimen in the present study was not sufficient to fully reverse age-related cognitive impairment. Graphs in Figure 3.6C show distance traveled per day to the escape hole in acquisition training (left, day, $F_{2.211, 117.2} = 69.14$, $p < 0.0001$; age, $F_{1, 53} = 8.281$, $p < 0.01$; diet, $F_{1, 53} = 0.9082$, $p = 0.3449$; no interaction between day and age, day and diet, age and diet, or day, age and diet) and reversal training (right, day, $F_{2.376, 125.9} = 7.445$, $p < 0.001$; age, $F_{1, 53} = 9.125$, $p < 0.01$; diet, $F_{1, 53} = 0.3886$, $p = 0.5357$; no interaction between day and age, day and diet, age and diet, or day, age and diet). All data are mean ± SEM and are pooled from WT and VGAT cohorts. The data included in Figure 3.6C were analyzed by a repeated measure three-way ANOVA with Fisher's LSD post hoc test. Significance ($p < 0.05$) is shown in the figure with multiple comparisons indicated by letters a-f. Values of 'N' indicate number of mice.

We also investigated possible age-related differences in search strategy to navigate to the escape hole. Search strategies are defined in the Materials and Methods, but basically, different search strategies were divided into 2 categories: spatial and non-spatial, as shown in Figure 3.7. During the acquisition training, all four groups gradually

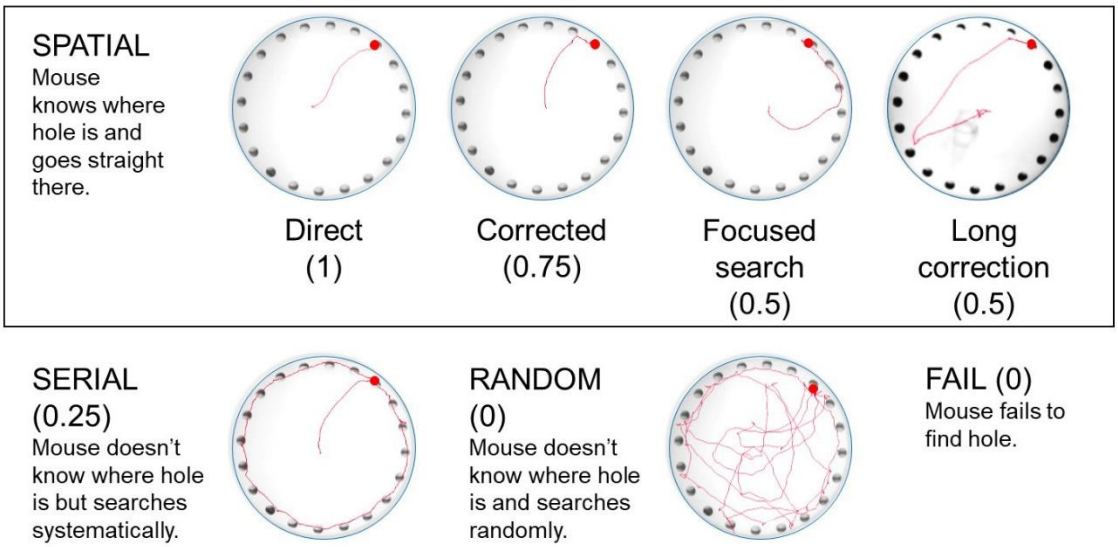

Figure 3.7. Spatial search strategies in mouse Barnes maze test. Examples shown range from highly spatial (top) to non-spatial and failures. Spatial strategies are shown in the box and include Direct, Corrected, Focused search, Long correction. Non-spatial strategies include Serial search, Random search, and Failure. Each strategy was scaled to quantitate cognitive score and values are shown in parentheses. Higher total cognitive scores indicate greater use of spatial search strategies. The focused search strategy is distinguished from the serial search when the mouse does not visit holes on the opposite side from the escape hole.

used a more spatial strategy across the training days, although both aged diet groups relied less frequently on spatial strategies than young groups throughout the training (Figure 3.8A, left). The pattern of search strategies was very similar between the aged IF and aged control. Young IF showed a delay in acquiring spatial search strategies relative to young control and continued to show a slight relative deficit throughout acquisition training. During the reversal training (Figure 3.8A, right), similar to the acquisition phase, all four groups displayed an increased use of a spatial strategy between days 1 and 4, although the aged control and aged IF did not achieve the levels of spatial strategies observed in the young diet groups. Both aged control and aged IF showed more random searches and failures throughout reversal training. Young IF displayed a slight delay in switching to a predominately spatial strategy relative to young control. These results show that the 4-week IF diet does not appear to improve cognitive performance in aged mice.

To quantify the cognitive capacity of individual mice, a cognitive score was calculated based on the data from Figure 3.8A and the cognitive score numerical values shown in Figure 3.7 (further details in Materials and Methods). All four tested groups showed an increase in their cognitive score between days 1 and 4 of acquisition and reversal training (Figure 3.8B). Young controls showed significantly higher cognitive scores than aged control and/or aged IF on the day 1, 2, and 4 in acquisition and on day 1 of reversal training, with young IF showing intermediate scores (Figure 3.8B), indicating age-related deficits in spatial learning. In addition, aged IF showed higher cognitive score on most of days in acquisition and reversal training when compared to aged

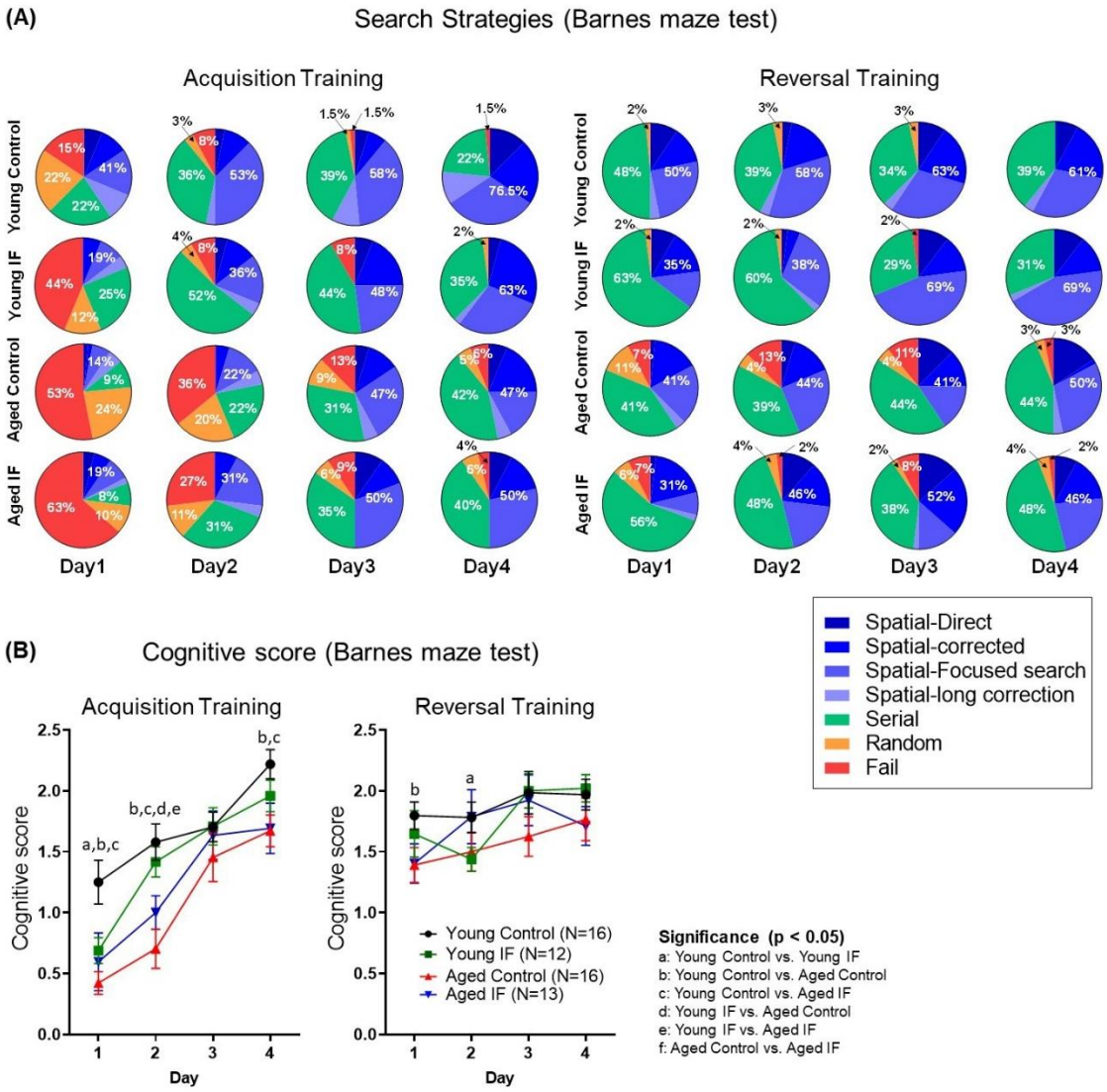

Figure 3.8. Late-onset short-term intermittent fasting did not improve an age-related reduction in the use of spatial search strategies. (A) The percentage of search strategy for each mouse group in the Barnes maze task was recorded during the acquisition training (left) and the reversal training (right). The percentages for the spatial search strategies (blue hues) are pooled. (B) Line graphs show cognitive scores for each mouse group per day during acquisition training (left, day, $F_{2.953, 156.5} = 62.91$, $p < 0.0001$; age, $F_{1, 53} = 13.20$, $p < 0.001$; diet, $F_{1, 53} = 0.1104$, $p = 0.7410$; no interaction between day and age, day and diet, age and diet, or day, age and diet) and during reversal training (right, day, $F_{2.542, 134.7} = 5.256$, $p < 0.01$; age, $F_{1, 53} = 3.655$, $p = 0.0613$; diet, $F_{1, 53} = 0.02204$, $p = 0.8826$; no interaction between day and age, day and diet, age and diet, or day, age and diet). Values are mean ± SEM and are pooled from WT and VGAT cohorts. The data in panel B were analyzed by a repeated measure three-way ANOVA with Fisher's LSD post hoc test. Significance ($p < 0.05$) is indicated by letters a-f in the figure. Values of 'N' indicate number of mice.

control, but it was not statistically significant, suggesting that short-term IF diet regimen on aged animals is not sufficient to reverse age-related cognitive impairment. In contrast, by day 4 in the reversal training, there were no statistically significant differences in cognitive score between all tested groups (Figure 3.8B, right). The legend for Figure 3.8 contains the summarized statistical analysis.

3.4.7 Correlation between cognitive behavioral scores and age-related changes in Ca^{2+} buffering and inhibitory synaptic transmission

Previously, we reported that age-related changes in calcium buffering and in sIPSC frequency are associated with cognitive impairment during aging in rats (Murchison et al., 2009; Griffith et al., 2014). We therefore examined the relationship between three cellular parameters that we measured in the present study (intracellular Ca^{2+} buffering slope, sIPSC frequency and quantal content) and cognitive function (cognitive score) across aging. Only control animals of both ages were used in this analysis to eliminate the effects of the IF diet. In addition, we used the cognitive score from the day 1 of acquisition and reversal training which showed the most significant age-related differences in cognitive function. Figure 3.9 shows the correlation plots for both acquisition (top graphs) and reversal training (bottom graphs). Each point on the graphs represents an individual animal. The intracellular Ca^{2+} buffering slope values were positively correlated with cognitive scores, suggesting that higher slopes (less buffering) are beneficial for cognitive function (Figure 3.9A, top, acquisition, $r = 0.5355$, $p = 0.0346$; bottom, reversal, $r = 0.7861$, $p = 0.0005$). Likewise, Figure 3.9B shows a

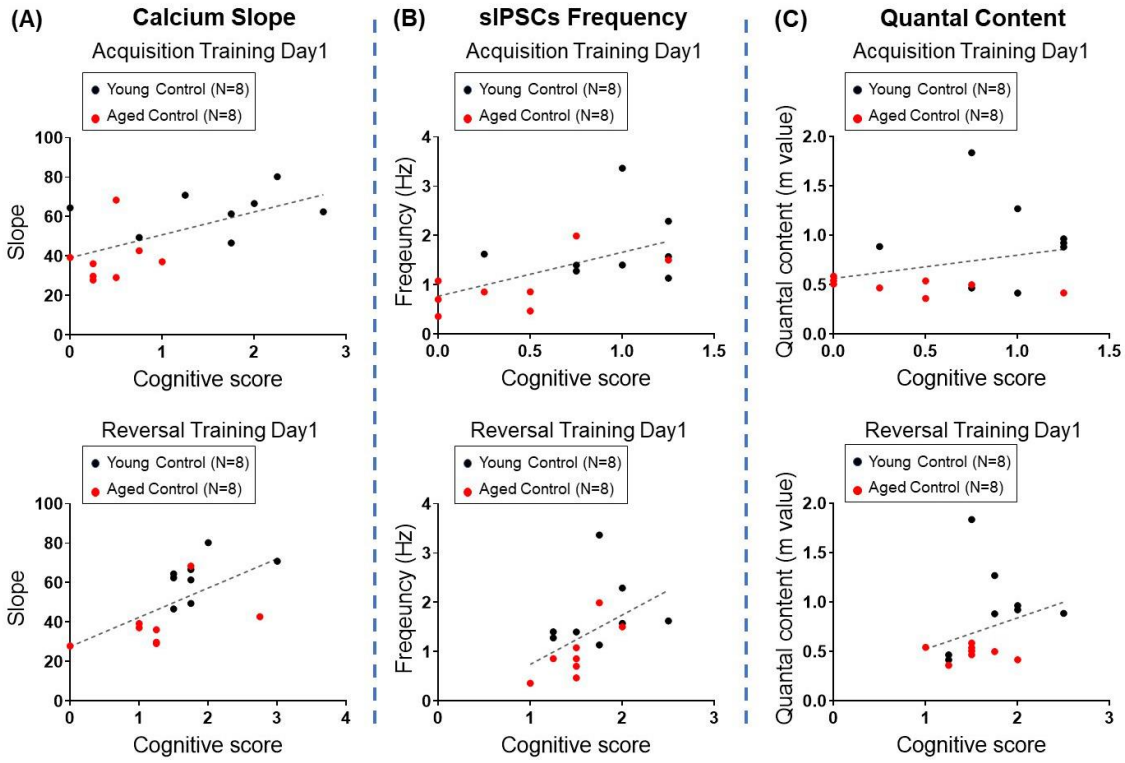

Figure 3.9. Cognitive scores in the Barnes maze task correlate with physiological measures of calcium buffering and synaptic transmission. (A) Intracellular calcium buffering slopes show a significant correlation with cognitive scores, such that greater slopes (lower buffering) are associated with higher cognitive scores (top, acquisition, r = 0.5355, p = 0.0346; bottom, reversal, r = 0.7861, p = 0.0005). (B) Scatter plots show that sIPSC frequency is significantly positively correlated with cognitive score (top, acquisition, r = 0.6468, p = 0.0083; bottom, reversal, r = 0.6900, p = 0.0040). (C) Scatter plots show that quantal content of inhibitory synaptic transmission is not significantly correlated with cognitive score (top, acquisition, r = 0.1643, p = 0.5397; bottom, reversal, r = 0.4821, p = 0.0608). All data were analyzed by Spearman's correlation with significance $p < 0.05$. Values of 'N' indicate number of mice.

positive correlation between sIPSC frequency and cognitive score. (top, acquisition, r = 0.6468, p = 0.0083; bottom, reversal, r = 0.6900, p = 0.004). No correlation between quantal content and cognitive score was found (Figure 3.9C, top, acquisition, r = 0.1643, p = 0.5397; bottom, reversal, r = 0.4821, p = 0.0608). When all animals (control and IF diet) were included in the analysis, there were no correlations (data not shown). This is predictable in that the aged IF diet reversed the changes in the neurophysiological parameters, but not the cognitive score deficits. Consistent with the previous rat data, we observed significant positive correlation between calcium buffering slope/sIPSC frequency and cognitive score. It is unclear why quantal content (m) from GABAergic synapses failed to correlate significantly with cognitive score (Figure 3.9C), other than that the aged mice had similar m-values regardless of cognitive score. Future studies are required to test whether IF may affect different releasable pools of neurotransmitter as an explanation for the differences between sIPSC frequency and evoked quantal release. Overall, our results suggest that changes in intracellular Ca^{2+} buffering and sIPSC frequency in the mouse BF are relevant to age-related changes in cognitive function.

3.5 Discussion

The substantial burden of age-related cognitive impairment associated with an aging population has led to increased interest in potential therapeutics and lifestyle changes intended to alleviate this mental deterioration. Caloric restriction (CR) is one such intervention that has been shown to ameliorate cognitive deficits during aging (Idrobo et al., 1987; Ingram et al, 1987; Stewart et al., 1989; Pitsikas and Algeri, 1992; Pitsikas et al, 1992; Eckles et al, 1997; Eckles-Smith et al, 2000; Fontán-Lozano et al.,

2007; Singh et al., 2012; Mattson, 2012; Mattson and Arumugam, 2018). In this study, we investigated the hypothesis that late-onset short-term intermittent fasting (IF) could have benefits similar to those imparted by long-term CR. We show that aged mice displayed cognitive decline and increased intracellular Ca^{2+} buffering, decreased sIPSC frequency and decreased quantal content of GABA release from presynaptic terminals. Late-onset short-term (4-6 weeks) IF reverses all of these age-related physiological changes, but fails to prevent cognitive impairment in aged mice. These results are consistent with other studies reporting the beneficial effects of short-term dietary interventions on age-related impairments (Cao et al. 2001; Kaur et al., 2008). Because we have shown that life-long CR can prevent enhancement of Ca^{2+} buffering in aged rat BF neurons (Murchison et al., 2009) and in aged mice BF neurons (Supplementary figure 3.1), we suggest that late-onset IF may have several beneficial effects on age-related function without the need for a long-term commitment to a CR diet.

In BF neurons, enhancement of Ca^{2+} influx was observed during aging. This increase occurred through larger amplitude low-voltage activated (LVA) currents, and reduced current inactivation of high-voltage activated (HVA) currents (Murchison and Griffith, 1995, 1996). Interestingly, basal $[Ca^{2+}]_i$ of aged BF neurons was unaltered, and the peak amplitude of Ca^{2+} transients ($\Delta[Ca^{2+}]_i$) induced by either High K^+ or Ca^{2+} current stimulation was decreased in BF cholinergic neurons of aged rats (Murchison and Griffith, 1998, 1999; Griffith et al., 2000). These findings suggest that the age-related increase in rapid Ca^{2+} buffering in aged BF neurons may be a possible compensatory mechanism to limit the rise of intracellular Ca^{2+} concentrations. However,

it is unclear if this potential compensatory increase in Ca^{2+} buffering is beneficial or detrimental, as it is associated with cognitive impairments in aged rats (Murchison et al., 2009. Alterations in Ca^{2+} dependent physiology during aging contributes to altered synaptic function and is believed to account for much age-related cognitive impairment (Disterhoft et al., 1996; Thibault and Landfield, 1996; Foster and Norris, 1997; Foster, 1999, 2007, 2012; Tombaugh et al., 2005; Murphy et al., 2006; Gant et al., 2015, 2018; Kumar and Foster, 2019; Abu-Omar et al., 2018).

The contribution of Ca^{2+} buffering to the synaptic functions in rat BF neurons was demonstrated indirectly with the addition of the exogenous Ca^{2+} buffer, BAPTA-AM. In these experiments using the reduced synaptic preparation, increased Ca^{2+} buffering with BAPTA-AM in synaptic terminals reduced the frequency of sIPSCs in the young BF neurons, suggesting that increased Ca^{2+} buffering at synaptic terminals could mediate the deficit in BF synaptic transmission with age and contribute to cognitive impairment (Griffith et al., 2014). Our current study demonstrated that the late-onset short-term IF diet regimen could reverse the age-related increase in Ca^{2+} buffering in aged mouse BF neurons with no change in baseline $[Ca^{2+}]_i$. Although the precise mechanisms underlying the impact of late-onset short-term IF on Ca^{2+} buffering in aged BF neurons have not been determined at this time, several alternatives may be possible. Given that increased Ca^{2+} buffering may be a compensatory mechanism against increased Ca^{2+} entry, the IF diet may prevent age-related enhancement of Ca^{2+} influx, thereby eliminating the stimulus for increased buffering. Alternatively, IF may interact more directly with rapid Ca^{2+} buffers, preventing their age-related upregulation. In

hippocampal CA1 pyramidal neurons, increased spike-mediated Ca^{2+} accumulation and slow after-hyperpolarization (sAHP) with age were prevented by CR, independent of Ca^{2+} clearance mechanisms (Hemond and Jaffe, 2005). Another study reported that CR offers neuroprotective effects under excitotoxic conditions by increasing both calcium uptake rates and maximal uptake capacity in mitochondria (Amigo et al., 2017).

It has been well established that CR attenuates age-related synaptic dysfunctions (Hori et al., 1992; Eckles-Smith et al., 2000; Mattson et al., 2003; Fusco and Pani, 2013; Wahl et al., 2016). In the current study, the IF regimen restored the age-related reduction in sIPSC frequency to levels observed in young BF neurons. Because changes in spontaneous frequency may represent changes in probability of neurotransmitter release from presynaptic sites, we further investigated possible presynaptic mechanisms with age and IF by measuring quantal content of inhibitory synaptic transmission. Quantal content is significantly reduced with age and reversed by IF. A reduction in quantal content alone however, is unlikely to explain reduced sIPSC frequency with age even though both are restored by IF. Because the probability of neurotransmitter release is directly affected by the level of Ca^{2+} within the synaptic terminal (Zucker, 1993; Wu and Saggau, 1997), the restoration of youthful Ca^{2+} buffering by IF may be the most important influence on presynaptic function in the BF neurons. It is noteworthy that both Ca^{2+} buffering and sIPSC frequency were significantly correlated with cognitive performance, while quantal content was not.

Despite the attractive link between Ca^{2+} buffering and sIPSC frequency, other targets for IF modulation cannot be ruled out. For instance, our laboratory has shown

that sIPSCs in aged rat BF are more dependent on tetrodotoxin-sensitive Na^+ channels than in young rat (Griffith et al., 2014) and this mechanism could be modulated by IF. Also, it was previously reported in animals with obesity-induced diabetes, that CR improved diabetes-induced cognitive deficits by reversing high-fat diet-induced expression of neurogranin which regulates Ca^{2+}/calmodulin-dependent synaptic function (Kim et al., 2016). Additional mechanisms could be involved as well, such as modulating synaptic function by changes in neurotrophic factors or oxidative stress, both of which have been studied extensively with CR (Granger et al., 1996; Lee et al., 2002; Merry, 2002, 2004; Mattson et al., 2004; Gredilla and Barja, 2005; Hunt et al., 2006; Hyun et al., 2006; Rex et al., 2006; Tapia-Arancibia et al., 2008; Kishi et al., 2015). A recent electrophysiological study also provides another possible mechanism of influence on GABAergic inhibitory synaptic transmission by IF. In this study, the CA1 hippocampal neurons from mice on IF diets for 1 month showed up-regulation of GABAergic synaptic activity via a mechanism requiring the mitochondrial protein deacetylase sirtuin 3 (SIRT3) and involving a reduction in mitochondrial oxidative stress (Liu et al., 2019). SIRT3 protects mitochondria and neurons against metabolic and excitotoxic stress (Cheng et al., 2016).

One of the most consistent synaptic plasticity-associated impairments during aging is the reduction in the neurotrophic factors and their signaling. However, CR protects against age-related deficits in synaptic plasticity and neuronal networks via upregulation of brain derived neurotrophic factor (BDNF)/TrkB (Rex et al., 2006; Granger et al., 1996; Tapia-Arancibia et al., 2008; Mattson et al., 2004; Kishi et al.,

2015). Our findings on the presynaptic mechanisms of IF may be explained by either direct or indirect BDNF modulation of synaptic transmission (Porcher et al., 2018; Crozier et al., 1999; Tanaka et al., 1997; Frerking et al., 1998; Tyler et al., 2006). Furthermore, BDNF is negatively correlated to oxidative stress (Jain et al., 2013). In hypertensive rats, CR alone could not improve cognitive decline (Kishi and Sunagawa, 2012) but administration of antioxidant reagent could protect against cognitive decline via BDNF/TrkB in the hippocampus of hypertensive rats (Kishi et al., 2012), indicating that CR coupled with reduction of oxidative stress could be efficacious against cognitive decline. Another finding showed that the beneficial effect of CR on cognitive function was attenuated by blockade of BDNF receptors in the hippocampus of metabolic syndrome model rats but CR-mediated improvements in BDNF expression and oxidative stress were not altered (Kishi et al., 2015). In the present study, our data demonstrated the beneficial effect of short-term IF on calcium homeostasis and synaptic transmission, even started later in life. However, this late-onset short-term IF regimen could not fully improve age-related cognitive decline. The aged group that was on IF for 4 weeks showed only marginally better performance in the Barnes maze compared to aged control group. Our findings therefore suggest that the IF regimen in the current study may require a longer duration or supplementation in order to reverse age-related deficits in cognitive function.

In conclusion, our findings provide evidence that late-onset short-term IF can reverse age-related changes in calcium homeostasis and inhibitory synaptic function in mouse BF neurons. However, only 4 weeks of IF may not have been long enough to

reverse age-related impairment in cognition. Importantly, we also show that intracellular Ca^{2+} buffering and sIPSC frequency in the mouse BF are correlated with cognitive performance in mice. Notably, reductions in quantal content (m) of GABAergic synapses were not correlated with cognitive status, which might be attributed to various pools of synaptic vesicles participated differently in spontaneous and evoked quantal release of IPSCs. Together these results suggest that short-term IF, even initiated late in life, is a promising avenue on which to pursue therapeutic interventions designed to improve age-related alterations in cognitive function.

3.6 Materials and Methods

3.6.1 Animals and Treatments

Male wildtype (WT) C57 Bl/6 mice and VGAT-ChR2(H134R)-EYFP optogenetic mice of two ages, young (4-8 months) and aged (18-25 months) were used for all experiments. Breeding pairs were purchased from Jackson Laboratory (Stock 014548, Bar Harbor, ME; Zhao et al., 2011; Bang et al., 2021) and an aging colony was maintained for both genotypes. For the intermittent fasting (IF) experiments, mice were singly housed and were identified as WT or VGAT by standard tail-clip genotyping methods after weaning (EZ tissue/tail PCR genotyping kit, EZ BioResearch, St. Louis, MO) as described by Bang et al., 2021. In aged animals, IF was initiated later in life. Calcium imaging experiments utilized WT mice, while VGAT mice were used for whole-cell patch-clamp recordings. Mice were randomly assigned to a control diet (ad libitum, AL) or an IF diet (alternate-day fasting) and diet groups were age-matched. IF mice received the AL diet until the initiation of the IF diet and for 24 h on alternate days

during the fasting regimen. After 4 weeks from the start of the diet, mice underwent two weeks of behavioral testing for a total of 6 weeks of diet treatment. Individual mice were then used daily for either calcium imaging or whole-cell patch-clamp experiments and this required approximately two weeks. During this time, mice were maintained on their respective diets. Mice were fed the NIH-31 chow which contained crude protein (18%), crude fat (5%), crude fiber (5%), minerals and vitamins. Water was available ad libitum. The body weight and food consumption were recorded daily in both IF and control groups. Food intake was calculated on feeding days for IF mice. All mice were maintained in the AAALAC-accredited vivarium at the Texas A&M University Health Science Center under controlled conditions (22 – 25°C; lights 0700-1900 h) in accordance with policies of the Texas A&M University Laboratory Animal Care Committee and NIH guidelines.

3.6.2 Enzyme-treated, acutely dissociated neurons for calcium imaging

Mice were euthanized after isoflurane anesthetization and the brain quickly removed and sectioned at 320-μm thickness in a coronal plane. Slices were cut using a carbogen-equilibrated ice-cold cutting solution containing (in mM): 120 NaCl, 2.7 KCl, 0.5 $CaCl_2$, 6 $MgCl_2$, 5 HEPES, 26 $NaHCO_3$, 11 D-glucose, and 0.3 kynurenic acid (pH 7.4 with NaOH, 310-330 mOsm). BF slices were then micro dissected to isolate the medial septum and nucleus of the diagonal band (MS/nDB) and enzymatically treated (trypsin, Sigma, type XI or type I, St. Louis, MO), as described previously (Murchison and Griffith, 1996, 1998; Murchison et al., 2009). Enzyme-treated tissues were continuously suspended in a holding solution (in mM): 140 NaCl, 2.7 KCl, 0.5 $CaCl_2$,

1.2 $MgCl_2$, 10 HEPES, and 33 D-glucose (pH 7.4 with NaOH, 310-330 mOsm) by agitation of a small magnetic stir bar and were kept oxygenated with 100% O_2. MS/nDB slices were then gently triturated using a series of increasingly smaller diameter fire-polished glass pipettes. The dissociated cells were plated on the glass floor of a recording chamber containing bath solution (in mM): 140 NaCl, 2.7 KCl, 2 $CaCl_2$, 1.2 $MgCl_2$, 10 HEPES, and 33 D-glucose, then perfused at a rate of about 2 ml/min. Experiments were performed at room temperature within 5 h of dispersal.

3.6.3 Calcium imaging

In order to measure intracellular Ca^{2+} buffering in mouse BF neurons, we utilized a dual wavelength ratiometric fura-2 microfluorimetry system (Murchison and Griffith, 1998, 2007; Murchison et al., 2009). Enzyme-treated, acutely dissociated mouse BF neurons were loaded with ratiometric fluorescent Ca^{2+}-indicator fura-2AM (1 μM, Molecular Probes, Eugene, OR) for 12 min in the presence of 10 μM pluronic acid (Invitrogen, Carlsbad CA), after which they were washed for 40-45 min to allow for fura de-esterification. The Fura-2 fluorescence was excited using alternating 340 nm and 380 nm wavelengths and the resulting 340/380 intensity ratio was determined. The intracellular calcium concentrations ($[Ca^{2+}]_i$) were estimated using in vitro calibration as described previously (Murchison and Griffith, 1998). The Ca^{2+}-transients ($\Delta[Ca^{2+}]_i$) were triggered by pressure application of elevated $[K^+]$ (20 mM) solution (High $[K^+]$), using a focal picospritzer (Picospritzer II, General Valve, Fairfield NJ). Application of different stimulus durations (0.2-1.2s) resulted in increasing amplitudes of $\Delta[Ca^{2+}]_i$. The amplitude of the transients was then plotted against the stimulus intensity to calculate a

buffering slope. Unlike the traditional buffering curve generated by voltage-clamp stimulation (Murchison et al., 2009), this less invasive technique produces plots of transient amplitude vs. stimulus intensity calculated in arbitrary units (stimulus duration X 10) with a greater slope value indicating less intracellular Ca^{2+} buffering. Fluorescent signals were recorded using a Sutter lambda DG-4 excitation switcher (Sutter Instrument ®, Novato, CA), a Hamamatsu ORCA flash2.8 CCD camera (Hamamatsu Photonics, Bridgewater Township, NJ), an Olympus IX70 fluorescent scope and Metafluor imaging software (Molecular Devices, San Jose, CA). The resting $[Ca^{2+}]_i$ was determined before any stimulation of the cell.

3.6.4 Reduced synaptic preparation using enzyme-free, acutely dissociated neurons to study synaptic transmission across aging

We used a reduced synaptic preparation to examine synaptic transmission in acutely dissociated BF neurons across aging (Griffith et al., 2014; Bang et al., 2021; Montgomery et al., in submission). In this preparation, there is a very low frequency of glutamatergic spontaneous excitatory postsynaptic currents (sEPSCs) which show rapid kinetics with decay time constant (τ_d =~5 ms). In contrast, much slower GABAergic spontaneous IPSCs are easily identifiable with decay constants of τ_d = 20-30 ms. With CsCl in the recording pipette, the IPSCs have a reversal potential of 0 mV and are often larger than the faster, occasional sEPSCs. No excitatory amino acid antagonists were used. All recordings were visually inspected and analyzed. Slices from the MS/nDB region (320-μm) were cut and neurons were acutely dissociated as described above, but

without enzyme pre-treatment. These neurons retain functional presynaptic boutons (Figure 3.1).

3.6.5 Electrophysiology

Standard whole-cell patch voltage-clamp recording was used for measuring spontaneous inhibitory postsynaptic currents (sIPSCs) and optically-evoked IPSCs (oIPSCs). Recordings for sIPSCs and oIPSCs were made from a holding potential of -60 mV, low-pass filtered at 2 kHz and digitized at 10 kHz with Digidata 1440A interface, Multiclamp 700B amplifier (Molecular Devices, San Jose, CA), and pClamp 10 software (Molecular Devices, San Jose, CA). Membrane capacitance (pF) was obtained by digital cancellation of whole-cell capacitance transients. Recording electrodes were pulled from glass capillary tubing (KG-33, 1.5mm OD, King Precision Glass, Claremont, CA) on a Flaming/Brown P-87 pipette puller (Sutter Instrument ®, Novato, CA) with final electrode resistance 4-8 MΩ when filled with a pipette solution. The internal pipette solution for whole-cell recordings contained (in mM): CsCl, 130; ethylene glycol-bis (β-aminoethyl ether)-N,N,N',N'-tetraacetic acid (EGTA), 10; $MgCl_2$, 2; HEPES, 10; Mg-ATP, 4; GTP, 0.1 (pH 7.2 with CsOH; 295-300 mOsm).

Mini Analysis (6.0.7; Synaptosoft, Decatur, GA) and Clampfit 10 (Molecular Devices, San Jose, CA) software were employed for the analysis and we visually identified and measured spontaneous IPSCs. The optically-evoked response was calculated as the peak current over 20ms from the time when response begins. Mean data were compared using a two-way ANOVA followed by Fisher's least significant

difference (LSD) test (GraphPad Prism 9, GraphPad software, San Diego, CA). Cumulative probability curves were compared using a Kolmogorov-Smirnov test.

3.6.6 Optically-induced current recordings and quantal content analysis

Optically-induced inhibitory postsynaptic currents (oIPSCs) were recorded using whole-cell clamp from a holding potential of -60 mV. Enzyme-free, acutely dissociated neurons from VGAT mice were stimulated with 5-ms duration light stimulation (470 nm) at 15 s intervals using an optogenetic illumination system (DC2100, Thor Labs, Ann Arbor, MI). Power density was calculated by dividing the measured power using a PM200 optical power and energy meter (ThorLabs, Ann Arbor, MI) connected to an S120C photodiode sensor (ThorLabs, Ann Arbor, MI) by the illuminated area. Initial measurements using a 400 μm cannula revealed a maximum power density of approximately 10mW/mm^2, and a power density of 1.76 mW/mm^2 corresponding to 100mA drive current. LED intensity was controlled by adjusting the drive current (1mA-1A). For the quantal content analysis, 50-100 consecutive traces of oIPSCs were recorded, and minimal light stimulation was used to ensure a sufficient number of failures. Using the method of failures ($m = \ln(N/N0)$) in the Poisson model, quantal content (m) was calculated where, N is the total number of stimuli, and N0 is the number of failures where stimulation did not evoke a synaptic response (Bang et al., 2021).

3.6.7 Barnes Maze

Cognitive function was assessed using the Barnes Maze (BM) spatial learning task (Barnes, 1979; Bizon et al., 2012; Pitts et al., 2018). The apparatus is a circular platform (92 cm in diameter) with 20 circular holes (5.1 cm in diameter) evenly spaced

around the periphery and an escape box is placed under one of the holes. The platform is located 92 cm above the floor to discourage mice from jumping down. Four bright floodlights were affixed above the maze as a negative reinforcement to motivate the mice to search for the escape chamber using spatial cues which surround the Barnes table. Video was acquired using an EQ610 Polestar II Everfocus camera and data were quantified using Ethovision XT version 15 video tracking software (Noldus). Mice were habituated by allowing each mouse to freely explore the maze without an escape box under modest light for 5 minutes to become accustomed to the room, table, and extra- and intra-maze layout. On the pre-training day which is 48 hrs after habituation, mice learned the presence of the escape hole by exploring the maze under bright light for 3 minutes and then being guided gently toward the escape hole positioned randomly on the maze and allowing the mouse to enter the hole and remain inside for 1 minute. Acquisition training began 24 hrs after the conclusion of pre-training and started with mice in a 2 L transparent glass beaker in the center of the table. A trial started when the beaker was lifted, and mice were allowed 3 minutes to locate and enter the escape box. The trial session ended when the mouse entered the escape hole or after 3 minutes had elapsed. If the mouse was unable to find the escape box, it was gently guided and allowed to remain there for one minute. All mice received 4 trials per day for 4 days. 72 hrs after the last acquisition training, reversal learning trials were performed in which the escape chamber position was changed 180˚ from its previous location in the acquisition training. Similar to the acquisition training, all mice were given 4 trials per day for 4 days. The platform and escape box were cleaned with 70% ethanol and water to prevent

odor cues between subsequent trials. Distance travelled to the escape hole and search strategies used per trial during acquisition and reversal training were measured from the recorded video. Search strategies were determined by examining each mouse's daily session and separating them into six main categories (Illouz et al.,): (1) Direct (spatial), navigating directly to target hole, (2) corrected (spatial), making a minor correction (± 1 hole away from the target hole), (3) long-correction (spatial), re-angulating from a distal region of environment and making a direct movement toward the target, (4) focused search (spatial), searching the region surrounding the target (± 3 holes away from the target hole) (5) serial search (non-spatial), systematic sequential hole searches; and (6) random search (non-spatial), localized searches of holes separated by paths crossing the maze center. Strategies during each trial session were scored with a numerical value to quantify a cognitive score for each animal: direct = 1, corrected = 0.75, focused search = 0.5, long-correction = 0.5, serial = 0.25, random = 0. Failure of a mouse to find the target hole was also assigned a score of "0" (Figure 3.7).

3.6.8 Statistical analysis

Aa Comparisons were performed using a two-way or repeated measures three-way ANOVA with Fisher's least significant difference (LSD) post hoc test using GraphPad Prism 9 (GraphPad software, San Diego, CA). Values are expressed as means ± S.E.M. Differences were considered significant at $p < 0.05$.

3.7 References

Abu-Omar, N., Das, J., Szeto, V., Feng, Z.P. (2018). Neuronal Ryanodine Receptors in Development and Aging. *Mol. Neurobiol.* 55, 1183-1192. doi: 10.1007/s12035-

016-0375-4.

Amigo, I., Menezes-Filho, S.L., Luévano-Martínez, L.A., Chausse, B., Kowaltowski, A.J. (2017). Caloric restriction increases brain mitochondrial calcium retention capacity and protects against excitotoxicity. *Aging Cell.* 16, 73-81. doi: 10.1111/acel.12527.

Cao, S.X., Dhahbi, J.M., Mote, P.L., Spindler, S.R. (2001). Genomic profiling of short- and long-term caloric restriction effects in the liver of aging mice. *Proc. Natl. Acad. Sci. U S A.* 98, 10630-5. doi: 10.1073/pnas.191313598.

Cheng, A., Yang, Y., Zhou, Y., Maharana, C., Lu, D., Peng, W., Liu, Y., Wan, R., Marosi, K., Misiak, M., Bohr, V.A., Mattson, M.P. (2016). Mitochondrial SIRT3 Mediates Adaptive Responses of Neurons to Exercise and Metabolic and Excitatory Challenges. *Cell Metab.* 23, 128-42. doi: 10.1016/j.cmet.2015.10.013.

Crozier, R.A., Black, I.B., Plummer, M.R. (1999). Blockade of NR2B-containing NMDA receptors prevents BDNF enhancement of glutamatergic transmission in hippocampal neurons. *Learn. Mem.* 6, 257-66.

Disterhoft, J.F., Thompson, L.T., Moyer, J.R. Jr., Mogul, D.J. (1996). Calcium-dependent afterhyperpolarization and learning in young and aging hippocampus. *Life Sci.* 59, 413-20. doi: 10.1016/0024-3205(96)00320-7.

Eckles, K.E., Dudek, E.M., Bickford, P.C., Browning, M.D. (1997). Amelioration of age-related deficits in the stimulation of synapsin phosphorylation. *Neurobiol. Aging.* 18, 213-7. doi: 10.1016/s0197-4580(97)00008-0.

Eckles-Smith, K., Clayton, D., Bickford, P., Browning, M.D. (2000). Caloric restriction

prevents age-related deficits in LTP and in NMDA receptor expression. *Brain. Res. Mol. Brain. Res.* 78, 154-162. doi: 10.1016/s0169-328x(00)00088-7.

Fontán-Lozano, A., Sáez-Cassanelli, J.L., Inda, M.C., de los Santos-Arteaga, M., Sierra-Domínguez, S.A., López-Lluch, G., Delgado-García, J.M., Carrión, A.M. (2007). Caloric restriction increases learning consolidation and facilitates synaptic plasticity through mechanisms dependent on NR2B subunits of the NMDA receptor. *J. Neurosci.* 27, 10185-95. doi: 10.1523/JNEUROSCI.2757-07.2007.

Foster, T.C. (1999). Involvement of hippocampal synaptic plasticity in age-related memory decline. *Brain Res. Brain Res. Rev.* 30, 236-49. doi: 10.1016/s0165-0173(99)00017-x.

Foster, T.C. (2007). Calcium homeostasis and modulation of synaptic plasticity in the aged brain. *Aging Cell.* 6, 319-25. doi: 10.1111/j.1474-9726.2007.00283.x.

Foster, T.C. (2012). Dissecting the age-related decline on spatial learning and memory tasks in rodent models: N-methyl-D-aspartate receptors and voltage-dependent Ca2+ channels in senescent synaptic plasticity. *Prog. Neurobiol.* 96, 283-303. doi: 10.1016/j.pneurobio.2012.01.007.

Foster, T.C., Norris, C.M. (1997). Age-associated changes in Ca(2+)-dependent processes: relation to hippocampal synaptic plasticity. *Hippocampus.* 7, 602-12. doi: 10.1002/(SICI)1098-1063(1997)7:6<602::AID-HIPO3>3.0.CO;2-G.

Fusco, S., Pani, G. (2013). Brain response to calorie restriction. *Cell Mol. Life Sci.* 70, 3157-70. doi: 10.1007/s00018-012-1223-y.

Gant, J.C., Blalock, E.M., Chen, K.C., Kadish, I., Thibault, O., Porter, N.M., Landfield,

P.W. (2018). FK506-binding protein 12.6/1b, a negative regulator of [Ca^{2+}], rescues memory and restores genomic regulation in the hippocampus of aging rats. *J. Neurosci.* 38, 1030-1041. doi: 10.1523/JNEUROSCI.2234-17.2017.

Gant, J.C., Chen, K.C., Kadish, I., Blalock, E.M., Thibault, O., Porter, N.M., Landfield, P.W. (2015). Reversal of aging-related neuronal Ca2+ dysregulation and cognitive impairment by delivery of a transgene encoding FK506-binding protein 12.6/1b to the hippocampus. *J. Neurosci.* 35, 10878-87. doi: 10.1523/JNEUROSCI.1248-15.2015.

Granger, R., Deadwyler, S., Davis, M., Moskovitz, B., Kessler, M., Rogers, G., Lynch, G. (1996). Facilitation of glutamate receptors reverses an age-associated memory impairment in rats. *Synapse.* 22, 332-7. doi: 10.1002/(SICI)1098-2396(199604)22:4<332::AID-SYN4>3.0.CO;2-C.

Gredilla, R., Barja, G. (2005). Minireview: the role of oxidative stress in relation to caloric restriction and longevity. *Endocrinology* 146, 3713-3717. doi: 10.1210/en.2005-0378.

Griffith, W.H., Dubois, D.W., Fincher, A., Peebles, K.A., Bizon, J.L., Murchison, D. (2014). Characterization of age-related changes in synaptic transmission onto F344 rat basal forebrain cholinergic neurons using a reduced synaptic preparation. *J. Neurophysiol.* 111, 273-86. doi: 10.1152/jn.00129.2013.

Griffith, W.H., Jasek, M.C., Bain, S.H., Murchison, D. (2000). Modification of ion channels and calcium homeostasis of basal forebrain neurons during aging. *Behav. Brain Res.* 115, 219-33. doi: 10.1016/s0166-4328(00)00260-6.

Hemond, P., Jaffe, D.B. (2005). Caloric restriction prevents aging-associated changes in spike-mediated Ca2+ accumulation and the slow afterhyperpolarization in hippocampal CA1 pyramidal neurons. *Neuroscience* 135, 413-20. doi: 10.1016/j.neuroscience.2005.05.044.

Hori, N., Hirotsu, I., Davis, P.J., Carpenter, D.O. (1992). Long-term potentiation is lost in aged rats but preserved by caloric restriction. *Neuroreport* 3, 1085-1088. doi: 10.1097/00001756-199212000-00013.

Hunt, N.D., Hyun, D.H., Allard, J.S., Minor, R.K., Mattson, M.P., Ingram, D.K., de Cabo, R. (2006). Bioenergetics of aging and calorie restriction. *Ageing Res. Rev.* 5, 125-143. doi: 10.1016/j.arr.2006.03.006.

Hyun, D.H., Hernandez, J.O., Mattson, M.P., de Cabo, R. (2006). The plasma membrane redox system in aging. *Ageing Res. Rev.* 5, 209-20. doi: 10.1016/j.arr.2006.03.005.

Idrobo, F., Nandy, K., Mostofsky, D.I., Blatt, L., Nandy, L. (1987). Dietary restriction: effects on radial maze learning and lipofuscin pigment deposition in the hippocampus and frontal cortex. *Arch. Gerontol. Geriatr.* 6, 355-62. doi: 10.1016/0167-4943(87)90014-8.

Ingram, D.K., Weindruch, R., Spangler, E.L., Freeman, J.R., Walford, R.L. (1987). Dietary restriction benefits learning and motor performance of aged mice. *J. Gerontol.* 42, 78-81. doi: 10.1093/geronj/42.1.78.

Jain, S., Banerjee, B.D., Ahmed, R.S., Arora, V.K., Mediratta, P.K. (2013). Possible role

of oxidative stress and brain derived neurotrophic factor in triazophos induced cognitive impairment in rats. *Neurochem. Res.* 38, 2136-47. doi: 10.1007/s11064-013-1122-0.

Kaur, M., Sharma, S., Kaur, G. (2008). Age-related impairments in neuronal plasticity markers and astrocytic GFAP and their reversal by late-onset short term dietary restriction. *Biogerontology* 9, 441-54. doi: 10.1007/s10522-008-9168-0.

Kim, H., Kang, H., Heo, R.W., Jeon, B.T., Yi, C.O., Shin, H.J., Kim, J., Jeong, S.Y., Kwak, W., Kim, W.H., Kang, S.S., Roh, G.S. (2016). Caloric restriction improves diabetes-induced cognitive deficits by attenuating neurogranin-associated calcium signaling in high-fat diet-fed mice. *J. Cereb. Blood Flow Metab.* 36, 1098-110. doi: 10.1177/0271678X15606724.

Kishi, T., Hirooka, Y., Nagayama, T., Isegawa, K., Katsuki, M., Takesue, K., Sunagawa, K. (2015). Calorie restriction improves cognitive decline via up-regulation of brain-derived neurotrophic factor: tropomyosin-related kinase B in hippocampus of obesity-induced hypertensive rats. *Int. Heart J.* 56, 110-5. doi: 10.1536/ihj.14-168.

Kishi, T., Hirooka, Y., Sunagawa, K. (2012). Telmisartan protects against cognitive decline via up-regulation of brain-derived neurotrophic factor/tropomyosin-related kinase B in hippocampus of hypertensive rats. *J. Cardiol.* 60, 489-94. doi: 10.1016/j.jjcc.2012.08.004.

Kishi, T., Sunagawa, K. (2012). Exercise training plus calorie restriction causes

synergistic protection against cognitive decline via up-regulation of BDNF in hippocampus of stroke-prone hypertensive rats. *Annu. Int. Conf. IEEE Eng. Med. Biol. Soc.* 2012, 6764-7. doi: 10.1109/EMBC.2012.6347547.

Kumar, A., Foster, T.C. (2019). Alteration in NMDA receptor mediated glutamatergic neurotransmission in the hippocampus during senescence. *Neurochem. Res.* 44, 38-48. doi: 10.1007/s11064-018-2634-4.

Lee, J., Duan, W., Mattson, M.P. (2002). Evidence that brain-derived neurotrophic factor is required for basal neurogenesis and mediates, in part, the enhancement of neurogenesis by dietary restriction in the hippocampus of adult mice. *J. Neurochem.* 82, 1367-1375. doi: 10.1046/j.1471-4159.2002.01085.x.

Liu, Y., Cheng, A., Li, Y.J., Yang, Y., Kishimoto, Y., Zhang, S., Wang, Y., Wan, R., Raefsky, S.M., Lu, D., Saito, T., Saido, T., Zhu, J., Wu, L.J., Mattson, M.P. (2019). SIRT3 mediates hippocampal synaptic adaptations to intermittent fasting and ameliorates deficits in APP mutant mice. *Nat. Commun.* 10, 1886. doi: 10.1038/s41467-019-09897-1.

Mattson, M.P. (2012). Energy intake and exercise as determinants of brain health and vulnerability to injury and disease. *Cell Metab.* 16, 706-22. doi: 10.1016/j.cmet.2012.08.012.

Mattson, M.P., Arumugam, T.V. (2018). Hallmarks of brain aging: adaptive and pathological modification by metabolic states. *Cell Metab.* 27, 1176-1199. doi: 10.1016/j.cmet.2018.05.011.

Mattson, M.P., Duan, W., Guo, Z. (2003). Meal size and frequency affect neuronal

plasticity and vulnerability to disease: cellular and molecular mechanisms. *J. Neurochem.* 84, 417-31. doi: 10.1046/j.1471-4159.2003.01586.x.

Mattson, M.P., Maudsley, S., Martin, B. (2004). BDNF and 5-HT: a dynamic duo in age-related neuronal plasticity and neurodegenerative disorders. *Trends Neurosci.* 27, 589-94. doi: 10.1016/j.tins.2004.08.001.

Merry, B.J. (2002). Molecular mechanisms linking calorie restriction and longevity. *Int. J. Biochem. Cell Biol.* 34, 1340-1354. doi: 10.1016/s1357-2725(02)00038-9.

Merry, B.J. (2004). Oxidative stress and mitochondrial function with aging—the effects of calorie restriction. *Aging Cell* 3, 7-12. doi: 10.1046/j.1474-9728.2003.00074.x.

Murchison, D., Griffith, W.H. (1995). Low-voltage activated calcium currents increase in basal forebrain neurons from aged rats. *J. Neurophysiol.* 74, 876-87. doi: 10.1152/jn.1995.74.2.876.

Murchison, D., Griffith, W.H. (1996). High-voltage-activated calcium currents in basal forebrain neurons during aging. *J. Neurophysiol.* 76, 158-74. doi: 10.1152/jn.1996.76.1.158.

Murchison, D., Griffith, W.H. (1998). Increased calcium buffering in basal forebrain neurons during aging. *J. Neurophysiol.* 80, 350-64. doi: 10.1152/jn.1998.80.1.350.

Murchison, D., Griffith, W.H. (1999). Age-related alterations in caffeine-sensitive calcium stores and mitochondrial buffering in rat basal forebrain. *Cell Calcium.* 25, 439-52. doi: 10.1054/ceca.1999.0048.

Murphy, G.G., Rahnama, N.P., Silva, A.J. (2006). Investigation of age-related cognitive

decline using mice as a model system: behavioral correlates. *Am. J. Geriatr. Psychiatry* 14, 1004-11. doi: 10.1097/01.JGP.0000209405.27548.7b.

Pitsikas, N., Algeri, S. (1992). Deterioration of spatial and nonspatial reference and working memory in aged rats: protective effect of life-long calorie restriction. *Neurobiol. Aging.* 13, 369-73. doi: 10.1016/0197-4580(92)90110-j.

Pitsikas, N., Garofalo, P., Manfridi, A., Zanotti, A., Algeri, S. (1991). Effect of lifelong hypocaloric diet on discrete memory of the senescent rat. *Aging (Milano)* 3, 147-52. doi: 10.1007/BF03323992.

Porcher, C., Medina, I., Gaiarsa, J.L. (2018). Mechanism of BDNF modulation in GABAergic synaptic transmission in healthy and disease brains. *Front. Cell Neurosci.* 12, 273. doi: 10.3389/fncel.2018.00273.

Rex, C.S., Lauterborn, J.C., Lin, C.Y., Kramár, E.A., Rogers, G.A., Gall, C.M., Lynch, G. (2006). Restoration of long-term potentiation in middle-aged hippocampus after induction of brain-derived neurotrophic factor. *J. Neurophysiol.* 96, 677-85. doi: 10.1152/jn.00336.2006.

Singh, R., Lakhanpal, D., Kumar, S., Sharma, S., Kataria, H., Kaur, M., Kaur, G. (2012). Late-onset intermittent fasting dietary restriction as a potential intervention to retard age-associated brain function impairments in male rats. *Age (Dordr)* 34, 917-33. doi: 10.1007/s11357-011-9289-2.

Stewart, J., Mitchell, J., Kalant, N. (1989). The effects of life-long food restriction on

spatial memory in young and aged Fischer 344 rats measured in the eight-arm radial and the Morris water mazes. *Neurobiol. Aging.* 10, 669-75. doi: 10.1016/0197-4580(89)90003-1.

Südhof, T.C. (2012). Calcium control of neurotransmitter release. *Cold Spring Harb. Perspect. Biol.* 4, a011353. doi: 10.1101/cshperspect.a011353.

Tapia-Arancibia, L., Aliaga, E., Silhol, M., Arancibia, S. (2008). New insights into brain BDNF function in normal aging and Alzheimer disease. *Brain Res. Rev.* 59, 201-20. doi: 10.1016/j.brainresrev.2008.07.007.

Thibault, O., Landfield, P.W. (1996). Increase in single L-type calcium channels in hippocampal neurons during aging. *Science* 272, 1017-20. doi: 10.1126/science.272.5264.1017.

Tombaugh, G.C., Rowe, W.B., Rose, G.M. (2005). The slow afterhyperpolarization in hippocampal CA1 neurons covaries with spatial learning ability in aged Fisher 344 rats. *J. Neurosci.* 25, 2609-16. doi: 10.1523/JNEUROSCI.5023-04.2005.

Van Cauwenberghe, C., Vandendriessche, C., Libert, C., Vandenbroucke, R.E. (2016). Caloric restriction: beneficial effects on brain aging and Alzheimer's disease. *Mamm. Genome.* 27, 300-19. doi: 10.1007/s00335-016-9647-6.

Wahl, D., Cogger, V.C., Solon-Biet, S.M., Waern, R.V., Gokarn, R., Pulpitel, T., Cabo, R.d., Mattson, M.P., Raubenheimer, D., Simpson, S.J., Le Couteur, D.G. (2016). Nutritional strategies to optimise cognitive function in the aging brain. *Ageing Res Rev.* 31, 80-92. doi: 10.1016/j.arr.2016.06.006.

3.8 Supplementary information

3.8.1 Supplementary Materials and Methods

3.8.1.1 Animals and treatments

We acquired male wildtype (WT) C57 Bl/6 mice of aged lifelong CR (aged CR, 21 months, N = 6), aged AL (aged control, 21 months, N = 6) and young AL (young control, 3 months, N = 6) from the National Institute of Aging (NIA) colony. Upon arrival at Texas A&M, we continued the same dietary regimen until mice were sacrificed for experiments, including at least 3 weeks of habituation. According to NIA protocol, both CR and control mice were individually housed. CR was initiated at 14 weeks of age at 10% restriction, increased to 25% restriction at 15 weeks, and to 40% restriction at 16 weeks where it was maintained throughout the life of the animal. Control animals were given NIH-31, the autoclavable form of a commonly used open formula feed, or NIH-31 fortified with extra vitamin supplementation (1.67 times standard) for CR animals. Water was available ad libitum in individual water bottles in each cage. All mice were maintained in the AAALAC-accredited vivarium at the Texas A&M University Health Science Center under controlled conditions (22 – 25℃; lights 0700-1900 h) in accordance with policies of the Texas A&M University Laboratory Animal Care Committee and NIH guidelines.

3.8.1.2 Enzyme-treated, acutely dissociated neurons and calcium imaging

Mice were euthanized after isoflurane anesthetization and the brain quickly removed and sectioned at 320-μm thickness in a coronal plane. Slices were cut using a carbogen-equilibrated ice-cold cutting solution containing (in mM): 120 NaCl, 2.7 KCl,

0.5 $CaCl_2$, 6 $MgCl_2$, 5 HEPES, 26 $NaHCO_3$, 11 D-glucose, and 0.3 kynurenic acid (pH 7.4 with NaOH, 310-330 mOsm). BF slices were then micro-dissected to isolate the medial septum and nucleus of the diagonal band (MS/nDB) and enzymatically treated (trypsin, Sigma, type XI or type I, St. Louis, MO), as described previously (Murchison and Griffith, 1996, 1998; Murchison et al., 2009). Enzyme-treated tissues were continuously suspended in a holding solution (in mM): 140 NaCl, 2.7 KCl, 0.5 $CaCl_2$, 1.2 $MgCl_2$, 10 HEPES, and 33 D-glucose (pH 7.4 with NaOH, 310-330 mOsm) by agitation of a small magnetic stir bar and were kept oxygenated with 100% O_2. Sections were then gently triturated using a series of fire-polished glass Pasteur pipettes of successively smaller tip diameters. The dissociated cells were plated on the glass floor of a recording chamber containing bath solution (in mM): 140 NaCl, 2.7 KCl, 2 $CaCl_2$, 1.2 $MgCl_2$, 10 HEPES, and 33 D-glucose, then perfused at a rate of about 2 ml/min. Experiments were performed at room temperature within 5 h of dispersal.

In order to measure intracellular calcium buffering in mouse BF neurons, we utilized a dual wavelength ratiometric fura-2 microfluorimetry system (Murchison and Griffith, 1998, 2007; Murchison et al., 2009). Enzyme-treated, acutely dissociated mouse BF neurons were loaded with ratiometric fluorescent Ca^{2+}-indicator fura-2AM (1 μM, Molecular Probes, Eugene, OR) for 12 min in the presence of 10 μM pluronic acid (Invitrogen, Carlsbad CA), after which they were washed for 40-45 min to allow for fura de-esterification. The Fura-2 fluorescence was excited using 340 nm and 380 nm alternating excitation and the resulting 340/380 ratio was determined. The intracellular calcium concentrations ($[Ca^{2+}]_i$) was calculated using in vitro calibration as described

previously (Murchison and Griffith, 1998). The Ca^{2+}-transients ($\Delta[Ca^{2+}]_i$) were triggered by pressure application of elevated [K^+] (20 mM) solution (High [K^+]), using a focal picospritzer (Picospritzer II, General Valve, Fairfield NJ). Application of different stimulus durations (0.2-1.2s) resulted in increasing amplitudes of $\Delta[Ca^{2+}]_i$. The amplitude of the transients was then plotted against the stimulus intensity (duration X 10) to calculate a buffering slope, as described in the general methods. Using this minimally invasive technique (compared to patch-clamping), greater buffering slopes are indicative of reduced buffering. Fluorescent signals were recorded using a Sutter lambda DG-4 excitation switcher (Sutter Instrument ®, Novato, CA), a Hamamatsu ORCA flash2.8 CCD camera (Hamamatsu Photonics, Bridgewater Township, NJ), an Olympus IX70 fluorescent scope and Metafluor imaging software (Molecular Devices, San Jose, CA).

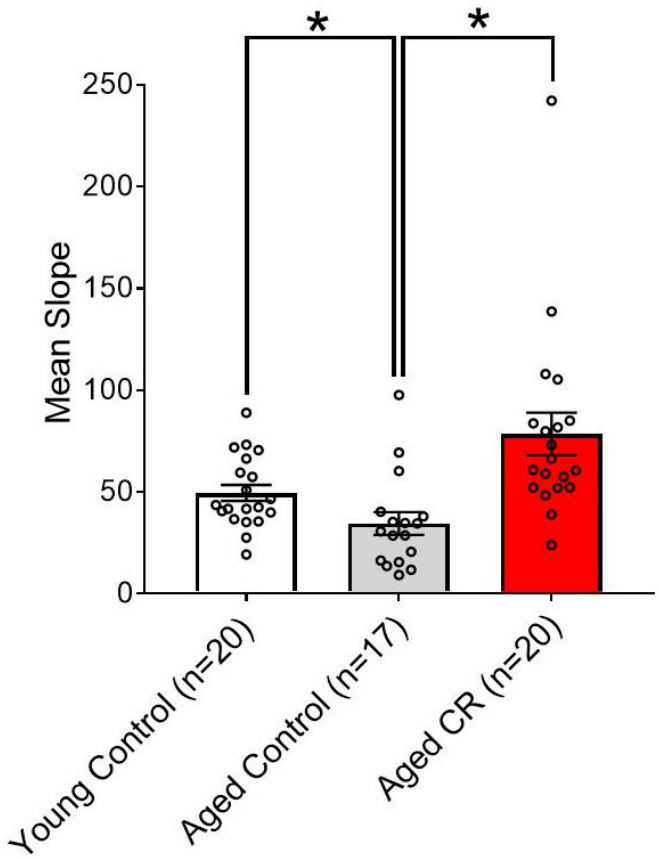

Supplementary figure 3.1. Increased Ca^{2+} buffering during aging is prevented by life-long caloric restriction. Bar graphs and scatter plots show mean (± SEM) buffering slopes in young control, aged control and aged CR groups (Young control: 49.49 ± 3.92, Aged control 34.43 ± 5.58, Aged CR 78.45 ± 10.42, n = 17-20 per group, *$p < 0.05$, unpaired t-test).

CHAPTER IV

AGING ALTERS SYNAPTIC EXCITATION/INHIBITION BALANCE IN THE MOUSE BASAL FOREBRAIN

4.1 Abstract

Imbalance between synaptic excitation and inhibition within neural circuits has been implicated in age-related brain dysfunction. Previously, we used a reduced synaptic preparation in the mouse basal forebrain (BF), to demonstrate a decreased frequency of spontaneous inhibitory postsynaptic currents (sIPSCs) with age (Chapter III). It is unknown if excitatory synaptic transmission changes in the BF across aging. Because the frequency of spontaneous excitatory postsynaptic currents (sEPSCs) is low in the BF reduced synaptic preparation, we recorded from neurons in brain slices where neuronal circuits are more intact and the frequencies of sEPSCs are much higher. Using whole-cell patch clamp recordings, the frequency and amplitude of sEPSCs and sIPSCs were measured in neurons from both young (2-3 months) and aged (19-23 months) C57/Bl6 mice. We observed no change in mean sEPSC frequency or amplitude with age and confirmed the reduced frequency of sIPSCs in aged brain slices. Moreover, there was no correlation between action potential firing frequencies and sEPSC frequencies in slices. All of these data suggest that there is no change in spontaneous excitatory synaptic transmission across aging in the BF, although decreased inhibition results in the overall excitatory/inhibitory (E/I) balance increasing with age. A disinhibition of cholinergic

neurons could serve as a compensatory mechanism for the diminished cholinergic signaling during aging.

4.2 Introduction

The balance of excitatory and inhibitory synaptic inputs (E/I balance) to neurons and circuits are fundamental for neuroplasticity and normal brain function. However, significant disruption in E/I balance has been described during aging with this imbalance variable across different brain regions. In the dentate gyrus, an increased excitation/inhibition ratio results in reduced cognitive performance in aged rats (Tran et al., 2019). While in the hippocampus, there was a selective upregulation of tonic inhibition in CA1 pyramidal cells only in aged-unimpaired rats, with neither the mEPSCs nor mIPSCs changing with age (Tran et al., 2018). These data suggest that maintaining adequate levels of inhibition could be a requirement for unimpaired cognitive performance during aging. In the hippocampus, the frequency but not the amplitude of spontaneous and miniature GABA IPSCs was reduced in aged rats, suggesting a presynaptic alteration (Potier et al., 2006). Furthermore, upregulation of excitatory synapses at depolarizing potentials is suggestive of an upregulation of hippocampal synaptic NMDA receptors once rats reach advanced age (Sametsky et al., 2010). In addition to these studies showing increased excitation with age, others have described increased inhibition. In the prefrontal cortex of rats and monkeys, synaptic inhibition was increased while synaptic excitation was decreased with age (Bañuelos et al., 2014; Luebke et al., 2004). Carpenter et al. (2016) have suggested that the age-related increase in cortical tonic inhibition may contribute to impaired executive function

during aging. These examples indicate that there is no single pathway to explain E/I imbalance in aging brain.

The BF is a critical modulator of hippocampal and cortical areas of the brain that are important for cognitive function. Reduced BF volume (Grothe et al., 2012) and degeneration of BF cholinergic neurons (Davies and Maloney, 1976; Bartus et al., 1982; Whitehouse et al., 1982; Mufson et al., 2008; Schliebs et al., 2011) are well-established characteristics of normal aging and Alzheimer's disease (AD). Accordingly, altered synaptic inputs in the BF during aging may exacerbate the diminished BF cholinergic signaling in the brain. Degeneration and dysfunction of BF cholinergic neurons are one of the most studied aspects of brain aging, and a theory has been proposed that GABAergic dysfunction and subsequent E/I imbalance drives the pathogenesis of AD (Bi et al., 2020). Previously, we have reported that GABAergic IPSCs in rat cholinergic BF neurons are decreased with age and associated with cognitive impairment (Griffith et al., 2014), and we show here (Chapter III) as well, that in mouse BF, synaptic inhibition is decreased. It is unknown whether the excitatory glutamatergic synaptic transmission in the BF is altered during aging. To address this, the present study was designed to determine whether the excitatory glutamatergic synaptic signaling in the BF is altered with age and to examine the E/I synaptic balance during aging, using the *ex vivo* mouse brain slice preparation.

4.3 Results

The aim of the study is to assess excitatory glutamatergic synaptic transmission in young and aged mouse BF neurons and to determine how excitation contributes to the

E/I balance during aging. Previously, we have utilized the reduced synaptic preparation which consists of enzyme-free, acutely dissociated neurons, in order to investigate inhibitory synaptic physiology more efficiently from aged subjects. However, in the reduced synaptic preparation, sEPSCs are rarely observed. In bicuculline, the mean frequency of sEPSCs from the reduced synaptic preparation was 0.016 ± 0.011 Hz (Griffith et al., 2014). Therefore, in this present study, experiments were performed in BF brain slices prepared from young and aged mice using whole-cell patch clamp recordings. We recorded sIPSCs in the presence of the NMDA receptor antagonist, APV (40 μM) and in AMPA/kainate receptor antagonist, DNQX (10 μM). We recorded sEPSCs in the presence of $GABA_A$ receptor antagonist, bicuculline (30 μM). Figure 4.1 shows representative examples of sIPSCs and sEPSCs obtained from BF slices both before (control) and after the application of antagonists, either APV/DNQX, bicuculline or both. In APV/DNQX, sEPSCs were blocked as shown in the bottom of Figure 4.1A. Bicuculline blocked sIPSCs (Figure 4.1B). Bath application of both bicuculline and APV/DNQX completely blocked both sIPSCs and sEPSCs in BF neurons of brain slices (Figure 4.1C, bottom), suggesting that these concentrations of antagonists are sufficient to enable us to selectively record either sIPSCs or sEPSCs in the BF slices.

4.3.1 Age-related decrease in sIPSC frequency in the BF neurons

To confirm our findings from the reduced synaptic preparation (Chapter III) that sIPSC frequency was reduced in aged BF neurons, sIPSCs were measured in APV/DNQX in BF neurons from young and aged mouse brain slices. As seen in voltage-clamp (V_h = -60 mV) recordings in Figure 4.2A, the frequency of sIPSCs in aged BF

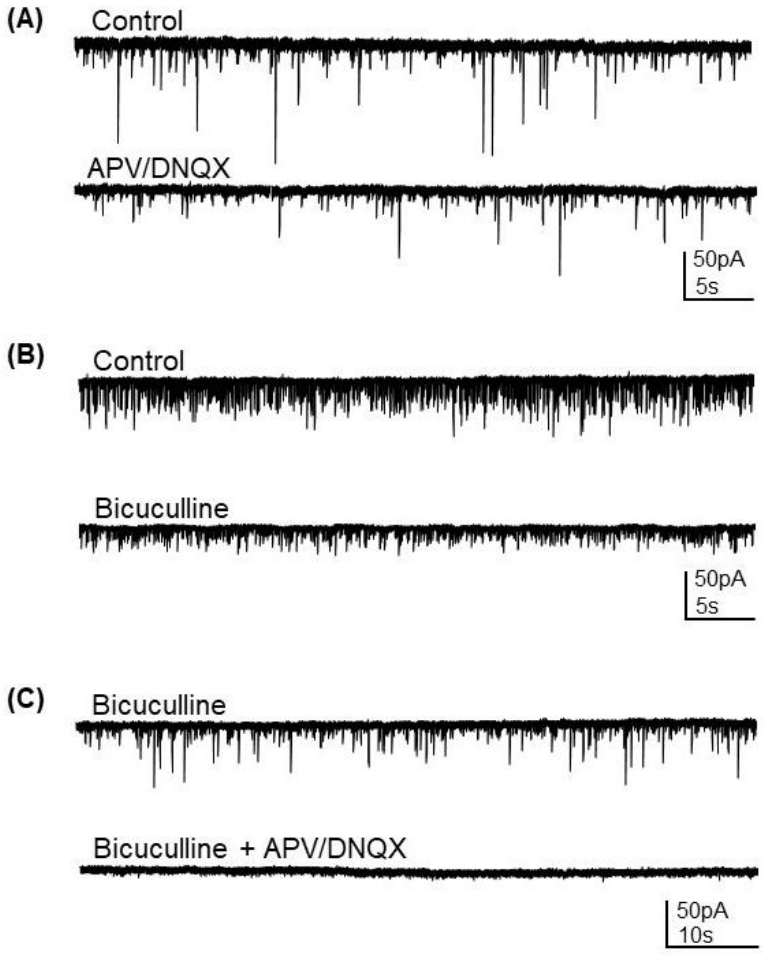

Figure 4.1. Antagonist sensitivity of spontaneous inhibitory postsynaptic currents (sIPSCs) and spontaneous excitatory postsynaptic currents (sEPSCs) from BF neurons in mouse brain slices. Examples from three different cells are shown. (A) Whole-cell voltage-clamp recordings (V_h = -60mV) of mixed spontaneous PSCs (top, control) and of sIPSCs in the presence of APV (40 μM)/DNQX (10 μM, bottom) are shown. (B) Control recordings (V_h = -75mV) of sPSCs are shown in another BF neuron (top) and below, recordings in bicuculline (30 μM). (C) Trace shows sEPSCs recorded (V_h = -75mV) in bicuculline (30 μM, top). Following the addition of APV/DNQX (bottom) all sPSCs were blocked.

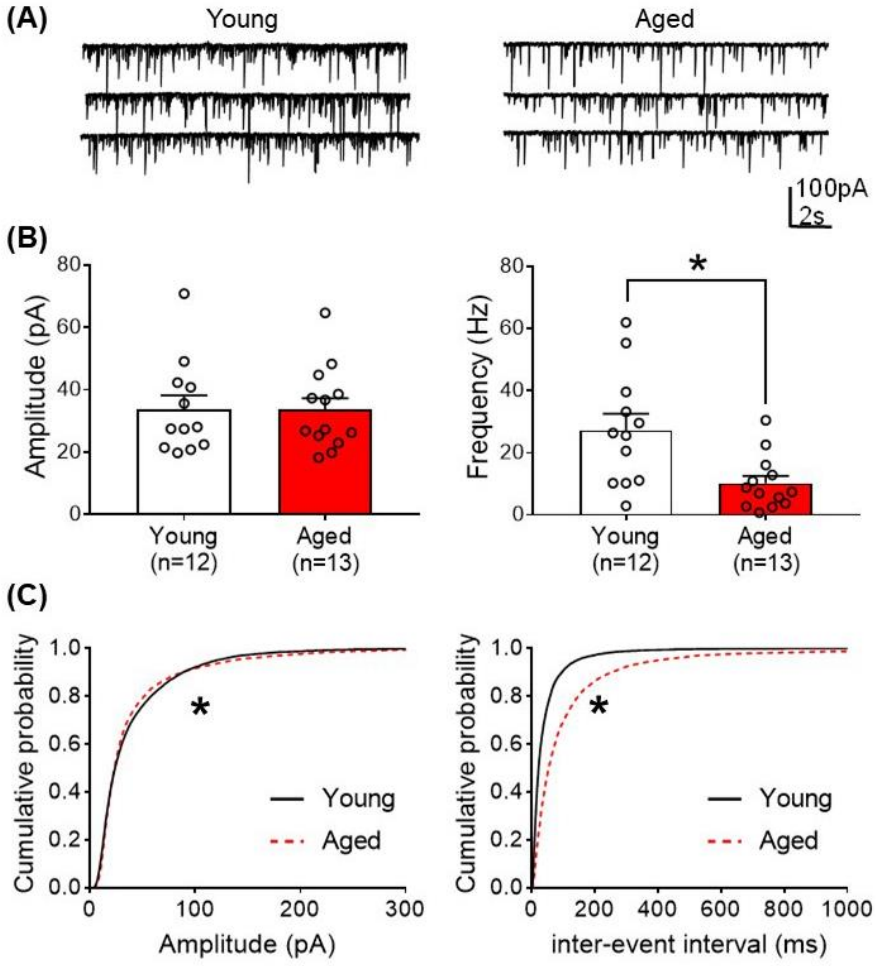

Figure 4.2. Changes in sIPSC amplitude and frequency in BF neurons from mouse brain slice during aging. (A) Representative whole-cell voltage-clamp recordings (V_h = -60mV) of sIPSCs in the presence of APV (40 μM)/DNQX (10 μM) are shown from both young (left) and aged (right) BF neurons. (B) Bar graphs and scatter plots show mean ± SEM of sIPSC amplitude (left, young: 33.88 ± 4.34 pA, aged: 33.66 ± 3.67 pA, unpaired t-test, p = 0.97) and frequency (right, young: 27.27 ± 5.27 Hz, aged: 10.14 ± 2.39 Hz, unpaired t-test, *p<0.01) for young and aged BF neurons. (C) Plots show cumulative probability distribution of sIPSC amplitude (left) and inter-event-intervals (right) for young and aged BF neurons. The data in panel C were analyzed by a Kolmogorov-Smirnov test (*p<0.05). n = number of neurons.

neurons were significantly decreased (right in Figure 4.2B, young: 27.27 ± 5.27 Hz, aged: 10.14 ± 2.39 Hz, unpaired t-test, *p<0.01). In contrast, the sIPSC amplitude was not significantly different between young and aged BF neurons (Figure 4.2B left, young: 33.88 ± 4.34 pA, aged: 33.66 ± 3.67 pA, unpaired t-test, p = 0.97)). Figure 4.2C show the cumulative probability plots of sIPSC amplitude (left) and inter-event interval (right) in young and aged BF neurons. These plots showed a significant age-related reduction in sIPSC frequency and a subtle difference in sIPSC amplitude (Kolmogorov-Smirnov test, *p<0.0001).

4.3.2 No age-related changes in the amplitude and frequency of sEPSCs in the BF neurons

To assess the effect of aging on excitatory synaptic activity, we performed whole-cell voltage-clamp recordings on BF neuron from young and aged mouse brain slices. Recordings were performed in the presence of bicuculline to isolate sEPSCs from a holding potential of -75 mV. Figure 4.3A shows recordings of sEPSCs from both young and aged BF neurons. Aged mice showed no change from young mice in the mean amplitude or frequency of sEPSCs. The mean sEPSC amplitudes were 13.23 ± 3.25 pA for young and 13.65 ± 0.66 pA for aged (left in Figure 4.3B, unpaired t-test, p = 0.65). For sEPSC frequency, the means were 5.09 ± 0.57 Hz in young and 5.04 ± 0.57 Hz in aged (right in Figure 4.3B, unpaired t-test, p = 0.95). Cumulative probability plots of sEPSC amplitudes and inter-event intervals comparing between young and aged are shown in the left and right panels of Figure 4.3C, respectively (amplitude: *p<0.0001,

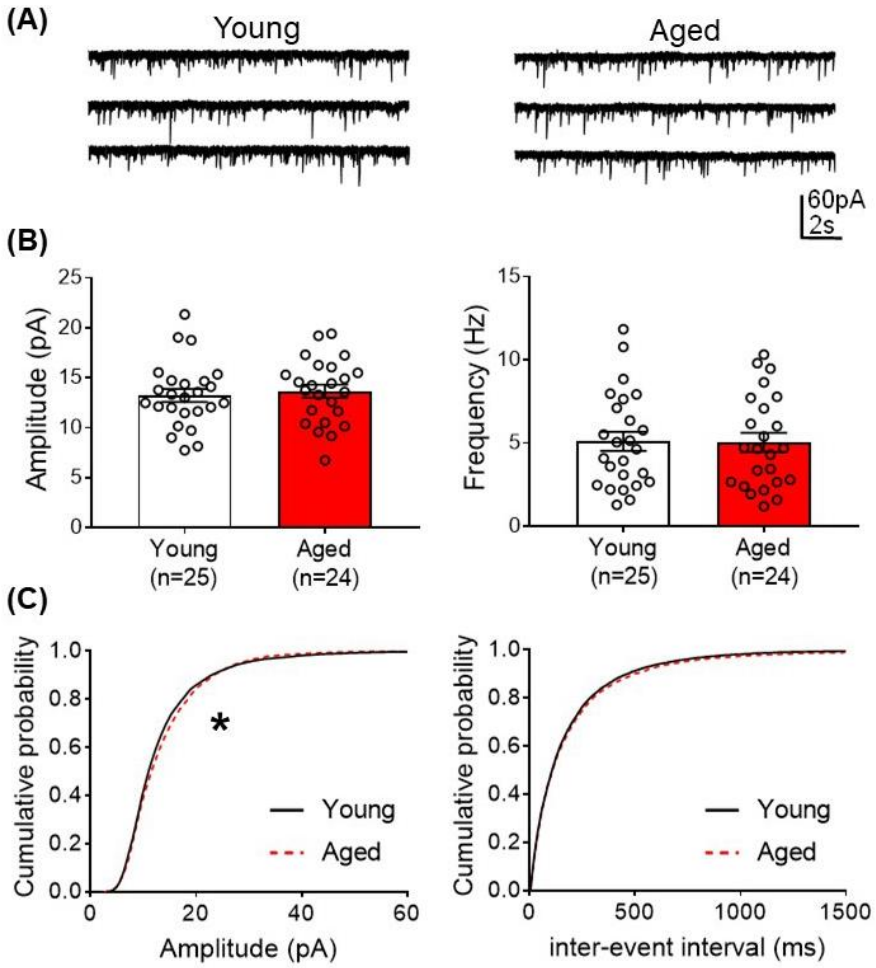

Figure 4.3. Amplitude and frequency of sEPSCs in BF neurons of mouse brain slice are unchanged during aging. (A) Representative whole-cell voltage-clamp recordings (V_h = -75mV) of sEPSCs in the presence of bicuculline (30 μM) from young (left) and aged (right) mice are shown in BF neurons. (B) Bar graphs and scatter plots show the mean (± SEM) amplitude (left, young: 13.23 ± 3.25 pA, aged: 13.65 ± 0.66 pA, unpaired t-test, p = 0.65) and frequency (right, young: 5.09 ± 0.57 Hz, aged: 5.04 ± 0.57 Hz, unpaired t-test, p = 0.95) of sEPSCs from young and aged mice. Number of cells are shown (n). (C) Cumulative probability distribution of sEPSC amplitude (left) and inter-event interval (right). The data in panel C were analyzed by a Kolmogorov-Smirnov test (*p<0.05).

frequency: p=0.2739, Kolmogorov-Smirnov test). Despite the significance of the amplitude cumulative probability, there is essentially no age-related difference in sEPSC amplitude.

4.3.3 The frequencies of sEPSCs are similar in different BF neuronal cell types

Our results thus far demonstrated no age-related change in sEPSCs frequency in the BF neurons, however, it is unclear whether age-related changes in sEPSCs frequency may be specific to different neuronal cell types in the mouse BF. Although we did not use molecular techniques to identify neuronal cell types in these experiments, different BF cell types are characterized by different action potential firing patterns (Griffith, 1988; Garrido-Sanabria et al., 2007; Murchison et al., 2009; Komendantov et al., 2019). Therefore, we measured action potential (AP) firing frequency for every neuron using whole-cell current-clamp recordings in order to differentiate neuron types. In current clamp, BF neurons in both young and aged mice demonstrated stereotypical firing patterns from slow- to fast-firing, consistent with cholinergic and GABAergic neurons respectively. Figure 4.4A shows examples of the range of firing frequencies and there was no significant difference in AP firing rate between young and aged BF neurons sampled (Figure 4.4B). We examined also, the relationship between sEPSCs and AP firing rate in each cell. There was no correlation between sEPSC frequency and AP firing rate in either young or aged neurons, suggesting that the frequency of sEPSCs during aging are not dependent on the neuronal cell types (Figure 4.4C).

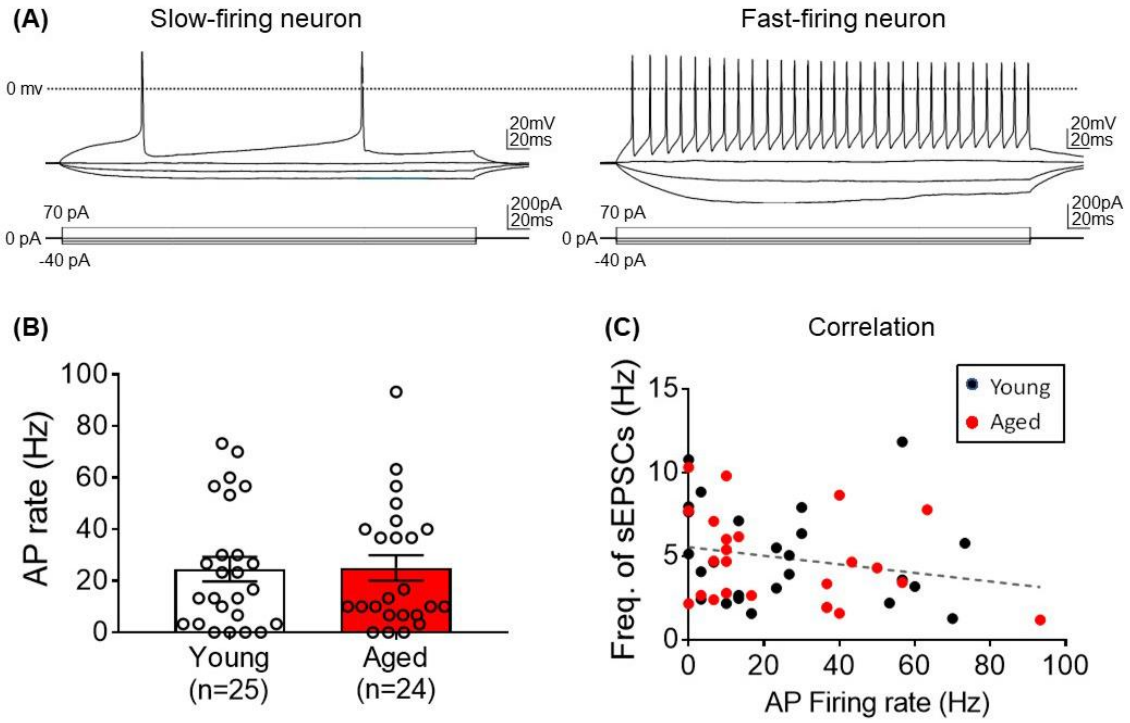

Figure 4.4. No significant correlation between action potential (AP) firing frequency and sEPSC frequency from BF neurons in mouse brain slices. (A) Typical examples of evoked action potentials (APs) from a slow-firing neuron (left) and a fast-firing neuron (right). Both examples are from aged mice and show current-clamp data of membrane voltage records during a series of current steps with resting membrane potential about -60 mV. The slow-firing neurons (<20 Hz) showed membrane properties consistent with BF cholinergic neurons, while the fast-firing neurons showed properties consistent with GABAergic BF neurons. (B) Bar graphs and scatter plots show mean (± SEM) AP firing rate at 60 pA current injection (young: 24.53 ± 4.73 Hz, aged: 25 ± 4.97 Hz, unpaired t-test, p = 0.95). Note that the distribution between young and aged was very similar. (C) Plot shows the correlation between sEPSC frequency and the AP firing rate in both young (black circle) and aged (red circle) BF neurons. The data in panel C was analyzed by Pearson's correlation (r = -0.22, p = 0.13).

4.4 Discussion

Understanding alterations in BF neuronal circuitry and E/I balance during aging is an important determinant as to how the BF modulates hippocampal and cortical activity and eventually influences cognitive function during aging. Age-related alterations in the intrinsic neuronal excitability and E/I balance have been implicated in cognitive impairment occurring during brain aging but has been studied primarily in hippocampus and cortex (Chang et al., 2005; Disterhoft and Oh, 2007; Matthews et al., 2009; Oh et al, 2010; Wang et al., 2011; Tran et al., 2018, 2019). In the present study, we aimed to explore changes in E/I balance in the BF during aging. Although the previous studies (Chapter III) demonstrated reduced sIPSC frequency in the BF during aging, it was shown in enzyme-free, acutely dissociated neurons with intact synaptic boutons, called the "reduced synaptic preparation". This preparation has many advantages but does not preserve cellular architecture and circuitry compared to brain slices. In addition, sEPSCs are infrequent in the BF reduced synaptic preparation. Therefore, we measured sEPSCs and sIPSCs in BF brain slices and found no change in the amplitude or frequencies of sEPSCs and we were able to confirm our previous results of an age-related reduction in sIPSC frequency in aged BF brain slices.

Basal forebrain cholinergic and GABAergic neurons receive synaptic input from both intrinsic and extrinsic GABAergic terminals and display spontaneous IPSCs (Leranth and Frotscher, 1989; Gaykema et al., 1991; Tóth et al., 1993; Gao et al, 1995; Griffith et al., 2014). Previous pharmacological studies which cannot distinguish between intrinsic and extrinsic GABA inputs on the BF, shows either facilitation or

impairment of learning and memory by intraseptal GABAergic antagonists or GABAergic agonists, respectively (Lamour et al., 1984; Henderson and Jones, 2005; Manseau et al., 2005), whereas studies with selective activation or lesion of intrinsic BF GABAergic neurons demonstrated that the intrinsic BF GABAergic neurons play an important role in learning and memory. More specifically, rats with damage to GABAergic neurons in the BF were slower to update changes to previous contingencies, indicating GABAergic neurons in the BF are critical for controlling proactive interference (Pang et al., 2011). In addition, the rats given GABAergic lesions of the BF showed reduced evoked hippocampal acetylcholine (ACh) efflux and impaired performance under the conditions of high cognitive load even though destruction of GABAergic MSDB neurons did not alter baseline hippocampal ACh efflux or ACh efflux by baseline behavior such as exploration (Roland et al., 2014). On the other hand, optogenetic activation of parvalbumin-positive GABAergic neurons in the BF can recruit hippocampal rhythmicity with high temporal precision, which is required for hippocampal theta synchronization (Dannenberg et al., 2015). Hippocampal theta rhythm is associated with integrative processes required for higher cognitive functions (Weiss et al., 2000; Bischof and Boulanger, 2003; Choi et al., 2010; Nuñez A and Buño, 2021). The underlying circuit mechanisms explaining the role of BF GABAergic neurons has been demonstrated also. According to Dannenberg et al. (2015), BF cholinergic neurons recruit GABAergic BF neurons which inhibit hippocampal inhibitory interneurons, resulting in disinhibition of hippocampal principal cells and increase of theta rhythms in the hippocampus. Indeed, disinhibition of hippocampal

principal cells by GABAergic BF neurons have long been suggested to be important for the generation of hippocampal theta rhythm (Freund and Antal, 1988; Freund, 1989; Serafin et al., 1996; Tóth et al., 1997; Hangya et al., 2009). Additionally, projection BF cholinergic neurons possess local axon collaterals (Zarborszky and Duque, 2000; Duque et al., 2007) and several other studies also demonstrated that BF cholinergic neurons excite BF GABAergic neurons (Yang et al., 2014; Damborsky et al., 2017). During aging, BF cholinergic neuron loss and dysfunction is well documented (Mufson et al., 2008; Schliebs and Arendt, 2011; Schmitz et al., 2016; Balu, 2017), which could be one plausible cause reducing GABAergic inhibitory tone in the BF via loss of cholinergic excitatory inputs on BF GABAergic neurons. Moreover, Damborsky and colleagues (2017) suggested that galanin decreases inhibitory synaptic transmission, as well as disrupts the ability of endogenous cholinergic activation to increase GABA release onto cholinergic neurons. During AD, there is hyperinnervation of BF by galanin-containing fibers (Mufson et al., 1993; Bowser et al., 1997), concurrent with an increase of galanin receptor expression (Mufson et al., 2000). Taken together, it is plausible that reduced inhibitory synaptic transmission during aging may serve as a compensatory mechanism via disinhibition of cholinergic neurons to mitigate the age-related dysfunction of BF cholinergic circuitry.

Excitatory synaptic inputs to the BF are also a heterogenous group from intrinsic BF glutamatergic neurons to extrinsic glutamatergic sources including the lateral hypothalamus, the amygdala, the intralaminar and midline nuclei of the thalamus, and the brain stem whereas BF glutamatergic neurons project to local cholinergic and

GABAergic neurons in the BF as well as to other brain areas. (Záborszky et al., 1984, 1991; Wu et al., 2004; Gielow and Zaborszky, 2017). BF glutamatergic neurons participate in the intra-septal mechanism which is responsible for hippocampal theta generation by connecting to GABAergic and cholinergic neurons within the BF (Robinson et al., 2016). Moreover, optogenetic investigation demonstrated that activation of BF VGluT2 neurons promote arousal, conceivably via both the intra-BF connections as well as the extra-BF projections to other arousal-promoting regions such as cortex, hypothalamus, and thalamic regions (thalamo-cortical nuclei) (Agostinelli et al., 2017; Steriade et al., 1993; Van der Werf et al., 2002; Gent et al., 2018; Dolleman-van der Weel et al., 2019). Both *in vivo* and *in vitro* applications of glutamate or glutamate agonists increases extracellular adenosine levels in the BF (Wigren et al., 2007; Sims et al., 2013). However, the elevated adenosine in the BF inhibits local glutamate release on local cholinergic and GABAergic neurons by activating A1 receptor, thus promoting sleep (Hawryluk et al., 2012; Yang et al., 2013). BF glutamatergic neurons are also projecting to VTA and lateral habenula which are part of the reward system in the brain, promoting avoidance behavior (Geisler et al., 2007; Tian and Uchida, 2015; Baker et al., 2016; Tooley et al., 2018; Wulff et al., 2019; McKenna et al., 2021) Although there are many studies that investigated the role of BF glutamatergic neurons, no research has been conducted to study age-related changes in excitatory synaptic transmission. In young mice, the study conducted by Damborsky et al. (2017) demonstrated the effect of galanin or β-amyloid peptide on glutamatergic excitatory synaptic transmission in the BF. In this study, galanin had no effect on sEPSC

frequency or amplitude but there was a significant decrease in mEPSC frequency, but not amplitude, suggesting that galanin may inhibit glutamatergic transmission presynaptically by a mechanism that acts on action potential-independent glutamate release without altering action potential-dependent glutamate release. Amyloid beta (Aβ) significantly decreased sEPSC frequency, with no change in amplitude. Additionally, it has been reported that BF cholinergic neurons inhibit BF glutamatergic neurons, possibly projection neurons (Xu et al., 2015; Yang et al., 2017). Because cholinergic neurons in the BF become dysfunctional during aging, it is plausible that the loss of cholinergic signaling within the BF may disinhibit BF glutamatergic neurons and enhance glutamatergic excitatory signaling in the BF. In the present study, we showed that BF sEPSCs amplitude and frequency are not altered during aging, which is consistent with the effect of galanin but not Aβ. However, we only showed changes in spontaneous (action potential-dependent plus action potential-independent) EPSCs, but not in miniature (action potential-independent) EPSCs. Thus, further studies are required to distinguish the aging effect on different underlying mechanisms of excitatory synaptic transmission and its relationship with behavior.

In summary, much is known about the circuitry and functions of the rodent BF, but much less is known about changes in the E/I balance in response to age, disease or drug treatment. As a start, we determined changes in the E/I balance across aging that resulted in an overall increase in excitation, due to the reduced sIPSC frequency. Future investigations of synaptic mechanisms will be necessary to understand the consequences of E/I imbalance on BF circuitry and function during aging.

4.5 Materials and Methods

4.5.1 Mice and Brain slice preparation

WT C57/BL6 mice of two ages were used, young (2-3 months) and aged (19-23). Mice were euthanized after isoflurane anesthetization and decapitated. The brain was quickly removed and placed in a chilled cutting solution containing (in mM): NaCl, 40; sucrose, 148.5; KCl, 2; NaH_2PO_4, 1.25; $NaHCO_3$, 26; $CaCl_2$, 0.5; $MgSO_4$, 7; D-glucose, 10; Ascorbate, 1; sodium pyruvate, 3; myo-inositol, 3; kynurenic acid, 0.8 and saturated with 95% O_2 and 5% CO_2 (pH 7.4 with NaOH, 310-330 mOsm). After blocking of the brain by trimming the cerebellum and olfactory bulb with a razor blade, the brain is immediately glued on a cutting stage of a tissue slicer and immersed in carbogen-equilibrated (95% O_2/5%CO_2) cutting solution at < 4℃. From rostral to caudal, 250-μm-thick brain slices containing the medial septum and nucleus of the diagonal band (MS/nDB) region are cut using a vibrating tissue slicer. Slices are then incubated in a 1:1 mixture of cutting solution and external bath solution at 35℃ for 45 min and are allowed to return to 25℃. The external bath solution contained the following (in mM): NaCl, 124; KCl, 3; CaCl2, 2.4; $MgSO_4$, 1.5; NaH2PO4, 1.25; NaHCO3, 26; sucrose, 15; D-glucose, 15 and saturated with 95% O2 and 5% CO2 (pH 7.4 with NaOH, 310-330 mOsm).

4.5.2 Electrophysiology

Standard whole-cell patch voltage-clamp recording was used for measuring spontaneous inhibitory postsynaptic currents (sIPSCs) and spontaneous excitatory postsynaptic currents (sEPSCs). The basic action potential firing patterns were assessed

by whole-cell current-clamp recordings. Slices were placed in a recording chamber and then perfused with the external bath solution at a rate of about 2 ml/min. Recordings for sIPSCs and sEPSCs were made from a holding potential of -60 and -75mV, respectively. For sIPSC recordings, 2-amino-5-phosphonopentanoic acid (APV, 40 μM) and 6,7-dinitroquinoxaline-2,3-dione (DNQX, 10 μM) were applied to the external bath solution to block excitatory amino acid receptors N-methyl-D-aspartate (NMDA), α-amino-3-hydroxy-5-methyl-4-isoxazolepropionic acid (AMPA) and kainate. The $GABA_A$ receptor antagonist, bicuculline (30 μM) was present in the external bath solution throughout the measurements of sEPSCs. All recordings were conducted at 32°C, low-pass filtered at 2 kHz and digitized at 10 kHz with Digidata 1440A interface, Multiclamp 700B amplifier (Molecular Devices, San Jose, CA), and pClamp 10 software (Molecular Devices, San Jose, CA). Membrane capacitance (pF) was obtained by digital cancellation of whole-cell capacitance transients. Recording electrodes were pulled from glass capillary tubing (KG-33, 1.5mm OD, King Precision Glass, Claremont, CA) on a Flaming/Brown P-87 pipette puller (Sutter Instrument ®, Novato, CA) with final electrode resistance 4-8 MΩ when filled with a pipette solution. The internal pipette solution for sIPSC recordings contained (in mM): CsCl, 130; ethylene glycol-bis (β-aminoethyl ether) N,N,N',N'-tetraacetic acid (EGTA), 10; $MgCl_2$, 2; HEPES, 10; Mg-ATP, 4; GTP, 0.1; pH 7.2 with CsOH; 295-300 mOsm. For sEPSC and current-clamp experiments, the internal pipette solution contained (in mM): K-gluconate, 136; NaCl, 25; HEPES, 10; $MgCl_2$, 2; ATP, 4 and EGTA, 0.05, pH 7.2, 290 mOsm.

4.5.3 Electrophysiological analysis

Mini Analysis (6.0.7; Synaptosoft, Decatur, GA) and Clampfit 10 (Molecular Devices, San Jose, CA) software were employed for the analysis. Mean data were compared using a paired t-test, Kolmogorov-Smirnov test or Pearson's correlation test with significance determined by $p < 0.05$ (GraphPad, San Diego, CA). Values were expressed as mean ± S.E.M.

4.6 References

Agostinelli, L.J., Ferrari, L.L., Mahoney, C.E., Mochizuki, T., Lowell, B.B., Arrigoni, E., Scammell, T.E. (2017). Descending projections from the basal forebrain to the orexin neurons in mice. *J. Comp. Neurol.* 525, 1668-1684. doi: 10.1002/cne.24158.

Baker, P.M., Jhou, T., Li, B., Matsumoto, M., Mizumori, S.J., Stephenson-Jones, M., Vicentic, A. (2016). The Lateral habenula circuitry: reward processing and cognitive control. *J. Neurosci.* 36, 11482-11488. doi: 10.1523/JNEUROSCI.2350-16.2016.

Balu, D.T. (2017). Cognitive deficits in prematurely born adults are associated with reduced basal forebrain integrity. *Biol. Psychiatry.* 82, e15-e16. doi: 10.1016/j.biopsych.2017.04.004.

Bañuelos, C., Beas, B.S., McQuail, J.A., Gilbert, R.J., Frazier, C.J., Setlow, B., Bizon, J.L. (2014). Prefrontal cortical GABAergic dysfunction contributes to age-related working memory impairment. *J. Neurosci.* 34, 3457-66. doi: 10.1523/JNEUROSCI.5192-13.2014.

Bartus, R.T., Dean, R.L. 3rd., Beer, B., Lippa, A.S. (1982). The cholinergic hypothesis of geriatric memory dysfunction. *Science* 217, 408-14. doi: 10.1126/science.7046051.

Bi, D., Wen, L., Wu, Z., Shen, Y. (2020). GABAergic dysfunction in excitatory and inhibitory (E/I) imbalance drives the pathogenesis of Alzheimer's disease. *Alzheimers Dement.* 16, 1312-1329. doi: 10.1002/alz.12088.

Bischof, W.F., Boulanger, P. (2003). Spatial navigation in virtual reality environments: an EEG analysis. *Cyberpsychol. Behav.* 6, 487-95. doi: 10.1089/109493103769710514.

Bowser, R., Kordower, J.H., Mufson, E.J. (1997). A confocal microscopic analysis of galaninergic hyperinnervation of cholinergic basal forebrain neurons in Alzheimer's disease. *Brain Pathol.* 7, 723-30. doi: 10.1111/j.1750-3639.1997.tb01058.x.

Carpenter, H.E., Kelly, K.B., Bizon, J.L., Frazier, C.J. (2016). Age-related changes in tonic activation of presynaptic versus extrasynaptic γ-amniobutyric acid type B receptors in rat medial prefrontal cortex. *Neurobiol. Aging.* 45, 88-97. doi: 10.1016/j.neurobiolaging.2016.05.015.

Chang, Y.M., Rosene, D.L., Killiany, R.J., Mangiamele, L.A., Luebke, J.I. (2005). Increased action potential firing rates of layer 2/3 pyramidal cells in the prefrontal cortex are significantly related to cognitive performance in aged monkeys. *Cereb. Cortex.* 15, 409-18. doi: 10.1093/cercor/bhh144.

Choi, J.W., Jung, K.Y., Kim, C.H., Kim, K.H. (2010). Changes in gamma- and theta-

band phase synchronization patterns due to the difficulty of auditory oddball task. *Neurosci. Lett.* 468, 156-60. doi: 10.1016/j.neulet.2009.10.088.

Damborsky, J.C., Smith, K.G., Jensen, P., Yakel, J.L. (2017). Local cholinergic-GABAergic circuitry within the basal forebrain is modulated by galanin. *Brain Struct. Funct.* 222, 1385-1400. doi: 10.1007/s00429-016-1283-0.

Dannenberg, H., Pabst, M., Braganza, O., Schoch, S., Niediek, J., Bayraktar, M., Mormann, F., Beck, H. (2015). Synergy of direct and indirect cholinergic septo-hippocampal pathways coordinates firing in hippocampal networks. *J. Neurosci.* 35, 8394-410. doi: 10.1523/JNEUROSCI.4460-14.2015.

Davies, P., Maloney, A.J. (1976). Selective loss of central cholinergic neurons in Alzheimer's disease. *Lancet* 2, 1403. doi: 10.1016/s0140-6736(76)91936-x.

Disterhoft, J.F., Oh, M.M. (2007). Alterations in intrinsic neuronal excitability during normal aging. *Aging Cell* 6, 327-36. doi: 10.1111/j.1474-9726.2007.00297.x.

Dolleman-van der Weel, M.J., Griffin, A.L., Ito, H.T., Shapiro, M.L., Witter, M.P., Vertes, R.P., Allen, T.A. (2019). The nucleus reuniens of the thalamus sits at the nexus of a hippocampus and medial prefrontal cortex circuit enabling memory and behavior. *Learn. Mem.* 26, 191-205. doi: 10.1101/lm.048389.118.

Duque, A., Tepper, J.M., Detari, L., Ascoli, G.A., Zaborszky, L. (2007). Morphological characterization of electrophysiologically and immunohistochemically identified basal forebrain cholinergic and neuropeptide Y-containing neurons. *Brain Struct. Funct.* 212, 55-73. doi: 10.1007/s00429-007-0143-3.

Freund, T.F. (1989). GABAergic septohippocampal neurons contain parvalbumin. *Brain*

Res. 478, 375-81. doi: 10.1016/0006-8993(89)91520-5.

Freund, T.F., Antal, M. (1988). GABA-containing neurons in the septum control inhibitory interneurons in the hippocampus. *Nature* 336, 170-3. doi: 10.1038/336170a0.

Gao, B., Hornung, J.P., Fritschy, J.M. (1995). Identification of distinct GABAA-receptor subtypes in cholinergic and parvalbumin-positive neurons of the rat and marmoset medial septum-diagonal band complex. *Neuroscience* 65, 101-17. doi: 10.1016/0306-4522(94)00480-s.

Garrido-Sanabria, E.R., Perez, M.G., Banuelos, C., Reyna, T., Hernandez, S., Castaneda, M.T., Colom, L.V. (2007). Electrophysiological and morphological heterogeneity of slow firing neurons in medial septal/diagonal band complex as revealed by cluster analysis. *Neuroscience* 146, 931-45. doi: 10.1016/j.neuroscience.2007.02.047.

Gaykema, R.P., Gaál, G., Traber, J., Hersh, L.B., Luiten, P.G. (1991). The basal forebrain cholinergic system: efferent and afferent connectivity and long-term effects of lesions. *Acta. Psychiatr. Scand. Suppl.* 366, 14-26. doi: 10.1111/j.1600-0447.1991.tb03105.x.

Geisler, S., Derst, C., Veh, R.W., Zahm, D.S. (2007). Glutamatergic afferents of the ventral tegmental area in the rat. *J. Neurosci.* 27, 5730-43. doi: 10.1523/JNEUROSCI.0012-07.2007.

Gielow, M.R., Zaborszky, L. (2017). The Input-output relationship of the cholinergic basal forebrain. *Cell Rep.* 18, 1817-1830. doi: 10.1016/j.celrep.2017.01.060.

Gent, T.C., Bandarabadi, M., Herrera, C.G., Adamantidis, A.R. (2018). Thalamic dual control of sleep and wakefulness. *Nat. Neurosci.* 21, 974-984. doi: 10.1038/s41593-018-0164-7.

Griffith, W.H. Membrane properties of cell types within guinea pig basal forebrain nuclei in vitro. *J. Neurophysiol.* 59, 1590-612. doi: 10.1152/jn.1988.59.5.1590.

Griffith, W.H., Dubois, D.W., Fincher, A., Peebles, K.A., Bizon, J.L., Murchison, D. (2014). Characterization of age-related changes in synaptic transmission onto F344 rat basal forebrain cholinergic neurons using a reduced synaptic preparation. *J. Neurophysiol.* 111, 273-86. doi: 10.1152/jn.00129.2013.

Grothe, M., Heinsen, H., Teipel, S. (2013). Longitudinal measures of cholinergic forebrain atrophy in the transition from healthy aging to Alzheimer's disease. *Neurobiol. Aging 34*, 1210–1220. doi: 10.1016/j.neurobiolaging.2012.10.018.

Hangya, B., Borhegyi, Z., Szilágyi, N., Freund, T.F., Varga, V. (2009). GABAergic neurons of the medial septum lead the hippocampal network during theta activity. *J. Neurosci.* 29, 8094-102. doi: 10.1523/JNEUROSCI.5665-08.2009.

Hawryluk, J.M., Ferrari, L.L., Keating, S.A., Arrigoni, E. (2012). Adenosine inhibits glutamatergic input to basal forebrain cholinergic neurons. *J. Neurophysiol.* 107, 2769-81. doi: 10.1152/jn.00528.2011.

Henderson, Z., Jones, G.A. (2005). GABAB receptors in the medial septum/diagonal band slice from 16-25 day rat. *Neuroscience* 132, 789-800. doi: 10.1016/j.neuroscience.2005.01.027.

Komendantov, A.O., Venkadesh, S., Rees, C.L., Wheeler, D.W., Hamilton, D.J., Ascoli, G.A. (2019). Quantitative firing pattern phenotyping of hippocampal neuron types. *Sci. Rep.* 9, 17915. doi: 10.1038/s41598-019-52611-w.

Lamour, Y., Dutar, P., Jobert, A. (1984). Septo-hippocampal and other medial septum-diagonal band neurons: electrophysiological and pharmacological properties. *Brain Res.* 309, 227-39. doi: 10.1016/0006-8993(84)90588-2.

Leranth, C., Frotscher, M. (1989). Organization of the septal region in the rat brain: cholinergic-GABAergic interconnections and the termination of hippocampo-septal fibers. *J. Comp. Neurol.* 289, 304-14. doi: 10.1002/cne.902890210.

Luebke, J.I., Chang, Y.M., Moore, T.L., Rosene, D.L. (2004). Normal aging results in decreased synaptic excitation and increased synaptic inhibition of layer 2/3 pyramidal cells in the monkey prefrontal cortex. *Neuroscience* 125, 277-88. doi: 10.1016/j.neuroscience.2004.01.035.

Manseau, F., Danik, M., Williams, S. (2005). A functional glutamatergic neurone network in the medial septum and diagonal band area. *J. Physiol.* 566, 865-84. doi: 10.1113/jphysiol.2005.089664.

Matthews, E.A., Linardakis, J.M., Disterhoft, J.F. (2009). The fast and slow afterhyperpolarizations are differentially modulated in hippocampal neurons by aging and learning. *J. Neurosci.* 29, 4750-5. doi: 10.1523/JNEUROSCI.0384-09.2009.

McKenna, J.T., Yang, C., Bellio, T., Anderson-Chernishof, M.B., Gamble, M.C.,

Hulverson, A., McCoy, J.G., Winston, S., Hodges, E., Katsuki, F., McNally, J.M., Basheer, R., Brown, R.E. (2021). Characterization of basal forebrain glutamate neurons suggests a role in control of arousal and avoidance behavior. *Brain Struct. Funct.* doi: 10.1007/s00429-021-02288-7. Epub ahead of print.

Mufson, E.J., Cochran, E., Benzing, W., Kordower, J.H. (1993). Galaninergic innervation of the cholinergic vertical limb of the diagonal band (Ch2) and bed nucleus of the stria terminalis in aging, Alzheimer's disease and Down's syndrome. *Dementia* 4, 237-50. doi: 10.1159/000107329.

Mufson, E.J., Counts, S.E., Perez, S.E., Ginsberg, S.D. (2008). Cholinergic system during the progression of Alzheimer's disease: therapeutic implications. *Expert Rev. Neurother.* 8, 1703-18. doi: 10.1586/14737175.8.11.1703.

Mufson, E.J., Deecher, D.C., Basile, M., Izenwasse, S., Mash, D.C. (2000). Galanin receptor plasticity within the nucleus basalis in early and late Alzheimer's disease: an in vitro autoradiographic analysis. *Neuropharmacology* 39, 1404-12. doi: 10.1016/s0028-3908(00)00011-3.

Murchison, D., McDermott, A.N,, Lasarge, C.L., Peebles, K.A., Bizon, J.L., Griffith, W.H. (2009). Enhanced calcium buffering in F344 rat cholinergic basal forebrain neurons is associated with age-related cognitive impairment. *J. Neurophysiol.* 102, 2194-207. doi: 10.1152/jn.00301.2009.

Nuñez, A., Buño, W. (2021). The Theta Rhythm of the Hippocampus: From Neuronal and Circuit Mechanisms to Behavior. *Front. Cell Neurosci.* 15, 649262. doi: 10.3389/fncel.2021.649262.

Oh, M.M., Oliveira, F.A., Disterhoft, J.F. (2010). Learning and aging related changes in intrinsic neuronal excitability. *Front. Aging Neurosci.* 2, 2. doi: 10.3389/neuro.24.002.2010.

Pang, K.C., Jiao, X., Sinha, S., Beck, K.D., Servatius, R.J. (2011). Damage of GABAergic neurons in the medial septum impairs spatial working memory and extinction of active avoidance: effects on proactive interference. *Hippocampus* 21, 835-46. doi: 10.1002/hipo.20799.

Potier, B., Jouvenceau, A., Epelbaum, J., Dutar, P. (2006). Age-related alterations of GABAergic input to CA1 pyramidal neurons and its control by nicotinic acetylcholine receptors in rat hippocampus. *Neuroscience* 142, 187-201. doi: 10.1016/j.neuroscience.2006.06.040.

Robinson, J., Manseau, F., Ducharme, G., Amilhon, B., Vigneault, E., El Mestikawy, S., Williams, S. (2016). Optogenetic activation of septal glutamatergic neurons drive hippocampal theta rhythms. *J. Neurosci.* 36, 3016-23. doi: 10.1523/JNEUROSCI.2141-15.2016.

Roland, J.J., Stewart, A.L., Janke, K.L., Gielow, M.R., Kostek, J.A., Savage, L.M., Servatius, R.J., Pang, K.C. (2014). Medial septum-diagonal band of Broca (MSDB) GABAergic regulation of hippocampal acetylcholine efflux is dependent on cognitive demands. *J. Neurosci.* 34, 506-14. doi: 10.1523/JNEUROSCI.2352-13.2014.

Sametsky, E.A., Disterhoft, J.F., Geinisman, Y., Nicholson, D.A. (2010). Synaptic

strength and postsynaptically silent synapses through advanced aging in rat hippocampal CA1 pyramidal neurons. *Neurobiol. Aging* 31, 813-25. doi: 10.1016/j.neurobiolaging.2008.05.029.

Schliebs, R., Arendt, T. (2011). The cholinergic system in aging and neuronal degeneration. *Behav. Brain Res.* 221, 555-63. doi: 10.1016/j.bbr.2010.11.058.

Schmitz, T.W., Nathan Spreng, R.; Alzheimer's Disease Neuroimaging Initiative. (2016). Basal forebrain degeneration precedes and predicts the cortical spread of Alzheimer's pathology. *Nat. Commun.* 7, 13249. doi: 10.1038/ncomms13249.

Serafin, M., Williams, S., Khateb, A., Fort, P., Mühlethaler, M. (1996). Rhythmic firing of medial septum non-cholinergic neurons. *Neuroscience* 75, 671-5. doi: 10.1016/0306-4522(96)00349-1.

Sims, R.E., Wu, H.H., Dale, N. (2013). Sleep-wake sensitive mechanisms of adenosine release in the basal forebrain of rodents: an in vitro study. *PLoS One* 8, e53814. doi: 10.1371/journal.pone.0053814.

Steriade, M., McCormick, D.A., Sejnowski, T.J. (1993). Thalamocortical oscillations in the sleeping and aroused brain. *Science* 262, 679-85. doi: 10.1126/science.8235588.

Tian, J., Uchida, N. (2015). Habenula lesions reveal that multiple mechanisms underlie dopamine prediction errors. *Neuron* 87, 1304-1316. doi: 10.1016/j.neuron.2015.08.028.

Tooley, J., Marconi, L., Alipio, J.B., Matikainen-Ankney, B., Georgiou, P., Kravitz,

A.V., Creed, M.C. (2018). Glutamatergic ventral pallidal neurons modulate activity of the habenula-tegmental circuitry and constrain reward seeking. *Biol. Psychiatry* 83, 1012-1023. doi: 10.1016/j.biopsych.2018.01.003.

Tóth, K., Borhegyi, Z., Freund, T.F. (1993). Postsynaptic targets of GABAergic hippocampal neurons in the medial septum-diagonal band of broca complex. *J. Neurosci.* 13, 3712-24. doi: 10.1523/JNEUROSCI.13-09-03712.1993.

Tóth, K., Freund, T.F., Miles, R. (1997). Disinhibition of rat hippocampal pyramidal cells by GABAergic afferents from the septum. *J. Physiol.* 500, 463-74. doi: 10.1113/jphysiol.1997.sp022033.

Tran, T., Bridi, M., Koh, M.T., Gallagher, M., Kirkwood, A. (2019). Reduced cognitive performance in aged rats correlates with increased excitation/inhibition ratio in the dentate gyrus in response to lateral entorhinal input. *Neurobiol. Aging* 82, 120-127. doi: 10.1016/j.neurobiolaging.2019.07.010.

Tran, T., Gallagher, M., Kirkwood, A. (2018). Enhanced postsynaptic inhibitory strength in hippocampal principal cells in high-performing aged rats. *Neurobiol. Aging* 70, 92-101. doi: 10.1016/j.neurobiolaging.2018.06.008.

Van der Werf, Y.D., Witter, M.P., Groenewegen, H.J. (2002). The intralaminar and midline nuclei of the thalamus. Anatomical and functional evidence for participation in processes of arousal and awareness. *Brain Res. Brain Res. Rev.* 39, 107-40. doi: 10.1016/s0165-0173(02)00181-9.

Wang, M., Gamo, N.J., Yang, Y., Jin, L.E., Wang, X.J., Laubach, M., Mazer, J.A., Lee,

D., Arnsten, A.F. (2011). Neuronal basis of age-related working memory decline. *Nature* 476, 210-3. doi: 10.1038/nature10243.

Weiss, S., Müller, H.M., Rappelsberger, P. (2000). Theta synchronization predicts efficient memory encoding of concrete and abstract nouns. *Neuroreport.* 11, 2357-61. doi: 10.1097/00001756-200008030-00005.

Whitehouse, P.J., Price, D.L., Struble, R.G., Clark, A.W., Coyle, J.T., Delon, M.R. (1982). Alzheimer's disease and senile dementia: loss of neurons in the basal forebrain. *Science* 215, 1237-9. doi: 10.1126/science.7058341.

Wigren, H.K., Schepens, M., Matto, V., Stenberg, D., Porkka-Heiskanen, T. (2007). Glutamatergic stimulation of the basal forebrain elevates extracellular adenosine and increases the subsequent sleep. *Neuroscience* 147, 811-23. doi: 10.1016/j.neuroscience.2007.04.046.

Wu, M., Zaborszky, L., Hajszan, T., van den Pol, A.N., Alreja, M. (2004). Hypocretin/orexin innervation and excitation of identified septohippocampal cholinergic neurons. *J. Neurosci.* 24, 3527-36. doi: 10.1523/JNEUROSCI.5364-03.2004.

Wulff, A.B., Tooley, J., Marconi, L.J., Creed, M.C. (2019). Ventral pallidal modulation of aversion processing. *Brain Res.* 1713, 62-69. doi: 10.1016/j.brainres.2018.10.010.

Xu, M., Chung, S., Zhang, S., Zhong, P., Ma, C., Chang, W.C., Weissbourd, B., Sakai, N., Luo, L., Nishino, S., Dan, Y. (2015). Basal forebrain circuit for sleep-wake control. *Nat. Neurosci.* 18, 1641-7. doi: 10.1038/nn.4143.

Yang, C., Franciosi, S., Brown, R.E. (2013). Adenosine inhibits the excitatory synaptic inputs to Basal forebrain cholinergic, GABAergic, and parvalbumin neurons in mice. *Front. Neurol.* 4, 77. doi: 10.3389/fneur.2013.00077.

Yang, C., McKenna, J.T., Brown, R.E. (2017). Intrinsic membrane properties and cholinergic modulation of mouse basal forebrain glutamatergic neurons in vitro. *Neuroscience* 352, 249-261. doi: 10.1016/j.neuroscience.2017.04.002.

Yang, C., McKenna, J.T., Zant, J.C., Winston, S., Basheer, R., Brown, R.E. (2014). Cholinergic neurons excite cortically projecting basal forebrain GABAergic neurons. *J. Neurosci.* 34, 2832-44. doi: 10.1523/JNEUROSCI.3235-13.2014.

Záborszky, L., Cullinan, W.E., Braun, A. (1991). Afferents to basal forebrain cholinergic projection neurons: an update. *Adv. Exp. Med. Biol.* 295, 43-100. doi: 10.1007/978-1-4757-0145-6_2.

Zaborszky, L., Duque, A. (2000). Local synaptic connections of basal forebrain neurons. *Behav. Brain Res.* 115, 143-58. doi: 10.1016/s0166-4328(00)00255-2.

Záborszky, L., Gombkoto, P., Varsanyi, P., Gielow, M.R., Poe, G., Role, L.W., Ananth, M., Rajebhosale, P., Talmage, D.A., Hasselmo, M.E., Dannenberg, H., Minces, V.H., Chiba, A.A. (2018). Specific basal forebrain-cortical cholinergic circuits coordinate cognitive operations. *J. Neurosci.* 38, 9446-9458. doi: 10.1523/JNEUROSCI.1676-18.2018.

Záborszky, L., Léránth, C., Heimer, L. (1984). Ultrastructural evidence of amygdalofugal axons terminating on cholinergic cells of the rostral forebrain. *Neurosci. Lett.* 52, 219-25. doi: 10.1016/0304-3940(84)90165-4.

CHAPTER V

CONCLUSIONS

This research dissertation was designed to utilize our optogenetic BF aging model to test the efficacy of a pharmacological treatment across aging and to test the effects of late-onset, short-term intermittent fasting (IF) on well-characterized age-related changes in synaptic and Ca^{2+} signaling. IF was tested as a possible new therapeutic alternative to help offset some the detrimental effects of aging. We focused on Ca^{2+} and synaptic modulation because these parameters are associate with cognitive changes during aging. In order to study presynaptic mechanisms in more detail, we also developed an optogenetic reduced synaptic preparation that allows measurements of quantal content (m) by specific stimulation of GABAergic presynaptic terminals. Finally, we explored whether age-related alterations in synaptic excitation and inhibition occur in the BF. Results from all of these studies will help advance our knowledge of the neurobiology of the aging brain and suggest possible new therapeutic avenues for drug research and/or lifestyle changes. Figure 5.1 summarizes the overall results of the project.

In Chapter II, we tested the effects of acute application of AMI on synaptic transmission using therapeutic concentrations that are well below those that block voltage-gated Ca^{2+} channels. The major finding is that AMI acts presynaptically to reduce neurotransmitter release and that this action is maintained during aging. We used a concentration of 3 μM which is within the therapeutic range (3-6 μM) for depression treatment (Glotzbach and Preskorn, 1982; Lavoie et al., 1990). In our reduced synaptic

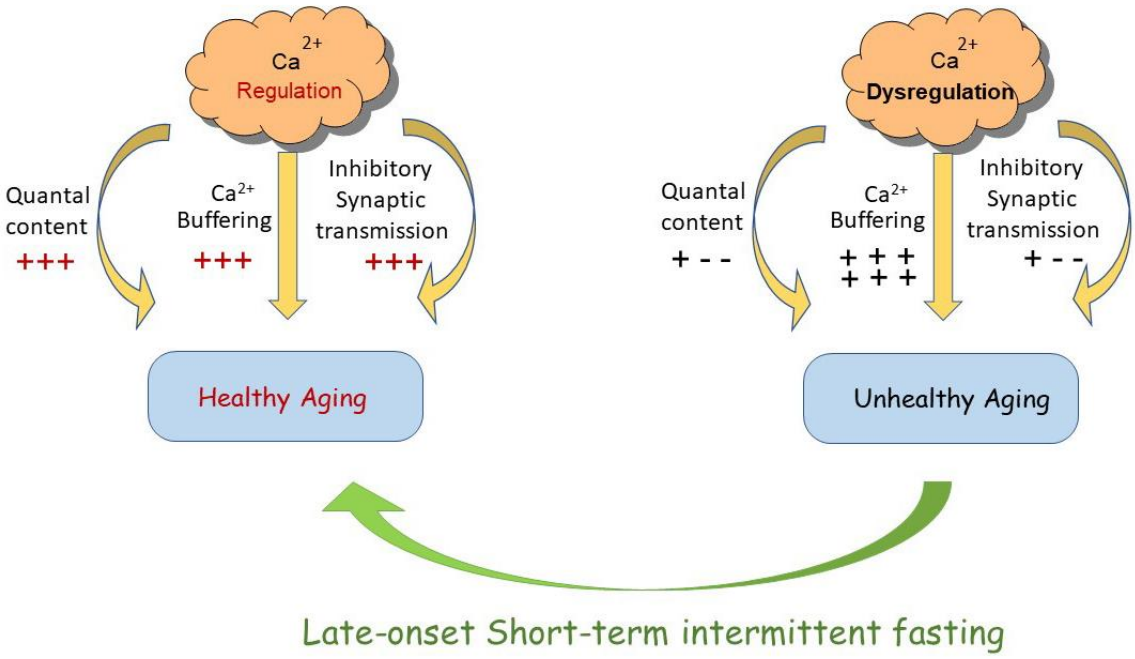

Figure 5.1. Overview of Ca^{2+} and synaptic parameters influenced by late-onset short-term intermittent fasting. Summary of our results in the context of the 'Ca^{2+} hypothesis of aging', as described in the text. Diagram on the left illustrates that healthy aging occurs when intracellular Ca^{2+} regulation is normal and synaptic mechanisms continue to function optimally, as in young subjects. Unhealthy aging is shown to the right and results in general Ca^{2+} dysregulation, which in turn decreases quantal content, increases intracellular Ca^{2+} buffering and decreases inhibitory synaptic transmission. Late-onset short-term intermittent fasting reversed or prevented these age-related changes.

preparation, 3 μM AMI reduced sIPSC frequency in both young and aged mice. The amplitude of sIPSCs was reduced also in young mice, and the amplitude of light-evoked oIPSCs was reduced in both young and aged. In contrast, the same concentration of AMI did not block HVA Ca^{2+} currents and high K^{+} induced intracellular Ca^{2+} transients. Considering the clinical effects of AMI are maintained in the elderly (Barber and Gibson, 2009), inhibition of GABAergic synaptic transmission is one plausible mechanism of action for AMI across aging. These results could have clinical implications suggesting that other drugs targeting GABA release presynaptically could be useful in treatment of depression in the elderly. Because AMI decreased sIPSC frequency, which represents a presynaptic change, we examined additional presynaptic mechanisms of AMI by utilizing quantal analysis. AMI decreased quantal content at GABAergic synaptic terminals which is another mechanism by which AMI modulates inhibitory transmission. AMI regulation of synaptic transmission has been shown also in another study using mechanically isolated medullary dorsal horn neurons (Cho et al., 2012). In that study, 30 μM AMI increased glycinergic neurotransmission presynaptically by increasing the intraterminal Ca^{2+} concentration, which they suggested was mediated by Ca^{2+} release from the intracellular Ca^{2+} stores rather than by extracellular Ca^{2+} influx. Although AMI concentrations used by Cho et al., 2012 are much higher than the therapeutic concentration that we used in Chapter II, it is interesting to speculate that, AMI might reduce the sIPSC frequency by regulating intraterminal Ca^{2+} stores. Although we did not measure intraterminal Ca^{2+} in this study,

we did not observe changes in somatic baseline $[Ca^{2+}]_i$ after 3 or 30 μM AMI. Further investigation will be required to determine actions of AMI on calcium signaling.

Another possible mechanism for presynaptic modulation of neurotransmitter release by AMI is through BDNF/TrkB signaling as AMI acts as a TrkA and TrkB receptor agonist and possesses marked neurotrophic activity (Jang et al., 2009). In the hippocampus, BDNF decreases inhibitory GABAergic transmission (Tanaka et al., 1997; Frerking et al., 1998) but increases excitatory transmission (Tyler et al., 2006), indicating a bidirectional control of synaptic transmission by BDNF. Thus, it is possible that AMI either acts directly or indirectly through BDNF/TrkB signaling to modulate synaptic transmission depending on the specific synapses and releasable pools of neurotransmitter. Future study is required to examine whether AMI modulates GABAergic synaptic transmission in the BF via BDNF/TrkB signaling.

Another interesting aspect of AMI is its influence on cognitive function. Many studies have reported the effects of AMI on memory and cognition in both humans and rodents, although the conclusions are different depending on the experimental conditions. Most studies following administration a single dose of AMI reported cognitive impairment (Branconnier et al., 1982; Curran et al., 1988; Parra et al., 2002), while chronic treatment with AMI demonstrated benefits to cognitive function (Sternberg and Jarvik, 1976; Staton et al., 1981; Yau et al., 2002; Chadwick et al., 2011). It would be an interesting future study to compare the effect of acute versus chronic treatment of AMI on synaptic transmission in the BF and cognitive function. Taken together, in Chapter II we demonstrate that clinically relevant concentrations of AMI

decreased sIPSC frequency and the quantal content in the mouse BF neurons and that these effects were maintained across aging. AMI also significantly decreased sIPSC amplitude in young BF neurons, as well as the amplitude of light-induced oIPSCs in both young and aged BF neurons without age-related differences. In general, changes in the frequency represent changes in probability of neurotransmitter release from presynaptic sites whereas changes in the amplitude could reflect changes in postsynaptic response and/or reduced quantal content. AMI may work at both pre- and post-synaptic sites, probably with a greater impact at presynaptic sites. Future studies will be needed to investigate further plausible mechanisms underlying the action of AMI.

In Chapter III, we investigated the effect of short-term IF initiated later in life on age-related alterations in calcium homeostasis and synaptic transmission in the BF and on cognitive impairment. Several studies have reported the beneficial effect of short-term CR as being comparable to life-long CR (Cao et al., 2001; Kaur et al., 2008). We observed age-related cognitive decline, as well as increased intracellular Ca^{2+} buffering, decreased sIPSC frequency, and decreased quantal content (m) of GABA release in the aged BF neurons. We demonstrated that late-onset short-term IF could reverse age-related alterations in calcium homeostasis and inhibitory synaptic transmission of BF neurons, but cognitive function was not restored.

Impairments in calcium homeostasis and synaptic function have been implicated during aging. In BF neurons, Ca^{2+} influx was increased through enhanced amplitude of LVA currents and reduced inactivation of HVA current (Murchison and Griffith, 1995, 1996). However, concomitantly Ca^{2+} buffering was increased during aging and this may

provide a possible compensatory mechanism to limit the rise of intracellular Ca^{2+} concentrations as there was no change in basal $[Ca^{2+}]_i$ of aged BF neurons (Murchison and Griffith, 1998). Although it is unclear whether this compensatory mechanism is beneficial (Murchison et al., 2009), late-onset short-term IF could significantly reverse the increased Ca^{2+} buffering during aging which is consistent with other studies reporting neuroprotective effects of CR by preventing or reversing age-related impairments in calcium signaling (Hemond and Jaffe, 2005; Amigo et al., 2017). We did not examine further mechanisms underlying the effect of late-onset short-term IF on Ca^{2+} homeostasis in aged BF neurons. Future studies are required to investigate the precise mechanisms by which IF could reverse age-related increases of Ca^{2+} buffering in the BF.

IF reversed the decreased quantal content of GABAergic synaptic transmission with age, and this change in quantal content was considered a presynaptic mechanism. Interestingly though, quantal content was not correlated with cognitive performance, although both Ca^{2+} buffering and sIPSC frequency were significantly associated with cognitive performance. Therefore, reduced sIPSC frequency is unlikely to be explained by a decrease in quantal content alone, but more likely Ca^{2+} signaling mechanisms to control presynaptic release are involved.

The calcium hypothesis of aging and AD was postulated decades ago (Gibson and Peterson, 1987; Khachaturian, 1994) suggesting that dysregulation of Ca^{2+} homeostasis may be a unifying hypothesis for age-related brain dysfunction and neurological diseases. A corollary of this hypothesis is that Ca^{2+} dysregulation results in

synaptic dysfunction that may be a critical mechanism directly contributing to age-related neurological diseases such as AD. Our results in Chapter III consistently demonstrate an age-related decrease in synaptic inhibition, with no change in excitation shown in Chapter IV. This age-related plasticity of synaptic inhibition was further demonstrated by reversal of these age-related changes by short-term intermittent fasting (Chapter III). The exact mechanisms responsible for the interactions of Ca^{2+} signaling and disrupted synaptic function is unknown, but a plausible mechanism for age-related synaptic dysfunction is disruption of Ca-dependent synaptic vesicle release and/or recycling processes.

Presynaptic boutons are packed with synaptic vesicles with a small fraction of vesicles available for immediate release which are called the readily releasable pool (RRP). Additional vesicular pools include a recycling pool and a reserved pool with additional molecular heterogeneity of vesicular pools based on the segregation of vesicular soluble N-Ethylmaleimide sensitive factor (NSF) attachment protein receptor (v-SNARE) proteins (reviewed by Crawford and Kavalali, 2015). During exocytosis, SNARE protein complexes bind to the plasma membrane when Ca^{2+} is available, resulting in vesicular fusion (Pang and Südhof, 2010). It is believed that presynaptic calcium influx controls neurotransmitter release, in part, by regulating the size of the RRP (Neher, 2015). It is thought that newly produced synaptic vesicle proteins are preferentially used in synaptic transmission (Truckenbrodt et al., 2018) and that synaptic strength is determined by the size of the RRP and the probability of release of each vesicle (Kaeser and Regehr, 2017). Overall, the synaptic vesicle cycle (SVC) is a

sophisticated and organized process that has many potential avenues for modulation and regulation. Modulation of this presynaptic function could be an underlying mechanism for age-dependent impairment and synaptic dysregulation.

In addition to disruption of the RRP and release mechanisms during aging, modulation can occur at additional steps in the process. During development and in normal synaptic function, amyloid β (Aβ) functions as a positive regulator of neurotransmitter release probability (Abramov et al., 2018), however, pathological buildup of Aβ, as seen during AD, results in disruption of numerous steps in the SVC including, membrane trafficking, docking, and priming of vesicles for fusion and transmitter release (review Ovsepian et al., 2018). In addition, impairments in cytoskeleton-based protein-transporter systems often underlie cognitive deficits, such as those associated with aging and neurodegenerative diseases (Martin-Peña and Ferrus, 2020). One goal for future studies will be to measure directly the size of the RRP across aging. In this way, direct measurements of vesicular pools can be determined. Many methods are available to test this idea but the best methods are those with the fewest experimental assumptions, including measuring the capacitance change within the presynaptic terminals in response to vesicle docking, or utilizing newer fluorescence measurements that detect changes in vesicle fusion. (reviewed by Kaeser and Regehr, 2017).

Other mechanisms for regulating synaptic function may be involved also, including changes in neurotrophic activity or oxidative stress which are the well-established mechanisms of aging and CR (Granger et al., 1996; Lee et al., 2002; Merry,

2002, 2004; Mattson et al., 2004; Gredilla and Barja, 2005; Hunt et al., 2006; Hyun et al., 2006; Rex et al., 2006; Tapia-Arancibia et al., 2008; Kishi et al., 2015). Future studies are needed to investigate mechanisms underlying synaptic changes in greater detail during aging and with dietary interventions.

Although our results in Chapter III demonstrated the beneficial effect of short-term IF on calcium homeostasis and synaptic transmission, even when started later in life, this IF regimen could not fully improve age-induced cognitive impairments. We believe reversing cognitive dysfunctions during aging is possible with a longer duration of IF. In summary, our findings in Chapter III provide evidence that late-onset short-term IF can reverse age-related changes in calcium homeostasis and inhibitory synaptic function in mouse BF neurons, but reversal of age-related impairment in cognition may require a longer period of IF.

In our final study (Chapter IV), we assessed changes in excitatory glutamatergic synaptic transmission in young and aged mouse BF neurons to determine how excitation contributes to the E/I balance during aging (Figure 5.2). In Chapters II and III, we utilized the reduced synaptic preparation with optogenetics for specific stimulation of inhibitory presynaptic terminals. Due to the very low frequency of sEPSCs in that preparation, we measured sEPSCs using BF brain slices where cellular architecture and circuitry are better represented. The major finding in this Chapter is that there is no change in the amplitude or frequency of sEPSCs during aging. We also confirmed our previous finding of an age-related decrease in sIPSC frequency, suggesting that the reduced synaptic preparation mirrors the results from slices. An imbalance toward

excitation results because of decreased inhibition with no change in excitation. Significant disruption in E/I balance has been implicated during aging, but with variation in E/I ratios between brain regions (Luebke et al., 2004; Potier et al., 2006; Sametsky et al., 2010; Bañuelos et al., 2014; Carpenter et al., 2016; Tran et al., 2018, 2019). Interestingly, cognitively impaired aged subjects showed distinguishable changes in E/I balance, not only from young but also from cognitively unimpaired aged subjects (Tran et al., 2019). Further studies are required to distinguish the aging effect on different underlying mechanisms of excitatory and inhibitory synaptic transmission and its consequences on BF circuitry, projection targets and behavior.

In conclusion, dysregulation of calcium signaling and synaptic transmission has been well described during aging, and abnormal calcium dynamics has been suggested as a common cause of synaptic dysfunction. Prolonged fasting and caloric restriction are known to extend lifespan and are associated with healthy aging in both human and animal models. Here, in this dissertation, we provide evidence that late-onset, short-term intermittent fasting can help restore the detrimental effects of aging as a possible new therapeutic alternative (Figure 5.1). Late-onset short-term IF can reverse age-related alterations in calcium homeostasis and synaptic functions although 4-week short-term diet restriction is not sufficient to reverse age-related impairment in cognitive function. We also determined changes in E/I balance in the BF neurons during aging. We demonstrated that the overall E/I balance increases during aging with reduced inhibition and no change in excitation in the BF. Although reduced inhibitory synaptic transmission in the BF is associated with cognitive decline during aging, we

hypothesized that the origin of the age-related E/I imbalance could be an effort at compensating for diminished cholinergic function in the BF by disinhibiting cholinergic neurons (Figure 5.2). This hypothesis can be addressed in future investigations.

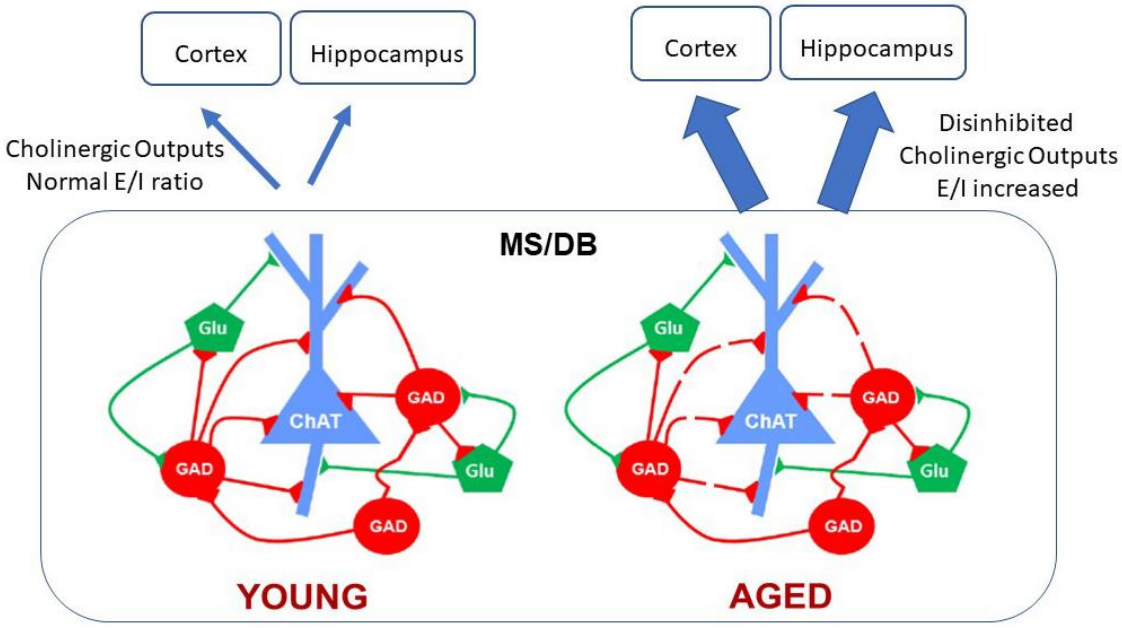

Figure 5.2. Overview of the simplified circuitry of the BF medial septum/diagonal band (MS/DB) and cholinergic projections to the cortex and hippocampus. Hypothesized summary of the age-related changes in cholinergic projection pathways following excitatory/ inhibitory (E/I) imbalance. Circuitry in young (left) shows inter-synaptic pathways within the MS/DB nucleus. Note the multiple synaptic connections on different cell types. GABAergic and glutaminergic projecting pathways are not included. Cholinergic outputs to the cortex and hippocampus are shown with arrows above. During aging (right) GABAergic inhibitory synaptic transmission is decreased and marked by dashed lines resulting in an overall increase in the E/I ratio because excitatory transmission remains unchanged with age. We hypothesize that the net result is increased excitation to cholinergic projection systems as a possible compensatory mechanism to offset cortical/hippocampal decreases in cholinergic function associated with age or disease.

5.1 References

Abramov, E., Dolev, I., Fogel, H., Ciccotosto, G.D., Ruff, E., Slutsky, I. (2009). Amyloid-beta as a positive endogenous regulator of release probability at hippocampal synapses. *Nat. Neurosci.* 12, 1567-76. doi: 10.1038/nn.2433.

Amigo, I., Menezes-Filho, S.L., Luévano-Martínez, L.A., Chausse, B., Kowaltowski, A.J. (2017). Caloric restriction increases brain mitochondrial calcium retention capacity and protects against excitotoxicity. *Aging Cell.* 16, 73-81. doi: 10.1111/acel.12527.

Bañuelos, C., Beas, B.S., McQuail, J.A., Gilbert, R.J., Frazier, C.J., Setlow, B., Bizon, J.L. (2014). Prefrontal cortical GABAergic dysfunction contributes to age-related working memory impairment. *J. Neurosci.* 34, 3457-66. doi: 10.1523/JNEUROSCI.5192-13.2014.

Barber, J. B., and Gibson, S. J. (2009). Treatment of chronic non-malignant pain in the elderly. *Drug-Safety* 32, 457-474. doi: 10.2165/00002018-200932060-00003.

Branconnier, R. J., Devitt, D. R., Cole, J. O. and Spera, K. F. (1982). Amitriptyline selectively disrupts verbal recall from secondary memory of the normal aged. *Neurobiol. Aging* 3, 55-59. doi: 10.1016/0197-4580(82)90061-6.

Cao, S.X., Dhahbi, J.M., Mote, P.L., Spindler, S.R. (2001). Genomic profiling of short- and long-term caloric restriction effects in the liver of aging mice. *Proc. Natl. Acad. Sci. U S A.* 98, 10630-5. doi: 10.1073/pnas.191313598.

Carpenter, H.E., Kelly, K.B., Bizon, J.L., Frazier, C.J. (2016). Age-related changes in

tonic activation of presynaptic versus extrasynaptic γ-amniobutyric acid type B receptors in rat medial prefrontal cortex. *Neurobiol. Aging.* 2016 Sep;45:88-97. doi: 10.1016/j.neurobiolaging.2016.05.015.

Chadwick, W., Mitchell, N., Caroll, J., Zhou, Y., Park, S-S., Wang, L., Becker, K. G., Zhang, Y., Lehrmann, E., Ill, W. H. W., Martin, B., and Maudsley, S. (2011). Amitriptyline-mediated cognitive enhancement in aged 3XTg Alzheimer's disease mice is associated with neurogenesis and neurotrophic activity. *PLoS One* 6, e21660. doi: 10.1371/journal.pone.0021660.

Cho, J. H., Choi, I. S., Lee, M. G., and Jang, I. S. (2012). Effect of amitriptyline on glycinergic transmission in rat medullary dorsal horn neurons. *Brain Res.* 1455, 10-18. doi: 10.1016/j.brainres.2012.03.030.

Crawford, D.C., Kavalali, E.T. (2015). Molecular underpinnings of synaptic vesicle pool heterogeneity. *Traffic.* 16, 338-64. doi: 10.1111/tra.12262.

Curran, H. V., Sakulsripron, M., and Lader, M. (1988). Antidepressants and human memory: An investigation of four drugs with different sedative and anticholinergic profiles. *Psychopharmacology* 95, 520-527. doi: 10.1007/BF00172967.

Frerking, M., Malenka, R. C., and Nicoll, R. A. (1998). Brain-derived neurotrophic factor (BDNF) modulates inhibitory, but not excitatory, transmission in the CA1 region of the hippocampus. *J. Neurophysiol.* 80, 3383-3386. doi: 10.1152/jn.1998.80.6.3383.

Gibson, G.E., Peterson, C. (1987). Calcium and the aging nervous system. *Neurobiol.*

Aging. 8, 329-43. doi: 10.1016/0197-4580(87)90072-8.

Glotzbach, R. K., and Preskorn, S. H. (1982). Brain concentrations of tricyclic antidepressants: single-dose kinetics and relationship to plasma concentrations in chronically dosed rats. *Psychopharmacology (Berl).* 78, 25-27. doi: 10.1007/BF00470582

Granger, R., Deadwyler, S., Davis, M., Moskovitz, B., Kessler, M., Rogers, G., Lynch, G. (1996). Facilitation of glutamate receptors reverses an age-associated memory impairment in rats. *Synapse.* 22, 332-7. doi: 10.1002/(SICI)1098-2396(199604)22:4<332::AID-SYN4>3.0.CO;2-C.

Gredilla, R., Barja, G. (2005). Minireview: the role of oxidative stress in relation to caloric restriction and longevity. *Endocrinology* 146, 3713-3717. doi: 10.1210/en.2005-0378.

Hemond, P., Jaffe, D.B. (2005). Caloric restriction prevents aging-associated changes in spike-mediated Ca2+ accumulation and the slow afterhyperpolarization in hippocampal CA1 pyramidal neurons. *Neuroscience* 135, 413-20. doi: 10.1016/j.neuroscience.2005.05.044.

Hunt, N.D., Hyun, D.H., Allard, J.S., Minor, R.K., Mattson, M.P., Ingram, D.K., de Cabo, R. (2006). Bioenergetics of aging and calorie restriction. *Ageing Res. Rev.* 5, 125-143. doi: 10.1016/j.arr.2006.03.006.

Hyun, D.H., Emerson, S.S., Jo, D.G., Mattson, M.P., de Cabo, R. (2006). Calorie

restriction up-regulates the plasma membrane redox system in brain cells and suppresses oxidative stress during aging. *Proc. Natl. Acad. Sci. U S A* 103, 19908-12. doi: 10.1073/pnas.0608008103.

Jang, S. W., Liu, X., Chan, C. B., Weinshenker, D., Hall, R. A., Xiao, G., and Ye, K. (2009). Amitriptyline is a TrkA and TrkB receptor agonist that promotes TrkA/TrkB heterodimerization and has potent neurotrophic activity. *Chemistry & Biology* 16, 644-656. doi: 10.1016/j.chembiol.2009.05.010.

Kaeser, P.S., Regehr, W.G. (2017). The readily releasable pool of synaptic vesicles. *Curr. Opin. Neurobiol.* 43, 63-70. doi: 10.1016/j.conb.2016.12.012.

Kaur, M., Sharma, S., Kaur, G. (2008). Age-related impairments in neuronal plasticity markers and astrocytic GFAP and their reversal by late-onset short term dietary restriction. *Biogerontology* 9, 441-54. doi: 10.1007/s10522-008-9168-0.

Khachaturian, Z.S. (1994). Calcium hypothesis of Alzheimer's disease and brain aging. *Ann. N. Y. Acad. Sci.* 747, 1-11. doi: 10.1111/j.1749-6632.1994.tb44398.x.

Kishi, T., Hirooka, Y., Nagayama, T., Isegawa, K., Katsuki, M., Takesue, K., Sunagawa, K. (2015). Calorie restriction improves cognitive decline via up-regulation of brain-derived neurotrophic factor: tropomyosin-related kinase B in hippocampus of obesity-induced hypertensive rats. *Int. Heart J.* 56, 110-5. doi: 10.1536/ihj.14-168.

Lavoie, P. A., Beauchamp, G., and Elie, R. (1990). Tricyclic antidepressants inhibit

voltage-dependent calcium channels and Na(+)-Ca2+ exchange in rat brain cortex synaptosomes. *Can. J. Physiol. Pharmacol.* 68, 1414-1418, doi: 10.1139/y90-215.

Lee, J., Duan, W., Mattson, M.P. (2002). Evidence that brain-derived neurotrophic factor is required for basal neurogenesis and mediates, in part, the enhancement of neurogenesis by dietary restriction in the hippocampus of adult mice. *J. Neurochem.* 82, 1367-75. doi: 10.1046/j.1471-4159.2002.01085.x.

Luebke, J.I., Chang, Y.M., Moore, T.L., Rosene, D.L. (2004). Normal aging results in decreased synaptic excitation and increased synaptic inhibition of layer 2/3 pyramidal cells in the monkey prefrontal cortex. *Neuroscience* 125, 277-88. doi: 10.1016/j.neuroscience.2004.01.035.

Martin-Peña, A., Ferrus, A. (2020). CCB is involved in actin-based axonal transport of selected synaptic proteins. *J. Neurosci.* 40, 542-556. doi: 10.1523/JNEUROSCI.0915-18.2019.

Mattson, M.P., Maudsley, S., Martin, B. (2004). BDNF and 5-HT: a dynamic duo in age-related neuronal plasticity and neurodegenerative disorders. *Trends. Neurosci.* 27, 589-94. doi: 10.1016/j.tins.2004.08.001.

Merry, B.J. (2002). Molecular mechanisms linking calorie restriction and longevity. *Int. J. Biochem. Cell Biol.* 34, 1340-1354. doi: 10.1016/s1357-2725(02)00038-9.

Merry, B.J. (2004). Oxidative stress and mitochondrial function with aging—the effects of calorie restriction. *Aging Cell* 3, 7-12. doi: 10.1046/j.1474-9728.2003.00074.x.

Murchison, D., Griffith, W.H. (1995). Low-voltage activated calcium currents increase

in basal forebrain neurons from aged rats. *J. Neurophysiol.* 74, 876-87. doi: 10.1152/jn.1995.74.2.876.

Murchison, D., Griffith, W.H. (1996). High-voltage-activated calcium currents in basal forebrain neurons during aging. *J. Neurophysiol.* 76, 158-74. doi: 10.1152/jn.1996.76.1.158.

Murchison, D., Griffith, W. H. (1998). Increased calcium buffering in basal forebrain neurons during aging. *J. Neurophysiol.* 80, 350-364. doi: 10.1152/jn.1998.80.1.350

Murchison, D., McDermott, A.N., Lasarge, C.L., Peebles, K.A., Bizon, J.L., Griffith, W.H. (2009). Enhanced calcium buffering in F344 rat cholinergic basal forebrain neurons is associated with age-related cognitive impairment. *J. Neurophysiol.* 102, 2194-207. doi: 10.1152/jn.00301.2009.

Neher, E. (2015). Merits and limitations of vesicle pool models in view of heterogeneous populations of synaptic vesicles. *Neuron* 87, 1131-1142. doi: 10.1016/j.neuron.2015.08.038.

Ovsepian, S.V., O'Leary, V.B., Zaborszky, L., Ntziachristos, V., Dolly, J.O. (2018). Synaptic vesicle cycle and amyloid β: Biting the hand that feeds. Alzheimers Dement. 14, 502-513. doi: 10.1016/j.jalz.2018.01.011.

Pang, Z.P., Südhof, T.C. (2010). Cell biology of Ca2+-triggered exocytosis. *Curr. Opin. Cell Biol.* 22, 496-505. doi: 10.1016/j.ceb.2010.05.001.

Parra, A., Everss, E., Monleón, S., Vinader-Caerols, C., and Arenas, M. C. (2002).

Effects of acute amitriptyline administration on memory, anxiety and activity in male and female mice. Neurosci. Res. Comm. 31, 135-144. doi: 10.1002/nrc.10046.

Potier, B., Jouvenceau, A., Epelbaum, J., Dutar, P. (2006). Age-related alterations of GABAergic input to CA1 pyramidal neurons and its control by nicotinic acetylcholine receptors in rat hippocampus. *Neuroscience* 142, 187-201. doi: 10.1016/j.neuroscience.2006.06.040.

Rex, C.S., Lauterborn, J.C., Lin, C.Y., Kramár, E.A., Rogers, G.A., Gall, C.M., Lynch, G. (2006). Restoration of long-term potentiation in middle-aged hippocampus after induction of brain-derived neurotrophic factor. *J. Neurophysiol.* 96, 677-85. doi: 10.1152/jn.00336.2006.

Sametsky, E.A., Disterhoft, J.F., Geinisman, Y., Nicholson, D.A. (2010). Synaptic strength and postsynaptically silent synapses through advanced aging in rat hippocampal CA1 pyramidal neurons. *Neurobiol. Aging.* 31, 813-25. doi: 10.1016/j.neurobiolaging.2008.05.029.

Staton, R. D., Wilson, H., and Brumback, R. A. (1981). Cognitive improvement associated with tricyclic antidepressant treatment of childhood major depressive illness. Percept. Mot. Skills 53, 219-234. doi: 10.2466/pms.1981.53.1.219.

Sternberg, D. E., and Jarvik, M. E. (1976). Memory functions in depression. *Arch. Gen. Psychiatry* 33, 219-224. doi: 10.1001/archpsyc.1976.01770020055009.

Tanaka, T., Saito, H., and Matsuki, N. (1997). Inhibition of GABAA synaptic responses

by brain-derived neurotrophic factor BDNF in rat hippocampus. *J. Neurosci.* 17, 2959–2966. doi: 10.1523/JNEUROSCI.17-09-02959.1997.

Tapia-Arancibia, L., Aliaga, E., Silhol, M., Arancibia, S. (2008). New insights into brain BDNF function in normal aging and Alzheimer disease. *Brain Res. Rev.* 59, 201-20. doi: 10.1016/j.brainresrev.2008.07.007.

Tran, T., Bridi, M., Koh, M.T., Gallagher, M., Kirkwood, A. (2019). Reduced cognitive performance in aged rats correlates with increased excitation/inhibition ratio in the dentate gyrus in response to lateral entorhinal input. Neurobiol. Aging. 82, 120-127. doi: 10.1016/j.neurobiolaging.2019.07.010.

Tran, T., Gallagher, M., Kirkwood, A. (2018). Enhanced postsynaptic inhibitory strength in hippocampal principal cells in high-performing aged rats. Neurobiol. Aging. 70, 92-101. doi: 10.1016/j.neurobiolaging.2018.06.008.

Truckenbrodt, S., Viplav, A., Jähne, S., Vogts, A., Denker, A., Wildhagen, H., Fornasiero, E.F., Rizzoli, S.O. (2018). Newly produced synaptic vesicle proteins are preferentially used in synaptic transmission. *EMBO J.* 37, e98044. doi: 10.15252/embj.201798044.

Tyler, W. J., Zhang, X. L., Hartman, K., Winterer, J., Muller, W., Stanton, P. K., and Pozzo-Miller, L. (2006). BDNF increases release probability and the size of a rapidly recycling vesicle pool within rat hippocampal excitatory synapses. *J. Physiol.* 574, 787-803. doi: 10.1113/jphysiol.2006.111310.

Yau, J. L. W., Noble, J., Hibberd, C., Rowe, W. B., Meaney, M. J., Morris, R. G. M.,

and Seckl, J. R. (2002). Chronic treatment with the antidepressant amitriptyline prevents impairments in water maze learning in aging rats. *J. Neurosci.* 22, 1436-1442. doi: 10.1523/JNEUROSCI.22-04-01436.2002.